Experimental and Numerical Modelling of the Hydraulic Stability of Geotextile Sand Containers for Coastal Protection

Von der
Fakultät Architektur, Bauingenieurwesen und Umweltwissenschaften
der Technischen Universität Carolo-Wilhelmina
zu Braunschweig

zur Erlangung des Grades einer
Doktoringenieur (Dr.-Ing.)
eingereichte

Dissertation

von
Darshana T. B. D. Dassanayake Mudiyanselage
geboren am 29.12.1977
aus Kurunegala, Sri Lanka

Eingereicht am: 12. April 2013
Disputation am: 02. Juli 2013

Berichterstatter: Prof. Hocine Oumeraci
Prof. Adam Bezuijen

2013

Preface

Several series of experimental and numerical modelling on the hydraulic stability of geotextile sand containers were carried out at Leichtweiss Institute, Technische Universität Braunschweig, Germany (LWI). LWI and NAUE GmbH & Co. KG are gratefully acknowledged for their financial support to conduct the laboratory investigations. Financial support provided for myself to pursue my PhD in Germany by German Academic Exchange Service (DAAD) is greatly acknowledged.

I would like to express my deep gratitude to my PhD supervisor, Prof. Dr.-Ing. Hocine Oumeraci, who gave me this opportunity to conduct my PhD at LWI and allowed me to use the laboratory facilities to perform various experimental studies. Also his valuable guidance and spending his precious time on discussions and on correcting the thesis etc. are highly appreciated.

I am very much thankful to all LWI staff for their assistance and friendship during my stay in Germany. Also, valuable advices from Dr.-Ing. Andreas Kortenhaus and kind care from Ms. Gabriele Fournier are highly appreciated.

Finally I like to express my gratitude deeply from the heart to my parents who have been continuously supporting and encouraging me during my studies, and specially to my wife Dilani, for her patience, encouragement and support during my study period.

July 2013 / Braunschweig, Germany Darshana T. B. D. Dassanayake Mudiyanselage

Kurzfassung

Vielseitige und innovative Lösungen für die Bemessung effektiver Küstenschutzbauwerke sowie Verstärkung existierender, bedrohter Küstenbarrieren werden benötigt. Dies beinhaltet auch Dünenverstärkungen und Kolkschutzmaßnahmen. Sandcontainer aus Geotextilien (GSC) sind eine günstige, flexible und reversible Lösung, die schon mehr als 50 Jahre im marinen und wasserbaulichen Bereich Anwendung findet. Viele erfolgreiche Küstenschutzprojekte mit GSCs wurden weltweit, vor allem in Australien und Deutschland, ausgeführt. Trotzdem befinden sich GSCs immer noch in der Entwicklung und es sind bisher keine Richtlinien zur Bemessung von GSC-Bauwerken auf Grundlage wissenschaftlicher Erkenntnisse vorhanden. Aufgrund der Beweglichkeit und der geringen Dichte von GSCs im Vergleich zu Steinschüttungen oder Betonformsteinen verhalten sich GSCs anders. Daher sind auch die bewährten Bemessungsansätze für Gesteinsschüttungen nicht anwendbar.

Die vorliegende Arbeit ist fokussiert auf die Evaluierung der Einflüsse der wichtigsten Eigenschaften auf die hydraulische Stabilität von GSC-Bauwerken sowie der Entwicklung eines neuen Ansatzes zur Vorhersage der hydraulischen Stabilität von Kronen-GSCs von Unterwasser- bzw. sehr niedrigen GSC- Bauwerken. Die wichtigsten Eigenschaften von GSCs sind die mechanischen Eigenschaften des Geotextils, der Füllstand, die Art des Füllmaterials und die Oberflächenrauigkeit. Tatsächlich beeinflussen die meisten dieser Eigenschaften die Deformation der GSCs und die Bewegung des Sandes innerhalb der Container. Vor allem interagieren die Effekte der einzelnen Eigenschaften miteinander. Die Bedeutung dieser Aspekte wurde in vielen Studien und Projekten weltweit hervorgehoben. Trotzdem sind die Kenntnisse über den Einfluss des Füllstands, der Eigenschaften des Füllmaterials und die Oberflächenrauigkeit der GSCs auf die hydraulische Stabilität von GSC-Bauwerken sehr gering.

Zunächst wurde der Wissensstand zu den betreffenden Eigenschaften von GSCs und ihrem Einfluss auf die Stabilität von GSC-Bauwerken und bestehende hydraulische Stabilitätsansätze kritisch bewertet. Anschließend wurden vier speziell entwickelte Experimente durchgeführt, welche Einblick in den Einfluss der oben genannten Eigenschaften auf GSC-Bauwerke gewährte und die Randbedingung für die numerische Modellierung der Stabilität festlegte. Unterschiedliche Arten von Experimenten wurden durchgeführt: zwei Laborexperimente (Fall- und Zugversuche), kleinmaßstäbliche Wellenkanalversuche (hydraulische Stabilität) und Versuche im Strömungskanal (Durchlässigkeit). Weiterhin wurden numerische Simulationen der GSC-Bauwerke mit Hilfe eines schwach gekoppelten RANS-VOF und FEM-DEM Modells durchgeführt. Dies war die bestmögliche Variante die hydraulische Stabilität von GSC-Bauwerken innerhalb der Doktorarbeit numerisch zu modellieren. Zuletzt wurden die Ergebnisse der experimentellen und numerischen Untersuchungen zusammengeführt und neue Stabilitätskurven und einfache Berechnungsansätze für die hydraulische Stabilität von Kronen-GSCs entwickelt.

Auch wenn die meisten früheren Studien und Richtlinien einen Füllstand von 80% für GSC im Küstenbereich empfehlen, ist eine höhere Stabilität für einen Füllstand von 100% zu beobachten. Desweiteren erhöhen geneigt platzierte GSCs und Geotextilien mit einer höheren Oberflächenrauigkeit die hydraulische Stabilität und verlangsamen auch den Schadensverlauf. Generell zeigen die numerischen Ergebnisse eine gute Übereinstimmung mit den experimentellen Daten. Daher hat das CFD-CSD Modell auch ein vielversprechendes Potential zur Anwendung in der Praxis. Es wird erwartet, dass die neu entwickelten Stabilitätsberechnungsansätze und Stabilitätskurven eine Verwendung von GSCs im Küstenbereich begünstigen.

Abstract

More versatile materials and innovative solutions are required for the design of new, cost effective shore protection structures as well as for the reinforcement of existing threatened coastal barriers, including dune reinforcement and scour protection. Geotextile Sand Containers (GSC) is a relatively low cost, soft and reversible solution for the above problem with a history of more than 50 years in hydraulic and marine applications. A range of successful coastal protection structures using GSCs has been constructed in many parts of the world, especially in Australia and Germany. Nevertheless, GSC is still an emerging technology and no proper guidelines are available for the design of GSC-structures on a sound scientific base. Due to the flexibility and the lower specific gravity of GSCs as compared to rock or concrete armour units, GSCs behave differently and therefore, the established design formulae for rock or concrete units are not applicable.

This PhD study attempts to evaluate the effect of the most important engineering properties of GSCs on the hydraulic stability of GSC-structures and to develop new formulae for the hydraulic stability of crest GSCs of submerged/low-crested GSC-structures. The most important engineering properties of GSCs are the mechanical properties of the geotextile material, the sand fill ratio, the type of the fill material and the interface friction. In fact, most of these properties will affect the deformation of GSCs and the movement of sand inside the container. More importantly, the effects of these properties on the stability of GSCs are interrelated. The significance of these aspects has been highlighted in many studies and projects worldwide. However, the knowledge about the influence of the sand fill ratio, the properties of fill material and the interface friction of GSCs on the hydraulic stability of GSC-structure is still very poor.

First, the present knowledge related to the engineering properties of GSCs and their effects on the stability of GSC-structures and the existing hydraulic stability formulae for GSC-structures were critically reviewed. Second, four series of especially designed laboratory experiments, which allowed us to have an insight into the influence of the above mentioned properties on the stability of GSC-structures and also to obtain the required parameters for the numerical modelling of their stability were performed. Experimental investigations consisted of two types of laboratory experiments (drop tests and pullout tests), small scale wave flume tests (hydraulic stability tests) and hydraulic flume tests (permeability tests). Third, numerical modelling of GSC-structures was conducted using the weakly coupled RANS-VOF model and FEM-DEM models. This was the best feasible option to numerically model the hydraulic stability of GSC-structures within the framework of this PhD. Overall the numerical results show a relatively good agreement with the experimental data. Hence, this Computational Fluid Dynamic-Computational Structural Dynamic (CFD-CSD) model system has an encouraging potential for practical applications.

Though most of the previous studies and design guidelines on the use of GSCs in coastal structures recommend a sand fill ratio of 80%, 100% filled GSC show higher hydraulic stability compared to 80% filled GSC. Moreover, inclined placement of GSCs and geotextile materials with high friction properties also enhance the hydraulic stability. Moreover, they also slow down the damage progress. Finally, combining both the experimental and numerical results, new stability curves and simple formulae were developed for the hydraulic stability of crest GSCs. This newly developed stability curves and stability formulae are expected to foster the applications of GSC structures for coastal protection.

Table of Contents

List of Figures

List of Tables

List of Notations and Symbols

a : length of the flat bag

A : total cross sectional area

A_f : final cross sectional area

A_0 : Initial cross sectional area

A_m : mean cross sectional area

A_{max} : maximum cross sectional area

A_S : projected area of the containers normal to the wave direction

A_T : projected area of the containers in wave direction

b : length of flat bag

c : constant depending on the type of structure of the formulae of Oumeraci and Muttray (2001)

C_D : drag coefficient

C_L : lift coefficient

C_M : inertia coefficient

Cu : coefficient of uniformity

D_g : diameter of geotextile tube.

D_w : opening size of geotextile based on hydrodynamic sieving

D : displacement

d : water depth

d_n : cubic root of volume

D : diameter of grain

D_x : soil particle size corresponding to x% passing

FR : sand fill ratio

g : acceleration due to gravity

h_1 : water level in front of structure

h_2 : water level behind of structure

h_{cont} : height of container

h_{GSC} : height of geotextile sand container

$h_{structure}$: height of structure

H_i : significant wave height of incident wave

H_o : deep water wave height

$H_{2\%}$: mean of the highest 2% of the waves in the time series

H_r : significant wave heights of reflected wave

H_s : significant wave height

I : hydraulic gradient

k : Darcy's coefficient of permeability

K : stability coefficient

K_a : active soil pressure

KO_{CD} : deformation factor for the drag coefficient during overturning of container

KO_{CM} : deformation factor for the inertia force during overturning of container

KO_{CL} : deformation factor for the lift force during overturning of container

KO_R : deformation factor for the resisting force during overturning of container

kPa : kilopascal

KS_{CD} : deformation factor for the drag coefficient during sliding of container

KS_{CM} : deformation factor for the inertia force during sliding of container

KS_{CL} : deformation factor for the lift force during sliding of container

KS_R : deformation factor for the resisting force during sliding of container

K_r : reflection coefficient

l_c : length of container

L_0 : deep water wave length

n : porosity of filling material

Ns : stability parameter (known also as stability number

O_x : opening size of geotextile corresponding to x particle size based on dry glass bead sieving

P : perimeter

Q : flow rate

Q^*: relative overtopping rate

q: overtopping discharge per unit length of structure

Rc : crest freeboard

Rc^* : relative crest freeboard

R_d : run down

R_u : run up

$R_{u2\%}$: run-up level which is exceeded by two per cent of the incoming waves.

T_m : mean wave period of a regular waves

T_p : peak wave period of a wave spectrum

T : test duration

$T_{tension}$: tension of geotextile

v: characteristic flow velocity

V : volume of the container

V' : volume of the container with deformation effects

v_n : velocity at point n

W : weight of armour layer

W_s : weight of sand

W_{50} : average weight of the cover-layer element

w_{cont} : width of the container

z_n : measurement point in the direction of gravity

ξ_o : Iribarren number (surf similarity parameter)

μ : friction coefficient

λ : friction factor

ν : kinematic viscosity of water

γ_{fGSC} : reduction factor for GSC-revetments

ϕ : friction angle of soil material

α : angle of the slope of the structure

σ_1: principal stresses

σ_3: principal stresses normal to the load

γ_b: reduction factor for a berm

γ_β: reduction factor for oblique wave attack

γ_f: reduction factor for slope roughness

Δ : submerged density of armour element

ρ_s: density of sand

Δh: water head difference

β : angle of incidence of wave

$\frac{\partial v}{\partial t}$: wave induced horizontal particle acceleration

Abbreviations

AOS : Apparent Opening Size
CFD : Computational Fluid Dynamic
COBRAS : Cornel Breaking Wave and Structures
COBRAS-UC : Cornell Breaking Wave and Structures-University of Cantabria
CSD : Computational Structural Dynamic
CoV : Coefficient of Variation
GSC : Geotextile Sand Container
GWK: large wave flume at Hannover
FR : Fill Ratio
LVDT : Linear Variable Differential Transformer
LWI : Leichtweiss Institute
NW_x : Nonwoven geotextile
PET: polyethylene terephthalate
PP: Polypropylene
RANS : Reynolds Averaged Navier Stokes
SWL: Still Water Level
UDEC : Universal Distinct Element Code
VOF : Volume of Fluid
WG : Wave Gauge
W_x : Woven geotextile

1 Introduction

1.1 Motivation

Settlements in coastal lowlands are especially vulnerable to sea level rise and storm surges associated with climate change. However, these lowlands are often densely settled and the population living there is growing rapidly. When considering the area along the coast that is less than 10 metres above the mean sea level, this zone covers 2% of the world's land area but contains 10% of the world's population. This percentage is higher in developing countries than developed countries (McGranahan et al. 2007). Further, the value of the coastal ecosystems represents almost 40% of the value of all marine and terrestrial ecosystems (Oumeraci 2000). On the other hand, the still increasing socio-economic pressure on the use of coastal zones with the subsequent increase of the needs for more infrastructures has led to an increasing conversion of these vital zones to a built environment. Therefore, sustainable development of these valuable and sensitive coastal zones is essential (Oumeraci 2004). Hence, there is an urgent need for cost effective, environmentally friendly solutions to mitigate the risk of disasters related to climate change in coastal settlements.

More versatile materials and innovative solutions are required for the design of new, cost effective shore protection structures as well as for the reinforcement of existing threatened coastal barriers and structures, including dune reinforcement and scour protection (Oumeraci and Recio 2010). Geotextile Sand Containers (GSC) represent a low cost (Oberhagemann and Hossain 2011, Weerakoon et al. 2003, Jackson et al. 2012), soft and reversible solution for the above problem and the use of GSCs in hydraulic and marine applications has a history of more than 50 years. Coastal structures built with GSCs are obtained by substituting rocks or concrete units with containers made of geotextile and filled with locally available sand. A range of successful coastal protection structures using GSCs have been constructed in many parts of the world, especially in Australia, Germany, and South Africa (Heerten et al. 2000, Restall and Saathof 2002, Restall et al. 2004, Saathof et al. 2007, Bleck and Werth 2012, Corbella and Stretch 2012) (Figure 1-1).

Figure 1-1: Coastal structures made of geotextile sand containers (GSCs)

Apart from GSCs, geotextiles are widely used in coastal structures and harbour constructions. (e.g. Geotextiles are placed below the riprap along the coastline or harbour caissons to prevent

soil erosion). However, geotextiles used for GSC-structures in coastal and marine environments are subject to significantly different forces and exposure conditions than geotextiles used in other conventional applications such as road construction, geotechnics, etc. In the earlier applications, coastal GSC-structures were considered as temporary or short term solutions. Mainly, the use of exposed geotextile for GSCs and Geotextile Tubes is pushing the boundaries of geotextile with regards to the durability (Hornsey 2011). The main concerns were UV-resistance, biological effects, abrasion and damage resistance, etc. However, GSC-structures made of geotextiles that were manufactured more than two decades ago are still in service and proved that they can last longer than what initially estimated. Also the advancements in the field of geotextile manufacturing technology allow the fabrics to be engineered to have a wide variety of properties, enabling a tailored design of the material for a specific application (ASR 2005a). Furthermore, research studies carried out during the recent past provide a good insight of the durability of geotextile in marine environment (e.g. Heieh et al. 2006, TenCate 2007, Hornsey 2011). Table 1-1 summarises the strengths and the weaknesses of GSC-structures in coastal environment. However, the extensive research works conducted during the last two decades and their findings remarkably reduced the weaknesses of coastal structures made of GSCs.

Table 1-1: Strengths and weaknesses of GSC-structures (modified from Recio 2007)

Strength / weakness	Conventional hard structures	GSC-structures
Applicability as a coastal structure to solve conventional coastal engineering problems	high	high
Resistance against wave action and coastal related natural hazards, if properly designed.	high	high
Adaptability to changing site conditions and morphological foundation changes.	low*	high
Total construction and life cycle cost savings (compared with conventional structures)	not applicable	generally high
Respond to cyclic hydrodynamic loads	moderate	high
Wave runup and wave reflection	low	high
Removability, if engineering measures did not prove successful	low	high
deep understanding of the hydraulic processes affecting the stability of GSC-structures	high	moderate
reliable design tools which can compromise the safety under different conditions	high	low
Requirement of consideration of site specific conditions for design and construction	moderate	high
Understanding of long term effect on structural durability in marine environment	high	low

* however, riprap revetments show high adaptability to site conditions and morphological foundation changes
** generally, GSC structure are less permeable and consequently then will have large wave runup and wave reflection

Nevertheless, there are still several critical issues that require further research in order to enhance applications and performances of the GSC-structures. The hydraulic processes affecting the stability of GSC-structures were extensively investigated by Oumeraci et al. (2002a, 2002b, 2003, 2007a), Oumeraci and Recio (2010), Recio (2007) and Recio and Oumeraci (2008a, 2008b, 2009). Moreover, few formulae were developed for the prediction of the hy-

draulic stability of GSC-structures (see Table 2-8) and among those, the formulae developed by Recio (2007) are the only process-based hydraulic stability formulae for GSCs. However, these formulae still need to be simplified and refined in order to make them more user friendly for practicing engineers.

The sand fill ratio of geotextile containers has been identified as an important parameter for the stability of GSC-structures (Venis 1968, Oumeraci et al. 2007a, Recio 2007, Recio and Oumeraci 2009, Oumeraci and Recio 2010, Coghlan et al. 2009, Horney 2011, Wilms et al. 2011 etc.). Nevertheless, none of the exiting formulae for the hydraulic stability of GSC-structures accounts for the sand fill ratio. Moreover, a clear definition for the sand fill ratio is still lacking (Bezuijen et al. 2004). Therefore, a proper definition for the sand fill ratio based on a systematic investigation of the relationships between the sand fill ratio and the hydraulic stability of GSC-structures is crucial, to achieve a better understanding of the hydraulic functioning of GSC-structures under wave attack.

Furthermore, Recio (2007) identified that the interface friction between GSCs considerably affects the hydraulic stability of GSC-Structures. A friction factor between containers (μ) is already included in Recio's formulae. Despite of the interface friction already incorporated in the formulae, the effect of interface friction properties is still not fully explained or experimentally verified. Furthermore, the formulae were derived using the friction coefficient, which were obtained from the direct shear stress tests conducted with the conventional shear box apparatus (NAUE 2004a and Recio 2007). Some recent research studies showed that the conventional direct shear stress test results (performed under dry conditions) do not perfectly represent the interface friction of GSCs (Krahn et al. 2007, Matsushima et al. 2008).

Moreover, Recio (2007) has adopted and improved a numerical modelling system for GSC-structure, consisting of a computational fluid dynamic model (CFD) and two computational structural dynamic models (CSD). The modelling system was partially validated to the extent of the performed experimental model tests. This weakly coupled modelling system helps to gain an improved understanding of the processes that affect the stability of GSC-structures. Further advancement of this modelling tool will lead to a development of an operational design tool based on CFD and CSD models.

Lastly, despite of the formulae from Recio (2007) need to be improved by incorporating some more important parameters, the formulae are already complicated. Hence, apart from refining and simplifying the formulae, it will be very useful for the engineering practice to develop simple hydraulic stability formulae and/or a computational tool for the design of GSC-structures. There are computational tools available for the design of geosynthetic tubes. For example GeoCoPS by ADAMA Engineering, USA is an interactive program for the design of geosynthetic tubes. This programme is capable of determining the geometry of the tube and the circumferential and longitudinal required strength of the encapsulating geosynthetic for a given problem. The computations account for the reduction factors related to seam strength, durability, creep, and installation damage. Development of a similar tool will help to spread the geotextile sand container technology.

1.2 Objectives

The tentative objectives of the current research are to;

(i) Investigate the effect of the sand fill ratio on the hydraulic stability of GSC-structures
(ii) Study the friction between GSCs and its effect on hydraulic stability of GSC-structures
(iii) Refine, simplify and make the stability formulae of Recio (2007) more user friendly
(iv) Develop a simplified stability formulae for the hydraulic stability of GSC-Structures

1.3 Methodology

The tentative methodology, which will be specified in more details as a result of Chapter 2, is briefly illustrated in Figure 1-2.

First, the present knowledge related to the engineering properties of GSCs and their effect on the hydraulic stability of GSC-structures will be reviewed. Particular emphasis will be put on the sand fill ratio and the friction between containers, which may affect the stability of GSC-structures. Second, a range of different types of laboratory experiments will be designed and conducted, which will allows us to have an insight into the influence of above mentioned properties on the stability of structures made of GSCs subject to wave attack and also to obtain the required parameters for numerical modelling of GSC-structures. Third, the most appropriate numerical model system will be selected to simulate hydraulic stability of GSC-structures. Initially numerical modelling will start with the weakly coupled RANS-VOF model and FEM-DEM models as used by Recio (2007). The performance of this model system and capabilities of other available models will then be critically evaluated in order to identify the best modelling system. The hydraulic stability of GSC-structures will be modelled using the selected modelling system incorporating the results obtained from physical models tests. These models will be verified through the proposed and past laboratory experiments. Based on this knowledge, finally more simplified hydraulic stability formulae will be developed.

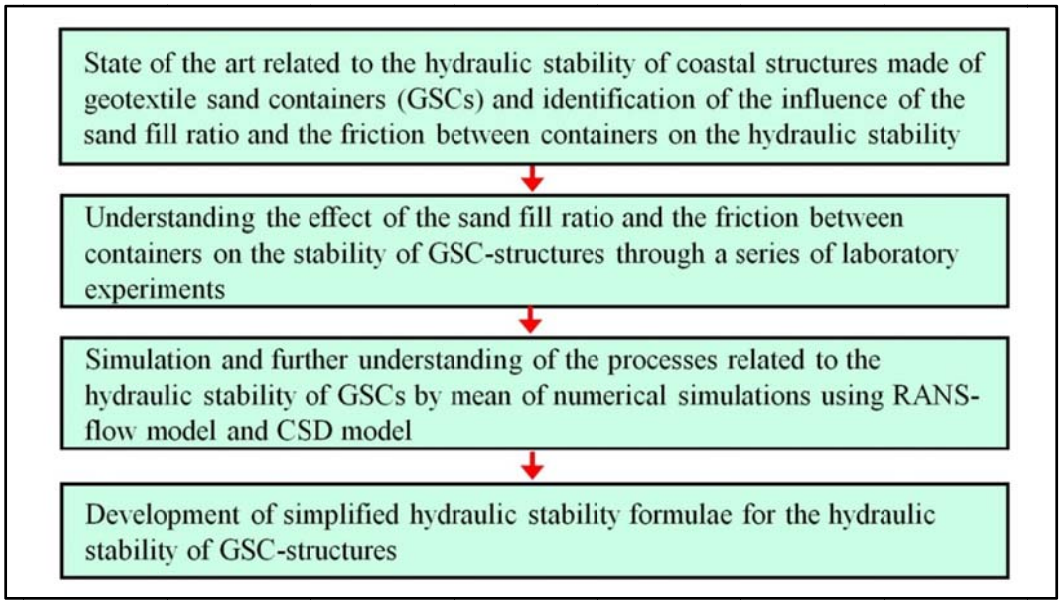

Figure 1-2: Tentative methodology of the research

2 Current State of Knowledge and Modelling

An extensive literature study on the important engineering properties of GSCs, which are relevant for the hydraulic stability, has been carried out in the framework of the PhD (see state-of-the art report - Dassanayake and Oumeraci 2009a). The most important engineering properties of GSCs are identified as the properties of geotextile material itself, the sand fill ratio, the type of fill material, the interface friction of GSCs and the deformability of GSCs. More importantly these properties are interrelated and their influence on the hydraulic stability of GSC-structure is not yet fully understood. This chapter aims at underlining the necessity of the knowledge of the aforementioned engineering properties of GSCs for an improved understanding of the hydraulic stability of GSC-structures and at proposing an experimental and numerical investigation programme. This investigation programme will bridge the knowledge gaps on engineering properties and their effect on the hydraulic stability of GSC-structures.

One of the most important findings of the literature study is that a systematic investigation of the relationships between these engineering properties of GSCs and the hydraulic stability of GSC-structures is crucial to achieve a better understanding of the hydraulic functioning GSC-structures under wave attack. Therefore, the ultimate objective is to introduce the sand fill ratio, the friction between GSCs, the inclination angle of GSCs, etc. as important parameters in the design guidance of GSC-structures subject to severe wave attack. As a result of this chapter which represents an updated summary of the aforementioned state-of-the art report, the tentative objectives and methodologies briefly introduced in Chapter 1 will be specified more precisely and modified where necessary.

2.1 Engineering Properties of Woven and Nonwoven Geotextile

The most widely used raw materials for manufacturing geotextiles are polypropylene and polyester. Physical properties of these materials can be improved by the use of additives and by changing the processing methods used to form the material into fibres, which is the building block of geotextiles. Geotextiles are divided into two main groups based on the manufacturing process, namely woven geotextile and nonwoven geotextile. Woven geotextiles have higher tensile strength and low elongations at rupture. Nonwoven geotextiles are generally thicker and formed by processes other than waving or knitting. They have randomly oriented fibres within the plane of geotextiles. Hence depending on each specific application, the most suitable type should be carefully selected. There are numerous successful projects carried out in coastal environment with both woven (Fowler and Trainer 1998, Lawson 2008) and nonwoven (Heerten et al. 2000, 2008, Jackson et al. 2006, Restall et al. 2004, Jackson and Corbett 2007, Saathof et al. 2007, Hornsey et at. 2011) geotextiles. Some of the properties and issues to be considered when selecting the most suitable material are summarised in Table 2-1. Generally standard test methods are used to evaluate the engineering properties of geotextiles in the laboratory. However, the measured (allowable) values determined must be adjusted when designing GSC-structures, to account for installation damages, long-term creep, chemical degradation, UV degradation, environmental degradation, etc. (Dassanayake and Oumeraci 2009a, Dassanayake et al. 2013).

As the engineering properties of both woven and nonwoven geotextiles may be appropriate or inappropriate for the GSC-structures, it is necessary to investigate both types of geotextile material in order to identify the most suitable material for GSC-structures. Therefore, the present research study did not favour a particular type of geotextile, instead, it equally considered both woven and nonwoven geotextiles.

Table 2-1: Engineering properties of geotextile materials related to coastal engineering applications

Property	Woven Geotextile	Nonwoven Geotextile
Material	Produced with high tensile yarns in orderly pattern	Produced as sheets of randomly orientated fibres
Tensile strength	High: • can be order of 200 kN/m (ASR 2005a) • can accommodate large stresses during installation & while in service without failure	Low: • can be order of 35 ~ 65 kN/m (ASR 2005a)
Elongation	Low: • cannot accommodate large strains without failure and reshaping is difficult • sand fill ratio of GSC will not change significantly due to elongation of the geotextile material during filling and installation operations or due to long term creep • Maximum elongations woven geotextile are in the order of 12% (PET) ~ 20% (PP).	High • can be in the order of 80% • high robustness during the installation (Lenze et al. 2002) • allows the GSCs to mould itself in with the existing features (Saathoff et al. 2007) • fill material will be distributed and induced local stress will be dissipated without failure • volume increase of the container will lead to low sand fill ratio • will creep over time and will thus fail to retain designated shape
Retention of fine material	Moderate • retention of fine material will be reduced with the uniaxial tensile strain • geotextile opening size (apparent opening size, AOS), which governs the size of the soil particles that can pass though the geotextile, will not significantly change	High • however, the tensile strain has more effect on relatively thinner materials, which increases geotextile opening size (apparent opening size, AOS), and decreases the fine retention capacity (Wu et al. 2008)
Friction	Low: • Relatively low angle of friction and may easily slide off • Interface friction angle = ca.13.33^0 (see Section 3.3.2)	High: • Relatively high angle of friction due to irregular structure • Interface friction angle = ca.22.64^0 (see Section 3.3.2)

2.2 Engineering Properties of GSCs

The closure of the estuary “Pluimpot”, The Netherlands in 1957 using sand filled Nylon bags is one of the first applications of GSCs in coastal engineering (Verhagen 2004, Bezuijen and Vastenburg 2008). Since then, various types and sizes of sand containers were used for coastal structures. Table 2-2 provides an overview of types of geotextile containments used in coastal engineering applications. Current research study focuses on geotextile containments those filled off-site and the term; “Geotextile Sand Containers” (GSCs) is used as a general term to describe them. The following sections describe the key engineering properties of

GSCs, which are related to hydraulic stability of GSC-structures, in detail. However, "Geotextile Tubes", which are hydraulically filled on-site and "Large Geotextile Containers", which are constructed and dumped using split bottom barges, will not be discussed in detail.

Table 2-2: Types of geotextile containments used in coastal engineering applications (modified from Oumeraci and Recio 2010)

Type	Volume [m3]	Sand Fill	Shape	Application
Geotextile Tubes	Generally >700 m^3	on site	cylindrical (D=1~55 m)	Geotextile Tubes are widely used in groins, containment dikes, dune reinforcements, etc. and as temporary structures
Large Geotextile Containers	Generally 100~700 m^3	split bottom barges	cylindrical/ pillow (D<5 m)	Large Geotextile Containers are used in reef structures (surf zone), defence structure against tsunami, etc.
GSCs or Geo-Bags	0.05~5.0 m^3	off site	pillow, box, mattress	as GSC units to build any type of coastal structures. also for scour protection and dune reinforcement.

2.2.1 Sand Fill Ratio

The sand fill ratio of geotextile containers has been identified for the first time by Venis (1968) as an important parameter for the hydraulic stability. Thereafter, many authors have highlighted the relevance of the sand fill ratio. Nevertheless, the optimum fill ratios for GSCs were more or less arbitrarily suggested (Delft Hydraulics 1975, Ray 1977, Oumeraci et al. 2002a, 2002b, 2003, Oumeraci et al. 2007a, Oumeraci and Recio 2010, Pilarczyk 2005, Recio 2007, Recio and Oumeraci 2008a, Recio and Oumeraci 2008b, Recio and Oumeraci 2009, Wilms et al. 2011, PIANC 2011, Hornsey et al. 2011, Corbella and Stretch 2012). Although the importance of the sand fill ratio was often highlighted, there are only very few publications available on the recommended sand fill ratio and most of them are limited to Geotextile Tubes or Large Geotextile Containers (e.g. Bezuijen et al. 2000). Moreover, most of the recent investigations were carried out with the sand fill ratio of 80% or "fill to capacity" (Coghlan et al. 2009, Hornsey et al. 2011). However, a systematic investigation of the influence of the sand fill ratio of GSCs on the hydraulic stability of GSC-structures is still lacking. Therefore, Oumeraci and Recio (2010) recommend to systematically investigate the influence of the sand fill ratio on the mechanisms responsible for the hydraulic failure of GSCs. The future research and design guidance/standards should be essentially directed towards an unambiguous and practical definition of the sand fill ratio as we all as towards the definition of an optimal sand fill ratio by accounting for the deformation properties of the geotextile and by balancing the advantages and drawbacks of high and moderate sand fill ratios (e.g. interface friction between GSCs).

a) Available definitions of the sand fill ratio

The sand fill ratio is defined as the ratio of the total available space within the geotextile container and the volume of the fill material. That is, an 80% fill ratio indicates that 80% of the geotextile container is filled with sand and 20% remains empty at its filling (vertical) position (Recio and Oumeraci 2008a). Even though this definition is apparently simple, calculation of the total available space within the geotextile is very complicated. Furthermore, the fill ratio

does not provide a clear description of the density of the sand. For example, when a GSC filled with dry sand is immersed in water, sand will be further compacted, and the new fill ratio will be less leaving more freedom for the internal movement of the sand. On the other hand, if the geotextile material undergoes elongation or relaxation over time, which then result in a smaller fill ratio too. Hence, the sand fill ratios of GSCs reported in the literature are often confusing (Bezuijen et al. 2004).

b) Factors influencing the sand fill ratio

The initial sand fill ratio of a GSC depends on: the properties of fill material (e.g. grain distribution, density, degree of saturation etc.), the method of filling / method of construction (e.g. hydraulic filling or dry filling) and the properties of geotextile material (e.g. elongation properties of geotextile). Even though, GSCs made of nonwoven geotextiles shows high robustness during installation (Lenze et al. 2002), it was found that the elongation of the geotextile adversely affects the sand fill ratio and hence, leads to other problems associated with the hydraulic stability. Meanwhile, there are no publications available to quantify the deformation of GSCs during the filling and handling process.

Furthermore, if a GSC is dropped from a certain height, the geotextile "skin" will be further elongated due to the impact of the GSC hitting the sea bottom. To date, no proper investigations have been carried out on the quantification of the deformations of GSCs during the different phases of construction. Sometimes, they are "filled to capacity" to compensate possible reduction in sand fill ratio during the construction and the installation processes.

c) Effect of the sand fill ratio on the hydraulic stability

Many authors (e.g. Venis 1968, Grüne et al. 2006, Recio and Oumeraci 2008b, Deltares 2008, Wilms et al. 2011, Hornsey et al. 2011) have mentioned the effect of the sand fill ratio on the stability of GSC-structures (Table 2-3). The results of these studies have proven that the sand fill ratio represents an important factor for the stability of GSC-structures. However, these results are not sufficient to understand the influence of the sand fill ratio on the hydraulic stability of GSC-structures. Therefore, optimum fill ratios were more or less arbitrarily suggested in the previous studies as aforementioned.

Table 2-3: Effect of the sand fill ratio on hydraulic stability of GSC-structures subject to severe wave attack (Grüne et al. 2006, Recio and Oumeraci 2008b, Deltares 2008, Wilms et al. 2011)

GSC property related to the hydraulic stability of GSC-structures	**Influence of the propriety on stability ["+" = favourable] ["-" = unfavourable]**	**Effect of the sand fill ratio**	
		low fill ratio	**high fill ratio**
flexibility: energy absorption	+	high	low
contact area: interface friction	+	high	low
stability of GSC (a group of GSCs) on sea bottom	+	low	high
internal stress in geotextile material: vulnerability to damage of GSCs	-	low	high
internal movement of sand: deformation	-	high	low
relative movement of geotextile or caterpillar mechanism (Deltares 2008)	-	high	low

In summary, despite of the sand fill ratio was identified as an important factor affecting the hydraulic stability of GSC-structures, not only systematic investigations of the relationship between the sand fill ratio and the hydraulic stability of GSC-structures are lacking, but also a proper definition of the sand fill ratio is not yet realised. In most of the projects, the sand fill ratio was determined rather on the basis of the construction methods than according to the hydraulic stability and the long-term durability.

2.2.2 Interface Friction Between GSCs

One of the most important parameters, which also contributes to the hydraulic stability of GSC-structures, is the interface friction. Not only during laboratory tests, but also in real life projects, "pullout" of GSCs (Figure 2-8) has been observed (Oumeraci et al. 2002b, Jackson et al. 2006). Recio (2007) attempted to experimentally and numerically investigate the process of pulling out of containers from a GSC-revetment due to wave attack and concluded that the interface friction between GSCs considerably affects the hydraulic stability of GSC-structures. Furthermore, the formulae suggested by Recio (2007) already account for the interface friction between GSCs. Moreover, Recio (2007) showed that even a small variation in the friction angle may induce completely different displacements of the GSCs by using the weakly coupled COBRAS/UDEC modelling system. When the interface friction angle is higher than a certain threshold limit, then a more or less gradual, but rather small movement towards the seaward direction was observed. However, the GSCs with smaller interface friction angles showed relatively large oscillatory movements with a clear resultant towards the seaward direction. Overall, the effect of interface friction properties is still not fully clarified or/and experimentally verified. Interface friction mainly depends on: the friction properties of geotextile material (both short term and long term), the contact area between two containers, the overlapping length (seaward slope), the sand fill ratio (shape of the GSCs), the type of fill material, etc.

Until recently the only available data to assess the friction between GSCs were obtained by means of laboratory tests. Conventionally, geotextile samples are tested in direct shear box apparatus (0.3 m × 0.3 m) to find their interface friction properties. However, Krahn et al. (2007) and Matsushima et al. (2008) showed that the estimation of interface friction between sand bags using the direct shear test results of geotextile materials are not accurate enough.

Krahn et al. (2007) tested interface shear strength of sand bags manufactured from woven geotextile and polyethylene sheets. In order to avoid the local distortions near the specimen edges, large scale direct shear test apparatus with a sheer box of 1 m × 1 m was used (Figure 2-1). This apparatus allowed tests to be carried out using large sand bag specimens and to minimize scale effects. The shear tests were carried out with different confining pressures (e.g. 25, 75 and 125 kPa) and typical results are shown in Figure 2-1. The most important finding of the research study by Krahn et al. (2007) is that the interface shear strength between filled sand bags is greater than that of the geotextile material alone. For example, the sand bags made of woven geotextile have been shown about 33% higher friction stiffness than that of the geotextile material.

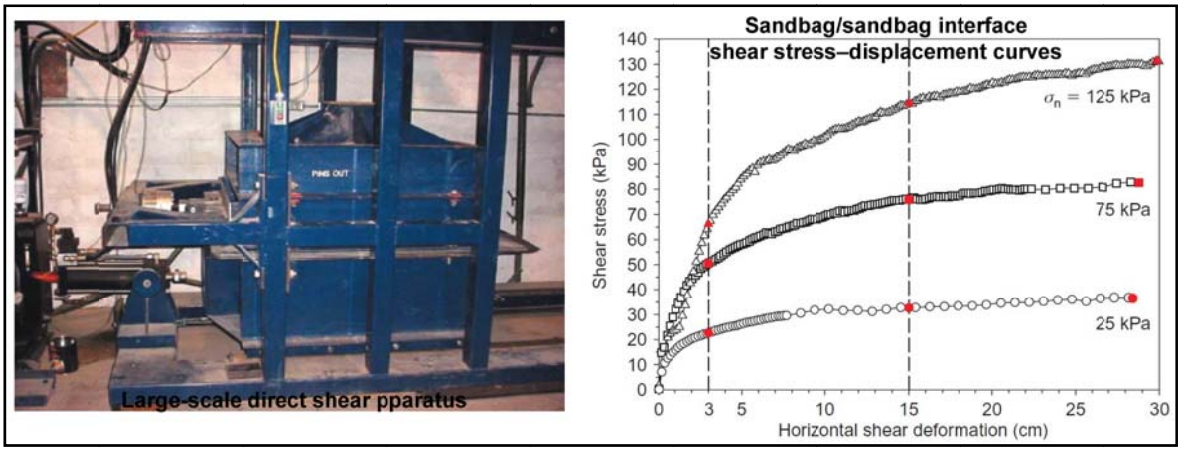

Figure 2-1: Large-scale direct shear apparatus and test result of sand bag-sand bag interface direct shear tests (Krahn et al. 2007)

Matsushima et al. (2008) carried out lateral shear tests on large scale soil bags stacked not only horizontally but also inclined. The objective of this study is to understand the anisotropic strength characteristics of stacked soil bags and to understand the differences in strength characteristics when stacked horizontally and inclined. A pile of three large scale soil bags were tested under different confining pressures (σ_v = 30kPa, 150kPa and 300kPa). When the soil bags were stacked inclined at an angle of 18^o to the loading direction, the lateral shear strength is approximately 2 times larger than that of horizontally placed soil bags. Results obtained by Matsushima et al. (2008) during their experimental investigation are promising and GSCs stacked inclined could be used for GSC-structures as well. When GSCs are placed inclined, they will have more friction force due to high resistance force and also due to larger overlapping length compared with the GSCs stacked horizontally. Furthermore, the container shape also contributes to the interface friction of GSCs. Jackson et al. (2006) mentioned that the higher fill ratios might lead to a smaller contact areas between GSCs thus result in relatively smaller resisting forces against the pullout.

2.2.3 Properties of Fill Material

One of the main concerns during the selection of the fill material for GSCs is the tendency of the fine grained particles to migrate (washout) during wave attack. Apart from the migration of fine particles, the properties of the fill material such as mean grain diameter, cohesion, degree of compaction, etc. will also affect the movement of material inside the container and hence the deformation of GSCs. Furthermore, the degree of compaction also depends on properties of fill material such as the moisture content, the grain size, and the grain size distribution. Granular material, such as sand will compact more or less immediately as the GSC is immersed in water, depending on the initial density, whereas a fill material with more fine particles and cohesive properties will take longer time to be fully compacted (or consolidated). In addition, the properties of the fill material influence the deformability of containers, when they are subject to confined loads. For example, Matsuoka et al. (2001) developed a stress strain relationship for woven sand bags including the properties of the fill material and the bag material.

2.2.4 Retention Properties of Geotextile

Most of the existing retention criteria consider only a unidirectional flow and valid only for elements not exposed to waves or not in the tidal range. However, a geotextile container, which is exposed to wave action and dynamic flow conditions, undergoes cyclic wetting and drying that creates oscillatory flow through geotextile and a stable soil structure (filter cake) may not develop under conditions of oscillatory flow (Giroud 1982). Hence, the pore size of the geotextile must be even smaller than that for unidirectional flow conditions. Ogink (1975) performed comparative experiments using several types of geotextile materials and with unidirectional (static) and bidirectional (dynamic) flow conditions. Based on the experimental results of nonwoven geotextile, Ogink (1975) recommends, (i) $O_{90}/D_{90} \geq 1$ for static flows and (ii) $O_{98}/D_{min} < 1$ for dynamic flows (where, O_{90} or O_{98} = characterise opening size which corresponds with the average sand diameter of the sand fraction of which 10% or 2% falls through the geotextile respectively and D_{90} or D_{min} = sand particle size correspond to, respectively 90% or 0% passing through the sieve). Moreover, some retention criteria under cyclic flow conditions are listed in Chen et al. (2008), but their applicability is yet to be verified. Furthermore, the cyclic deformation of containers (flapping) during the wave action will leads to different behaviours of fill material. Therefore, most of the recent studies, recommend to perform new experimental investigations instead of relying on existing retention criterion. Hence, a verified turbulence test should be used to assess the fines retention capability of the geotextile (Saathoff et al. 2007).

2.2.5 Deformability of Geotextile Sand Containers

Although the effect of the deformations of GSCs on the hydraulic stability is significant, until Recio (2007), no one has attempted to explain the hydraulic stability of coastal GSC-structures, taking into account the effect of the deformations and associated processes. The deformation of GSCs could be either as a result of the stresses from the neighbouring containers or as a result of the wave action or due to a combination of the both. Based on the experimental and numerical studies, Recio (2007) developed analytical stability formulae that account for the deformation of the individual GSCs.

The deformation of GSCs can be described as cyclic deformations (flapping during wave uprush and downrush) and progressive deformations (gradual enlargement of the seaward end due to the internal movement of sand). Due to soft, flexible nature of the GSC, cyclic deformation may occur during each wave cycle. This phenomenon has both positive and negative effects. Due to this cyclic deformation, GSC can dissipate more wave energy than a stiff block. On the other hand, this deformation adversely affects the force coefficients and reduces the resisting forces, thus increasing the mobilising forces. In addition, the cyclic deformation of GSCs will increase the washout of smaller particles during wave runup and rundown. Therefore, lower fill ratios intensify the migration of fine particles. In contrast, the deformation due to the internal movement of sand has only a negative effect on the stability of GSC-structure that increases the force coefficients of GSCs. The Internal movement of sand heavily depends on the fill ratio of the container (Recio and Oumeraci 2008b, Oumeraci and Recio 2010).

One of the factors governing the final geometry of the GSC is the properties of fill material. Matsuoka et al. (2001) performed unconfined and confined compression tests on sand containers. According to Matsuoka et al. (2001), sand bags have an "apparent cohesion" due to the effect of the geotextile material on the fill partials inside the container (Figure 2-2). Therefore, the stress-strain relationship of GSCs depends on the properties of both fill material and geotextile. Therefore, GSCs can be described as homogeneous blocks which have "average properties" (i.e. composite behaviour of the sand fill and the geotextile) of GSCs (e.g. "average" density, "average" bulk modulus and shear modulus, "apparent cohesion").

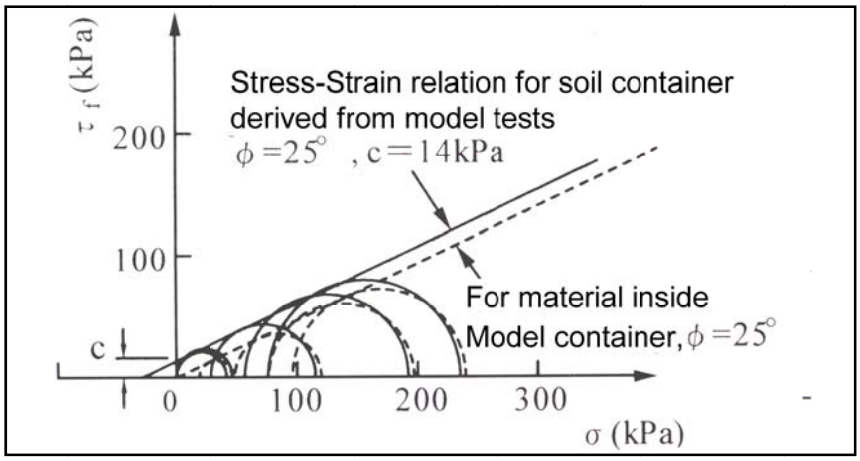

Figure 2-2: Results of biaxial compression test of soil containers (Matsuoka et al. 2001)

2.2.6 Discussion and Implications for the Present Study

Section 2.2 reviews the available knowledge on the properties of GSCs which may affect the hydraulic stability and points out the knowledge gaps and the implications for the present study. The most important engineering properties of GSCs affecting the stability, are the properties of geotextile material itself, the sand fill ratio, the type of fill material, the interface friction of GSCs, and the deformability of GSCs caused by the movement of sand inside the container. More importantly these properties are interrelated (Figure 2-3) and their influence on the hydraulic stability of GSC-structures is not yet fully understood.

Meanwhile, a more appropriate definition for the sand fill ratio of GSC should also be developed, as the applicability of the existing definitions for relatively smaller containers (GSCs) is questionable. The initial sand fill ratio, just after filling and the fill ratio just after installation of GSCs is different due to many factors such as the elongation of geotextile during the handling and the installation processes, the deformation of containers under the loads from neighbouring containers, the compaction of sand etc. Hence, the development of a clear and proper definition for the sand fill ratio is very challenging, but extremely important. Furthermore, Recio (2007) found out that the interface friction between GSCs considerably affects the hydraulic stability of GSC-Structures. A friction factor between containers (μ) is already included in the formulae of Recio (2007). However, the effect of interface friction properties is still not fully explained or experimentally verified.

Regarding the effect of deformation of GSCs on the stability of GSC-structures (Recio 2007), the factors responsible for the deformation are not yet adequately explained. A proper under-

standing of the effects of the above mentioned properties of GSCs on GSC deformations is essential for the further development of GSC technology. When studying the influence of these properties on stability of GSC-structures, attention should be paid to distinguish between the effects of each GSC property separately. On the other hand, a properly planned experiment can be used to study the effects of several properties on the hydraulic stability at the same time.

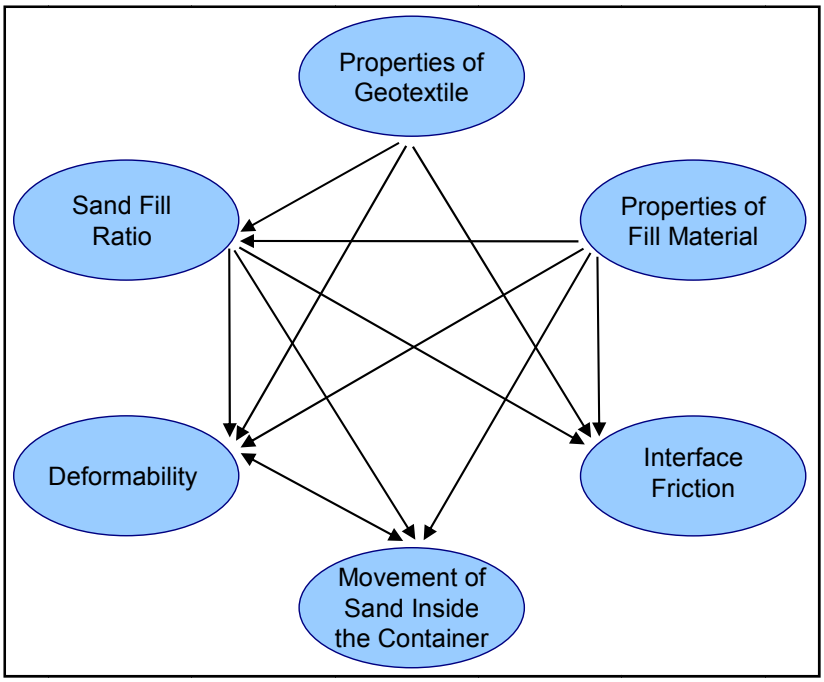

Figure 2-3: Interrelationship of properties of GSCs (Dassanayake and Oumeraci 2009b)

Table 2-4 summarises the conclusions drawn from the state of the art review on the properties of GSCs and identified the unsolved areas to be investigated. These unsolved issues should be systematically studied using both laboratory testing and numerical modelling.

Table 2-4: Conclusions drawn from the review of state of the art knowledge on properties of GSCs (modified from Dassanayake and Oumeraci 2009b)

Properties	Conclusions Drawn	Areas to be investigated
Properties of Geotextile	Elongation properties of geotextile influence the deformability of GSCs causing lower sand fill ratio and high AOS. However, due to 3D structure of thick nonwoven geotextiles, this effect is relatively low. Also, friction properties of geotextile influence the interface friction of GSCs.	• Influence of elongation properties of geotextile on deformation of GSC • Fine retention criteria of GSCs and its relation to properties of geotextile • Contribution of friction properties of geotextile to interface friction of GSCs
Properties of Fill Material	Properties of fill material are determinant for the migration of sand, the sand fill ratio, the deformability of container, the movement of sand inside the container, and the interface friction of GSCs	• Influence of properties of fill material on deformability and internal movement of sand of GSC • Influence of properties of fill material on migration of fine particles of a GSC subject to wave attack • Influence of fill material on stability of GSC-structures

Sand Fill Ratio	Identified as an important factor contributing to hydraulic stability. The sand fill ratio affects the deformability of container, the internal movement of sand, and the interface friction.	• Proper definition of the sand fill ratio • Influence of the sand fill ratio on stability of GSC-structures • Optimum fill ratio for different GSC applications • Methodology to incorporate the sand fill ratio in numerical modelling of GSCs
Deformability of GSCs	Deformability of GSCs depends on the elongation characteristics of geotextile material, the sand fill ratio, the properties of the fill material, the internal movement of sand and the stresses acting on GSCs	• Influence of these properties on the deformation of GSCs and ultimately on the hydraulic stability of GSC-structures
Interface Friction	Interface friction strongly affect the stability of GSCs. Interface friction depends on the type of geotextile material, the type of the fill material, the overlapping length and the sand fill ratio (shape of the GSCs).	• Influence of interface friction of GSCs on the hydraulic stability of GSC-structures • Relationship between direct shear test results of geotextile material and friction properties of GSCs
Movement of Sand inside the Container	Movement of the sand influences the deformation. It depends on the properties of the fill material, the sand fill ratio and the deformability of containers	• Influence of properties of the fill material and the sand fill ratio on the movement of particle inside the container and on the hydraulic stability of GSC-structures

2.3 Processes Affecting the Hydraulic Stability of GSCs

The analysis of the current knowledge about the hydraulic processes relevant for the hydraulic stability of GSC-structures is essential to achieve the objectives addressed under the section 1.2. The most important processes affecting the hydraulic stability of GSCs were identified as the wave reflection, the wave overtopping, the wave runup, the wave uprush and downrush, the permeability of the GSC-structure and the deformation of the constitutive GSCs. These engineering properties of GSCs, as addressed in section 2.2, influence most of the processes at different scales. The key findings related to the processes affecting the hydraulic stability of GSC-structures are given in Dassanayake and Oumeraci (2009a). Unlike parametric investigations, there is limited information regarding the hydraulic processes associated with the hydraulic stability of GSC-structures. Therefore, Recio (2007), reviewed present stage of the knowledge related to stone revetments since some of the processes are similar. Afterwards, an extensive series of experimental and numerical studies were carried out covering most of these processes and mechanisms. The results are reported in Oumeraci and Recio (2010) and Recio (2007). Apart from that, only Oumeraci et al. (2002a, 2002b, 2003, 2007) performed process oriented investigations on the stability of GSC-structures. However, most of the research studies were limited to horizontally placed, and 80% filled nonwoven GSCs. Therefore, a detailed investigation is required to broaden the knowledge on the hydraulic processes of GSC-structures while varying the key engineering properties. This section provides an overview of only three crucial processes. Further details on the other processes affecting the hydraulic stability of GSCs can be found in Dassanayake and Oumeraci (2009a).

2.3.1 Wave Uprush and Downrush and Forces Acting on GSCs

During his series of experimental investigations, Recio (2007) measured the wave induced pressure around GSCs during wave uprush and downrush using an instrumented GSC (Figure 2-4 and Figure 4-9). By integrating the pressure measurements around the GSC, the total wave-induced forces and moments were derived (Figure 4-10). The detailed analysis of the wave-induced loads on GSC-structures can be found in Recio and Oumeraci (2006b). Afterwards, COBRAS model was calibrated and validated using the date from the instrumented GSCs. Later, using the validated model, the wave-induced forces on each container were investigated to provide a further insight into the interaction between the wave loading of neighbouring containers. A detailed description of this approach and the shortcomings are discussed in section 4.4.

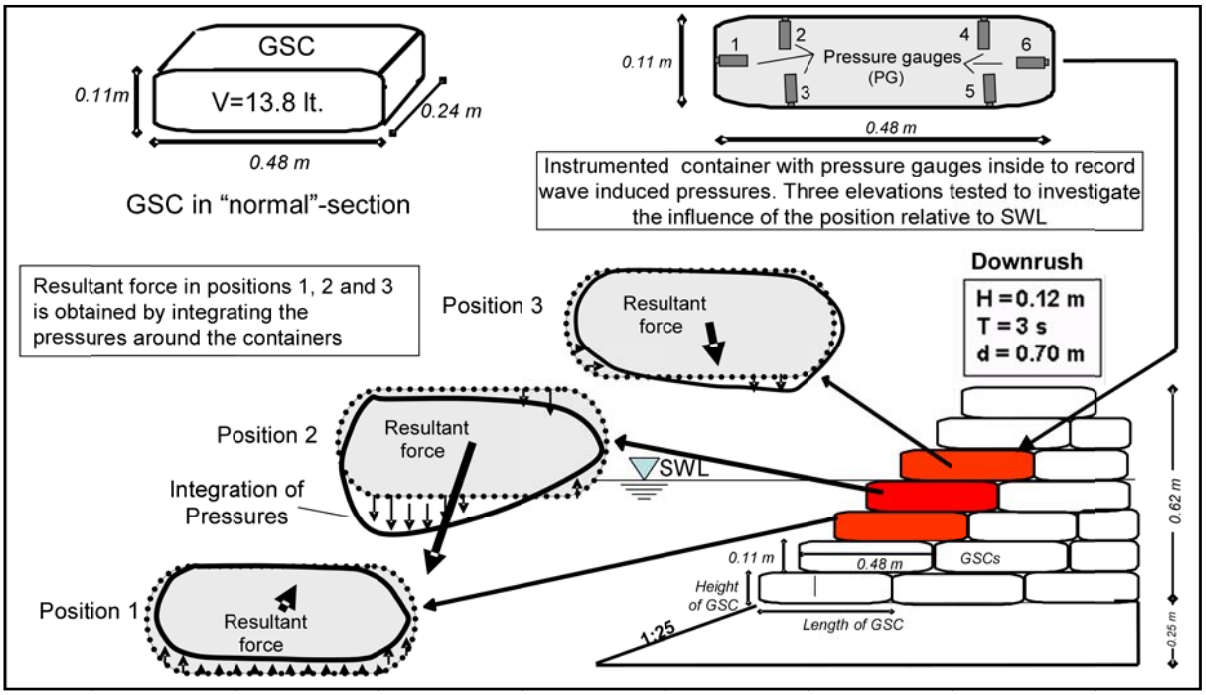

Figure 2-4: Wave induced load on instrumented sand container during wave downrush (Recio 2007)

2.3.2 Permeability of GSC-Structures

In general, the hydraulic permeability of the structure influences the hydraulic stability (Hendar 1960, Hudson 1956 and 1961, Pilarczyk 1998, Van der Meer 1998, etc.). The more permeable the structure, the more water can penetrate into the structure during wave runup and the smaller the forces on armour units will be, both during the wave runup and rundown phases. Higher permeability reduces the seepage forces and pressure "build-up" in the structure. Permeability also strongly affects the wave transmission and other processes associated with wave-structure interaction (Chao-Lung et al. 2004, Muttray and Oumeraci 2002). Hence, larger permeability will provide a more stable structure.

The flow through a GSC-structure is not homogeneous. A laminar flow is expected through the sand fill of GSCs while the flow through the gaps between containers is expected to be turbulent. Despite the in-homogeneity of the flow and its unsteadiness, the permeability of

GSC-structures will preferably be described by the Darcy permeability coefficient *k* (Recio 2007).

The first permeability analysis was conducted by Oumeraci et al. (2002b). The large scale model results by Oumeraci et al. (2002b) showed a permeability around $k = 2 \times 10^{-2}$ m/s for the cover layer made of 0.150 m^3 sand containers while the sand used in the tests inside the GSC had a permeability coefficient of $k = 1.6 \times 10^{-4}$ m/s. Then, it was concluded that the permeability of a GSC-structure is eventually governed by the gaps between the GSCs. Recio's (2007) small scale experimental investigations confirmed this finding. Apart from confirming that the size of the gaps governs the overall permeability of the GSC-structure, the other main conclusions, from that experimental study were;

(i) the smaller the container, the smaller the permeability coefficient of the structure and may vary from 8×10^{-3} m/s (medium containers) to 1.5×10^{-2} m/s (large containers)
(ii) longitudinal or transversal GSC arrangement will result in similar permeability.

However, as shown in Table 2-5, there is a significant variation in the permeability measurements (e.g. Permeability of a single column of large GSCs (vol. *13.8 l*) is lower than a complete structure with small GSCs (vol. *1.7 l*). Therefore, a different approach is necessary for the permeability tests, if it is necessary to find out the influence of the sand fill ratio or type of geotextile material on the hydraulic permeability.

Table 2-5: Comparison of permeability coefficients with different GSC sizes and different mode of placement (Recio and Oumeraci 2008a)

Cross section	Size of GSCs	Permeability K [m/s]	Remarks
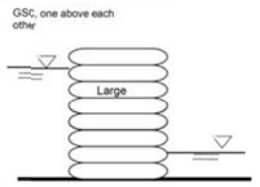	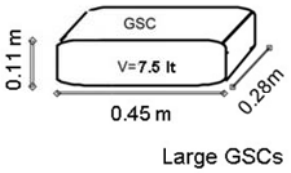	1.5×10^{-2}	Single column of GSCs, GSC volume: 13.8 l
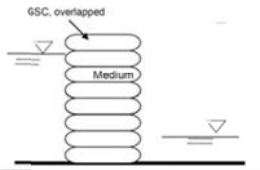	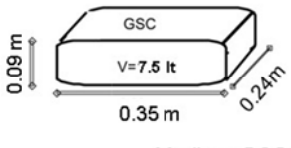	0.8×10^{-2}	Single column of GSCs, GSC volume: 7.5 l
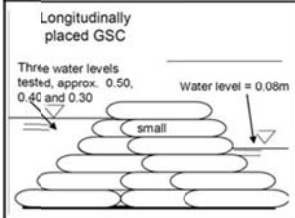	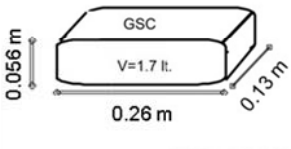	2.2×10^{-2}	Low crested GSC structure with 1:1 slope. Despite of the large width of the structure, permeability is higher than larger containers GSC volume: 1.7 l
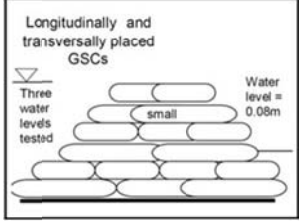	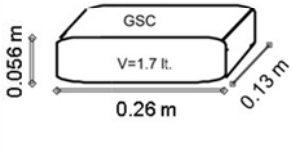	1.2×10^{-2}	Low crested GSC structure with 1:1 slope. Interlaid GSC-structure showed a relatively lower permeability but still higher than that of the 7.5 l

2.3.3 Cyclic Deformations of GSC

The deformation of sand containers represents is the most important mechanism that makes the GSC-structures unique as compared to other (hard) coastal structures. The deformation of GSCs can be divided as cyclic deformation (flapping during wave uprush and downrush) and progressive deformation (gradual enlargement of seaward end due to internal movement of sand). Recio (2007) followed two steps during the development of his hydraulic stability formulae. During the first step, no account is made for the effect of the cyclic deformation on the stability of GSCs. Then, drag (C_D), inertia (C_M) and lift (C_L) coefficient were determined for the rigid GSCs based on experimental investigations. During the second step, corrective factors were introduced to account for the cyclic deformation effects. Figure 2-5 shows an example calculation with all the available formulae for stability of GSC-structures (see Figure 5-1) including equations developed by Recio (2007). As shown in Figure 2-5, the formulae that account for cyclic deformation give the lowest stability and hence need the largest sand container for a given wave condition. Furthermore, the effect of cyclic deformation on the hydraulic stability of GSC-structure is more relevant for crest GSCs. Later, the formulae extended to five different applications of GSCs. However, only two failure mechanisms, sliding and overturning were considered. Also, the effect of cyclic deformation of GSCs on the hydraulic stability for each of these applications was considered equally, but not sufficiently verified.

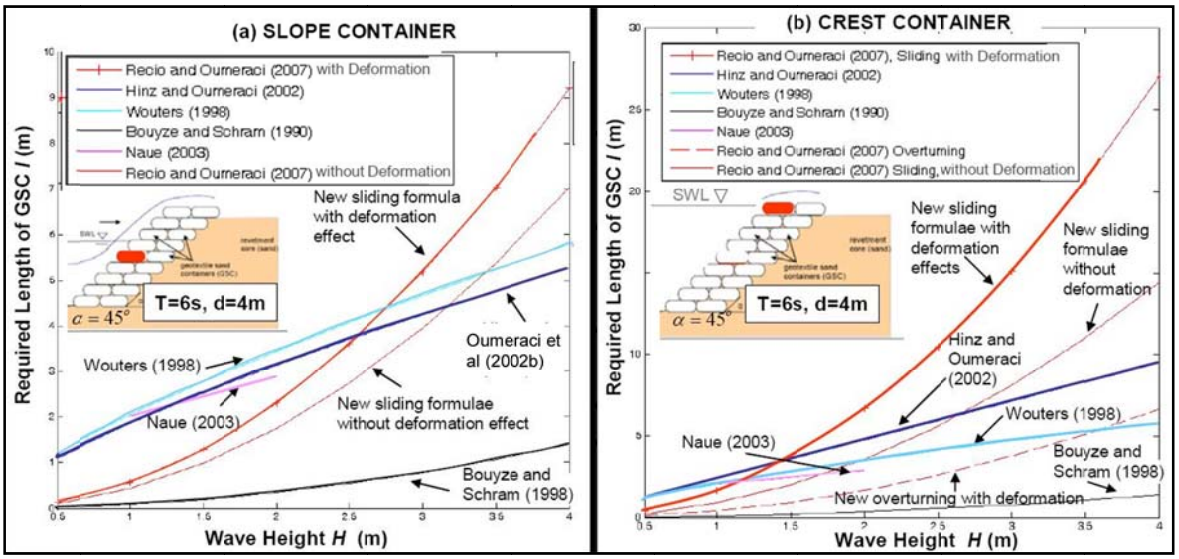

Figure 2-5: Comparison between available stability formulae with and without deformation effects (modified from Recio 2007)

2.3.4 Discussion and Implications for the Present Study

Only very few of process-oriented investigations have been performed on the stability of GSC-structures. Most of the research studies were limited to revetments with 1:1 seaward slope, horizontal placement, and 80% fill ratio. Therefore, more detailed investigations are required to broaden the knowledge on hydraulic processes of GSC-structures while varying the engineering properties of GSCs, the geometry of the GSCs, the geometry of the entire GSC-structure and the submergence depth.

The overall permeability of the GSC-structure is governed by the size of the gaps between containers (Recio 2007, Werth et al. 2008). The different fill ratios might result in different gap sizes and consequently will have different permeabilities. A smaller fill ratio more likely to result in smaller gaps. Apart from that, the different fill materials and the different types of geotextiles might also influence the permeability of GSCs.

The deformation of GSCs depends on many parameters, partially, the sand fill ratio and the properties of geotextile material. Therefore, a new series of experiments need to be performed to identify the deformation of GSC during each of the applications and the significance of the influencing factors on the deformation for each application. Hydraulic stability Formulae developed by Recio (2007) considered only the stability of the GSCs against two failure modes, sliding and overturning. Five different applications of GSC were identified. The effect of deformation of GSCs on the hydraulic stability for each of these applications was however, treated equally and yet to be verified. Therefore, formulae that are not limited to specific geometrical conditions and a sand fill ratio are still to be developed

In summary, most of the important engineering properties of GSCs influence the different processes affecting the hydraulic stability of GSC-structures. Therefore, future experimental and numerical investigations should be carried out only with a sound understanding of all the processes and the failure modes involved.

2.4 Failure Mechanisms of GSC-Structures

Due to the flexibility and low specific gravity of GSCs as compared to rock or concrete armour units, they behave differently and the established design formulae for rock or concrete units are not applicable. Furthermore, the stability of GSC is more complex and GSC-structures show a number of particular failure modes (Jackson et al. 2006). Figure 2-6 shows many of the different potential failure modes (After, Jackson et al. 2006, Deltares 2008, Lawson 2008, Oumeraci and Recio 2010). Most of these failure modes are influenced by the engineering properties of GSCs such as the sand fill ratio, the type of geotextile, etc. and some of them are already mentioned in section 2.3. A sound understanding of the potential failure modes of GSC-structures are required for the development of computational models for the stability of GSC-structures. This section describes the failure mechanisms of GSC-structures related to the hydraulic stability.

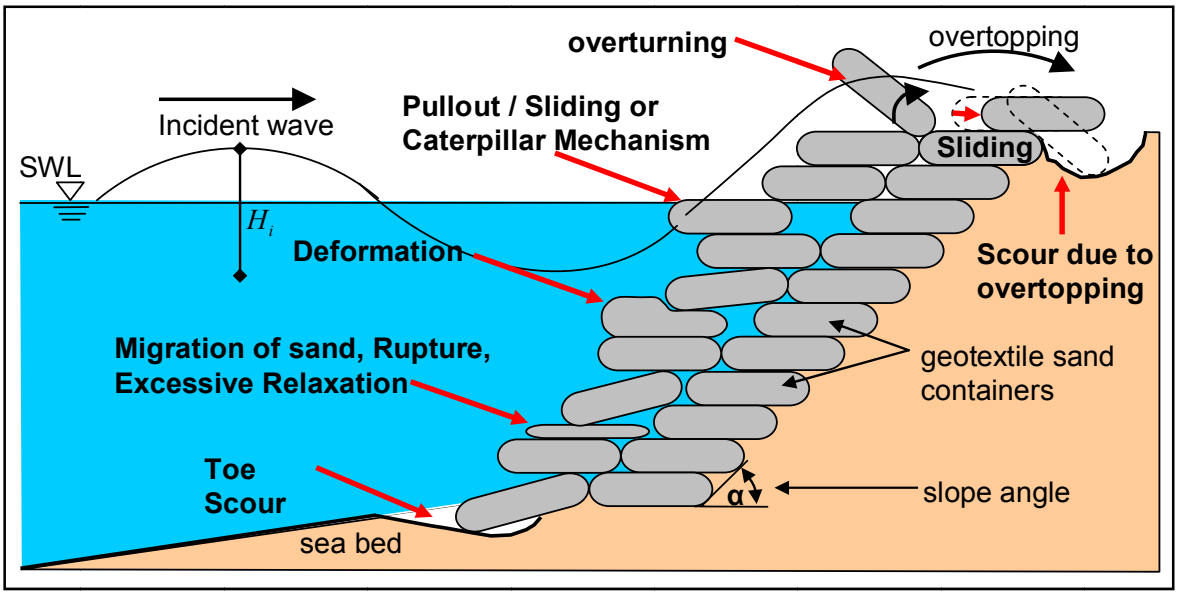

Figure 2-6: Potential failure modes of a GSC-revetment (Jackson 2006, Recio 2007, Deltares 2008, Lawson 2008, Oumeraci and Recio 2010, Dassanayake and Oumeraci 2009)

2.4.1 Failure due to Progressive Deformation

The progressive deformation (gradual enlargement of seaward end) of the GSC is caused by the internal movement of sand (Recio and Oumeraci 2008a, 2008b, Oumeraci and Recio 2010). Recio (2007) conducted an experimental investigation of the internal movement of sand using a transparent permeable container filled with coloured sand (Figure 2-7). Based on the video record analysis of the permeable transparent container with coloured sand subject to wave attack, the following observations were made. When a GSC structures subject to severe wave attack, wave uprush induced a rotational sand movement directed upward and wave downrush induced seaward movement of sand. After few cycles, the container deforms as the sand accumulates at the seaward end of the container. This behaviour reduces the contact area with the neighbouring containers. According to Recio (2007), unless the container further horizontally moves triggering the internal movement of sand, condition should prevails. However, forward movement will ease as a result of smaller contact areas with the neighbouring containers. Then the whole process of sand movement will repeat and GSCs will progressively deform. Furthermore, when compared with a normal container, a deformed container has less resisting forces and larger mobilizing forces induced by wave attack. If these processes continue, then the GSC will gradually move in the seaward direction and finally, it will be pulled out from the structure. Corbella and Stretch (2012) provided field evidence to validate these processes, which were originally explained by Recio (2007). In addition, the large scale experiments by Deltares (2008) also confirmed the movement of sand inside GSCs.

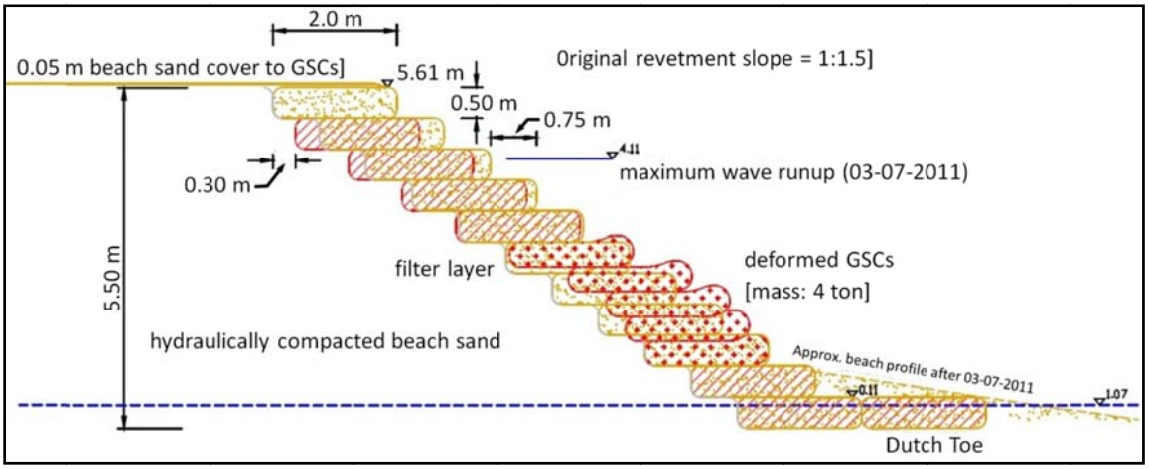

Figure 2-7: A cross-sectional drawing of a GSC-revetment in South Africa, which shows both the as-built structure and the progressive deformation and the motion in the seaward direction after a cyclone (Corbella and Stretch, 2012)

2.4.2 Failure due to Pulling Out

Jackson et al. (2006) describes the pullout of GSCs from revetment and the following influence factors were identified (see Figure 2-9). Even though Jackson et al. (2006) discussed about the failure modes of GSC-structures, they address neither the deformation of container nor the internal movement of sand (Figure 2-8). As mentioned in section 2.4.1, Recio (2007) explains the process behind the pullout of GSC and he termed this failure mechanism as "progressive sliding" towards the seaward direction.

(a). pullout of prototype 0.75 m³ GSCs from a temporary revetment in Maroochy, Australia (Jackson et a. 2006)

(b). pullout of model 0.025 m³ GSCs during wave flume tests at GWK, Germany (Oumeraci et al. 2002b)

Figure 2-8: Pullout of GSCs due to wave attack

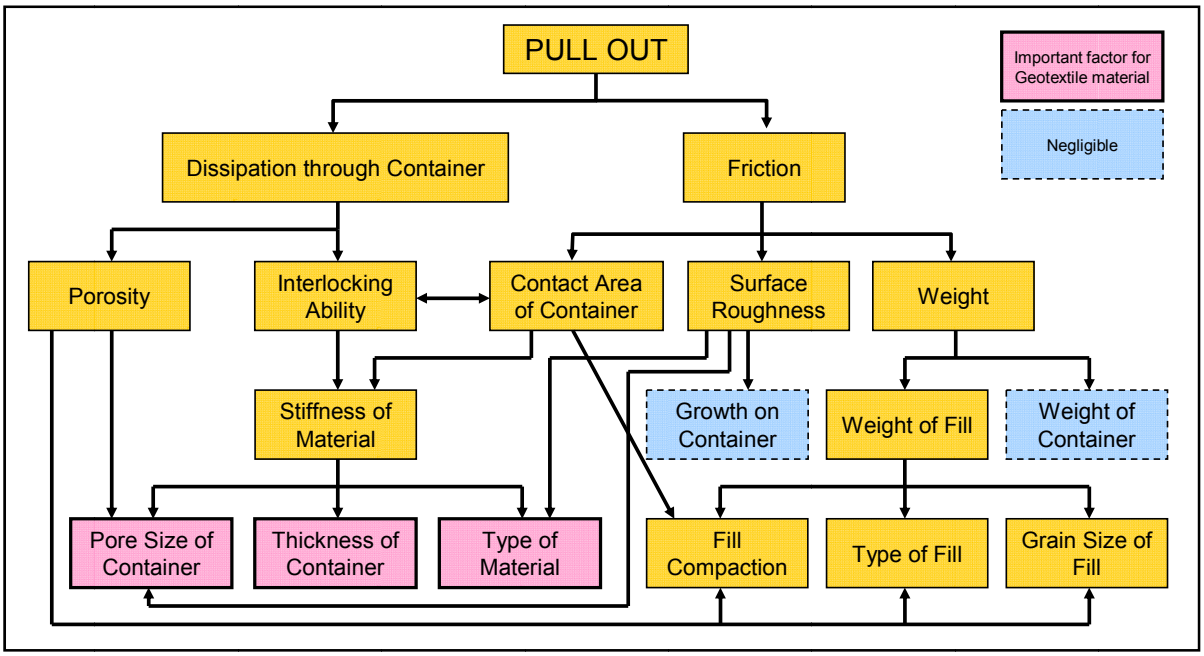

Figure 2-9: Factors influencing pullout of GSCs (modified from Jackson et al. 2006)

2.4.3 Failure due to Cyclic Deformations and Sliding of GSCs

One of the most common hydraulic failure modes of GSC is sliding. GSCs could progressively slide either towards the seaward direction (GSCs at the slope or at the crest) or towards the landward direction (only GSCs at the crest). During the wave runup, uprushing water uplifts the front part of the container and local vortices occur between the containers. As a result of the uplift, the effective contact areas between GSCs and thus the stabilizing forces are reduced. During the downrush, the uplifted part of the container moves again downward. However, the effective contact area further reduces due to the uplift deformations and internal movement of sand (Recio 2007). He suggested corrective factors for his sliding formulae to take the effect of deformation into account. Figure 2-5 provides an impression of effect of cyclic deformation on sliding failure mechanism for slope and crest containers (see Figure 5-1 and Figure 5-9).

The deformation of GSCs changes the location of centre of gravity and hence, increase the moment due to drag force and inertia force. As projected area reduces, moment due lift force will also be reduced. Meanwhile, there will be an additional vertical force component, due to the pressure exerted on the deformed section of the GSC. However, it is not clear whether this vertical force component was considered during the derivation of Recio's formulae (Dassanayake and Oumeraci 2009a)

2.4.4 Failure due to Overturning of GSCs

Generally, GSCs at the crest of the GSC-structure are more vulnerable for both sliding and overturning failures (Figure 2-10). Therefore, the crest containers are considered as the critical elements of low-crested GSC-structures (Oumeraci et al. 2002b and Oumeraci et al. 2003). Given the same incident wave conditions, the required weight of a crest container might be up

to 8 times larger than the required weight of a slope container. Not only the crest containers, but also the slope containers can overturn during extremely high wave conditions, which exert much higher destabilising forces on a GSC than the resisting forces (Recio 2007).

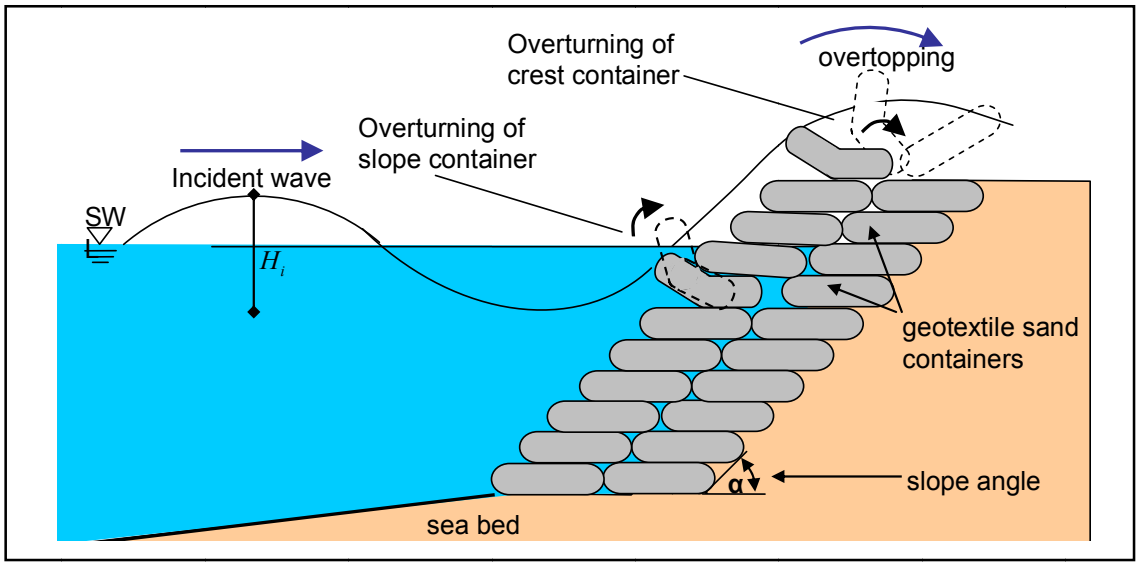

Figure 2-10: Cyclic deformation (flapping) and overturning of slope and crest GSCs

According to Recio (2007), the cyclic deformation (flapping) of GSC affects more adversely in the sliding than the overturning failure mechanism. The resisting moments against overturning will be 8% lower for a deformed container whereas the resisting forces against sliding will be 30% lower, when compared with a non-deformed container. This might also be due to the underestimation of additional moments due to forces acting on the deformed section of the GSC. However, the final results still show a considerable difference in terms of the required length of GSCs against overturning (Figure 2-11).

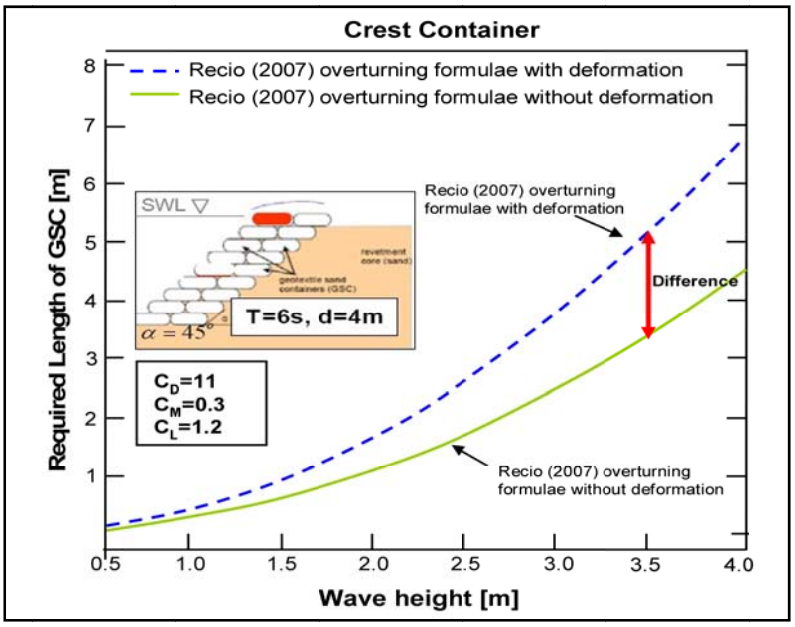

Figure 2-11: Comparison between Recio's overturning formula for the crest GSCs with and without deformation effect (Recio 2007)

2.4.5 Discussion and Implications for the Present Study

The knowledge of potential failure modes of GSC-structures is required for the development of new hydraulic stability formulae for the stability of GSC-structures. Recio (2007) provides a comprehensive description about the deformation of GSCs and resulting failure modes: sliding and overturning. Jackson et al. (2006) and Corbella and Stretch (2012) mentioned the pullout of GSCs, which is more likely to occur as explained by Recio (2007). Furthermore, Oumeraci et al. (2003) also identified sliding and overturning as two main modes of failure.

In addition to the failure mechanisms discussed above, Lawson (2008) and Deltares (2008) highlighted the problem of migration of fine particles (washout) from GSCs exposed to direct wave attack, but still there is no proper investigation on this issue. Also, scour at the toe is also important and more studies should be carried out to understand wave reflection from GSC-structures.

Most of the failure modes identified so far are influenced by the sand fill ratio, the type of fill material and the interface friction. Therefore, systematic investigations are required to properly understand the influence of the aforementioned factors on the hydraulic stability and to quantify the influence of each of these factors. Once this knowledge is gained, it is possible to develop simplified formulae and/or a computational tool for the hydraulic stability of GSCs.

2.5 Numerical Modelling of GSC-Structures

Empirical formulae developed based on scaled physical models showed several restrictions (e.g. relatively narrow range of applicability, difficulty to reproduce some of the important factors relative to hydraulic stability, such as friction between elements, flow in the porous structures, etc.). Hence, the simulation of wave-structure interactions using numerical models has been rapidly developing during last few decades. In order to simulate all the processes related to the hydraulic stability of GSC-structures, a fully coupled **C**omputational **F**luid **D**ynamic model (CFD) and a **C**omputational **S**tructural **D**ynamic Model (CSD) are required. Even though some research studies on combined CFD-CSD modelling have been conducted recently (Latham et al. 2008, Greben et al. 2008, Mindel 2008, Latham et al. 2009, Xiang et al. 2012) on the wave-structure interactions, most of these studies are still limited to stiff elements such as rocks or concrete armour units. However, due to the flexible nature of GSCs, these models cannot be directly applied to GSC-structures. Recio (2007) illustrated the possibilities to numerically simulate the hydraulic stability of GSC-structures considering their flexibility. He used a weakly coupled CFD and CSD model, which resulted in reasonably accurate results. Section 4.4 discusses the limitations of this modelling system in detail.

2.5.1 Computational Fluid Dynamic (CFD) Model

Several approaches have been followed to study the wave hydrodynamics around coastal structures. Among existing approaches, models based on Navier-Stokes equations have been incorporated in the last two decade to study the wave-structure interaction problems. The number of simplifying assumptions assumed in these model, is lower than in other approach-

es. Therefore, the ability of these models to deal with flows around complicated geometries and to provide detailed information on the velocity and pressure field are higher than other models (Lara et al. 2010b).

Recio (2007) showed that COBRAS (**Co**rnel **Br**eaking Wave **a**nd **S**tructures); a two dimensional RANS-VOF (**R**eynolds **A**verage **N**avier **S**tocks equation and the **V**olume of **F**luid concept) model is capable of simulating the wave-induced forces on GSCs. This numerical code has been developed by the research team of Professor Dr. Philip L.F. Liu in Cornell University, USA (Lin and Liu 1998, Liu 2004, Liu and Lin 1997, Liu and Lin 2002, Liu et al. 1999). Recently, the research group of Prof. Inigo Losada (Losada et al. 2005, Losada et al. 2008), modified the COBRAS code from Cornel University and introduced a new version with more simplified input options, which is called COBRAS-UC. The new version provides a complete description of the flux around rubble-mound breakwaters, being its only limitation is its 2D character (Sierra et. al. 2010). Both, COBRAS and COBRAS-UC have been used and validated by many researchers and their findings are reported in several publications, which describe different applications of these models. Garcia et al. (2004a, 2004b), Recio (2007) and Lara et al. (2006) successfully used COBRAS and COBRAS-UC codes to perform 2D numerical analysis of wave-structure interaction with low-crested and submerged permeable structures under regular waves. Hence, these codes can be successfully used to model wave-structure interaction of GSC-structures.

2.5.2 Structural Dynamic Models (CSD)

A GSC-structure is made of several flexible discontinuous elements. According to Itasca (2011), a numerical model must represent two mechanical behaviours: behaviour of the discontinuities (i.e. discontinuities between GSCs) and behaviour of solids (i.e. individual GSCs). Different approaches are available to model a discontinuous system. However, most of these approaches are capable of modelling deformable bodies (or elements), only few are capable of modelling deformable contacts. As deformable contacts are one of the key features in modelling of GSC-structures, it is easy to identify the most suitable method to numerically simulate GSCs.

The **U**niversal **D**istinct **E**lement **C**ode (UDEC) is a two-dimensional numerical code, which is based on of the distinct element method. This commercially available code combines both finite and discrete element methods for deformations and discontinum modelling. The stability of GSC-structure has been studied with the UDEC software (Recio 2007). UDEC can simulate the response of discontinuous media subject to either static or dynamic loading. The discontinuous medium is represented as an assemblage of discrete blocks or elements (FEM in UDEC).

2.5.3 Partially Coupled COBRAS/UDEC Model System (Recio 2007)

Basically there are two methods to couple the CFD and CSD: (i) One way coupling; where, the fluid flow exerts forces on the discrete elements and interactions of discrete elements are modelled by DEM and (ii) Two way coupling: where, in addition to the one way coupling, the

solid particle interactions are modelled by DEM that are in turn coupled to the fluid forces as they move and affect the fluid flow (Latham et al. 2008). The extent of the coupling also differs from one to another. In most of the cases, two independent codes are coupled with a "Connecting file". Two codes are running independently while sharing the information. This method is referred to as "weakly coupling", "partial coupling" (Recio 2007, Oumeraci and Recio 2010) or "loosely-coupling" (Wang and Lin 2008).

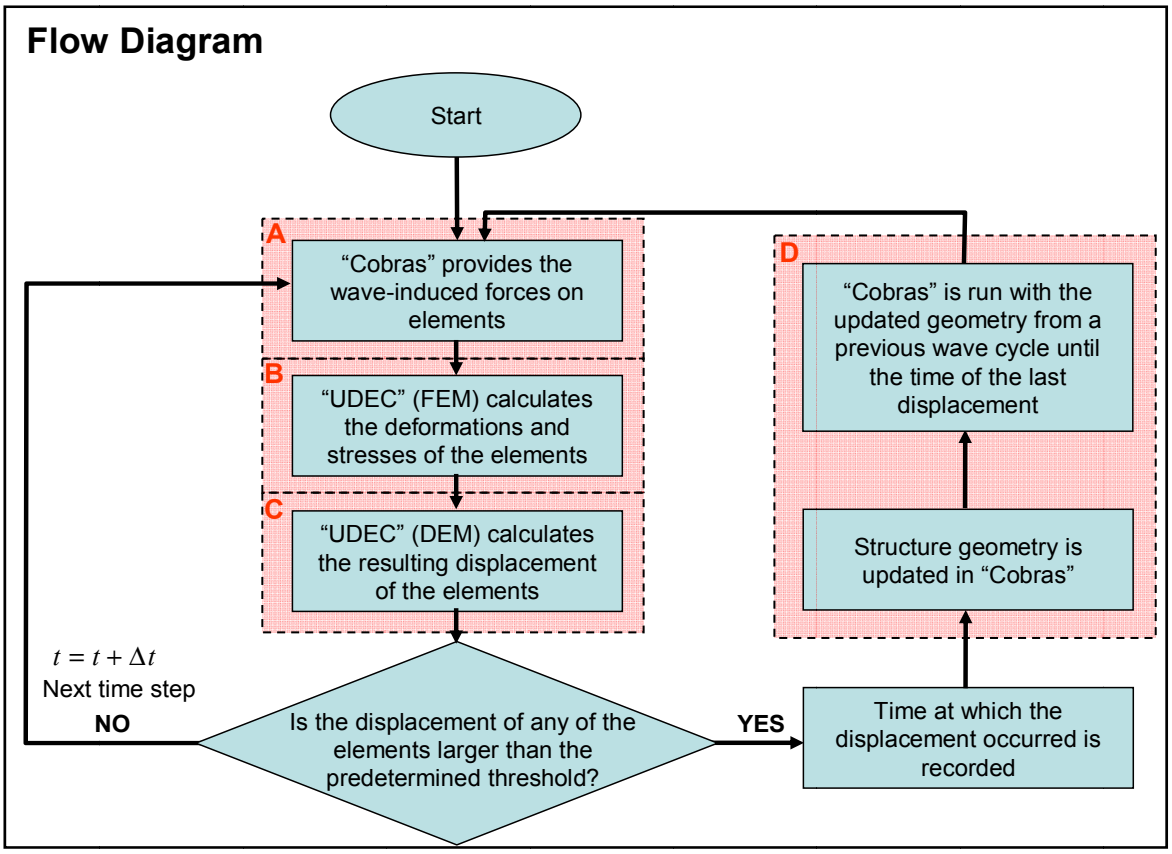

Figure 2-12: Numerical modelling concept followed by Recio (2007)

COBRAS/UDEC model system used by Recio (2007) is a weakly coupled system to model the hydraulic stability of GSC-structures. The modelling concept followed by Recio (2007) is shown in Figure 2-12. In this modelling system, the COBRAS and the UDEC are running independently while sharing the output information (see Figure 2-12). A similar method was used to solve many other fluid-deformable structure interaction problems in different disciplines (e.g. Wand and Lin 2008). This weakly coupled model system contains some crucial limitations in modelling following cases, (i) detached element is "floating" away from the structure (ii) displacement of several elements occur simultaneously and (iii) deformations during a time step are large enough to affect considerably and immediately the boundary conditions of neighbouring elements. Based on the knowledge obtained from various model tests and analysis of GSC-structures, the COBRAS code and UDEC were adapted to accurately represent the hydraulic process responsible for the instability of GSC-revetments. Similar Technique has been used by Greben et al. (2008) and Grobler et al. (2010). Detailed description of Recio's model and validation is given in section 4.4 and in Dassanayake and Oumeraci (2012f).

2.5.4 Discussion and Implications for the Present Study

Since the experimental investigations always involve, not only various expensive technical resources but also a lot of expensive consumables, the numerical modelling is considered as a cost effective technique. Furthermore, once a calibrated numerical model is established, a range of scenarios may be investigated with relatively little effort.

In spite of the limitations, COBRAS/UDEC is the most reasonable modelling system for GSC-structures up to date. Capabilities and limitations of this CFD-CSD codes for modelling of GSC-structures were documented by Recio (2007) and Dassanayake and Oumeraci (2012f). COBRAS/UDEC modelling system was initially developed to model the GSC-revetments and later applied for selected low-crested structures. Therefore, COBRAS/UDEC modelling system can be successfully used for the modelling of submerged GSC-structures.

Recio (2007) simulated the hydraulic stability of GSCs with different interface friction properties and found the significance of interface friction. However, the results are not yet experimentally verified. By simulating pullout tests and comparing with experimental results, the interface friction properties of the numerical models can be validated up to a certain extent.

Working with a 2D model is much simpler and required less computational power. Furthermore, Recio (2007) reasonably simplified the 3D problem of the hydraulic stability of GSCs into a 2D problem. The results from the weakly coupled modelling system were reasonably accurate, when compared with the experimental results from Oumeraci et al. (2002a). Therefore, the current research will focus on adopting the COBRAS/UDEC modelling system of Recio, to model the hydraulic stability of submerged GSC-Structures. This modelling system will be further verified and corrected based on the results of the proposed experimental investigations.

2.6 Physical Modelling of GSC-Structures

Starting from the works of Venis (1968), several model tests related to the hydraulic stability of GSC-structures were conducted worldwide. The results of a comparative analysis of the previous hydraulic model tests are outlined in this section.

2.6.1 Scale Modelling of GSC

Detailed information of the laboratory tests on the hydraulic stability of GSC-structures performed by Hudson (1956), Venis (1968), Porraz et al. (1979), Ray (1977), Kübler (2002), Tekmarine (1982), Jacobs and Kobayashi (1983 and 1985), Bouyze and Schram (1990), Pilarczyk (2000), Oumeraci et al. (2002b, 2002c, 2007), US-CEM (2004), Recio (2007), Recio and Oumeraci (2007d, 2008a, 2008b,2009), Mori et al. (2008), Mori (2009), Coghlan et al. (2009), Oumeraci and Recio (2010), Deltares 2010 and Wilms et al. (2011) are summarised in Figure 2-13. The cross sections of the model structures investigated are comparatively shown in the figure. Table 2-7 provides more detailed information and the contributions of them for the advancement of the knowledge on the hydraulic stability of GSC-structures.

One of the main challenges in modelling GSC is to accurately reproduce the properties of geotextile in small scale. The similitude conditions do not allow the use of identical geotextile material in prototype and small scale model. However, it is impossible to satisfy all the scaling rules simultaneously. Therefore, depending on the purpose of the experiment, a practical strategy to scale down the properties of geotextile should be defined. Table 2-6 shows interrelationship of properties of geotextile material and other engineering properties of GSCs.

Table 2-6: Relationship between engineering properties of GSCs and the properties of fill material of GSCs.

	Properties of GSCs			
	Sand Fill Ratio	**Deformability**	**Movement of Sand Inside the Container**	**Interface Friction**
(a) Properties of Geotextile Material				
• Mass per Area	-	-	-	-
• Thickness	-	X	-	-
• Tensile Strength	X	X	X	-
• Elongation	X	X	X	X
• Puncture Force	-	-	-	-
• Deformation by Penetration Test	-	X	X	-
• Permeability	X	X	X	-
• Transmitivity	-	-	-	?
• Characteristic Opening Size	X	?	X	-
• Surface Friction	-	-	-	X

***X**=relevant, **?**=unknown, **-** =not relevant*

Due to practical limitations, Pilarczyk (2000) recommends to use different scaling rules for different properties of geotextile. Therefore, the thinnest suitable material has been selected, which is one order of magnitude stronger in tensile strength. Similarly, it had been impractical to satisfy other model parameters such as the interface friction, the hydraulic conductivity of geotextile and the properties fill material. Deltares (2010), during the large scale hydraulic stability tests of geotextile tubes, studied the scaling problems of geotextiles and fill materials, but did not reach a proper conclusion. Though the selected scale was 1:4, Deltares (2010) followed a similar approach as described above and selected a thin geotextile with a sufficient sand retention capability and a sufficient strength for hydraulic filling.

2.6.2 Discussion and Implications to the Present Study

After an extensive review and analysis of the literature on the sand fill ratio of GSCs and its effect on the hydraulic stability of GSC-structures, it is found that the laboratory investigations are the most feasible and appropriate option to study the effect of different engineering properties of GSCs on the hydraulic stability of GSC-structures.

Most of the previous experimental studies were carried out to investigate the hydraulic stability of GSC-revetments. However, Mori at al. (2009) conducted a series of experiments with submerged GSC-structures. Other than that, only Delft Hydraulics (1994) and Oumeraci et al. (2002b) conducted experiments with submerged and low-crested GSC-structures while changing few parameters. Therefore, up to now a process oriented investigation of submerged GSC-

structures has not yet been performed. Hence, further systematic investigations are required, which cover the effect of the sand fill ratio, the interface friction between GSCs, and the inclination angles of GSCs, etc.

Scaling of geotextile material represents the one of the main concern when planning small scale experiments and it is impossible to achieve a perfect similitude. Therefore, the selections of the material for the experimental investigations should be based on a thorough understanding of the physical processes and properties of available materials. Therefore, it is recommended to conduct further studies to identify scaling problems related to geotextile material and fill material in the small scale GSC-structure models.

Table 2-7: Previous model tests related to the hydraulic stability of GSC-structures (modified from Recio 2007)

Author and Year	Type of Structure	Scale	Wave-flume dimensions (length)m x (width)m x (depth)m	Wave Type	Container Material	Container Dimensions (length)m x(width)m x(height)m	Filling Material	Fill ratio	Over-lapping	Stability Criteria	Contribution
VENIS (1968)	Submerged breakwater (1:n=1:1.5)	1:5; 1:20	U/3.0/U & U/0.6/U	Unknown	Jute and Nylon, plastic bag	without filling (1:5) 0.4x0.4 m & (1:20) 0.1x0.1	Dry sand ρ_s= 1600 kg/m^3 wet sand ρs=1900 kg/m^3	50%-90%	--	--	Recommendation of a sand fill ratio of 80%. lower filling ratio reduces the stability
DELFT Hydraulics (1975)	Revetment, sand tubes, (1:n=1=3)	01:25	Unknown	Spectra	Jute and linen	Tube diam. 0.9m and 1.5m	Sand	90%-100%	--	Movement starts H/(ΔDn) = 2.0 Damage =4.5	No consideration of wave period, tubes more stable than containers. Stability proportional to tube diameter. Larger mattresses give higher stability. Sand fill ratio does not influence the stability of mattresses
RAY (1977)	Breakwater and submerged breakwater	1:1	Unknown	Regular waves	Nylon	Without filling 2.44 x 1.52m full 2.15x1.2x0.33	Wet sand, ρ_s= 2000 kg/m3	75%	--	From H/(ΔDn) = 3.0 to = 5	Steep waves induce reduction in stability (specially on submerged breakwaters).
PORRAZ et al. (1979)	Breakwater (1:n:1:1 and 1:n=1:2)	1:60	70/0.6/1.2	Regular waves	Polyethylene	Full 5.6x2.3x0.5cm	Mortar ρ_s=2140 kg/m3	Un known	--	For 1:n=1:1 and H_{crit}=6cm H/(ΔDn)=2.0 for 1:n=1.2 and H_{crit}=9cm H/(ΔDn)=2.0	Steepness of slope, higher overlapping induces higher stability, higher loads are on the top of the slope. Recommendations for a larger crest element. Higher stability with containers perpendicular to the structure axis
TEKMARINE (1982)	Revetment slope (1:n=1:3)	1:6	107/3.7/4.6	Regular waves and Spectra	Unknown	Without filling 0,61 x 0.33m; full 0.54 x 0.26 x0.14m	Gravel ρ=1923 kg/m3 (cement)	Un known	50%	50% overlapping H/(ΔDn)=2.1 without overlapping 1.8 combination2.1	Overlapping length increases the K factor to 1.5, Elements near the SWL are critical for the stability, Recommendations for maximum possible overlapping
JACOBS & KOBAYASHI (1983/1985)	Revetment slope (1:n=1:3)	Unknown	24.4/0.61/1.4	Regular waves	Woven Geotextile	Without filling 12.7x8.9cm; full 12.4x6.2x3.3cm	dry sand ρ_s= 1699 kg/m3 wet sand 1955 kg/m3	Un known	50%	50% overlapping H/(ΔDn)=2.4	Increase in the overlapping increases the stability, Introduction of a empirical constant, Formulation of the relation between the stability number Ns and the surf similarity parameter ξ
BOUYZE & SCHRAM (1990)	Submerged breakwater (1:1)	Unknown	8/1/0.35/	Current	Geotextile	1m x 0.36 m full	Sand	Un known	50%	$\frac{u_{cr}}{\sqrt{g\Delta_t D}} = 0.5 \cdot to \cdot 1.0$	Critical velocity before movement of the elements. No particular contribution.
DELFT Hydraulics (1994)	3 Layers of containers in a submerged breakwater (1:n=1:1)	1:20	55/1.0/1.2	Pierson Moscowitz Spectra	Geotextile	Full 1.0x0.42x0.09	Sand	Un known	--	Movement starts H/(ΔDn)=1.83. Displacement H/(ΔDn)=2.33	Description of the dependency of the stability with the experiment parameters. No particular contribution

Table 2.7 cont: Previous model tests related to the hydraulic stability of GSC-structures cont. (modified from Recio 2007)

Author and Year	Type of Structure	Scale	Wave-flume dimensions (length)m x (width)m x (depth)m	Wave Type	Container Material	Container Dimensions (length)mx(width)m x(height)m	Filling Material	Fill ratio	Over-lapping	Stability Criteria	Contribution
VAN DER MEER (1987) :	Rubble mound breakwater	unknown	50/1.0/2.0	Pierson Moscowitz Spectra	Rock	--	--	--	--	Damage grade $S=A_E/D^{\wedge}2$ A_E= eroded area	Difference between regular waves and spectra but no relation with the type of spectra. The damage grade increases with the Iribarren number, Higher stability with higher permeability, Higher stability with long waves
WOUTERS (1998)	--	Develop stability formula from the experimental data of Porraz (1978), Tekmarine (1982) and Jacobs &Kobayashi (1983, 1985)								$H/(\Delta Dn) = 2.5/\sqrt{(\xi_o)}$	Develop of a function for describing the stability number with the surf similarity parameter
OUMERACI et al. (2002a) (small scale)	Dune protection, slope revetment and submerged breakwater (1:n=1:1; 1.5 ; 3)	1:8	100/2.0/1.2	JONSWAP Spectra	Geotextile and linen	Without filling 0.31x0.15 full 0.25x0.1x0.06m	Sand	80%	<=50%	$H/(\Delta Dn) = 2.0/\sqrt{(\xi_o)}$	High influence in the stability by the overlapping,
OUMERACI et al. (2002b) (large scale)	Revetment (1:1)	1:6	300/5.0/7.0	JONSWAP Spectra	Nonwoven Geotextile	150 lt and 25 lt	Sand	80%	<=50%	$H/(\Delta Dn) = 2.7/\sqrt{(\xi_o)}$	Some scale effects observed. Stability increased by the use of adhesive strips among elements. New stability formulae based on the Wouters formula. Formulas for crest and slope elements
Grüne et al (2006) (large scale)	Scour protection for offshore monopile	1:10	300/5.0/7.0	JONSWAP Spectra	Nonwoven Geotextile	0.282x.144x.033 - 0.487x0.252x0.118	sand	56% , 80% & 100%		--	percentage of filling and the direction of wave approach contribute to stability of a single GSC on the seabed (these are smaller for a group of GSC), stability increases with filling ratio
RECIO (2007) -1	Varies	1:8	5.0/2.0/1.5 tank	N/A	Nonwoven Geotextile	full 0.45x0.28x0.11 (13.8 lt) & 0.35x0.24x0.09 (7.5 lt)	Sand 1800kg/m^3	80%	varies	N/A	Permeability of GSC-structures governs by the gaps between GSCs
RECIO (2007)-2	GSC revetment	1:8	100/2.0/1.2	Regular waves and Spectra	Nonwoven Geotextile	full 0.26x0.13x0.06 (1.7 lt)	Sand 1800kg/m^3	80%	varies	N/A	Permeability Coefficient of GSC-structures is k=10^-2, Placement pattern affect the permeability, Random placement has the highest permeability. Longitudinal placement has almost same permeability as random and highest hydraulic stability

Table 2.7 cont: Previous model tests related to the hydraulic stability of GSC-Structures cont. (modified from Recio 2007)

Author and Year	Type of Structure	Scale	Wave-flume dimensions (length)m x (width)m x (depth)m	Wave Type	Container Material	Container Dimensions (length)mx(width)m x(height)m	Filling Material	Fill ratio	Over-lapping	Stability Criteria	Contribution
RECIO (2007)-3	GSC revetment 1:n=1:1	1:8	100/2.0/1.2	Regular waves and Spectra	Nonwoven Geotextile	full 0.48x0.24x0.11	Sand 1800kg/m^3	80%		see Table 2.8 (Process based stability formulae)	Permeability Coefficient of GSC-structures is k=1.4 x 10^{-2}, wave induced loads on GSCs and inside the GSCs
RECIO (2007)-4	GSC revetment 1:n=1:1	1:8	100/2.0/1.2	Regular waves and Spectra	Nonwoven Geotextile	full 0.25x0.10x0.06	Sand 1800kg/m^3	80%		see Table 2.8 (Process based stability formulae)	internal movement of sand and its effect on the stability, variation of contact area among neighbouring GSCs, types of displacement and effect of deformation on the stability were studied. Using PIV technique, wave induced flow on the seaward slope of the GSC-revetment were found
RECIO (2007)	Instrumented Container	1:8	100/2.0/1.2	Regular waves and Spectra	Stiff Wood Container covered with geotextile	0.30x0.15x0.06	N/A	N/A		see Table 2.8 (Process based stability formulae)	Drag, Inertia & Lift coefficients for GSC were obtained by testing varies configurations
Deltares (2008)	GSC burm	1:4	240/5/7	JONSWAP Spectra	Woven Geotextile	5.0x2.75x0.55	sand	Un known	-	-	caterpillar mechanism which caused by the movement of sand inside the container was found, migration of sand during wave attack up tp 8% and lower than theoretical value based on sieve analysis
Mori (2008)	GSC submerged breakwater 1:n=1:2	1:25	50/0.8/0.8	Spectra	Nonwoven Geotextile	0.11/0.08/0.036 0.083/0.08/0.035	sand	Un known	50%	unknown	type of geotextile materials used for the construction of GSCs might not affect the stability of GSC-structure, higher wave setup and lower wave transmission due to low permeability and stability is lower than that of rocks
Coughlan et al. (2009)	GSC-revetment 1:n= 1:1.5, 1:2	1:10	32/3/1.3	Regular waves and spectra	Nonwoven Geotextile	0.165/0.140/0.043	sand	100%	varies	design nomograms to find same wave height based on initial damage level	Double layer "stretched bond" revetment with 1:1.5 slope are more stable and less vulnerable for total failure

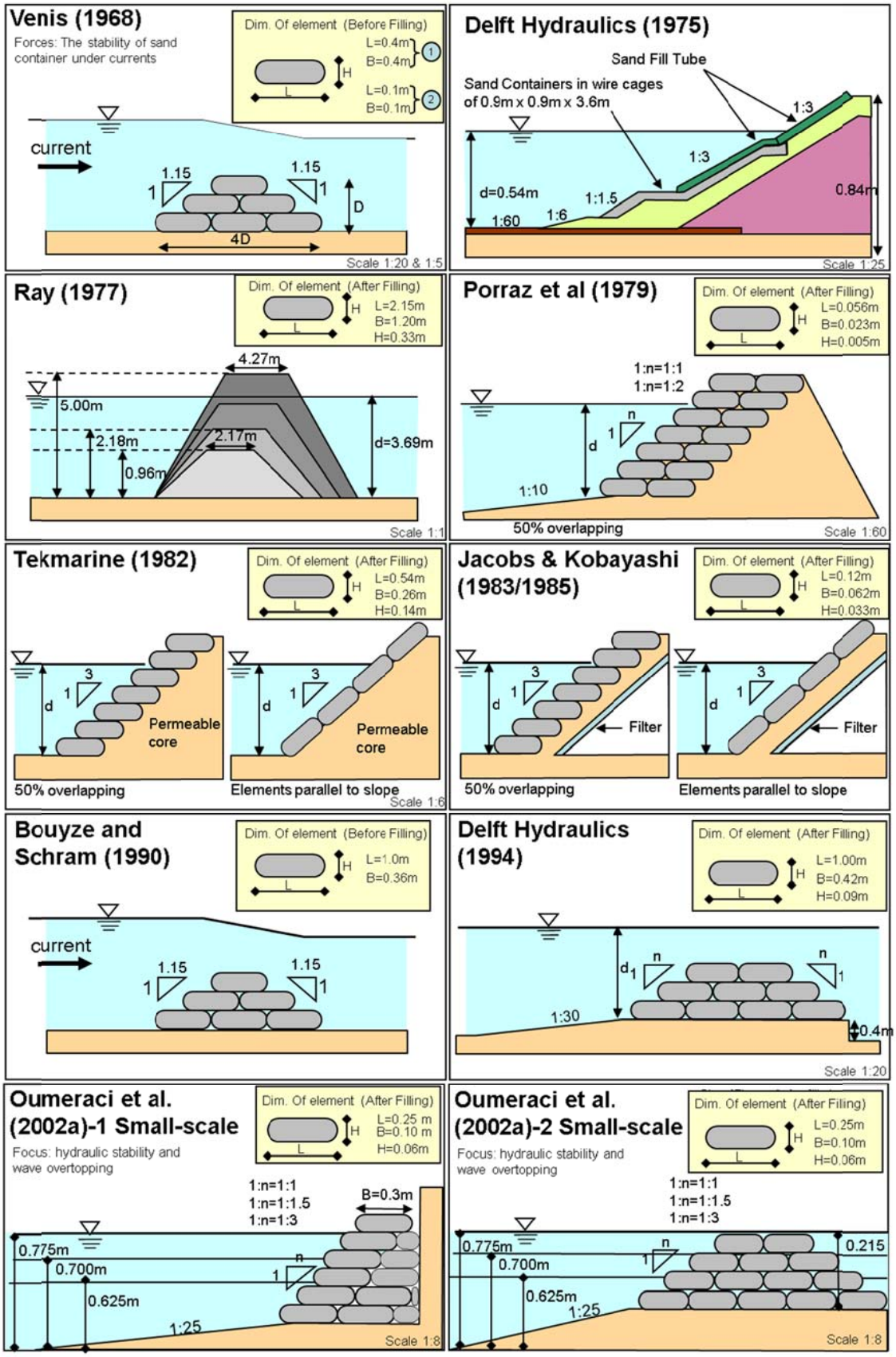

Figure 2-13: Comparative cross section of previous model tests of GSC-structures (modified from Oumeraci et al. 2002b).

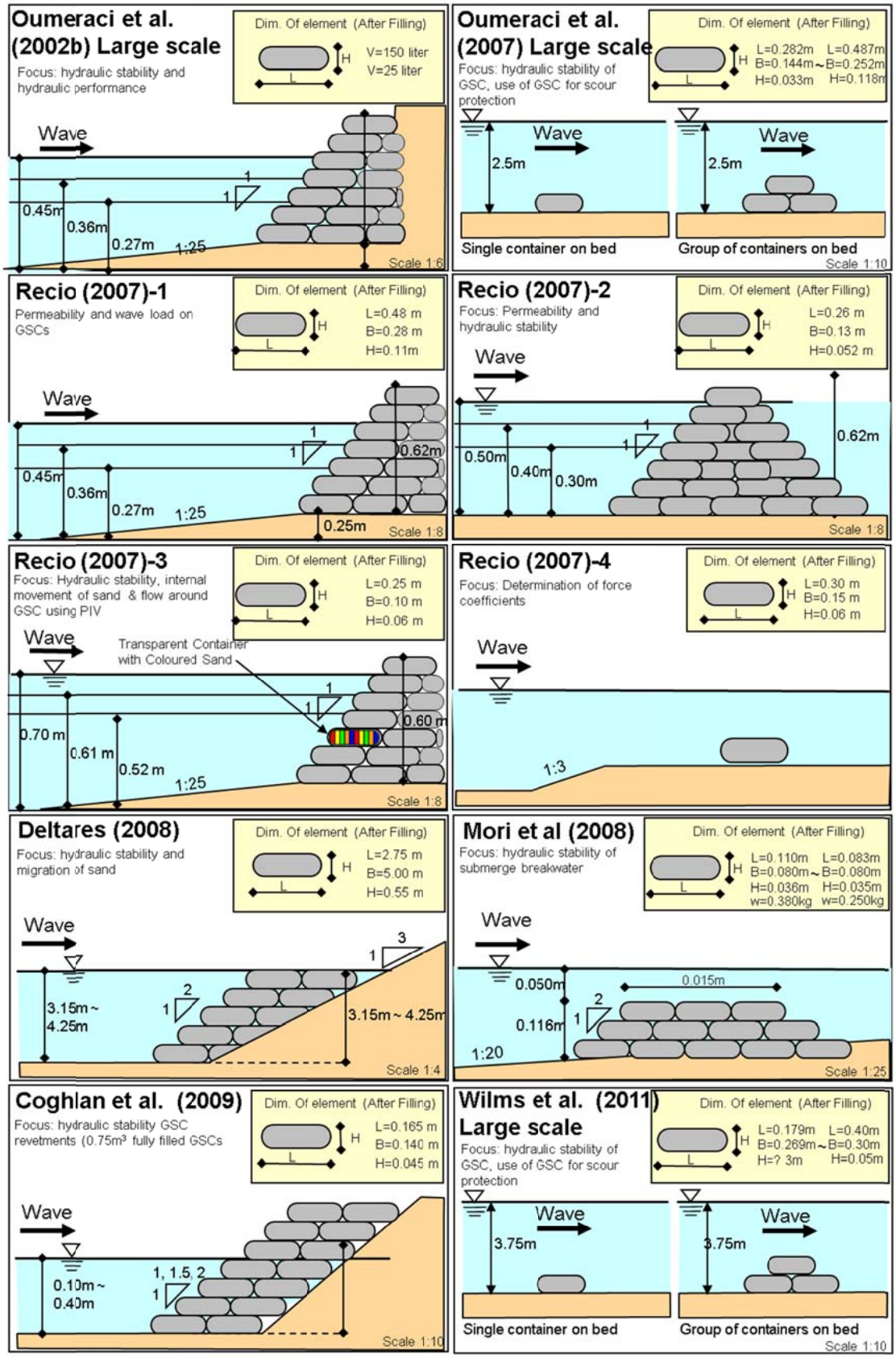

Figure 2.13 cont.: Comparative cross section of previous model tests of GSC-structures (modified from Oumeraci et al. 2002b)

2.7 Existing Hydraulic Stability Formulae and Nomograms

Several authors suggested several formulae for the hydraulic stability of GSC-structures. Among those works, contributions from Wouters (1998), Pilarczyk (2000), Oumeraci et al. (2002a, 2002b, 2002c, 2003, 2007), Recio (2007), Mori (2008), Recio and Oumeraci (2010), Coghlan et al. (2009), Recio et al. (2010) and Hornsey et al. (2011) are noteworthy. The existing hydraulic stability formulae can be categorised into the following three groups:

Group 1: Early GSC-structures were designed using the hydraulic stability formula for rock armour layers such as Hudson's formula (1956) or Van der Meer formula (1988). As a result the required weight of GSC is determined as a function of the design wave height similar to any other conventional rubble mound structure. (Figure 2-14a).

Group 2: The Hudson formula does not include the wave period and contains the empirical coefficients k_D, which is not appropriate for GSC-structures as the response of GSCs to wave loads basically differs from that of rigid armour units. Therefore, Wouters (1998) proposed a new stability formula (Eq. 2.2) for GSCs based on the Hudson formula and previous experimental data (e.g. Bouyze and Schram 1990). This new formula was developed explicitly for GSC-structures (Figure 2-14b) by introducing a modified stability number (N_s) which accounts for the wave period through surf similarity parameter ξ_0, together with a new empirical coefficient C_W as an appropriate substitute for k_d:

$$Ns = \frac{Hs}{(\rho_{GSC} / \rho_W - 1) \cdot D} = \frac{C_W}{\sqrt{\xi_0}} \quad \text{with} \quad \xi_0 = \tan\alpha / \sqrt{(\mathrm{Hs} / \mathrm{L}_0)} \tag{2.2}$$

where $D = lc \sin\alpha$ and lc = length of a GSC

Where,

N_s = stability number [-],
H_s = incident significant wave height [m],
ρ_W = density of water [kg/m^3],
ρ_{GSC} = density of GSCs [kg/m^3],
C_W = empirical parameter derived from the stability number N_s [-],
D = thickness of armour layer [m],
α = slope angle of the structure [°],
$L_0 = g\,T^2/(2\pi)$ = deep water wave length calculated using the mean wave period [m]

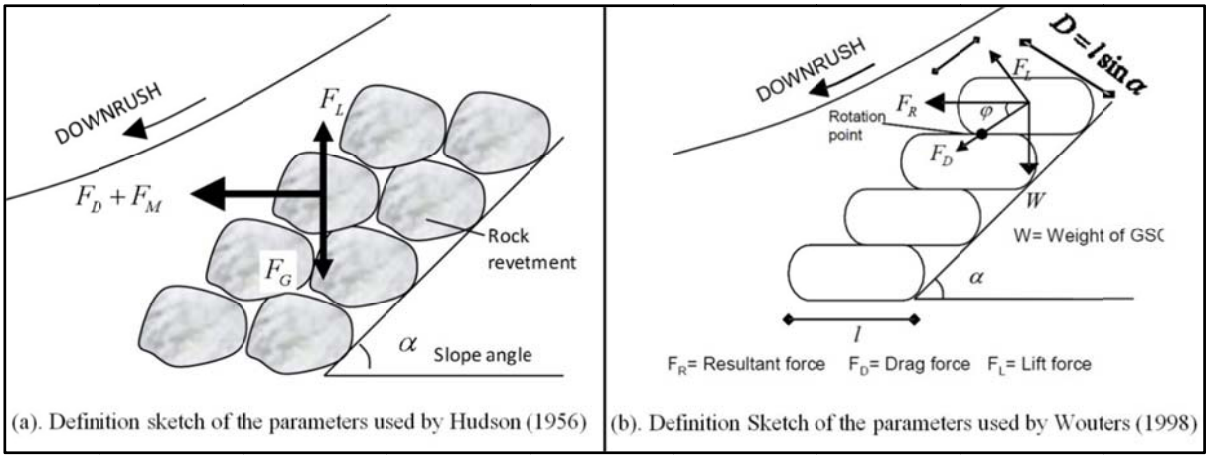

Figure 2-14: Definitions sketches of the parameters used in previous hydraulic stability formulae

Based on extensive small and large scale model tests, Oumeraci et al. (2002a, 2002b, 2003) confirmed the approach by Wouters (1998) using a modified stability number as a function of the surf similarity parameter for the GSCs on a slope of a sufficiently high revetment (i.e. without excessive overtopping). Moreover, another value was proposed for the empirical parameter (C_w = 2.75). As GSCs placed on the slope and on the crest of a coastal structure undergoing different wave loads under different boundary conditions, the slope GSCs of a high revetment and the crest GSCs of a comparatively lower structure with excessive wave overtopping expectedly showed different stability behaviours. Hence, a new formula was proposed for the stability of crest GSCs in which the relative freeboard Rc/H_s represents the governing influencing parameter. This formula is valid only for $Rc > 0$ and needs therefore to be verified for $Rc = 0$ and $Rc < 0$. Nevertheless, the second main development was the recognition of different behaviours of crest and slope GSCs.

Group 3: The simple stability formulae of Group 2 were developed without considering explicitly the effect of the deformation of GSCs. Though this effect is implicitly included to some extent in the empirical parameter C_w, it is necessary to understand the governing underlying failure mechanisms of GSCs, which basically differ from those of rigid armour units, and to take them into account in the stability formulae. According to Oumeraci and Recio (2010), previous experimental studies have shown that the dislodgment and pullout of the slope containers by wave action (including the sliding and the overturning of crest containers) are strongly affected by the deformation of the sand containers. Moreover, it was clearly shown by Oumeraci and Recio (2010) that the neglection this deformation might result in an unsafe design, especially for very high design waves. Simple stability formulae mentioned above cannot explicitly account for the deformation and other mechanisms affecting the hydraulic stability. Since GSCs are different from conventional rubble mound structures in many ways, a different approach was required. One of the remarkable steps in this direction is the development of the first process-based hydraulic stability formulae for GSC-structures by Recio (2007).

Recio (2007) conducted an extensive study on the processes affecting the hydraulic stability of GSCs and found that any formula deals with GSC-structures should account at least most

important processes (e.g. the cyclic deformation) and key parameters (e.g. the friction between containers). In order to account the effects of deformation, in the new process based formulae, the resisting forces (weight and friction force) and the mobilizing forces (drag, inertia and uplift forces) were explicitly introduced. Furthermore, two most common failure modes: sliding and overturning were dealt separately (Figure 5-2). Initially, the formulae have been derived without considering the deformation and as the second step; effects of the deformations were introduced as correction factors. Formulae to calculate force coefficients C_D, C_M and C_L, deformation factors K_{CD}, K_{CM}, K_{CL} and K_R, the definition of parameters and typical values to be used in the stability formulae are presented in Recio (2007). As these formulae are too complex for engineering applications, tentative nomograms based on Recio's (2007) formulae were recently proposed by Recio et al. (2010) for the hydraulic stability of GSC-structures to be used in feasibility studies (Table 2-8).

Apart from that Hornsey et al. (2011) also proposed design nomograms for the hydraulic stability of GSC-structures (Table 2-8), which are limited to two specific GSC geometries. However, GSC is still a developing technology and comprehensive design guidelines are not yet available. Certainly, the hydraulic stability of GSC is more complex as GSC-structures may experience a number of specific failure modes. Table 2-8 provides a summary of the available hydraulic stability formulae and nomograms for GSC-structures.

Table 2-8: Available hydraulic stability formulae and nomograms for the design of GSC- structures

Authors/Structure types **Formulae / Nomograms**	**Remarks**
Hudson (1956) / Rubble mound structures $N_S = \frac{H}{\Delta D_n} = (K_D \cot\alpha)^{1/3}$ $W_{50} = \frac{\rho_S g H^3}{K_D(\rho_S/\rho_W - 1)^3 \cot\alpha}$	The formula is based on the balance of wave generated flow forces (inertia force is neglected) on a (stiff, non-deformable) armour stone on a slope of a rubble mound structure. K_D is derived empirically from scale model tests. Later new K_D values for different types of armour units and for different types coastal structures were proposed by several other researchers. The formula does not include the wave period.
Wouters (1998) / GSC-revetments $N_s = \frac{H_s}{(\rho_E/\rho_w - 1)\cdot D} = \frac{C_w}{\sqrt{\xi_0}}$ $D = l \cdot \sin\alpha$ $lc = \frac{H_s\sqrt{\xi_0}}{(\rho_E/\rho_w - 1)\cdot \sin\alpha\, C_w}$	The formula describes the relationship between the stability number of GSCs and the surf similarity parameter which includes the wave period (particularly important for GSCs). Instead of the typical required weight of the armour unit (GSC), the thickness D of the cover layer was defined by the relationship $D = lc \sin\alpha$. Wouters (1998) proposed a value for $C_w = 2.0$ based on laboratory experiments. The applicability of the formula is limited to slope GSCs and not sufficiently validated with experimental results or field data.
Oumeraci et al. (2002b, 2002c, 2003) / High GSC-revetments and low crested overtopped structures Slope GSCs: $N_{s,slope} = \frac{H_s}{(\rho_E/\rho_w - 1)\cdot D} < \frac{C_w}{\sqrt{\xi_0}}$ $lc = \frac{H_s^{3/4}\sqrt{T}}{C_w\left(\frac{2\pi}{g}\right)\left(\frac{\rho_{GSC}}{\rho_w} - 1\right)\sqrt{\frac{\sin(2\alpha)}{2}}}$ Crest GSCs: $N_{s,crest} = \frac{H_s}{(\rho_{GSC}/\rho_w - 1)\cdot D} < 0.79 + 0.09\frac{R_c}{H_s}$ $lc = \frac{H_s}{\left(\frac{\rho_{GSC}}{\rho_w} - 1\right)\left(0.79 + 0.09\frac{R_c}{H_s}\right)\sin(\alpha)}$	Based on systematic hydraulic model testing, the stability formula of Wouters, was confirmed for slope GSCs of sufficiently high revetments (no excessive wave overtopping) and a new value for $C_w = 2.75$ was proposed (Oumeraci et al., 2003). However, for the crest GSCs of relatively low-crested structures (excessive wave overtopping) the surf similarity parameter. The stability number N_s is primarily affected by the relative freeboard Rc/Hs and the effect of the surf similarity parameter was comparatively negligible. For the first time (1:1 slope), different boundary conditions for the crest and the slope GSCs were treated separately. However, the formula for the crest GSCs considered only a limited range of Rc/Hs >0, so there is still room for further extension in the lower range of relative freeboards (Rc/Hs $\leq$ 0) . Even recently, Bezuijen and Vastenburg (2012) recommended these formula for high GSC-revetments without excessive overtopping as there are no other simple alternatives.
Recio (2007) and Oumeraci and Recio (2010) / GSC-revetments and submerged GSC-structures $l_{c(sliding)} \geq u^2 \frac{[0.5KS_{CD}C_D + 2.5KS_{CL}C_L\mu]}{\left[\mu KS_R\Delta g - KS_{CM}C_M\frac{\partial u}{\partial t}\right]}$ $l_{c(overturning)} \geq u^2 \frac{[0.05KO_{CD}C_D + 1.25KO_{CL}C_L]}{\left[0.5\Delta KO_R g - 0.1KO_{CM}C_M\frac{\partial u}{\partial t}\right]}$	Process based stability formulae for different types of GSC-structures were derived considering two key hydraulic failure modes: overturning and sliding. Force coefficients C_D, C_M and C_L were proposed as a result of extensive small scale experiments. These formulae explicitly take the cyclic deformation of GSCs into account and different deformation factors were proposed for different GSC-structures. A separate set of formulae were also provided for the calculation of the force coefficients. The main drawback of this set of formulae is that they are too complex for engineering applications. Furthermore, the final calculation is based on the horizontal particle velocities and accelerations without the structures, the changes in particle velocities due to the presence of the structure are implicitly embedded in the force coefficients.
Mori (2009) and Mori et al. (2008) / Submerged GSC-breakwaters $N_s = \frac{H_s}{(\rho_E/\rho_w - 1)\cdot D} < \frac{C_w}{\sqrt{\xi_0}}$	The applicability of the formula for slope GSCs by Oumeraci et al. (2003), to crest GSCs of a submerged GSC-structure was analysed based on experimental data. According to the experimental results, the formula seems to be applicable for surf similarity parameters between ξ_0 = 1.5 ~ 4.0. However. when the surf similarity parameter is less than 1.5, the formula over estimates the hydraulic stability. (seaward slope of the GSC-structure = 1:2)

Table 2 8: Available hydraulic stability formulae and nomograms for GSC- structures (cont.)

Authors/Structure types **Formulae / Nomograms**	**Remarks**
Recio et al. (2010) / Submerged GSC-reefs Example of nomogram for submerged GSC breakwater based on Recio's formulae (2007) to be applied for feasibility studies 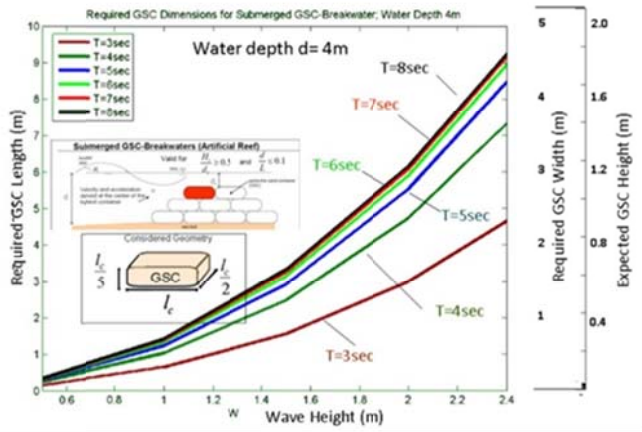 	A set of nomograms on the hydraulic stability of prototype GSC-structures were developed by extending Recio's formulae (2007) formulae. There are different nomograms for breakwaters, revetments, and scour protection systems. The assumptions and the limitations of the nomograms are: (i).The nomograms shall be applied for feasibility studies only, because they use average empirical force and deformation coefficients. (ii). The nomograms related to submerged breakwaters assume that the crest of the breakwater is submerged 1 m below the design water level. (iii). The nomograms are only applicable for containers in which its length is half of its width ($l_c = 2 \times b_c$) (iv). The nomograms use parameter values of nonwoven geotextiles. (v). The nomograms assume 80% sand fill ratio (vi). The nomograms are intended to assist during feasibility studies where GSC alternatives are compared with conventional structures
Coghlan et al. (2009) and Hornsey et al. (2011) / Non-overtopping GSC revetments Stability nomograms (example for 0.75 m^3 GSCs) were developed for two specific GSC geometries (GSC volumes: 0.75 m^3 and 2.5 m^3) based on scale model tests 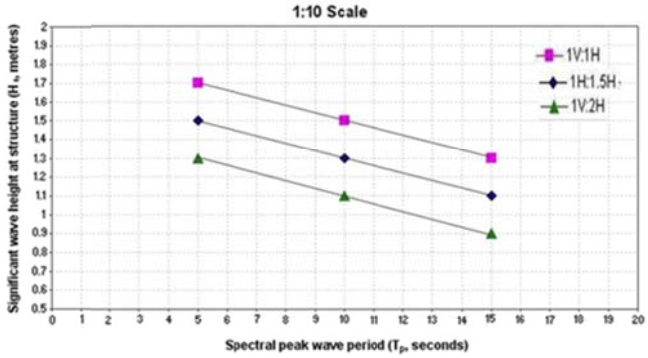 	Two nomograms which indicate the design wave heights Hs and peak wave periods Tp (at the structure) for the "Initial Damage" criterion (i.e. 0~2% of displaced GSCs on the double layer system) of non-overtopped revetment slopes were proposed. The design nomograms were developed from irregular wave tests (1100 waves) on the structure conducted with different revetment slopes (1:1, 1:1.5 and 1:2), foreshore slopes = 1:10 ~ 1:20, water depths = 3.0 m (in prototype scale), The wave heights and the wave periods in nomograms are in prototype scale. Nonwoven staple fibre geotextiles were used during the construction of model GSCs The nomograms represent two specific GSCs sizes: l_c = 2.4 m, b_c = 1.8 m and h_c = 0.65 [2.5 m^3] l_c = 1.6 m, b_c = 1.2 m and h_c = 0.40 [0.75 m^3] However, the nomograms are valid only for the tested conditions such as the stacking pattern, the sand fill ratio, the type geotextile material, the GSC geometry, etc. Hence, is it difficult to use the formulae for different types of GSCs.

b_c = width of the GSC [m]
C_D, C_L C_M = drag, lift and inertia coefficients
C_w = empirical parameter derived from N_S [-]
D_{50} = thickness of armour layer [m]
g = acceleration due to gravity
H_s = incident significant wave height [m]
h_c = height of the GSC [m]
K_D = stability coefficient (obtained experimentally)
KO = coef. account for deformation during overturning
KS = coef. account for deformation during sliding
$L_0 = g\,T^2/(2\pi)$ = deep water wave length using T_p [m]
l_c = length of the GSC [m]
N_s = stability number [-]
Rc = crest freeboard [m]

$Re = \left(\frac{uD}{\nu}\right)$ = Reynolds number
Tp= peak wave period
u=horizontal velocity
W_{50} = average weigh of element [kg]
α = slope angle of structure slope [°]
$\xi_0 = \tan\alpha/(H_s/L_0)^{1/2}$= Iribarren number [-]
$\Delta = (\rho s/\rho w - 1)$.
$\frac{\partial u}{\partial t}$ = horizontal acceleration[m/s^2]
μ = friction factor between geotextiles [-]
ρ_s = density of armour unit [kg/m^3]
ρ_W = density of water [kg/m^3]
ρ_E = density of GSC [kg/m^3]

Discussion and Implications for the Present Study

The requirement of new hydraulic stability formulae for GSCs has been discussed by many authors over the last few decades and Wouters (1998), Oumeraci at al. (2002b, 2002c, 2003) and Recio (2007) are the key contributors. Among them, the contribution from Recio (2007) for the advancement of the knowledge on the hydraulic stability of GSC-structures is undoubtedly significant. Most of his valuable contributions are the identification of processes related to the hydraulic stability of GSC-structures and also, the development of new process based stability formulae considering the cyclic deformations of GSCs. The deformation factors of the formulae of Recio (2007) were analytically derived, but not yet fully verified using experimental data. Therefore, it is important to verify these deformation factors experimentally.

Furthermore, process based formulae are largely influenced by the square of horizontal particle velocity, $\boldsymbol{u}$. Therefore, an accurate estimation of the horizontal particle velocity near the critical GSC is necessary. Any construction will alter the flow pattern and the particle velocities. Therefore, the estimation of horizontal particle velocity, after the construction of GSC-structure based on the linear wave theory is questionable. Therefore, a different approach to calculate the horizontal velocity and the acceleration might be necessary for more accurate designs (e.g. obtain the flow velocities and accelerations using a CFD model).

Moreover, the application method of the formulae is complicated due to its iteration process. The formula proposed by Hudson (1956) more than half a century ago is still the most preferred formula among the practicing engineers due its simplicity. However, there are few drawbacks in this formula. For example, Hudson's formula does not consider explicitly the influence of wave period on the hydraulic stability. Therefore, any new stability formula for the design of GSC-structure should focus on either to simplify the process based stability formula by Recio (2007) or to develop new formulae based on Hudson's formula and also, including the influence of wave period (e.g. by including surf similarity parameter). As mentioned earlier, Wouters (1998) and Oumeraci et al. (2002b, 2002c and 2003) attempted to come up with Hudson (1958) like empirical formulae for GSCs. However, due to lack of data, a detailed analysis was not performed. Therefore, it is necessary to reanalyse the small and large scale data from Oumeraci et al. (2002a, 2002b and 2003) to understand the relationship between the surf similarly parameter, the relative freeboards and the stability number.

In addition, the development of a simple computation tool (including process based and/or empirical formulae) or design monograms will be very much helpful to make GSC technology more attractive for the engineering practice.

2.8 Specification of Objectives and Methodology

Section 1.2 defines the tentative objectives and methodology for the current PhD research study. This section provides the specific objectives and the specific methodology to be adopted for this PhD study.

2.8.1 Specification of Objectives

The objectives of the PhD thesis may be specified as follows,

(i) Systematic study of the sand fill ratio and its effect on hydraulic stability of structures made of GSCs
- Identification of the factors influencing the sand fill ratio of GSCs
- Development of a physically-based and practically feasible definition of the sand fill ratio of GSC
- Development of a methodology to incorporate the sand fill ratio in the numerical modelling of GSC-structures
- Determination of the optimum sand fill ratio for different applications of GSCs in the coastal environment

(ii) Systematic study of the friction between GSCs and its effect on the hydraulic stability of structures made of GSCs
- Identification of the factors influencing the friction between GSCs
- Systematic study of the influence of the properties of geotextile materials and the sand fill ratio on the friction between GSCs and ultimately on the hydraulic stability of GSCs
- Development of a methodology to properly represent friction between GSCs in the numerical modelling of GSC-structures

(iii) Improvement/Development of an operational CFD-CSD modelling system
- Investigation of the capabilities and limitations of existing COBRAS/UDEC modelling system to model the submerged GSC-structures
- Further improvement of the COBRAS/UDEC modelling system and validate it based on the experimental results
- Carry out a systematic parameter study using validated COBRAS/UDEC modelling system

(iv) Refining and simplification of Recio's formulae to make them more user friendly.
- Evaluation of the feasibility of simplifying the Recio's formulae, mainly to avoid or shorten its iteration process
- Refining the Recio's formulae, mainly considering the stability of submerged GSC-structures

(v) Development of new nomograms/formulae for the hydraulic stability of submerged/low-crested GSC-structures
- Development of nomograms for the hydraulic stability of GSCs based on further experimental and numerical investigations
- Development of empirical relationships for the hydraulic stability of submerged/low-crested GSC-structures by combining both experimental and numerical modelling results

2.8.2 Specification of Methodologies

Figure 2-15 briefly illustrates the overall methodology, which will be adopted in this research study.

The results of this chapter have shown that the effect of the sand fill ratio and the friction between containers, are the most important factors affecting the stability of GSC-structures. Due to the complexity of the behaviour of GSC-structures, physical modelling is the best available tool to study these effects. Therefore, four series of especially designed laboratory experiments, which allow us to have an insight into the influence of above mentioned properties on the stability of structures made of GSCs and also to obtain the required parameters for the numerical modelling of GSC-structures, have to be performed. Experimental investigations consist of two laboratory experiments (drop tests and pullout tests), a small scale wave flume test (hydraulic stability tests) and hydraulic flume tests (permeability tests).

The first type of laboratory experiments should be focused on the variation of sand fill ratio during the manufacturing of GSCs and due to dropping in deeper waters. In order to find the expected deformation and elongation of geotextile materials due to impact with seabed, sink velocity and the sinking behaviour should be studied in detail. Therefore, drop tests will also focus on sinking behaviour and placing accuracy, in addition to the deformation and the changes in sand fill ratio.

One of the most common failure modes of GSC-structures has been identified as pulling out of GSCs during the wave run-down. Therefore the second type of tests were focused on the effect of the sand fill ratio, the type of geotextile material and the inclination angle on pullout forces. Apart from that, pullout tests will provide an idea about failures due to sliding of crest GSCs.

After the drop tests and pullout tests, it is expected to have a good insight into the sand fill ratio and the type of geotextile materials of GSCs and their importance in stability against sliding (or pulling out). The drop test results will provide information on more practical final sand fill ratios and placing accuracy.

Then, a series of wave flume tests (hydraulic stability tests) will be conducted to study the effect of the sand fill ratio, the type of geotextile material, the inclination angle of GSCs, etc. on the overall hydraulic stability of low-crested and submerged GSC-structures subject to wave attack. During the flume tests, effects of the sand fill ratios on cyclical deformation and movement of GSCs due to wave attack will also be studied, which are another important inputs when developing new stability formulae.

Finally, in order to quantify the effect of engineering properties of GSCs on the overall permeability of GSC-structures, new permeability tests should be performed in a hydraulic flume. These tests should be performed using the small scale GSCs constructed for wave flume test and with the same types of structures.

Numerical modelling of GSC-structures should then be conducted using the weakly coupled RANS-VOF model and FEM-DEM models as used by Recio (2007). This is the best feasible

option to model the hydraulic stability of GSC-structures. However, there are several shortcomings of the existing modelling system. Therefore, as the first step, pullout tests will be simulated to obtain the required parameters for proper representation of GSCs in two dimensional UDEC model. Then, the existing COBRAS/UDEC modelling system will be critically evaluated and the feasible modifications will be suggested. These models will be verified through the proposed and past laboratory experiments where necessary. Finally, the validated modelling system should be used for the performance of new simulations to obtain additional hydraulic stability data and also to perform a systematic parameter study.

Afterwards, using the results of experimental investigations and numerical models, the formulae of Recio (2007) will be simplified and furthermore, more simplified formulae/stability nomograms for design of GSC-structures will be developed as the main outcome of this PhD.

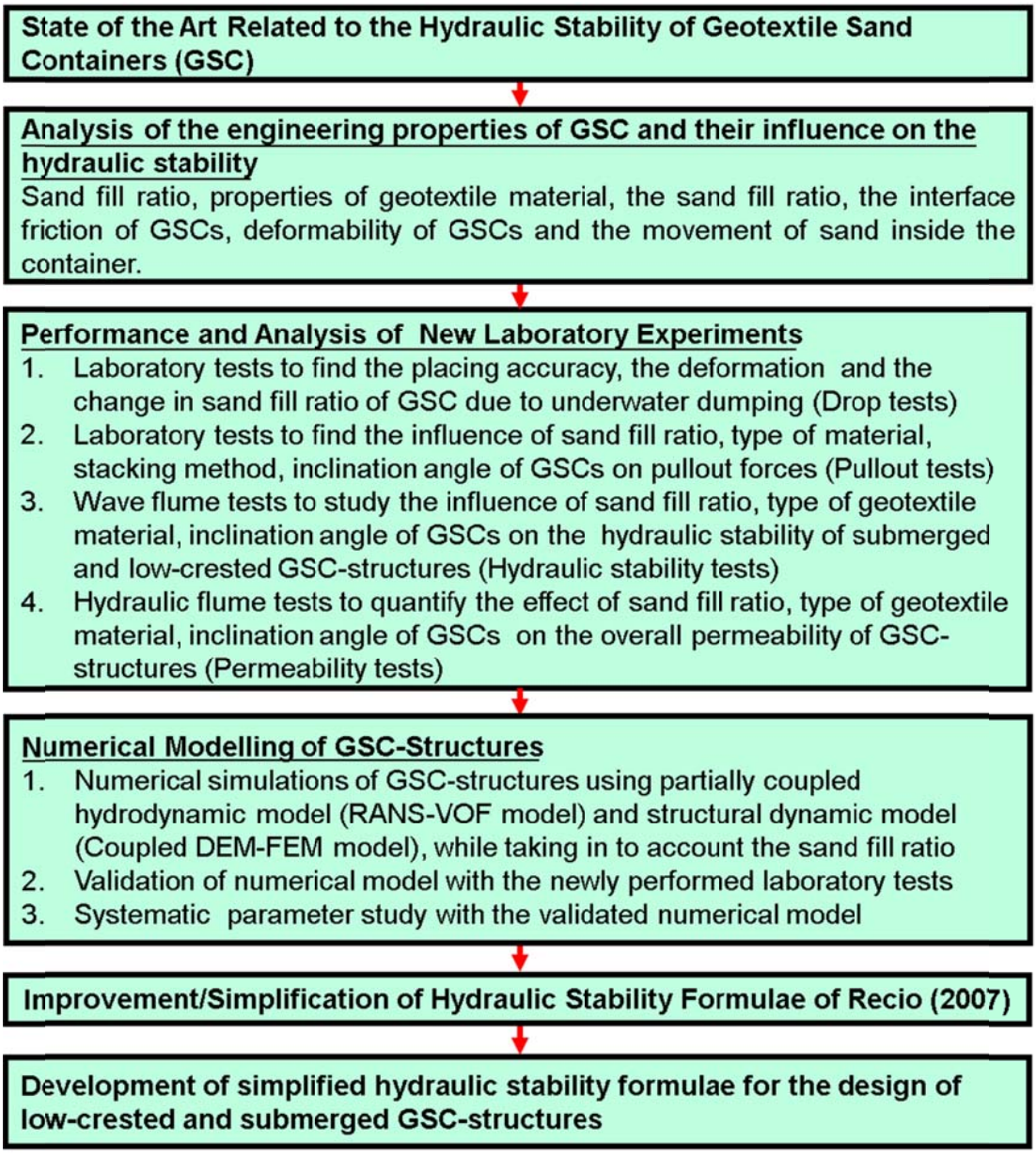

Figure 2-15: Revised methodology of the research

3 Effect of Engineering Properties of GSCs on the Hydraulic Stability – Experimental Studies and Results

As discussed in Chapter 2, the behaviour of GSC-structures is very complex and physical modelling is the best available tool to study the GSC-structures. Therefore, four types of laboratory experiments were performed at LWI and key results are summarised in this Chapter. First, several model GSCs were constructed with varying geometries and sand fill ratios; in order to determine practical sand fill ratios and to develop a method to predict the final external dimensions of a GSC, once the sand fill ratio and the dimensions of empty flat bag are known (Section 3.1). Four series of experimental investigations were then performed, which consisted of underwater drop tests (section 3.2), pullout tests (section 3.3), hydraulic stability tests (section 3.4) and permeability tests (section 3.5). These experiments allowed to have an insight into the influence of the engineering properties of GSCs on the hydraulic stability of GSC-structures, and also to obtain the parameters, which are required for the numerical modelling of GSC-structures.

3.1 Definition of the Sand Fill Ratio and Final Geometry of GSCs

3.1.1 Proposed Definition for the Sand Fill Ratio of GSCs

Even though the sand fill ratio is found to be a key factor governing the hydraulic stability of GSCs, none of the exiting stability formulae for the design of GSC-structures accounts for the sand fill ratio. Moreover, existing definitions for the sand fill ratio are very vague and not sufficiently appropriate to be implemented in the engineering practice. In order to overcome the drawbacks of existing definitions of the sand fill ratio, under the current study, a new definition was developed. This new definition for the sand fill ratio is based on the volume of a fully inflated geotextile bag and the dry bulk density of sand.

The shape of the geotextile bag is initially flat and two-dimensional. Once it is filled, it becomes a three dimensional pillow. The final shape of the filled GSC has a complicated geometry, which is difficult to idealize by a simple shape (Figure 3-1).

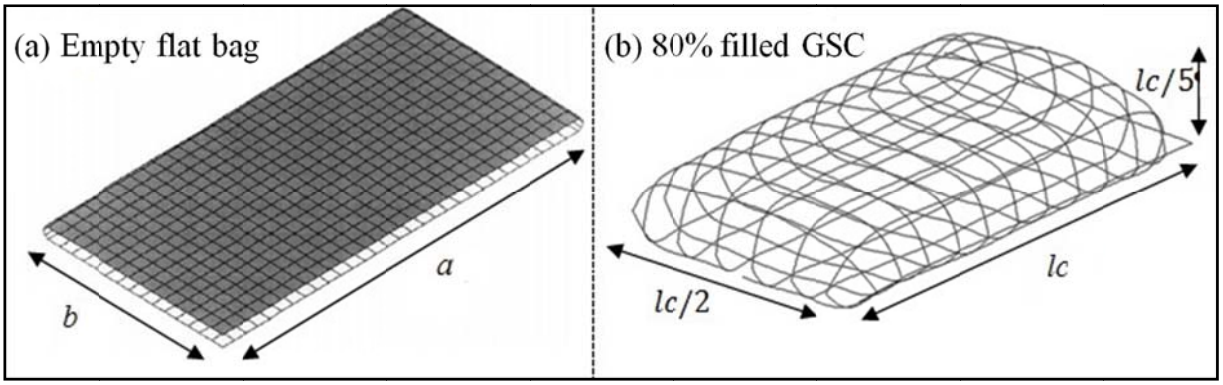

Figure 3-1: Empty flat bag and 80% filled GSC

The calculation of the maximum volume of a GSC is challenging due to its straight edges at the top and the bottom and the elliptical shape at the middle of the container (Figure 3-2). According to Robin (2004), when the dimensions of a flat rectangular bag which can neither stretch nor shear, with dimensions *a,b*, bounds for the maximum volume of closed sack obtained by inflating the bag are approximately given by;

$$V = a^3\left[\frac{b}{\pi a} - 0.142\left(1 - 10^{-b/a}\right)\right], \text{ where } V\text{= maximum theoretical volume} \qquad (3.1)$$

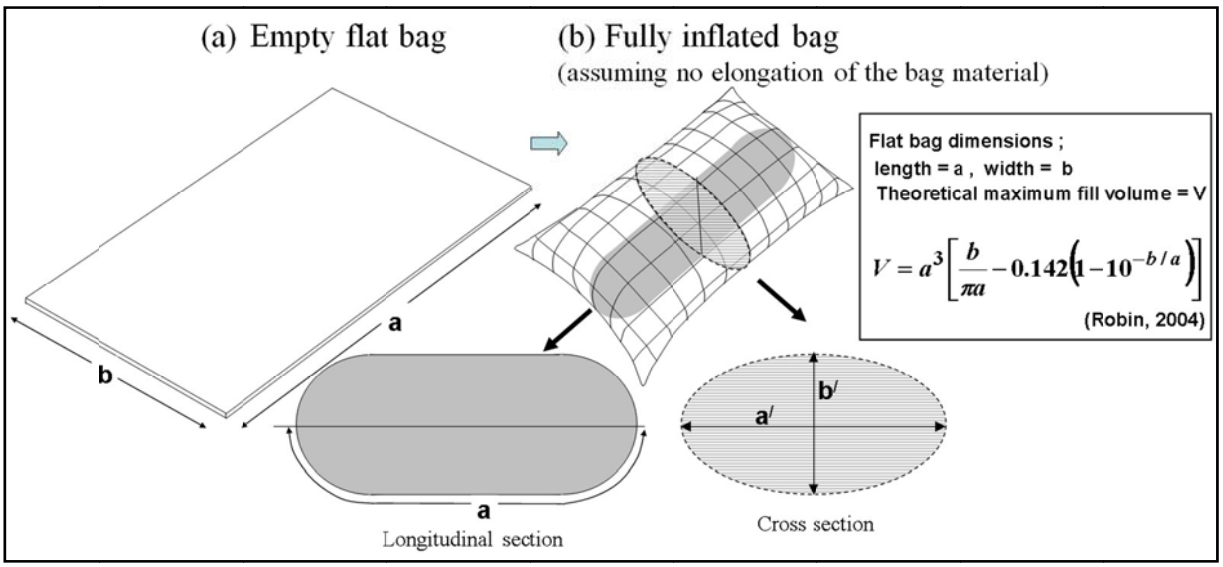

Figure 3-2: Theoretical maximum fill volume of flat rectangular bag

However, due to the elongation properties of geotextiles, the application of equation 3.1 for the calculation of maximum theoretical volume of geotextile sand container is still questionable. Therefore, the initial sand fill ratio can be used as the representative sand fill ratio value for GSCs. The initial sand fill ratio is calculated with equation 3.2, which is based on the theoretical maximum inflated volume that estimated using equation 3.1 of Robin (2004).

$$\text{Initial sand fill ratio of a GSC, } FR_0 = \frac{\left(\begin{array}{l}\text{Total volume of dry sand inside a GSC,}\\ \text{when the GSCs is filled under gravily, } V_{dry\ sand}\end{array}\right)}{\left(\begin{array}{l}\text{Calculated maximum inflated volume based on}\\ \text{the initial empty flat bag dimensions, assuming}\\ \text{no elongation (equation 3.1), } V_{max}\end{array}\right)}\% \qquad (3.2)$$

The initial sand fill ratio also varies with the sand density, which depends on the method of filling and the degree of compaction. Different compaction densities will result in different GSC weights. Furthermore, the sand fill ratio of GSCs is expected to be changed during different phases of a GSC-structure (Figure 3-3 and Figure 3-4). Therefore, it was required to find a practical density value of GSCs for the current study. The density of the sand fill was checked by filling several model geotextile containers in accordance with the general site practices such as filling dry sand under gravity (without compaction). After testing several

model GSCs with different sand fill ratios (GSC masses: 11.18 kg ~ 16.80 kg), the average dry bulk density of the sand fill was found as 1480 kg/m^3. This density value was used for the calculation of the required mass of the sand to achieve desired sand fill ratios during the construction of the other small scale GSCs. Apart from the lab tests, several publications on the field density measurements were also referred to find supportive evidences for the selected density figure and found out that most of the field densities, which have been reported in literature, are in the same range. For an example, Oumeraci et al. (2012) reported a field in-situ density of 1550 kg/m^3 where the average moisture content of fill material was 4.8% (range: 4.6% ~ 4.9%) by mass, then the dry bulk density of sand was reported as 1475 kg/m^3 and the fully saturated density as 1860 kg/m^3. Moreover, Blacka et al. (2007) found the average dry bulk density of the sand fill as 1327 kg/m^3 and fully saturated density as 1729 kg/m^3. Furthermore, Recio (2007) has used the value 1800 kg/m^3 as saturated density of the sand fill. Therefore, even though the final density of sand depends on the specific site practice, the selected density values (i.e. dry bulk density of the sand fill = 1480 kg/m^3) for the current research study adequately represent the approximate densities, which could be achieved in practice.

3.1.2 Final Geometry of GSCs

According to the literature (e.g. Pilarczyk 2000, Recio 2007, Oumeraci et al. 2002a, Oumeraci et al. 200b, 2003, PIANC 2011), typical GSCs used in the field are often 80% filled GSCs (except in Australia). The length l_c of an 80% filled GSC is generally twice as large as its width ($l_c/b_c = 2$) and five times as large as its height ($l_c/h_c = 5$)(Figure 3-1b). After many trials, the dimensions of the required empty flat bag, which result in the same geometrical relationship once they are 80% filled, were determined as: $a = 0.50$ m and $b = 28$ m to achieve a target size of 0.50 m long model GSC with the aforementioned geometrical ratios. Two types of geotextiles; a woven (mass per area = 110 g/m^2) and a nonwoven (mass per area = 200 g/m^2) were used for the construction of model GSCs (Dassanayake and Oumeraci 2012c).

During the small scale model experiments, it was found that the 0.5 m long model GSCs can be filled up to 120% of the initial theoretical maximum volume as a result of the elongation of geotextile material, even if the GSCs are filled carefully to avoid excessive elongations.

Once the sand fill ratio was defined, it is necessary to find out the relationship between the sand fill ratio and the final dimensions of GSCs. Several model GSCs were constructed with different fill ratios to develop a relationship between the sand fill ratio and the final external dimensions of GSCs. Model GSCs were constructed with different sand fill ratios; 80% (mass of sand = 11.18 kg), 90% (mass of sand = 12.58 kg), 100% (mass of sand = 13.98 kg), 110% (mass of sand = 15.39 kg), 120% (mass of sand = 16.80 kg). Due to its higher elongation properties, a container made of nonwoven geotextile can be filled up to 120% of the initial volume, whereas a container made of woven geotextile can only be filled up to 110% (Figure 3-3).

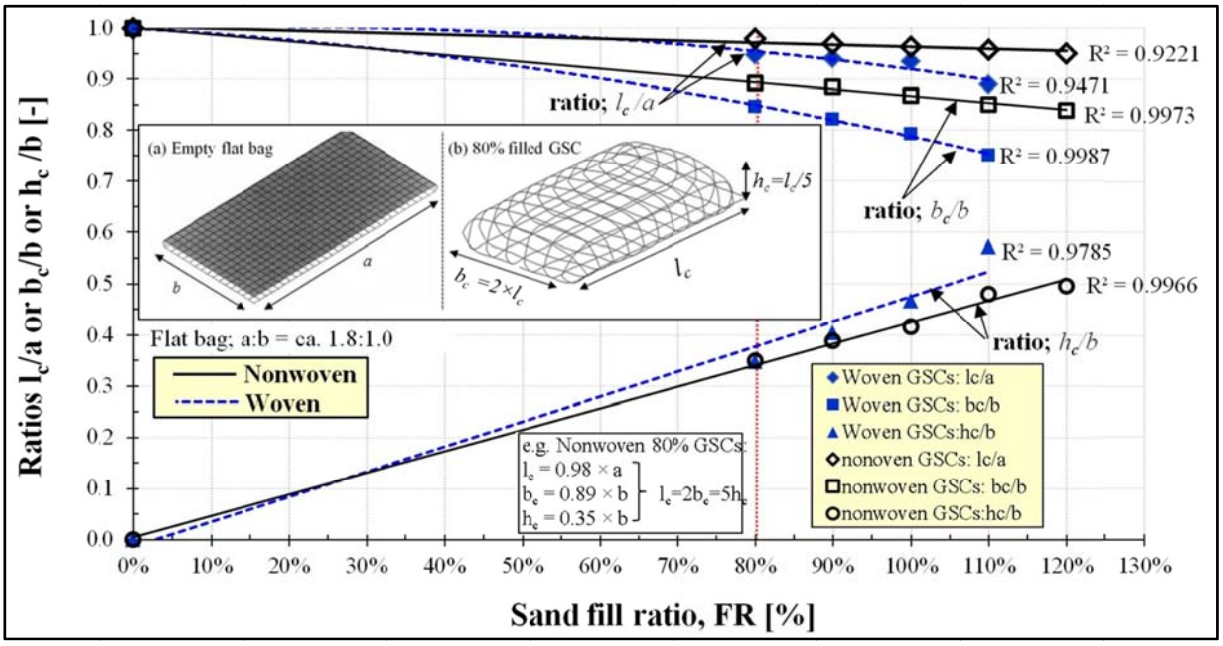

Figure 3-3: Prediction of the final dimensions of filled GSCs based on the empty initial flat bag dimensions

Different relationships were found for different types of geotextile material and for the different length-width ratios of empty flat bags (Dassanayake and Oumeraci 2010d). Based on model GSCs of length : width = 1.8 : 1.0 (i.e. for a typical GSC used in the field), a nomogram to predict the external dimensions of filled GSCs with different sand fill ratio is developed (Figure 3-3). If an empty bag with another length / width ratio is used, new nomogram should be developed accordingly.

3.1.3 Final Sand Fill Ratio

Figure 3-4 illustrates different phases of a GSC-structure, during which the sand fill ratio of GSCs is expected to change. Construction of a GSC starts with a rectangular flat bag. Then, the container will be filled with sand or any other fill material. During the filling process, the GSC will deform as a result of the elongation of the geotextile material. After the filling, GSC will be transported from the filling site to the location of the GSC-structure in construction. During transport, sand will be further compacted and also, the geotextile material will undergo additional elongations depending on the method of handling. Once the container is submerged, the sand fill will be further compacted (instantaneous compaction). Depending on the installation method, GSC will be further deformed (e.g. if the GSC is dropped from a certain height, the geotextile skin will be elongated due to the impact, when the GSC hits the bottom). Even after the placement of the container, due to weight of the GSCs above, it will deform more and the sand fill will be further compacted. Finally, the container will come into an equilibrium stage depending on the imposed stresses, the strength of the geotextile material, the properties of fill material, etc.

When a GSC-structure is exposed to wave attack, the next compaction phase of the fill material can be expected. However, while GSCs are in service, due to cyclic deformation and cyclic wetting and drying, finer particles will be washed out thus leading to a reduction of the volume of the sand fill. Furthermore, as a result of continuous stresses on the geotextile mate-

rial, it will be subject to creep over time. Both, the wash out of the fine particles and the creep of the geotextile material will lead to lower sand fill ratios. However, it is difficult to quantify the relative contribution of each of these processes since there are several factors involved (e.g. type of geotextile material, type of fill material, hydrodynamic conditions around GSCs, submergence depth, exposure time, etc.).

As shown in Figure 3-4, the final sand fill ratio (*FR*) is always lower than the initial sand fill ratio (FR_0). The quantification of the final sand fill ratio is difficult since it involves many factors. In order to experimentally simulate the GSC-structures, the new definition of the initial sand fill ratio was used (eq. 3.2), which is one of the main outcomes of this research study.

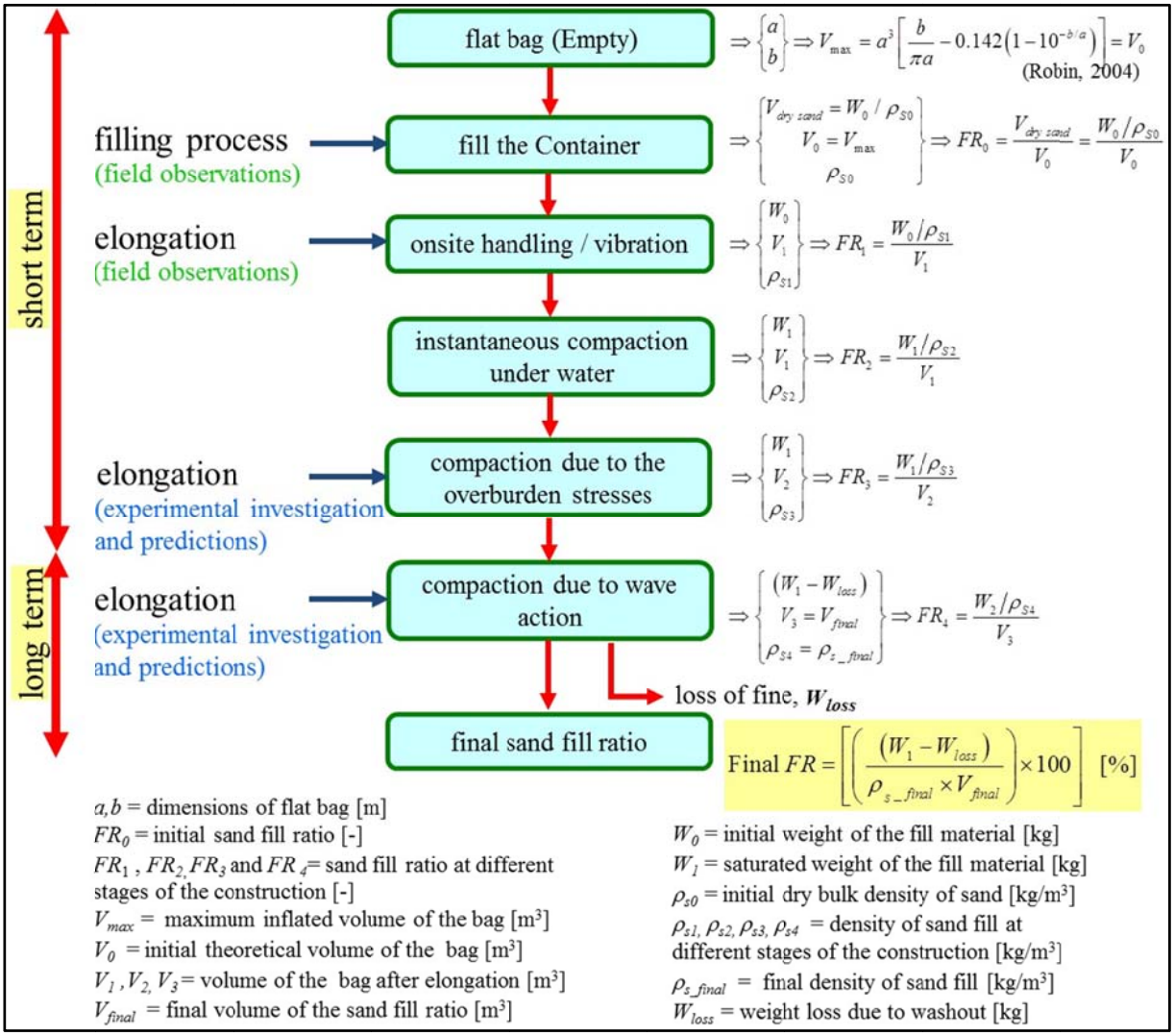

Figure 3-4: Processes influencing the final sand fill ratio of GSCs

Despite the difficulties associated with the deformation of the final sand fill ratio, a methodology to estimate the final sand fill ratio is proposed. This methodology considers the sand fill ratio of GSCs during different phases of construction and while in service (Figure 3-15). As mentioned above, GSCs will undergo some deformations during filling, handling, and the

installation processes. These deformations will result in a lower sand fill ratio compared to the initial value. If GSCs are dropped from a certain height during the installation process, the geotextile will be further elongated due to the impact of the GSC hitting the sea bottom. To date, there are no investigations on the quantification of the deformations of GSCs during the different phases of construction. Sometimes, sand containers are filled "as much as possible" to compensate possible reductions in the sand fill ratio during the construction and the installation processes. On the other hand, larger sand fill ratios will lead to larger sink velocities and might cause bursting of GSCs, when hitting the seabed. Therefore, a good knowledge of the sink velocities and the resulting deformations of GSCs due to the impact with the seabed are necessarily required (see Section 3.2).

3.1.4 Summary of Sand Fill Ratio Study and Concluding Remarks

After an extensive literature study (Dassanayake and Oumeraci 2009a and 2009b), several model GSCs were constructed with varying geometries, geotextile materials and sand fill ratios. The main objectives were to determine practical sand fill ratios and to develop a method to estimate the final external dimensions of a GSC, once the sand fill ratio and the dimensions of empty flat bag is known. The main outcomes of this exercise can be summarised as follows;

- A new definition for the sand fill ratio of GSCs was proposed, following a careful consideration of several parameters and processes that affect the sand fill ratio. The novel definition can be termed as the initial sand fill ratio, which can be used as the representative parameter to describe GSCs. The initial sand fill ratio of a GSC (FR_0) is defined using the fully inflated volume of the empty flat bags ($V_{max}=V_0$) described by the formula (equation 3.1) of Robin (2004) and the dry bulk density of the sand fill (ρ_{s0} = 1480 kg/m^3). Then, by constructing several model GSCs with varying geometries and sand fill ratios, a range of practical sand fill ratios was found. Under laboratory conditions, the sand fill ratio of GSC can be between 80%~120%. Under field conditions, it is expected that sand fill ratios of 90%~100% are feasible (e.g. Oumeraci et al. 2012).
- Two types of nomograms (for nonwoven and woven geotextile) were developed to estimate the final external dimensions of GSCs, once the sand fill ratio and the dimensions of unfilled flat bag is known (see Figure 3-3). However, these nomograms are valid only for the most commonly used length/width ratio of empty bag (length : width = 1.8 : 1.0). This nomogram will assist in the design of future GSC-structures, particularly to estimate the required amount of geotextile for the construction of GSCs and also for the calculation of the required number of GSCs to build a GSC-structure.
- Due to both short and long term processes, the sand fill ratio is expected to change. Most significant processes that contribute to the change of sand fill ratio were identified and the evolution of the sand fill ratio is presented as a flow chart (Figure 3-4).
- A methodology was developed to determine the final sand fill ratio of GSCs under field conditions (see Figure 3-15)

Among the different processes that affect the sand fill ratio, it is expected that dumping and sinking processes of GSCs in water will significantly alter the final sand fill ratio. Therefore,

it was necessary to conduct a series of small scale underwater drop tests with GSCs. Section 3.2 focuses on the underwater sinking behaviour and the deformation of GSCs based on the results of the drop tests. Furthermore, the possibility to develop a methodology to perform dry drop tests and to predict probable deformation caused during the underwater sinking of GSCs are also addressed (see Section 3.2.6).

3.2 Dumping GSCs in Deeper Waters – Drop Test Results

At present, there is a significant increase in near shore and offshore construction works (e.g. artificial reefs, submerged breakwaters). Moreover, there is a high potential for GSCs to be used as scour protection systems for offshore wind power plants (Grüne et al. 2006, Wilms et al. 2011, Oumeraci et al. 2012, etc.). However, there are still several critical issues which require further research in order to further enhance the application of GSCs for fully submerged marine structures. The lack of understanding of the behaviour of GSCs when sinking underwater, the ability to survive from instantaneous loads when GSCs hit the seabed and the final fill ratio after hitting the seabed are the main concerns, when building fully submerged GSC-structures. However, only a very limited amount of research studies are available on the dropping of GSCs in water. Most of the previous studies covered only very large GSCs (≈ 250 m^3) dropped from split bottom barges (e.g. Bezuijen et al. 2000, 2001, 2002a, 2002b, 2004, 2008, De Groot et al. 2003, 2004, Klein Breteler 2001, etc.). Therefore, the present knowledge on the dropping of smaller GSCs in water is relatively poor and a substantially improved knowledge is required for the design of submerged GSC-structures. The main objective of this research study is to fill this knowledge gap. Even rigid objects such as cylinders show highly complex motions, when sinking underwater. However, there is an urgent practical need to improve the predictability of the trajectory, the sink velocity, the final orientation, the impact velocity, and the deformation due to the impact of sinking GSCs in water.

Therefore, investigations were conducted on the variation of the sand fill ratio due to dropping in deeper waters, in addition to that occurring during the manufacturing of GSCs. In order to qualitatively determine the expected deformation and elongation of geotextile materials due to the impact with the seabed, the sink velocity and the sinking behaviour should be studied experimentally (drop tests). These tests also focused on the sinking process and the placing accuracy, in addition to the deformation and the changes in the sand fill ratio.

As this PhD study focuses on developing reliable design tools / simplified formulae for the hydraulic stability of GSC-structures by taking into account the effect of the sand fill ratio, variation of the sand fill ratio during the manufacturing process of GSCs and during the construction of submerged GSC-structures were studied in detail. Furthermore, it was also necessary to determine the sand fill ratios, which were to be tested in hydraulic stability tests. Therefore, the results from the drop tests were directly used for the planning of the hydraulic stability tests (wave flume tests) and the numerical modelling. Apart from that, this study answered some critical issues, which have yet limited the application of GSCs for fully submerged coastal and marine structures. These issues, which play a major role when designing fully submerged structures, are the lack of understanding of the behaviour of GSCs when fall-

ing underwater, the ability to survive from instantaneous loads when a GSC hits the seabed and the final fill ratio after hitting the seabed.

3.2.1 Theoretical Background

A body accelerating in a viscous fluid such as water undergoes several forces that can be categorised in different groups namely; buoyancy, drag force, inertia force and lift force (Figure 3-5). There are two possible approaches to study the fluid–body interaction. The first is to fix the body and let the fluid to flow and the second is to let the body to be moved with six degree of freedom in a fluid. However, according to the literature, even the behaviour of symmetrical bodies such as spheres shows a considerable difference when moving freely in a still fluid and when fixed in a moving fluid. Therefore, the only way to study the sinking behaviour of GSCs is to let them sink in water with six degree of freedom. Furthermore, available literature emphasize the importance of initial conditions to the sinking behaviour. Therefore, initial conditions should be dealt carefully.

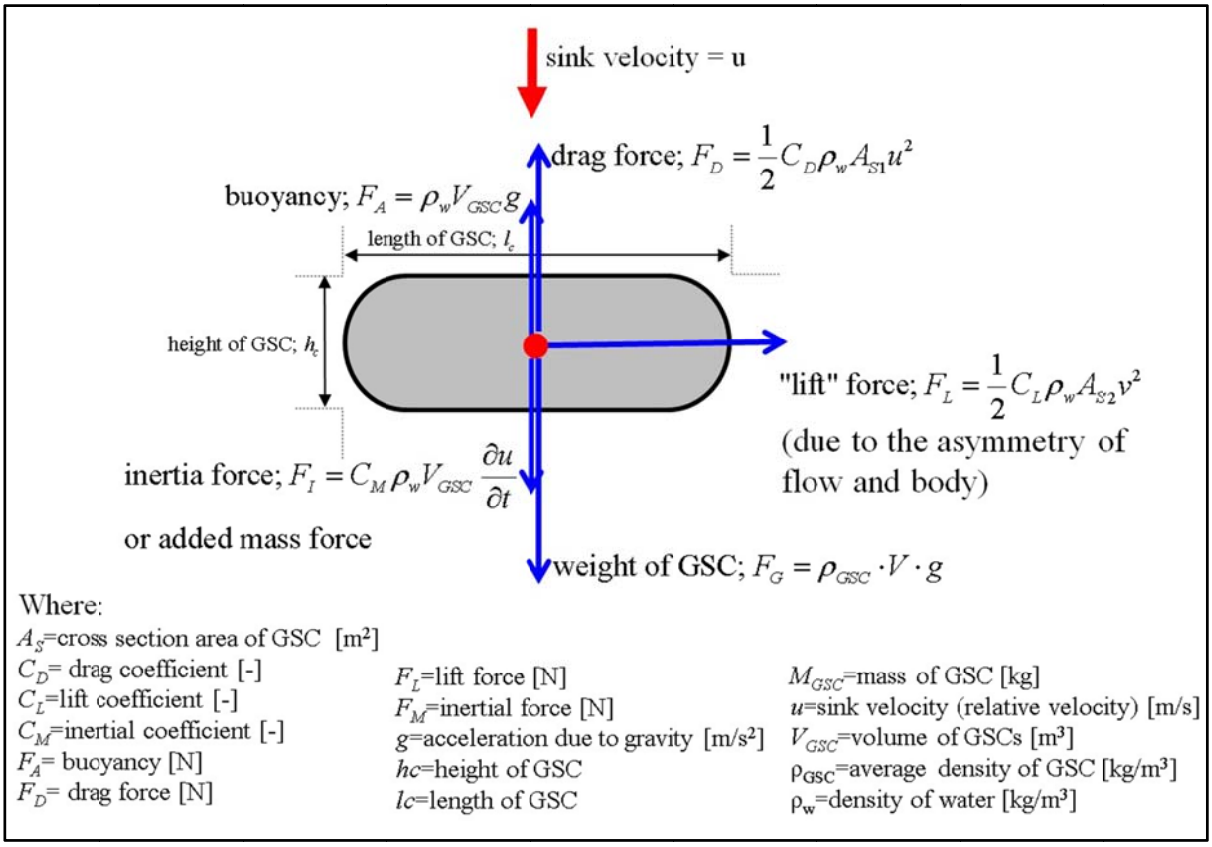

Figure 3-5: Forces acting on a sinking geotextile sand container (GSC) – definition sketch

The flow around a body that is moving through water can be described with the Reynolds number (dimensionless relationship between the inertial force and the viscous force). Reynolds number for the GSCs was defined by Recio (2007) as;

$$\mathrm{Re} = \frac{uD}{\nu} \qquad 3.3$$

Where, u = relative velocity (sink velocity of the body) [m/s], D = length scale of GSC in the flow direction (in Figure 3-5, $D = h_c$) [m], ν = kinematic viscosity of water [m^2/s]

The Reynolds number is used as a criterion to distinguish between laminar and turbulent flow. If the Reynolds number is very small (Re <<1) this is an indication that the viscous forces are dominant in the problem, and it may be possible to neglect the inertial effects; hence the density of the fluid might not be an important variable. On the other hand, for the large Reynolds number flows, viscous effects are small relative to inertial effects and for these cases it may be possible to neglect the effect of viscosity.

Bukreev and Gusev (1996) experimentally studied the motion of a sphere in a fluid due to gravity. Among their findings, the large difference that they observed between the motion of a free sphere and flow passing a fixed sphere at fairly large Reynolds numbers are remarkable. Particularly, it has been found that a freely sinking sphere can deviate from a straight trajectory, and its drag coefficient can exceed considerably that of a fixed sphere (by more than ca. 100%~200%). Furthermore, at Reynolds numbers of the order of 2×10^5, the drag coefficients were greatly reduced. Moreover, the spheres moved rectilinearly, while accelerating along a certain initial section of length. After the initial section, vortex separated from the sphere, and a sudden deflection of the initial dropping axis was observed. They were not able to draw concrete conclusions on the trajectory shapes and rather called them "random"

The motion of a large cylinder sinking freely at large (~10^6) Reynolds numbers were studied in USA through a series of experimental investigations and the results are reported in Chu et al. (2002), Abelev et al. (2003), Holland et al. (2004), etc. Throughout these experiments, number of parameters such as length, weight, centre of mass and nose shape combine with initial orientation (initial inclination angle), releasing height, etc. were varied to estimate the net drag force on six cylinder bodies under different conditions. These bodies were released in air and the underwater motion was studied with video records. During these experimental investigations, abrupt changes in position, orientation and sink velocity were observed, when cylinders, which are released above the water surface separated from a trapped cloud of bubbles. These cloud of bubbles resulted in a less predictable behaviours. These experimental results show nonlinear characteristics of the trajectory patterns and overall, six different trajectory patterns (straight, spiral, flip, flat, seesaw, combination) were detected. The transition between patterns depends on the initial conditions (the drop angle and the initial velocity) and the internal structure of the cylinder. The dynamics of trajectory pattern formation and transition are very complicated. It involves stability, nonlinear dynamics and fluid-body interactions (Chu et al. 2002). This is one of the first attempts to perform a detailed investigation on freely sinking irregular bodies (i.e. cylinders with eccentric mass and different shapes of noses). This research study provides a valuable foundation for the planning of new drop tests (of GSCs) and also warns the possible randomness of the sinking patterns. Moreover, Chu et al. (2004) proposed a set of empirical formulae to calculate the drag coefficient of sinking cylinders. These formulae are based on the Reynolds number, *Re* and the aspect ratio of cylinders.

They enable a direct comparison of the drag coefficients of a cylinder that sinks with six degree of freedom in a fluid and drag coefficients of fixed cylinders in fluid flow. According to the results, freely sinking cylinders resulted in approximately one magnitude smaller drag coefficients compared to a fixed cylinder in a fluid flow (Chu et al. 2005, Dassanayake and Oumeraci 2010a). Even though there are several characteristic differences between these cylinders and GSCs, these publications are helpful to select the most appropriate parameters that affect the sink velocities of GSCs. Further details and implications of these experimental investigations are provided in Dassanayake and Oumeraci (2010a).

Table 3-1 compares the behaviours of rigid and flexible bodies, when dropping from air and sinking in water. Details on the present knowledge on dumping GSCs in water are given in this report as well as in the state of the art of Dassanayake and Oumeraci (2010a). A summary of the most relevant finding of this report is provided in this section.

Table 3-1: Comparison of behaviours of rigid and flexible bodies, when dropping from air and sinking in water

Process	**Behaviour of a rigid body**	**Behaviour of a flexible body**
Releasing	Body will remain in the releasing mechanism, until the full body can move.	Body will starts to deform once the releasing mechanism started to open. When the flexible body leaving out from the releasing mechanism, shape will differ from the initial shape
Sinking in air	No change of the body shape	Body shape will remain the same, because , air pressures too small to change the body shape
Hitting the water surface	Body will hit the water surface causing some damping of its kinetic energy	Considerable amount of kinetic energy will be lost due to damping and deformation of the body
Sinking in water	Since the shape is predictable, sink velocity can be estimated more precisely	Shape of the body will change significantly causing changes in drag, inertia and lift coefficients. Furthermore, the body can absorb water and will release air, so the average density of the body will also be increased.
Trajectory in water	No asymmetry, but still difficult to predict the trajectory due to vortex shedding	Due to the asymmetry of the flexible bodies, it is more difficult to predict the trajectory and they will deviate from the starting vertical axis
Effect due to water pressure	No change of the shape	Water pressure is large enough to change the shape of the body
Hitting the seabed	No change of the shape and depending on the hardness of the seabed, body could bounce or penetrate into the seabed	Body will deform due to the impact

The necessity of improved formulae to estimate the sink velocity of GSCs was discussed in Dassanayake and Oumeraci (2010a). Bezuijen et al. (2000, 2004) developed formulae to estimate the underwater sink velocity of large woven geotextile containers with the sand fill ratios (*FR*) of 50% ~ 70%. These large GSCs contain hundreds of cubic meters of fill material

(generally 100 m^3 ~ 700 m^3) and sometimes referred as "Geotextile tubes". The formulae developed by Bezuijen et al. (2000, 2004) are the only available formulae to estimate the sink velocity and the deviation of GSCs. These formulae were developed based on small scale and large scale experimental investigations. Furthermore, these large GSCs are filled and dropped using split bottom barges and cross section of these containers can be approximated to a cylindrical cross section. In contrast, small GSCs are mechanically filled somewhere outside the construction site and then, moved to construction site and dropped from (or above) the water surface (e.g. by using stone dumping vessel). Therefore, the applicability of the formulae by Bezuijen et al. (2000, 2004) for the calculation of the underwater sink velocity of relatively small GSC with fill ratios of 80% or more is still questionable. Moreover, they used two main assumptions for the derivation of the formulae: GSC keeps its shape throughout the sinking process and GSC is not rotating while falling underwater. However, these assumptions might not be valid for sinking GSCs. Because, GSCs with relatively low fill ratios might reshape during the sinking process and there is a high possibility that GSCs might show rotational motions while sinking with six degree of freedom. As a result, the sink velocities and the drag coefficients will vary during the sinking process. Therefore, when planning new drop tests, it is important to provide a sufficient water depth and space for sinking GSCs to sink freely (e.g. the required water depth and space for a particular GSC to complete its rotation and to achieve a more stable orientation while sinking). If the aforementioned assumptions, which are relevant for large geotextile tubes, are not valid for GSCs, then the only method to find the sink velocities of GSCs is through drop tests (small scale or prototype).

Based on the experimental and field investigations, Bezuijen et al. (2000) argue that due to the small duration that a GSC takes to fall down underwater (few seconds), it will not be possible to fully saturate the GSC. In addition, entrapped air in the sand fill will resist the sand being fully saturated. Furthermore, Bezuijen et al. (2000) assumed that the flow inside the GSC may be described by Darcy's law, even though it might not be directly applicable to flow inside a falling GSC since Darcy's law is valid only for a steady flow.

Figure 3-6 show the most probable saturation process inside the GSC. Since the GSC is moving downward, pressure distribution on the surface of the GSC become more complex and might be influenced by the shape of the container, the sink velocity, etc. Moreover, the saturation process will increase the weight of GSC by occupying the voids. As a result, a wet GSC will move faster than a dry GSC. The weight of a fully dry GSC (density of the fill = 1480kg/m^3, degree of saturation = 0%) will be increased approximately by 18%, once it is fully saturated.

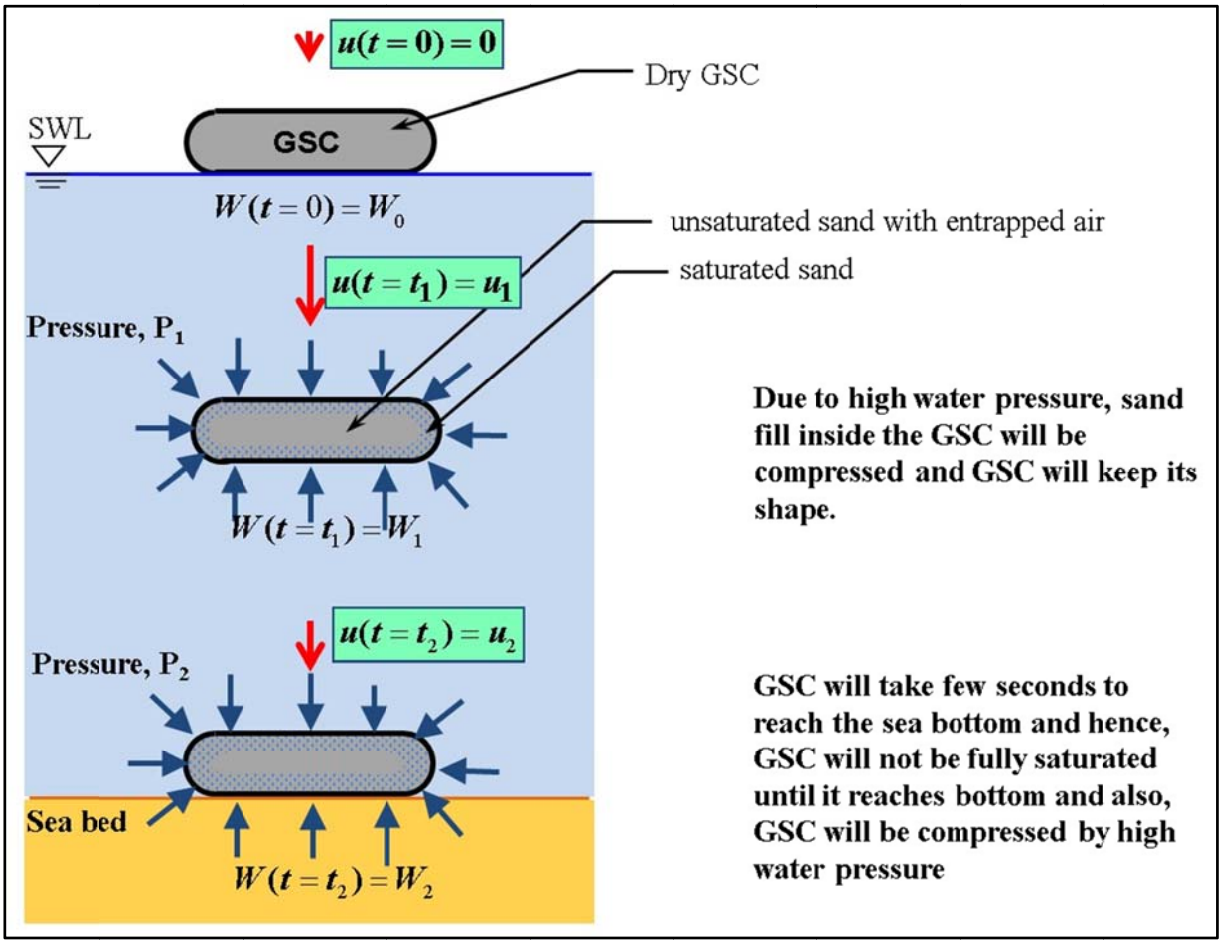

Figure 3-6: Saturation of sand inside a GSC as it falls underwater

Holland et al. (2004) used an analytical approach to derive formulae for the sink velocity of rigid cylindrical bodies. However, the most crucial step is to find the force coefficients. Bezuijen et al. (2000, 2004) suggested a single drag coefficient for "Geocontainers". While, Chu et al. (2004) proposed an empirical formula to calculate the drag coefficient for sinking cylinders. This formula is based on the Reynolds number and the aspect ratio of cylinders. Furthermore, it is expected to observe a reduction in sink velocity as a GSC approaches the bottom. However, a detailed study on flow around the GSC is necessary to describe the physical processes associated in the fluid-body interaction.

The GSC drop tests conducted by Oberhagemann et al. (2006) and Zellweger (2007) on the predictability of the final location of dropped GSCs and on the coverage, when dropped several GSCs as group, are the only references available directly related to the present research study. The quantitative analysis of the experimental data are however, not systematic and detailed enough to come up with conclusive results. Moreover, the target application of GSCs was the construction of river bank protection structures, which are normally constructed on a steep slope than the coastal/marine structures.

3.2.2 Specific Objectives of the Drop Test Study

In order to evaluate the behaviour of GSCs, when sinking underwater and to quantify the deformations of GSCs due to the impact at the seabed, laboratory investigations were conducted. The specific objectives of the experimental investigations were as follows: (i) Systematic study of the underwater behaviour of sinking GSCs and quantification of the impact velocity when hitting the seabed, (ii) Quantification of the subsequent GSC-deformations (iii) Evaluation of the possibility to conduct drop tests under dry conditions and to predict the deformation pattern of GSCs due to underwater dropping based on the results of the drop tests under dry conditions (sinking GSCs in air).

3.2.3 Experimental Setup

Small scale experiments were selected as the most feasible method to study the underwater sinking behaviour of GSCs in water. However, it is not possible to design a small scaled model to accurately simulate all the important engineering properties of GSCs simultaneously. Therefore, a relatively thin nonwoven material (mass = 200 g/m^2) was selected for the small scale model tests. Model GSCs were filled with washed sand (D_{50} = 0.25 mm and no fine materials below 0.10 mm). Three different sizes A_3, A_4, A_5 (Table 3-2) of empty flat bags were used for the drop tests. The sizes of GSCs were defined based on the length/width ratio of empty (flat) bags. The sand fill ratios were defined according to the definition given in Section 3.1 and using equation 3.2. Every different (size) type has been filled with the four different fill ratios (*FR*: 80%, 90%, 100%, 110%) that resulted in twelve different sizes of small scale GSCs (Table 3-2). The sand fill was either fully saturated (saturation = 100%) or completely dry (saturation = 0%). For each sand fill ratio, fully saturated GSCs and fully dry GSCs were prepared. Fully dry GSCs were constructed by introducing a water tight thin polythene layer in between geotextile and the fill material. That leads to an overall amount of 48 different GSCs. However, the aspect ratio (a/b) of all empty bags was kept constant to ca. 1:1.8. The model GSCs were released with three different initial orientations. Preliminary small scale tests were conducted in a 5 m high cylinder with 0.65 m diameter at Leichtweiß-Institute (LWI) and a still water tank at Delft University of Technology (Dassanayake and Oumeraci 2010e). Then a new Underwater Drop Testing Facility (UDTF) was developed/constructed at LWI (Figure 3-7) to systematically investigate the sinking behaviour of GSCs. Detailed tests were conducted at LWI using this newly built UDTF. Underwater motions were captured using two high speed (60 fps) video cameras (Figure 3-7b). In order to provide a precise time reference for the instant of hitting (or in some cases, releasing in water), infrared sensors were also used.

Since the ultimate objective of any scale model testing of a structure is to study the behaviour of the prototype structure, a sound knowledge on the possibilities and limitations of small scale modelling is important. The scaling laws relevant to GSC-structures and the interpretation of small scale model test results are discussed in Dassanayake and Oumeraci (2009a), Dassanayake and Oumeraci (2010e) and Dassanayake and Oumeraci (2011a) in detail. In this section, the drop test results are presented in prototype scale, assuming the mass of a proto-

type GSC is 1000 kg and the Froude similitude. This assumption resulted in three different scales as 1 : 6.77, 1 : 5.56 and 1 : 4.21 for the three sizes of small scale GSCs A_3, A_4 and A_5 respectively. Apart from that, whenever possible, the results are presented with non-dimensional parameters (e.g. Figure 3-11 and Figure 3-13).

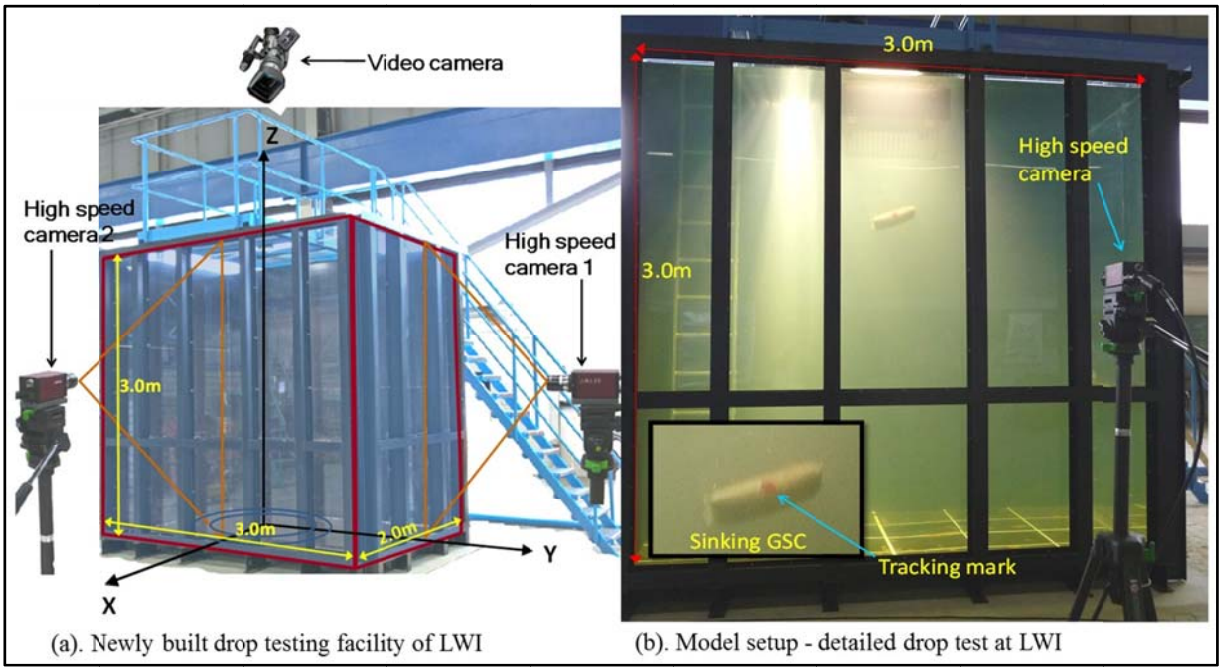

Figure 3-7: Model setup in the LWI Underwater Drop Testing Facility (UDTF)

Table 3-2: Combination of parameters for conducted drop tests

			GSC type (empty bag dimensions)								
			A_3 (a = 0.30m, b =0.18m)			A_4 (a = 0.36m, b = 0.21m)			A_5 (a =0.48m, b = 0.28m)		
		initial orientation of GSCs at SWL	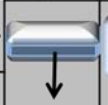								
		sand fill ratio									
Saturation of fill material	0% (fully dry)	80%	x	x	x	x	x	x	x	x	x
		90%	x	x	x	x	x	x	x	x	x
		100%	x	x	x	x	x	x	x	x	x
		110%	x	x	x	x	x	x	x	x	x
	100% (fully saturated)	80%	x	x	x	x	x	x	x	x	x
		90%	x	x	x	x	x	x	x	x	x
		100%	x	x	x	x	x	x	x	x	x
		110%	x	x	x	x	x	x	x	x	x

During the drop tests, high speed cameras were used to capture images during the sinking process with an average of 50 frames per second. Afterwards velocity plots were generated by tracking the movement of GSCs on each frame. The MATLAB code: SPAN 1.3 developed by Dael (2009) was adopted to manually track the movement of GSCs and to generate the velocity plot out of the distance the GSC is moving between two successive frames in order to make sure that the GSCs had the possibility to develop terminal velocity that unaffected by the rota-

tional effects. The depth required to achieve terminal velocity was compared with results of similar tests. When GSCs were sinking in a stable orientation, no abrupt changes in velocity diagrams could be seen, but a smooth increase in velocity.

3.2.4 Sinking Behaviour and Impact Velocity

Since GSCs sink freely with six degrees of freedom, the trajectories are influenced by the different motion patterns and these patterns could become rather random, so that the underwater sink trajectories vary according to the initial orientations. As shown in Figure 3-8, GSCs can rotate around vertical (yawing), transverse (pitching) and longitudinal (rolling) axis. In general, the sinking GSCs show a combination of several motion patterns. Nevertheless, one motion pattern always dominates the sinking process and could be identified as the principal motion. Moreover, even after GSCs hit the bottom, further movements were observed. These near horizontal movements are due to two reasons. First, the horizontal velocity component of GSCs, which results from rotation and oscillation processes, leads to further movement of GSCs near the bottom. Second, GSCs move due to the momentum balance. When a GSC approaches the bottom with an inclination to the horizontal plane, it tends to push water, which is trapped between the GSC and the bed, away during the process of settling down. Consequently, the GSC moves in the opposite direction.

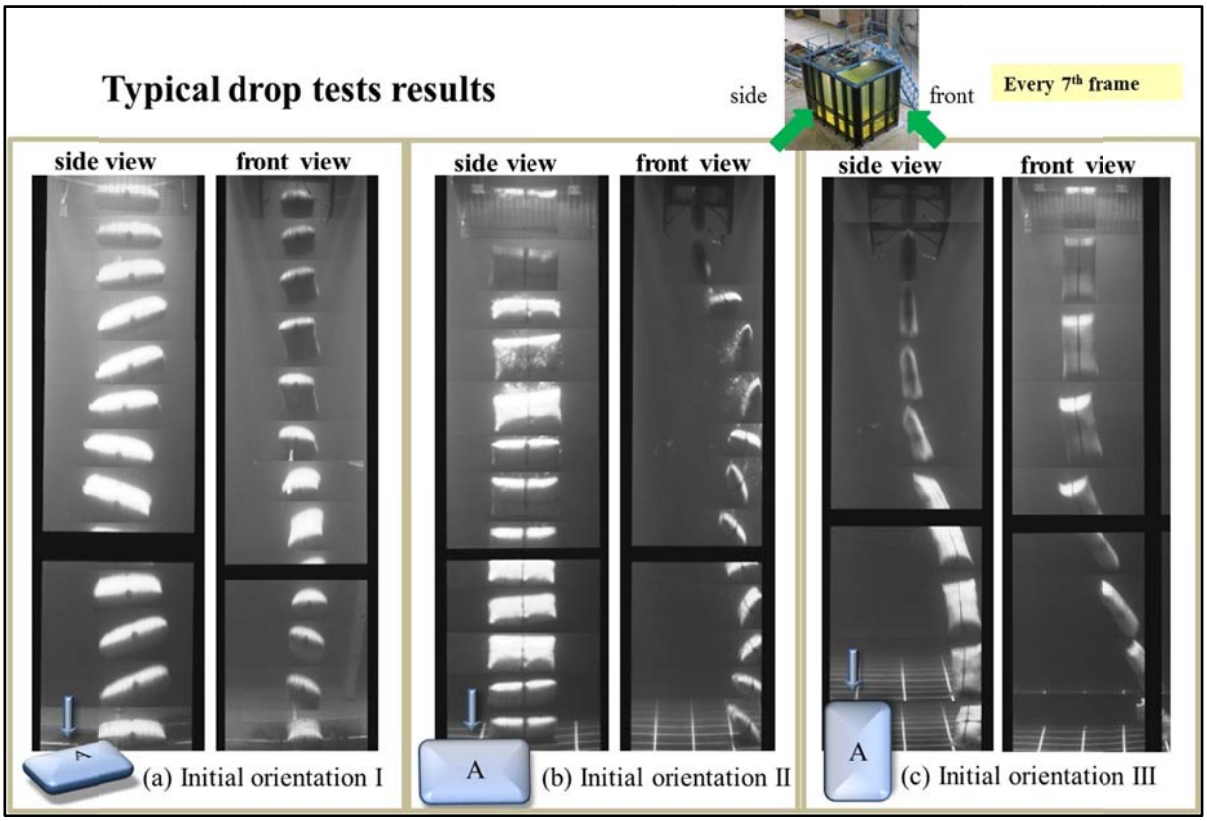

Figure 3-8: Sinking behaviours of dropped GSCs: effect of initial orientation at SWL on sinking patterns

Each drop test was repeated five times to reduce the risk of the results being biased by slight imperfections associated with the initial orientation. Figure 3-8 and Figure 3-9 show exemplary results for the sink trajectories and the sink velocities obtained from the drop tests of a small scale GSCs. The drop test results show that the asymmetry of model GSCs will have a significant influence on the behaviour of sinking GSCs. Moreover, it is extremely difficult to drop the GSC with an exact vertical orientation. Particularly in the case of drop tests, where the direction of movement is perpendicular to the smallest cross section, the GSC will turn about 90 degrees within the first meter of sink. Thereafter, the GSC will sink in its flat position. During the rotation, GSC will be deviated a significant distance horizontally. The analysis has shown that, irrespective of the initial orientation, GSCs sink underwater with their largest cross sectional area perpendicular to the direction of travelling if a sufficient water depth is available. Also, a significant decrease (20 ~ 50 %) in sink velocity was observed near the bottom and just before hitting the seabed. In the case of the largest model GSCs (dry GSC mass = 10.57 kg), final velocities were less than 0.8 m/s, which is equivalent to about 1.64 m/s in prototype scale when a 1000 kg prototype GSC is considered (scale 1 : 4.21). Hence the final velocity is significantly smaller than what was initially assumed (Figure 3-9).

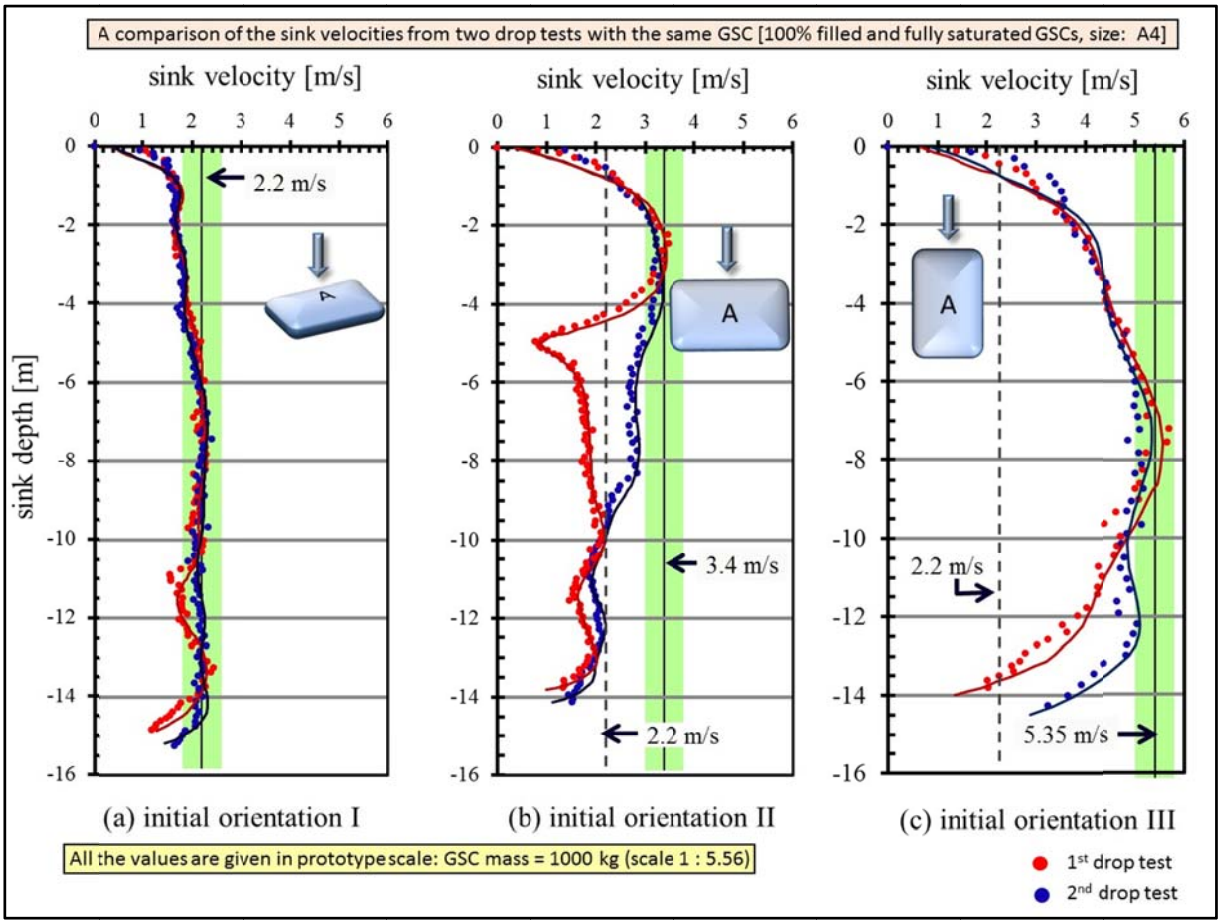

Figure 3-9: Terminal velocity of dropped GSCs with different initial orientations at SWL

Four different velocity phases during the sinking process could be identified. First, the GSC accelerates until the terminal velocity, then it sinks with the terminal velocity while keeping

its position stabile. However, after some distance, probably because of asymmetry of GSC, in several tests, the GSC changes its orientation (Figure 3-8b and c) and in some cases, shows an oscillatory motion while sinking (Figure 3-8a). As a result, sink velocity will also changes during this phase. Finally, when the GSC approaches the bottom, it slows down as shown in Figure 3-9.

Then by analysing the video records of the sinking GSCs, the depths until which GSCs were sinking while keeping their initial orientation were identified and their terminal velocities were tentatively determined using velocity plots. In order to make sure that each GSC had the possibility to reach its terminal velocity during this period, velocity plots were carefully examined and the depths required to achieve terminal velocities were compared with the results of similar tests and then, terminal velocities were finalised. Here the terminal velocity was defined as the maximum velocity at which a GSC sinks without showing any rotational motion. During the analysis, it was observed that the GSCs dropped in "initial orientation II" rotate very quickly into "orientation I" (see Figure 3-8). These changes in orientation lead to a significant decrease in sink velocity, because of the increase of cross sectional area perpendicular to the direction of movement. Hence, these GSCs did not have sufficient duration to reach their terminal velocities. Therefore, the analyses of terminal velocity were performed only for "initial orientation I" and "initial orientation III", which are relatively more stable (More details can be found in Dassanayake et al. 2011b).

Figure 3-10 compares the terminal velocity results from the model tests. Here, only the terminal velocities for "initial orientation I" is shown and for two saturation levels; 0% and 100%.

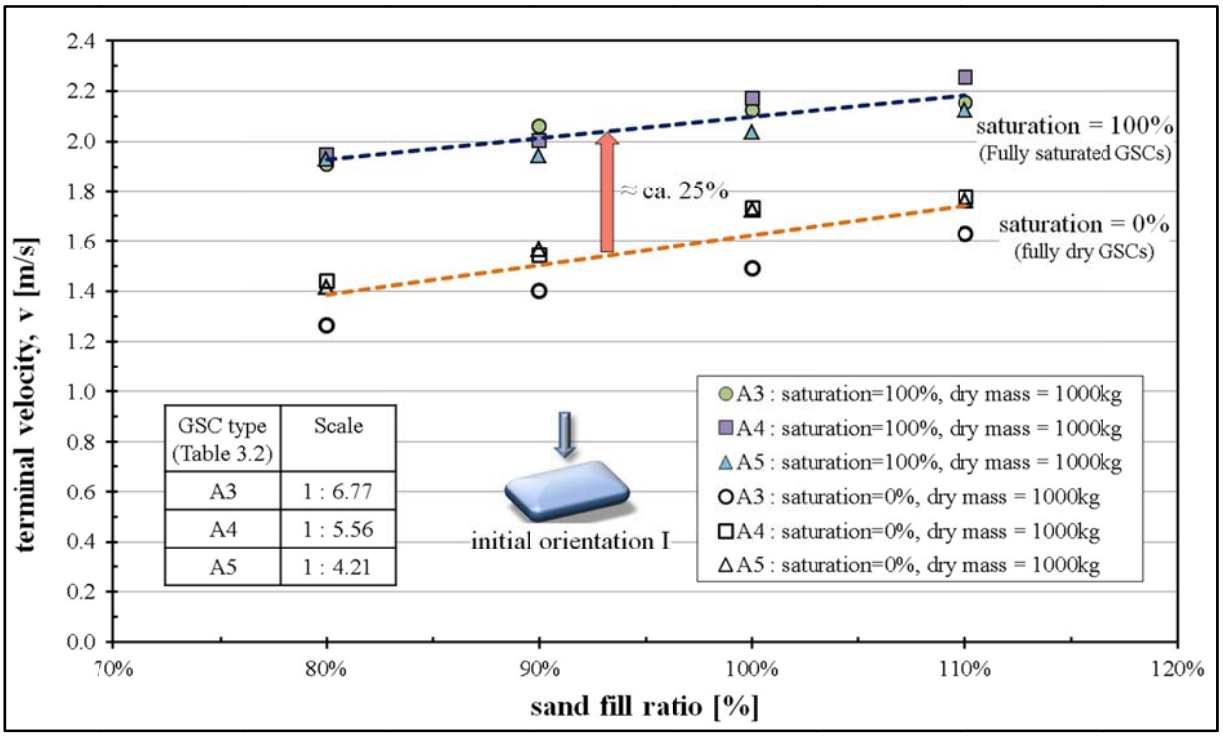

Figure 3-10: Comparison of terminal velocities of sinking GSCs with different sand fill ratios (result are shown in prototype scale assuming the mass of a 100% filled and fully saturated GSC is 1000 kg)

From the four different tested sand fill ratios (80%, 90%, 100%, and 110%) in 24 different testing scenarios, it was observed that the terminal velocities increase with increasing sand fill ratios (i.e. with decreasing cross sectional area perpendicular to the direction of sinking, see Figure 3-9). Furthermore, as shown in the figure, full saturation results in ca. 25% higher terminal velocities than fully dry GSCs. Figure 3-10 confirms the accuracy of the velocity measurements. These velocity measurements were later used for the calculation of drag coefficient of sinking GSCs.

The geometry of GSCs influences the underwater sinking behaviour and the development of terminal velocity as shown in Figure 3-9. When a GSC is moving at its terminal velocity in a steady vertical path, both inertia force and lift force (Figure 3-5) become zero and force balance reduced to equation 3.5, where only unknown is the drag coefficient (C_D).Therefore, for the calculation of drag coefficient, the forces acting on the GSCs in the state of terminal velocity in vertical direction were used. Lift force and inertia force were not taken into account, and no rotations of GSCs were assumed, when GSCs have reached terminal velocity. Although in reality inertia and lift forces cannot be fully omitted from the force balance. Therefore, the calculated drag coefficient might still contain the effect of inertia and lift forces.

$$(\text{drag force; } F_D) = (\text{weight of GSC; } F_G) - (\text{buoyancy; } F_A) \tag{3.4}$$

$$\frac{1}{2} C_D \rho_w A_{S1} u_T^2 = \rho_{GSC} V_{GSC} g - \rho_w V_{GSC} g$$

$$C_D = \frac{2 \times (\rho_{GSC} V_{GSC} g - \rho_w V_{GSC} g)}{(\rho_w A_S u_T^2)} \tag{3.5}$$

A_s = area perpendicular to the direction of travelling [m^2], C_D = drag coefficient [-], g = acceleration due to gravity, V_{GSC} = volume of GSCs [kg/m^3], ρ_W = density of water [kg/m^3], ρ_{GSC} = density of GSCs [kg/m^3], u_T = terminal velocity [m/s],

Finally, drag coefficients of GSCs were calculated from the model test results and values are shown in Figure 3-11.

- "initial orientation I" (when GSC dropped with its largest cross section parallel to the water surface): drag coefficients are comparable to that of fixed smooth cylinders in a steady flow (C_D = 1.0 ~ 1.2) for the tested Reynolds numbers ($Re = 2.0\times10^4 \sim 1.5\times10^5$ with Re; defined using the sink velocity, u and the length scale of GSC in the sinking direction, D).
- "initial orientation III" (when a GSC dropped with its smallest cross section parallel to the water surface): drag coefficients were between 0.6 and 1.2, which are higher than that of a fixed smooth cylinder in a steady flow for the associated Reynolds numbers $Re = 4.0\times10^5 \sim 1.5\times10^6$.

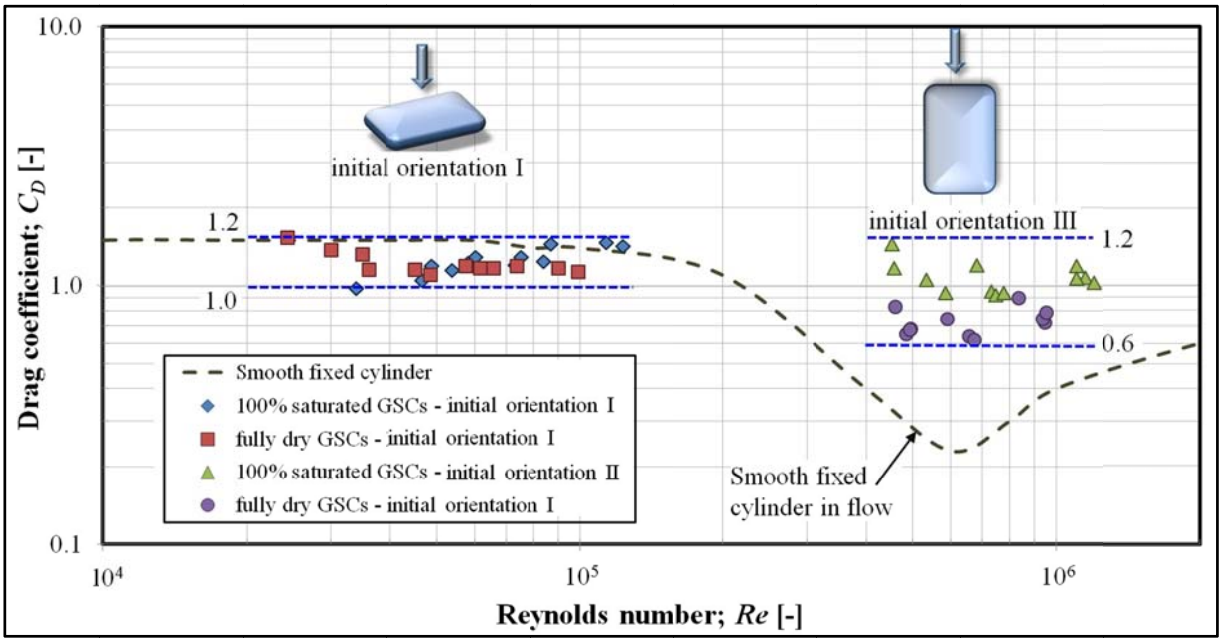

Figure 3-11: Drag coefficient C_D of freely sinking GSCs versus Reynolds number, Re

Apart from the sink velocities, the displacements of GSCs from the initial dropping axis, when they dropped in deeper water were also studied. As shown in Figure 3-12, placing accuracy of GSCs is higher, when GSCs are dropped with their largest cross sectional area parallel to the water surface. For example, 0.36 m long GSCs showed an average deviation of less than 50 % the container length from the initial dropping axis, when sunk about 8 times the container length. Other initial orientations resulted in much larger deviations (see Dassanayake et al. 2011a, 2011b for further details).

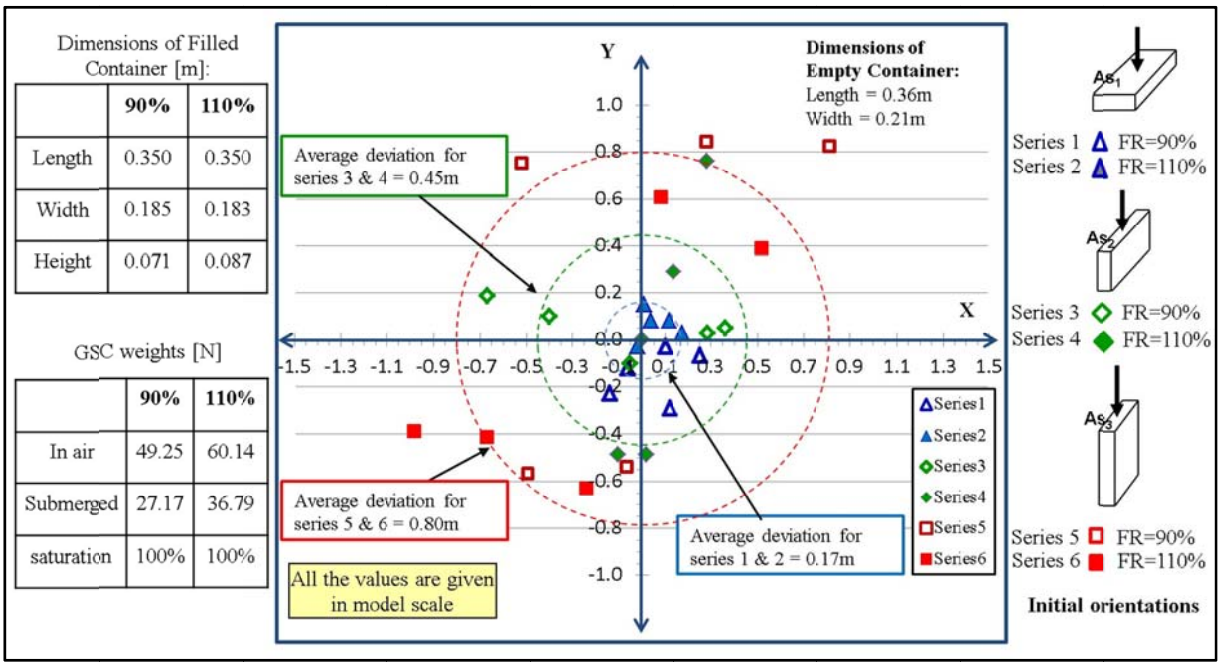

Figure 3-12: Deviation of the GSCs from the initial dropping axis (exemplary for GSC type A4)

Since 3 types of GSCs were used in the experiments, all the results were plotted together by introducing two non-dimensional parameters: relative sink depth and relative deviation. Here, the vertical sink depth was divided by GSC lengths (l_c) to find the non-dimensional relative depth and also, the deviations were divided by the GSC lengths (l_c) to obtain the non-dimensional deviation. Figure 3-13 shows a relative deviation of GSCs from their initial dropping axis for 3 relative depths. Even though, the sink trajectories are random, similar to Figure 3-12, general trend of spreading is clearly visible. From the three different tested relative depths (i.e. 5.9, 7.9 and 9.4) in 48 different testing scenarios, it was observed that the mean relative deviations (mean values of five repetitions with the same GSC) increase with increasing relative depths. When a GSC released with initial orientation I, even it sinks ca. 10 times its length, all deviation values are within one container length. However, if a GSC released with initial orientation III, it can move horizontally up to a maximum distance of ca. 5 times the container length from the initial dropping axis with a sink depth of 10 container lengths.

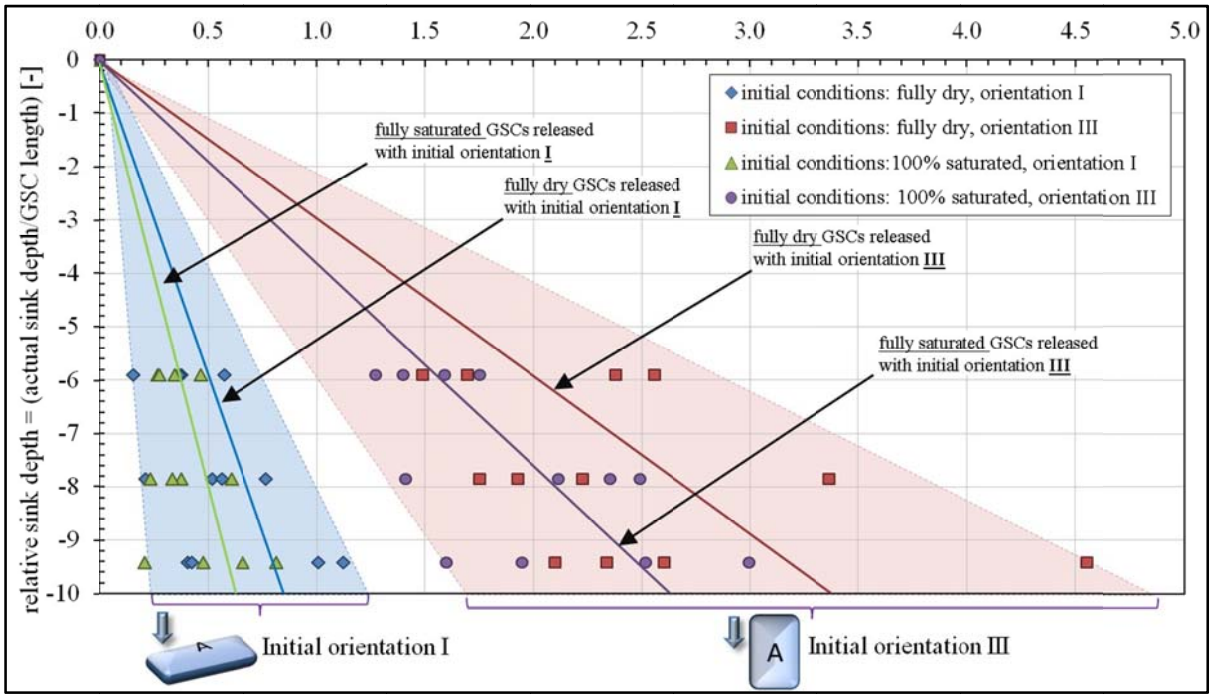

Figure 3-13: Mean relative deviation of dropped GSCs from the initial releasing axis

3.2.5 Changes in the Sand Fill Ratio

One of the main objectives of the drop tests was the quantification of the GSC-deformations during the filling process and due to the impact when GSCs hitting the seabed. From each GSC, two sets of elongation measurements were taken. The first set of measurements was taken right after the filling (elongation of geotextile due to construction, filling, and handling) and closing the GSCs and the second set of measurements was taken after the drop tests (elongation of geotextile due to dumping and hitting the seabed). Then, using all the deformation measurements, the new fully inflated volume was calculated using the Robin's (2004)

formula (see Figure 3-2 and equation 3.1). Among the different sand fill ratios tested, 90 % filled GSCs showed the lowest deformation during filling process as well as after performing several drop tests (Figure 3-14). However, the deformations due to filling and handling processes were observed to be much larger compared to the deformation due to the impact with the steel bottom of the drop testing facility (UDTF), after a drop test. The elongation measurement after the first drop tests with each small scale GSC (type A3, A4 and A5) showed almost no difference compared to the initial measurements. Therefore, the final deformation measurements (Table 3-3) were taken after 15 drop tests with three different initial orientations (see Table 3-2). Therefore, the deformations shown in Figure 3-14b cannot be quantitatively extrapolated to the prototype scale, rather only qualitatively conclude that the 90% (initial *FR*) filled GSCs show less deformation. Moreover, A4 (scale 5.56/medium) and A5 (scale 4.26/large) shows considerably different deformations. Type A5 (large) GSCs showed in average 8.5% larger deformation compared to type A4 GSCs (medium). Since both types of GSCs were manufactured using the same type of geotextile material, this difference might provide an indication on the importance of the tensile strength of geotextile material to avoid excessive deformation. For example, the ratio between the weight of GSCs and the maximum tensile strength of the bag material might be a relevant parameter to address the deformation of GSCs. However, the data from the model tests are not sufficient to come up with a conclusion. Nevertheless, the final deformation measurements provide valuable information regarding the changes in the sand fill ratio during the tests. Finally, these elongation measurements and the expansions of fully inflated volume of GSCs will enable the estimation of the average error (Table 3-3) concerning the sand fill ratio (only due to the elongation of the geotextile material).

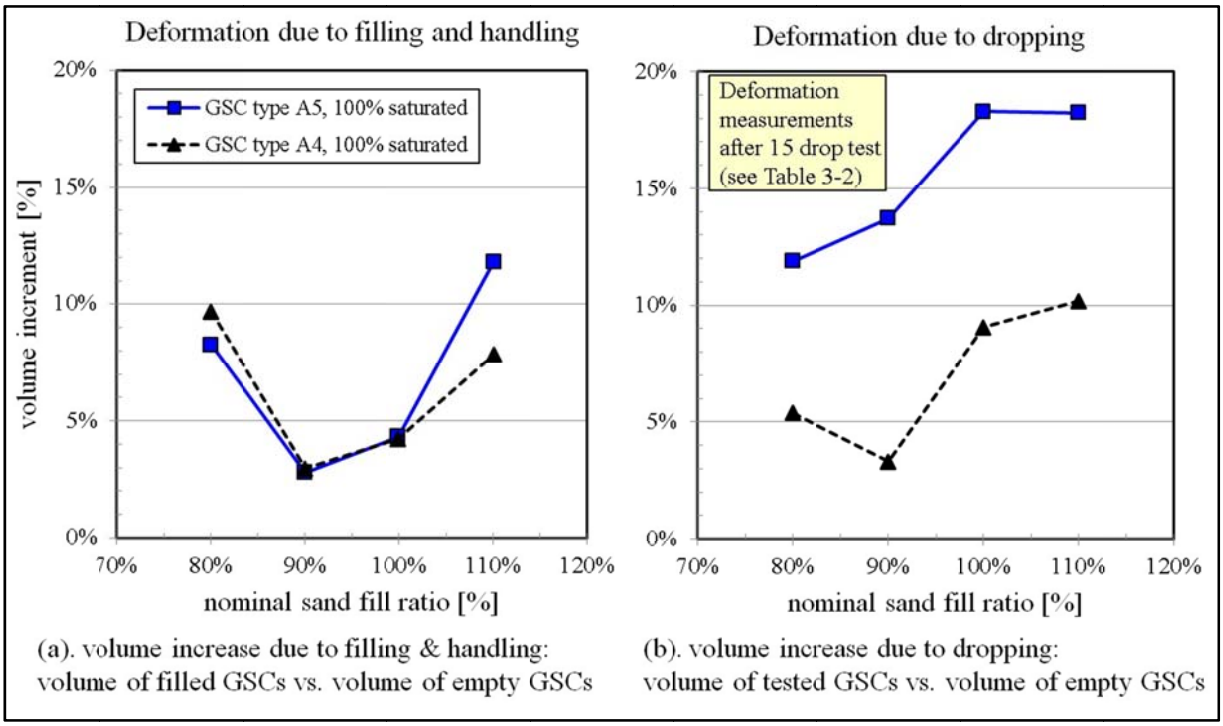

Figure 3-14: Increase of fully inflated volume of GSCs due to the elongation of geotextile material (see Table 3-2 for definition of type A4 and A5)

Table 3-3: change in sand fill ratio (FR) of type A_5 GSCs due to the elongation of geotextile material

GSC Mass [kg]	Initial FR based on fully inflated volume (before elongation) and actual GSC mass	FR after filling and handling in the lab	Final FR after small scale drop tests (after 15 drops)
10.57	80%	73%	65%
11.89	90%	87%	76%
13.22	100%	95%	80%
14.54	110%	97%	82%

Based on the small scale experimental result, (section 3.1 and 3.2), final sand fill ratios of 80% and 100% were selected for the hydraulic stability tests. If a GSC filled initially with 90% (initial FR = 90%), then, after the deformations due to filling, handling and installation, final fill ratio might be ca. 80%. Also, 80% is the most commonly used sand fill ratio for GSCs (Pilarczyk 2000, Oumeraci and Recio 2010, PIANC 2011). Moreover, if a GSC is filled more than 110%, then the final sand fill ratio will be ca. 100%. Therefore, 80% and 100% sand fill ratio were selected as they are more realistic values. Apart from that, it was required to have a significant difference between the two selected sand fill ratios due to the scale of the model tests (hydraulic stability tests, Section 3.4).

3.2.6 Tentative Method to Predict the Final Sand Fill Ratio

Based on small scale experimental results, a tentative method to predict the final sand fill ratio of GSCs is proposed. The main processes that influence the final sand fill ratio are categorised as short term and long term processes and the current research focuses only on the short term processes. Figure 3-4 outlines the key processes and the tentative methodology to predict the sand fill ratio and each of these processes are explained in Figure 3-15. Before starting any project, it is necessarily required to determine the actual mass, the expected dimensions and the target sand fill ratio of the prototype GSCs to be used for the planned GSC-structure. Once the required mass of the prototype GSC is defined based on hydraulic stability requirements, the dimensions of the empty bag, which will result in the desired GSC (with the correct sand fill ratio and the external dimensions), can be calculated as explained in sections 3.1.1 and 3.1.2. Apart from that, the only other method to find the final dimensions of GSCs is to construct prototype containers and to perform measurements. The necessary guidance to perform these field investigations are also summarized in Figure 3-15.

Since, GSCs will undergo some deformations starting from the filling process till the installation, it is necessary to carryout field investigation with sample prototype GSCs in order to quantify the deformations during the different phases of construction. The construction method of these prototype GSCs should be representative for the actual construction method, which will be adopted. Both geotextile material and fill material should be similar to the material which will be used in the project. The final dimensions of the GSC will be taken by placing the prototype GSC on a hard flat surface. In order to determine the final dimensions,

at least five longitudinal and cross sectional profiles should be taken. The deformation can be measured using a GSC with a grid system drawn on the surface of a GSC before filling and measuring the deformations of GSC by referring to the initial grid system without deformation. It is necessary to construct at least five GSCs to obtain different measurements since there is always an uncertainty associated with the geometry of GSCs. In case of deep water installation, it is important to predict the final deformation due to the impact with the seabed. This can be achieved by performing dry drop tests and few underwater drop tests discussed in Figure 3-15. Finally by adding all the deformation and compaction of the fill material, those result in during different phases of the construction, the sand fill ratios of GSCs in a newly constructed coastal/marine structure can be found. However, the final sand fill ratio also depends on the long term effects such as washout of fine particles, creep of geotextile, etc.

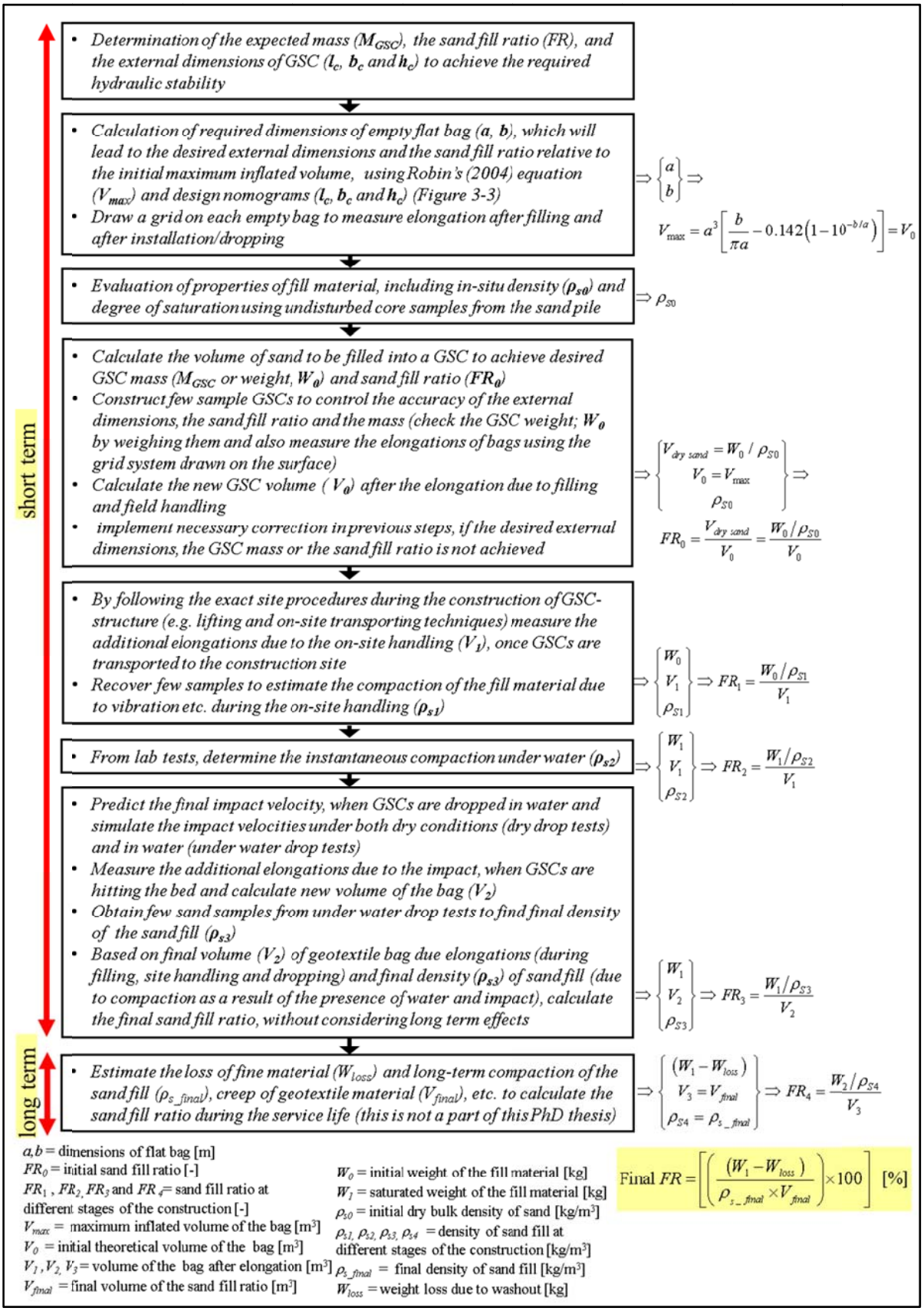

Figure 3-15: Proposed methodology to for the determination of the final sand fill ratio

3.2.7 Summary of Drop Test Results and Concluding Remarks

Within the framework of this study, a new Underwater Drop Testing Facility (UDTF) was developed and constructed at LWI to methodically investigate the sinking behaviour of GSCs. The main design concerns, when planning fully submerged GSC-structures in deeper waters such as sink velocities, spreading of GSCs when released from the water surface, deformations caused from filling, handling and due to instantaneous loads when hitting the seabed were studied and the most significant results can be summarised as follows.

- The sink trajectories and the deviations from the initial dropping axis in still water, mainly depend on the initial orientation of the GSCs. When a GSC dropped with its largest cross section parallel to the water surface, it deviates only 0.2 ~ 1.2 GSC lengths after it sinks 10 times its length, while other initial orientations result in much larger deviations, which could even reach 5 GSC lengths.
- Fully wet GSCs (100% saturation) showed about 25% higher sink velocities than those with fully dry GSC (0% saturation).
- Near the bottom (when the distance between the GSC and the bottom is less than ca. 0.5 GSC length), a significant decrease (20~50%) in sink velocity was observed just before hitting the seabed
- Based on the terminal velocity results of two different initial orientations, the behaviour of drag force against the Reynolds number was studied. Drag coefficients for "initial orientation I" (when GSC dropped with its largest cross section parallel to the water surface) are comparable to the drag coefficient of a fixed smooth cylinder in a steady flow ($C_D = 1.0 \sim 1.2$) for the tested Reynolds numbers $Re = 2.0\times10^4 \sim 1.5\times10^5$ with Re defined using the sink velocity, v and the length scale of GSC in the sinking direction, D. However, when a GSC dropped with its smallest cross section parallel to the water surface (initial orientation III), it shows drag coefficients between 0.6 and 1.2, which are higher than those of a fixed smooth cylinder for Reynolds numbers $Re = 4.0\times10^5 \sim 1.5\times10^6$.
- The deformation measurements were carried out for all the GSCs with sand fill ratios 80%~110%. The results show that 90% filled containers are insensitive to deform due to filling process and due to the impact on the bottom of the drop test tank, when dropped in deeper water. The small scale model test results show that GSCs can enlarge by 3% ~ 12% during the filling process (due to the elongation of the geotextile material). Furthermore, dropping in deep water could further elongate the geotextile (after 15 drop tests, the small scale GSCs showed further 3% ~ 18% expansions).
- The ratio between the weight of GSCs and the maximum tensile strengths of the bag material (geotextile) could be a relevant parameter to determine the degree of deformation during the construction and the installation process of GSCs. However, this could only be confirmed by prototype tests, because the tensile strength of the geotextile material cannot be properly scaled down to a small scale.
- Finally, a comprehensive methodology to determine the final sand fill ratio of a GSC is developed by considering all relevant processes associated with the construction of GSC structures, which can be applied in practice (Figure 3-15).

However, due to the limitations of small scaled models to accurately simulate all the important engineering properties of GSCs simultaneously and to simulate field construction methods (filling, handling, dumping, etc.) inside a laboratory, the performance of tests under prototype conditions will be required to validate the results of this study.

3.3 Interface Friction Properties of GSCs – Pullout Test Results

The interface friction between GSCs has been identified as one of the most important factors contributing to the hydraulic stability of GSC-structures. Also, the interface friction properties of GSCs are different from the results of direct shear tests (shear box) conducted only with sample geotextile materials (see Section 2.2.2). Therefore, a proper investigation on this topic is essential for a proper understanding of the hydraulic stability of GSC-structures.

The results of numerical modelling of Recio (2007) using the weakly coupled modelling system "COBRAS/UDEC" well illustrated the importance of the interface friction between GSCs. Also, the formulae suggested by Recio (2007) already account for the interface friction between GSCs. The derivation and the validation of the formulae were performed based on the results of the direct shear tests, which were carried out with the conventional shear box apparatus with dimensions of 0.30 m x 0.30 m. However, the recent large scale experiments (Lohani et al. 2006, Krahn et al. 2007, Matsushima et al. 2008) provide a better understanding of interface friction properties of sand bags. However, those studies showed that the estimations of interface friction between sand bags using direct shear test results with geotextile samples are not accurate enough to determine the interface friction characteristics of GSCs. Therefore, more investigations should be conducted to understand the friction between GSCs and its effect on the hydraulic stability of structures made of GSCs. Furthermore, the lateral displacement of GSCs made of geotextile with different friction properties should also be examined. With more insight into the interface friction of GSCs gained from specific experimental investigations, the findings can be used to improve the existing numerical modelling system (CFD-CSD) and the process-based hydraulic stability formulae of Recio (2007).

Moreover, the work of Matsushima et al. (2008) shows the importance of more investigations on the hydraulic stability of GSCs stacked with some inclination towards the structure core, so that the effect of friction for such a configuration also need to be examined.

According to literatures, pullout tests were conducted for different structures such as rocks, artificial armour units, etc. and in most of the cases, pulling out forces perpendicular to the slope was measured (e.g. Hald and Burcharth 2000, Muttray et al. 2005, Wang and Peene 1990).

Furthermore, Latham et al.(2008) used a DEM code to simulate the pullout tests of Hald and Burcharth (2000) and observed the similar distribution of pullout forces to the experimental results of Muttray and Oumeraci (2005). Therefore, it might be possible to use pullout force results to validate numerical models up to some extent. The lack of data for the displacement rate of armour units was the main obstacle to validate the numerical model of Latham et al.

(2008). Therefore, it is important to measure both the pullout forces and the displacement rates of GSCs.

This section summarises the key results of pullout tests, which are described in more details in Dassanayake and Oumeraci (2010d).

3.3.1 Main Objectives of GSC Pullout Test

The main objective of these tests is to study the effects of engineering properties of GSCs on the pullout forces of GSC-structures, with a special attention to the sand fill ratio. In order to achieve this goal, the effects of the following factors on the pullout forces were examined through a series of scale model tests: sand fill ratio of GSC, friction properties of geotextile material, seaward slope (overlapping length), and stacking method of GSCs. Apart from the determination of the influence of engineering properties of GSCs on the pullout forces, the specification of the required parameters for the numerical modelling of submerged GSC-structures represents a further objective of the pullout tests.

3.3.2 Experimental Setup and Test Programme

The pullout tests were conducted by constructing different GSC-structures in the 1 m wide LWI-wave flume (1 m wide and 1.25 m height). GSC models were constructed with five sand fill ratios; 80 % (mass = 11.18 kg), 90 % (mass = 12.58 kg), 100 % (mass = 13.98 kg), 110 % (mass = 15.39 kg), 120 % (mass = 16.80 kg) and two types of geotextiles, a woven and a nonwoven, were used during the manufacturing of model GSCs. The woven geotextile showed a friction angle of 13.33^0 (tan Φ=0.237), and the nonwoven material showed an angle of 22.62^0 (tan Φ=0.417) during underwater direct shear tests with standard shear box.

The dimensions of the empty flat bag were as: a = 0.50 m (length) and b = 28 m (width) to achieve a target size of 0.50 m long model GSCs. Then the GSC length l_c of an 80% filled GSC, is twice as large as its width ($l_c/b_c = 2$) and five times as large as its height ($l_c/h_c = 5$)(Figure 3-1b). Since nonwoven geotextile has higher elongation properties, nonwoven containers can be filled up to 120 % of the initial volume, whereas containers with woven geotextile materials can only be filled up to 110 % due to their limited elongation capability. After each pullout test, deformations of GSCs were checked and if GSCs were significantly deformed (i.e. if the deformation of any grid line is more than 10% it's original length) they were not reused and new GSCs were constructed. However, each test configuration was repeated at least five times and all the results were taken into consideration during the analysis.

The height of GSC-structures was varied depending on the model configuration. GSCs were pulled using an electric motor that has a capability to adjust the pulling speed (Figure 3-16). GSCs were modified by attaching a horizontal pipe made of the same geotextile material at the front side of GSC, which can accommodate a steel rod (Figure 3-17). This rod and the electric motor were connected using light weight steel cables. The pullout forces were measured using a force transducer (Figure 3-16) connected to the cables and GSCs were tested

only for steady pullout forces. The movement of GSCs under the pullout forces was measured using a displacement transducer (Liner Variable Differential Transformer, LVDT). The LVDT was connected with a light weight sliding frame attached to the back side of the container. This attachment provided more precise measurements of the movement of the container and the measurements are assumed to be free from errors caused by the deformations of the GSC caused by pullout force.

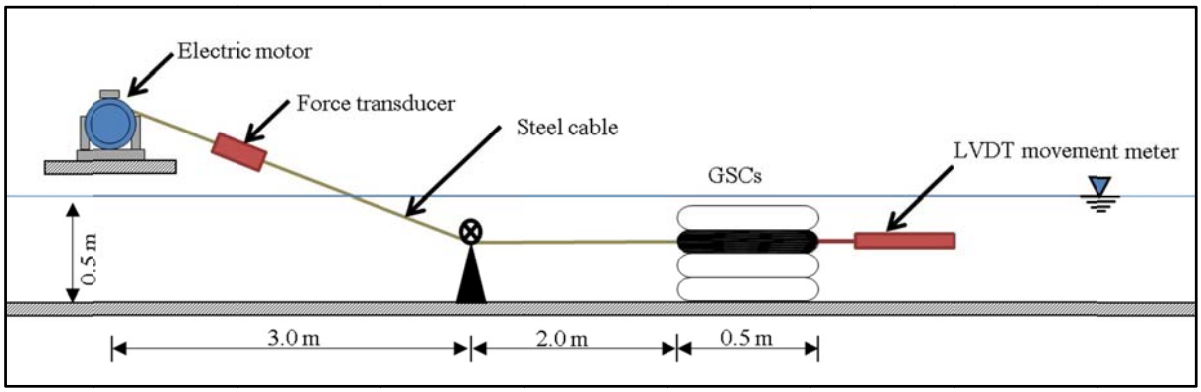

Figure 3-16: Experimental setup for pullout tests (note: all dimension in meter)

As aforementioned, GSCs with five fill ratios were tested in 96 different testing scenarios (Table 3-4). Each test configuration was repeated at least five times and all the results were taken into consideration during the analysis. In most cases, there were variations in the measured pullout forces. However, the general trends were clearly visible. Several explanations were found for the variations in the pullout force measurements. First, the pullout forces depend on the geometry of the interface between GSCs (e.g. longitudinal and lateral profile of GSCs at the lower layers, curvature of the GSCs, friction effects from two side by side neighbouring GSCs).

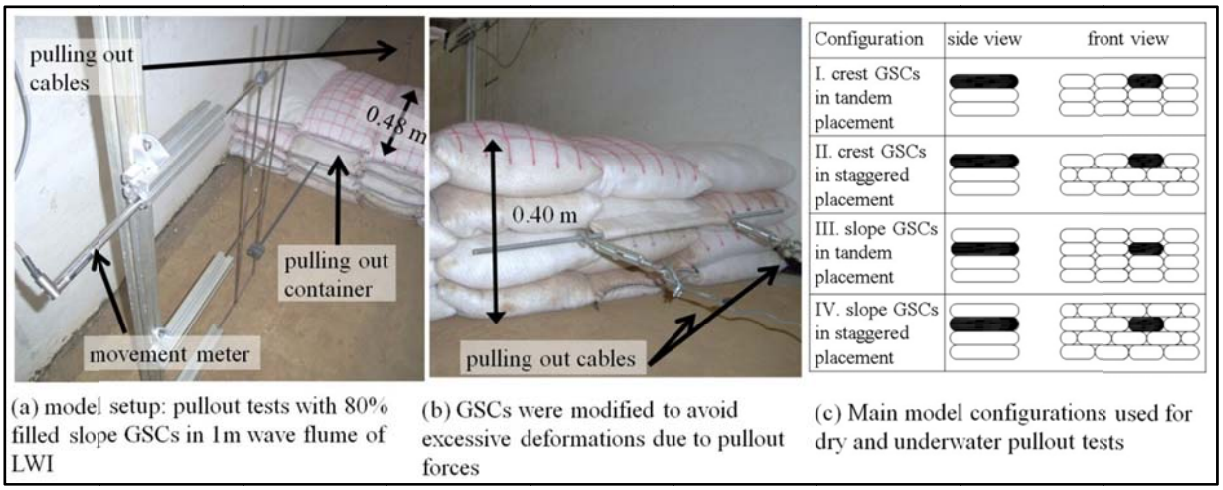

Figure 3-17: Front and rear views of the model with four model configurations for pullout tests

The friction properties (friction angel / friction coefficient between geotextile-geotextile interface) of geotextile materials are generally measured using small shear box tests (direct shear

box apparatus) and the tests are generally performed under dry conditions. In order to extrapolate the friction parameters obtained through small shear box tests to describe the interface fiction properties of GSCs, it is necessary to find a relationship between those two parameters. Therefore, the pullout tests were initially conducted under dry conditions (dry tests) and then, the calculated pullout forces based on friction angles obtained during the small shear box tests and the actual pullout force measured during the experiments were compared. Afterwards, most of the dry pullout tests were repeated underwater (wet tests / see Table 3-4) and the results were compared again to study the effect of the presence of water on the interface friction properties of GSCs (wet tests). Most of the results presented in this chapter are from underwater (wet tests) pullout tests and further information/results can be found in Dassanayake and Oumeraci (2010d).

Table 3-4: Testing programme for pullout tests (see Figure 3-17 for model configuration I~IV)

	seaward slope angle [deg]	45°	90°		45°	90°	
	inclination angle of GSCs [deg] / sand fill ratio	0°	0°	-15°	0°	0°	-15°
nonwoven geotextile* (dry and underwater)	80%		I,II,III & IV			I,II,III & IV	
	90%		I,II,III & IV			I,II,III & IV	
	100%		I,II,III & IV			I,II,III & IV	
	110%	I & III	I,II,III & IV		I & III	I,II,III & IV	
	120%	I & III	I,II,III & IV		I & III	I,II,III & IV	
woven geotextile** (dry)	80%		I,II,III & IV	I,II,III & IV		I,II,III & IV	I,II,III & IV
	90%		I,II,III & IV			I,II,III & IV	
	100%		I,II,III & IV	I,II,III & IV		I,II,III & IV	I,II,III & IV
	110%		I,II,III & IV			I,II,III & IV	
	120%	-	-	-	-	-	-
		slope container (S)			crest container (C)		

I = configuration I (tandem placement: crest GSCs) III = configuration III (tandem placement: slope GSCs)
II = configuration II (staggered placement: crest GSCs) IV = configuration IV (staggered placement: slope GSCs)
* all the pullout tests with nonwoven geotextiles tests were repeated with water (dry and underwater)
** only a few selected the pullout tests with woven geotextiles tests were repeated with water
(see Dassanayake and Oumeraci, 2010d)

Results from crest and slope GSCs were analysed separately as in some occasions, they showed different patterns. In most of the cases, there were variations in the measured pullout forces. However, the general trends are clearly visible.

3.3.3 Influence of the Sand Fill Ratio on Pullout Forces

The main focus of these test series was to find the influence of the sand fill ratio on pullout forces of both crest and slope GSCs of a structure with a vertical seaward front. For an empty geotextile bag with a given geometry, the weight of the GSC increases with the sand fill ratio. As a result, pullout forces were also increased with the sand fill ratio. However, the increase rate was decreasing. The ratio between the pullout force and the weight (when a GSC-structure is submerged, the weight of GSCs under buoyancy is considered) of the crest GSC was introduced as a relative pullout force for crest GSCs (see Figure 3-21). According to the

results, sand fill ratios of 90 %~100 % required a higher relative pullout force than for the other tested sand fill ratios (Figure 3-18 and Figure 3-19). In general, the sand fill ratio clearly affects the deformation (shapes) of GSCs, and consequently the interface friction forces. Therefore, there will be a significant difference in terms of the hydraulic stability for different sand fill ratios.

Interestingly, 120% filled crest and slope GSCs resulted in the lowest resistance (in terms of relative pullout force) against pulling out. Contrary to the common belief that the 80% filled GSCs provide better stability (e.g. PIANC 2011), 90% ~ 100% filled GSCs showed the highest resistance than the other sand fill ratios. For lower sand fill ratios (80%~100%), pullout tests do not show a significant difference between pullout forces of tandem and staggered arrangements. Surprisingly, both crest and slope GSCs with tandem arrangement show slightly higher pullout forces than staggered arrangement, when sand fill ratios are relatively higher (110% ~ 120%). This might be due to "interlocking" between GSCs as a result of upper GSCs follow the convex shape of lower GSCs, when compared to the staggered arrangement. The convex curvature is higher for larger sand fill ratios

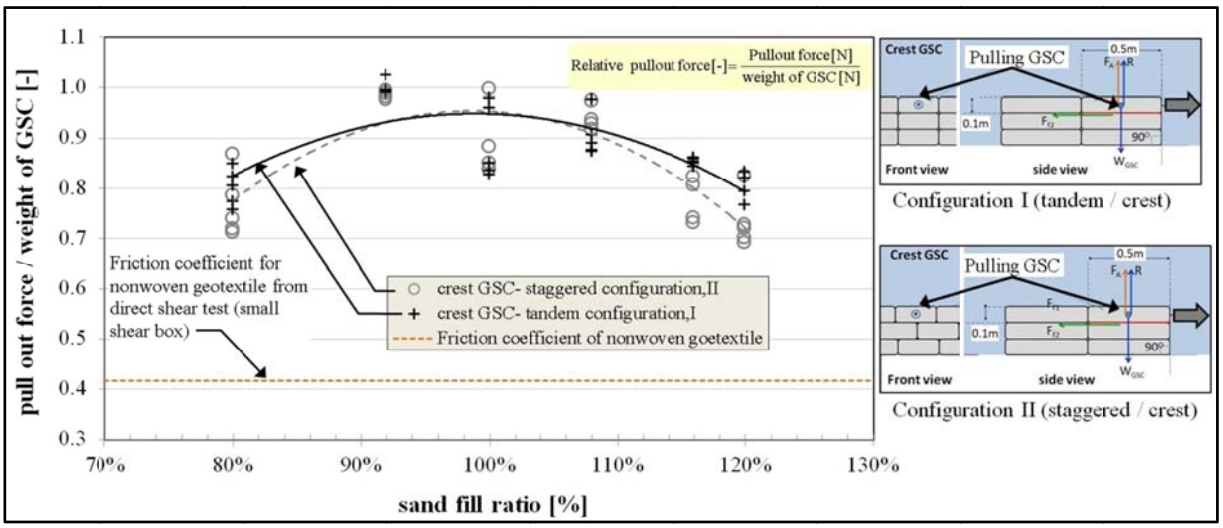

Figure 3-18: Effect of sand fill ratio on relative pullout forces on crest GSC (underwater pullout test results)

The effect of the sand fill ratio and the stacking pattern (tandem or staggered arrangements) of slope GSCs was studied by performing pullout tests on the GSCs from the second layer. The seaward front of the structure was kept vertical to obtained maximum pullout forces. Later, some of the pullout tests on the slope GSCs were repeated with 1:1 seaward slope (Figure 3-23). Unlike the crest GSCs, the slope GSCs have interfaces from both top and bottom sides. By taking these two surfaces and the perpendicular force acting on these two surfaces into account, the relative pullout force was redefined as the ratio between the pullout force and the three times the weight of a GSC (Figure 3-21). The slope GSCs did not display a large variation in relative pullout forces compared to the crest GSCs. However, both trend-lines drawn for slope GSCs with tandem and staggered arrangements show the higher resistance against pullout forces when the sand fill ratio is 90% ~ 100%.

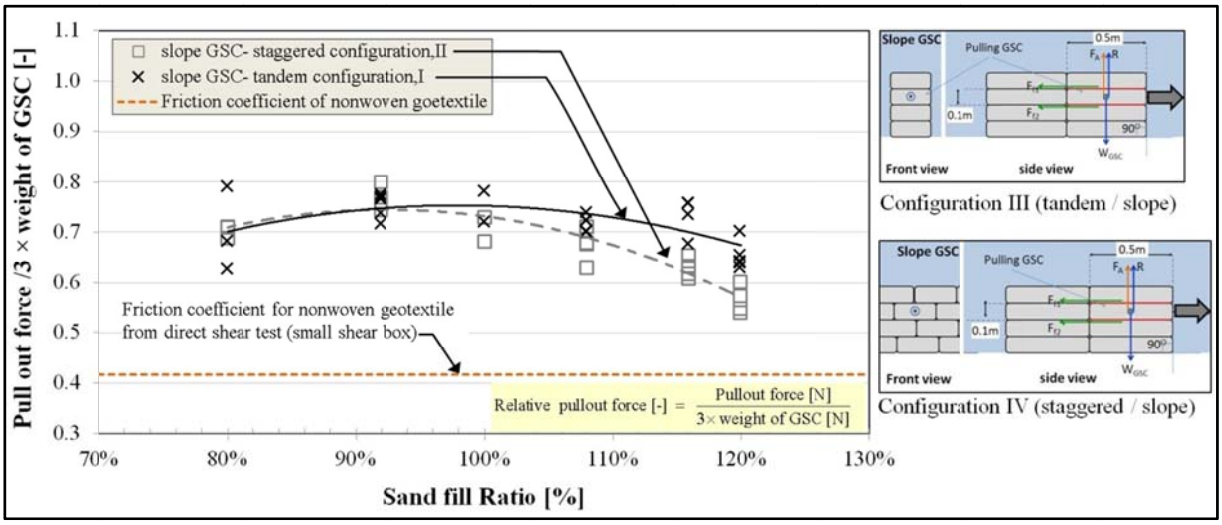

Figure 3-19: Effect of sand fill ratio on relative pullout forces on slope GSC for a vertical seaward front (underwater pullout test results)

3.3.4 Comparison of Slope and Crest GSCs

A comparison of the slope GSCs (from the second layer from the crest) and the crest GSCs shows that the slope containers have in average at least 130% higher resistance than the crest GSC (Figure 3-20), when the seaward front is vertical. Therefore, the crest GSCs are the critical elements from submerged or low-crested GSC-structures.

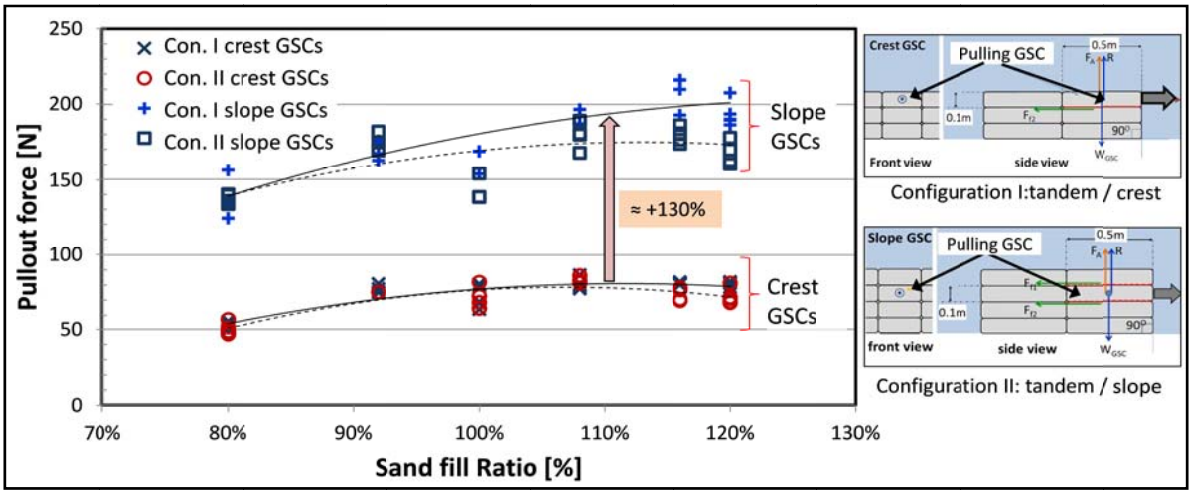

Figure 3-20: Comparison of pullout forces for crest and slope GSCs for a vertical seaward front (underwater pullout test results)

3.3.5 Effect of Geotextile Material Properties on Pullout Forces

Two different types of geotextile, a woven and a nonwoven, were used for the model GSCs. During underwater direct shear tests with standard shear box, the woven geotextile showed a friction angle of 13.33° (tan Φ=0.237) while the nonwoven material showed an angle of

22.62° (tan Φ=0.417). These two materials showed a clear difference in their pullout resistance, which is roughly proportional to the friction coefficients obtained from direct shear tests.

The relative pullout forces were calculated to find out the relationship between friction properties of geotextile materials and the interface friction properties of GSCs. According to the results, both types of GSCs showed more than 30% higher relative friction forces than the friction coefficients (Figure 3-22). When consider both dry and underwater pullout tests with nonwoven geotextiles, the lowest relative pullout force was 0.54, which can also be described as interface friction coefficient of two nonwoven GSCs (Figure 3-21). Similarly, when consider the pullout tests with woven geotextiles, the lowest relative pullout force was 0.31 (interface friction coefficient of two woven GSCs). Both these values (tan Φ=0.540 for the nonwoven GSCs and tan Φ=0.310 for the woven GSCs) are approximately 30% of the friction coefficients obtained from the direct shear test (tan Φ=0.417 for the nonwoven geotextiles and tan Φ=0.237 for the woven geotextiles).

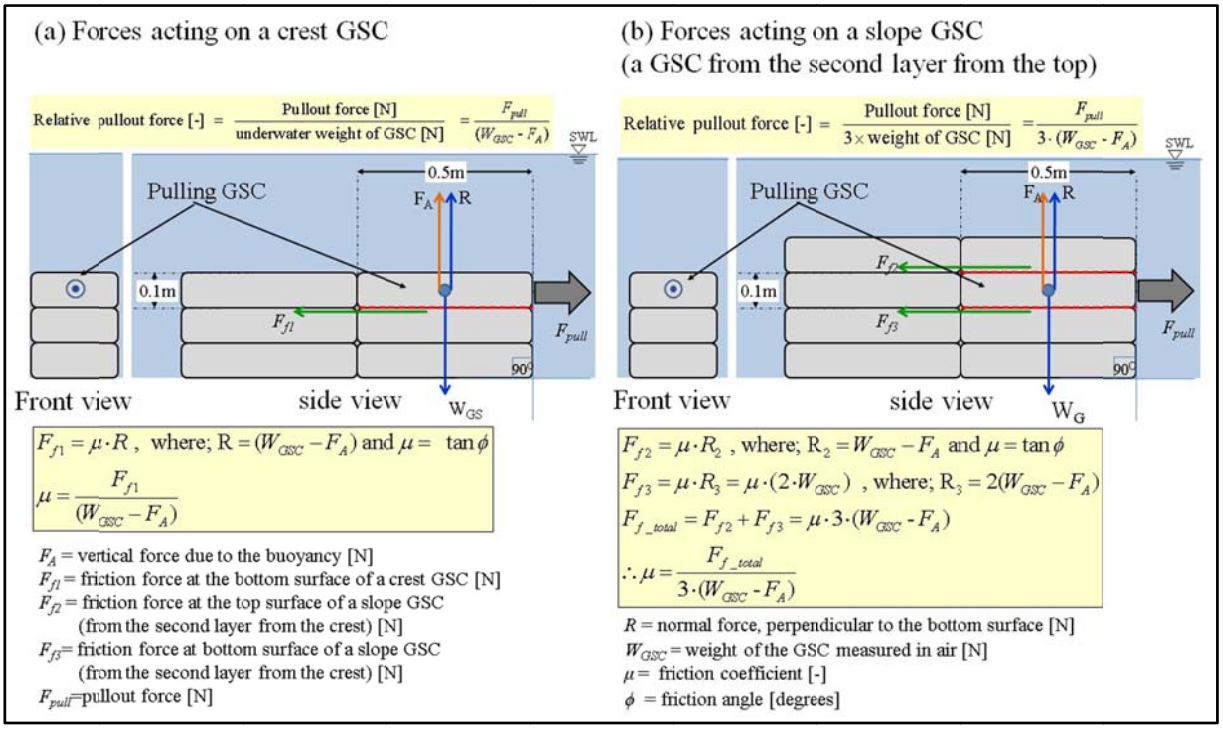

Figure 3-21: Calculation of interface friction coefficient of crest and slope GSCs

Therefore, for during design purpose, it is much safer to consider the friction properties of geotextile materials directly. Furthermore, GSCs-structures with nonwoven geotextile can be further optimised as they showed nearly 75% higher relative friction forces than GSC-structures with woven geotextile. However, stacking methods did not show any important effect during both nonwoven and woven GSCs.

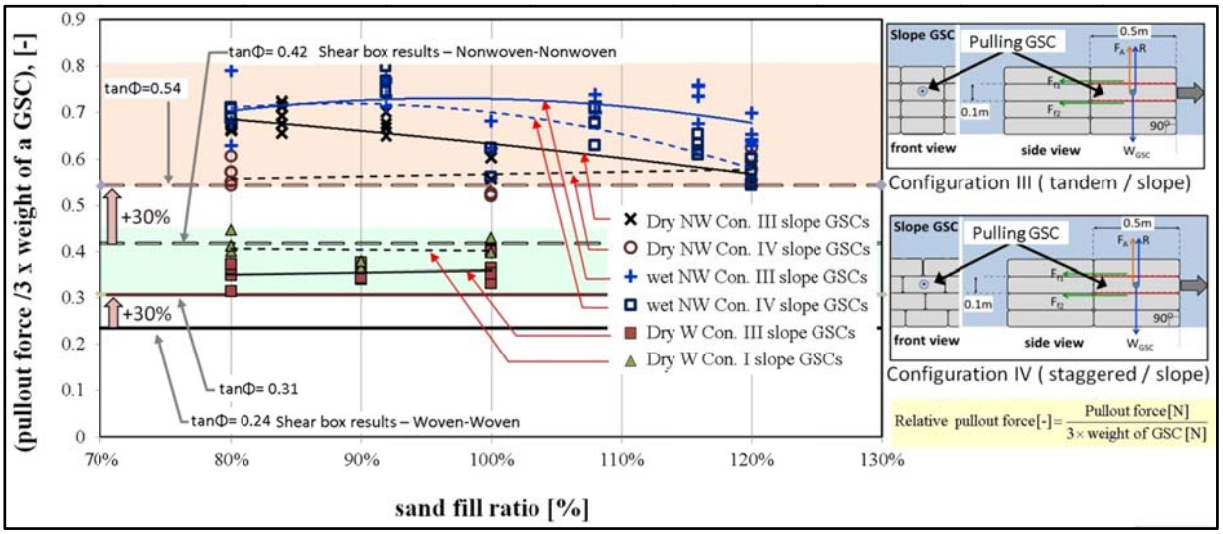

Figure 3-22: comparison of pullout forces for woven and nonwoven geotextile (exemplarily for slope GSCs)

3.3.6 Influence of the Seaward Slope Angle on Pullout Forces

Apart from vertical seawalls, the most common seaward slope from GSC-structures is 1:1 (or 45°). Therefore, GSCs were arranged as 1:1 slope and pullout forces were measured. The different types of nonwoven GSCs were used (fill ratios: 80%, 110%, 120%). The pullout tests with 1:1 seaward slope were conducted with only the tandem stacking method, because, the two GSC arrangements show almost similar pullout resistances. It is also expected that the effect of stacking method on pullout forces (specially for the GSCs with high sand fill ratios; FR=110%~120%) might not be significantly different from the tests with vertical seaward front.

According to the results, crest containers showed only an average of ca. 10% higher values compared with the vertical seaward slope cases and slope containers showed an average of ca. 10% reduction in pullout forces compared to the vertical seaward slope cases (Figure 3-23). Since the crest container lying on an uneven surface (due to the gap between first and second raw of GSCs from the second layer from the crest), "interlocking" might be higher. This might cause the increase (ca. 10% in average) in the pullout forces for the crest GSCs.

At the slope, there is a reduction in the contact area (overlapping area), which might lead to less "interlocking" and consequently lower pullout forces than a vertical seaward slope. In addition, only ca. 80% of the GSC length of the crest GSC is resting on the slope GSC (from the second layer from the top). Therefore, the force acting perpendicular to the contact surface between the crest and the second GSC from the top is also reduced by ca. 20%. Consequently, the friction force (F_{f2}, Figure 3-21) is lower than that of the vertical seaward front. As a result, total pullout forces are lower than those from the tests with vertical seaward front (ca. 10% lower in average).

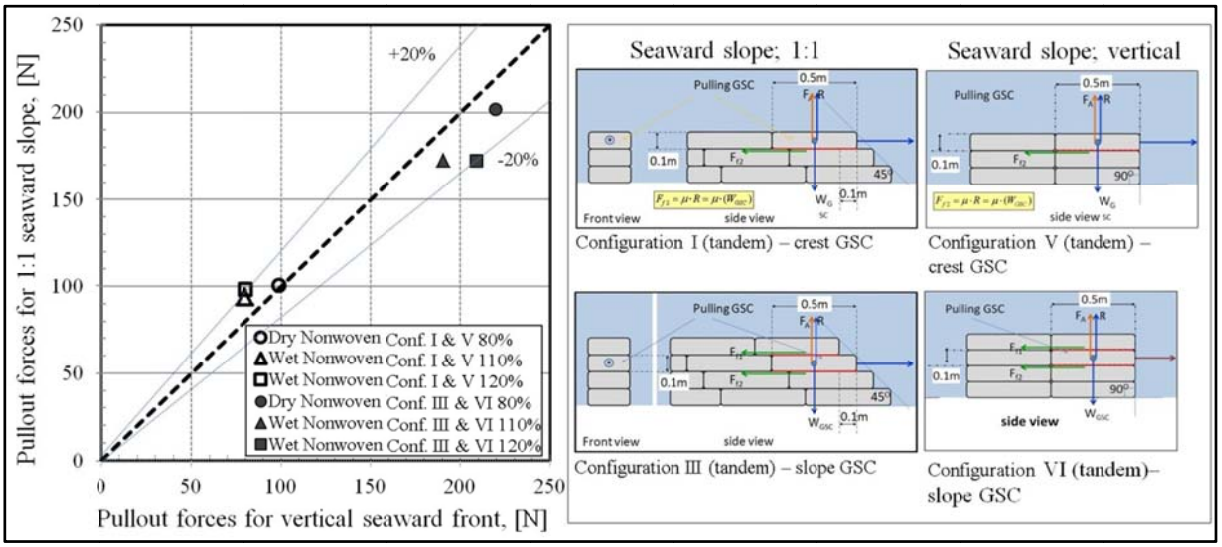

Figure 3-23: Influence of seaward slope angle of the GSC-structure on the pullout forces

3.3.7 Pullout Tests in Water

The effect of the presence of water on pullout forces was another important issue related to the overall hydraulic stability. Figure 3-24 shows experimental results of nonwoven crest GSCs. Pullout forces under dry and submerged conditions are different, however, this difference is mainly due to the different normal loads. When GSCs are submerged, because of the buoyancy, normal loads are smaller and as a result, pullout forces are also smaller. However, when relative pullout forces are considered, there is only slight different between dry and submerged GSCs. For the calculation of relative pullout forces, in case of dry pullout tests, GSCs weight in air and in case of submerged pullout forces, GSCs weight underwater were considered. Other than in tandem placed GSCs with low sand fill ratios, all the other GSCs showed ca. 10~15% higher pullout forces, when GSCs are submerged and there is no apparent reduction in interface friction properties. This slight difference could be due to the settlement of GSCs, once they are wet. Therefore, it is not required to alter the joint properties in numerical models, because, GSCs are wet at least once during a test, and all the GSCs will then show nearly the similar behaviour. Slope GSCs (Figure 3-21) also showed a similar behaviour, when compare the results from dry pullout tests and from the tests with water (Dassanayake and Oumeraci 2010d).

In addition, two GSC stacking methods: tandem arrangement and staggered arrangement showed almost the same pullout forces for crest GSCs during the underwater pullout tests. However, dry pullout tests showed ca. 20% high pullout forces for crest GSCs with tandem arrangement compared to crest GSCs with staggered arrangement. Once the GSC-structure is submerged, GSCs of large sand fill ratios (FR = 110% ~ 120%) with tandem arrangement showed ca. 5% ~ 10% higher pullout forces compared to the GSCs with staggered arrangement. Therefore, there was no apparent advantage in placing GSCs with staggered arrangement for the tested conditions.

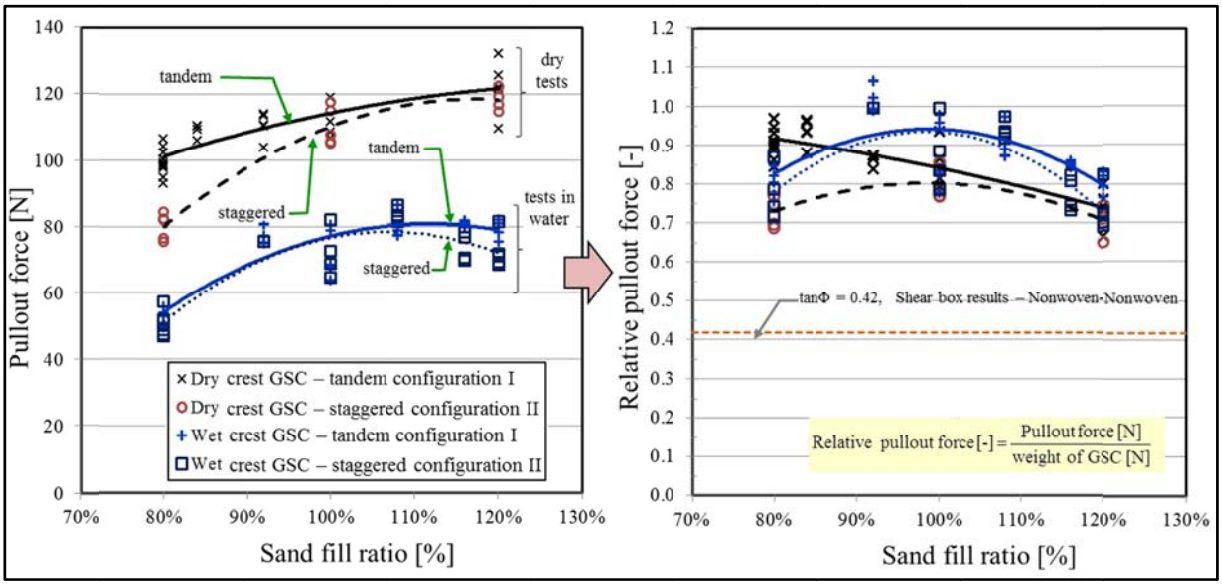

Figure 3-24: Comparison of pullout forces of crest GSCs under dry and submerged conditions

3.3.8 Summary of Pullout Test Results and Concluding Remarks

The small scale pullout tests were carried out to quantify the effect of key engineering parameters such as the sand fill ratio, the type of geotextile material, seaward slope of GSC-structures (overlapping length), stacking pattern, test conditions (dry or submerged), etc. on the pullout forces. The influence of these factors on pullout force of crest and slope GSCs were then analysed in detail and concluding remarks drawn from the study can be summarized in point form as follows.

- The results of the pullout tests that cover five different tested sand fill ratios (80%, 90%, 100%, 110%, and 120%), have shown that the pullout forces increase with increasing sand fill ratios. A non-dimensional parameter was introduced as relative pullout force (ratio between the pullout force and the weight of the GSCs). Optimal sand fill ratios in terms of the resistance against pullout of the GSCs (or the sand fill ratios that resulted in the highest relative pullout forces) were found to be between 90% ~ 100%. The slope containers have in average at least 130% higher resistance than the crest containers, when consider respective relative pullout forces. In this comparative analysis only the amount of sand filled into the GSCs was varied and the size of the empty bag was unchanged (same amount of geotextile). Hence, the weight of each GSC increases as the sand fill ratio increases.
- As expected, the slope GSCs showed higher pullout resistance than the containers at the crest. In average, slope GSCs showed at least 130% higher resistance than the crest GSCs.
- Among the two types of geotextiles, the woven geotextile showed a friction angle of 13.33° (tan Φ=0.237), and the nonwoven material had a friction angle of 22.62° (tan Φ=0.417) during underwater direct shear tests with standard shear box. These two geotextile materials displayed a clear difference in their pullout resistance, which is approximately proportional to the friction coefficients.

- The pullout resistance is roughly proportional to the friction coefficients obtained from direct shear tests. Interestingly, all the GSCs showed 30% ~ 50% higher pullout resistance than what was expected based on the interface friction properties of geotextile materials without the sand fill.
- As expected, slope containers in GSC-structures with a 1:1 seaward slope showed a lower resistance to pullout forces than GSCs in a structure with a vertical front. This is mainly due to the reduction in overlapping length between GSCs. However, in average, it is only about 10% lower than that of the vertical seaward front. In contrast, crest containers show slightly higher (or sometimes equal) values with an average of approximately 10% higher. This could be due to irregularities in the surface, which might increase the "interlocking" between GSCs.
- Even though the required pullout force to move a dry GSC is larger than that of a submerged container, submerged GSCs showed ca. 10~15% higher relative pullout forces than dry GSCs. There is no apparent decrease in interface friction properties due to the presence of water. Therefore, the settlement of GSCs, once they are wet, might be the reason for this slight difference. Consequently, it is not required to modify the joint properties in numerical models depending on whether GSCs are emerged or submerged. Because, GSCs are wet at least once during each test and all the GSCs will then show nearly a similar behaviour.

In general, sand fill ratio clearly influences the weight and the shapes of GSCs and consequently the interface friction forces. Therefore, there will be a significant difference in terms of the hydraulic stability, for GSCs of different sand fill ratios. Similarly, friction properties of geotextile materials showed a significant influence on the interface friction properties and ultimately on the pullout forces. However, the underwater pullout tests of GSCs structures with tandem and staggered GSC arrangements did not show a considerable difference in pullout forces, even though the tandem arrangement showed slightly higher pullout forces for several test configurations. Therefore, the hydraulic stability tests should mainly consider the parameters such as the sand fill ratio and friction properties of geotextile, but only the tandem arrangement. Since most of the previous experiments have been performed with 80% sand fill ratio, it will be necessary to include that in hydraulic stability tests. Even though the 90% filled GSCs showed highest resistance against pullout, 100% sand fill ratio might appropriate to achieve a considerable contrast in terms of sand fill ratio as it resulted in the next highest pullout forces.

Moreover, one of the main limitations of COBRAS/UDEC modelling system by Recio (2007) is the inadequate representation of GSC-GSC contacts. With the help of pullout test data, it is possible to find out proper joint models to represent GSC-GSC contacts with different engineering properties and to validate them. Therefore, the results from the pullout tests were helpful for the planning of hydraulic stability tests and also to obtain required GSC parameter for the numerical models.

3.4 Effect of Engineering Properties of GSCs on the Hydraulic Stability – Hydraulic Stability Test Results

The results of an extensive review and analysis of the literature on the sand fill ratio and on hydraulic stability of GSC-structures have shown that the laboratory investigations are the most feasible and appropriate option to study the effect of different sand fill ratios on the hydraulic stability of GSC-structures. Therefore, a series of hydraulic stability tests were performed and results are described in this section. These tests mainly focused on fulfilling the requirement of a process oriented systematic investigation of the effect of different fill ratios on the hydraulic stability of GSC-structures. Furthermore, the hydraulic stability tests also focused on the effects of other engineering properties of GSCs on the hydraulic stability of GSC-structures such as the type of fill material, the friction between containers and the inclination angle of GSC. The results of the literature analysis clearly showed a gap in the knowledge on hydraulic stability of low-crested and submerged GSC-structures (Figure 2-13). Therefore, the current study focuses mainly on submerged and low-crested GSC-structure for shore protection. More detailed results are given in Dassanayake et al. (2011c).

However, as described in Dassanayake and Oumeraci (2009a, 2009b), perfect similitude cannot be achieved in small scale experiments. Therefore, hydraulic stability tests need to be carefully planned with some insight of the physical processes involved in the wave-structure interaction and the associated scaling laws. Dassanayake and Oumeraci (2010a) describe the possibilities and the limitations of scaling of the most relevant materials for the small scale experiments on hydraulic stability of GSC-structures. Due to the complexity of the scaling the engineering properties of geotextile, final materials for the tests were selected based on both the analysis of expert opinions from the industry and on a comparative analysis of the properties of geotextile materials available in the market (Dassanayake and Oumeraci 2010a).

Though the small scale laboratory models are considered as the most reliable tool for designing and testing most types of coastal structures (Hughes 2003), they still have certain limitations. Due to scale effects, laboratory effects and measurement errors, model and prototype results might differ significantly. Therefore, test should be planned and results should be analysed cautiously.

3.4.1 Specific Objectives of Hydraulic Stability Tests

The overall objectives of the hydraulic stability tests were to study the effect of the sand fill ratio and the interface friction properties of GSCs on the hydraulic stability of GSC-structures with an improved understanding of the hydraulic stability of crest GSCs of low-crested and submerged GSC-structures and to obtain the required data for the validation of the numerical models. The specific objectives are threefold; (i) Identification and understanding of the effects of engineering properties of GSCs on the hydraulic stability of GSC-structures. (ii) Quantification and evaluation of the sensitivity and relative importance of identified and selected properties of GSCs on the hydraulic stability of submerged GSC-structures through a

set of appropriate laboratory experiments. (iii) Comparison of currently available stability formulae on GSCs with the analysed data from the laboratory experiments.

3.4.2 Experimental Setup

Hydraulic stability tests (Figure 3-25 and Figure 3-26) were conducted to investigate the effect of the most important engineering properties on the processes that govern the hydraulic stability. Approximately 350 model tests were performed while varying wave parameters, geometrical parameters (e.g. inclination angle of GSCs) and properties of GSC such as the sand fill ratio, the type of geotextile material, etc. During the model tests, incident and transmitted wave parameters, the behaviour of the structure (high speed video records), the flow velocity around the structure, the pressure variations at the crest of the GSCs structure are systematically recorded.

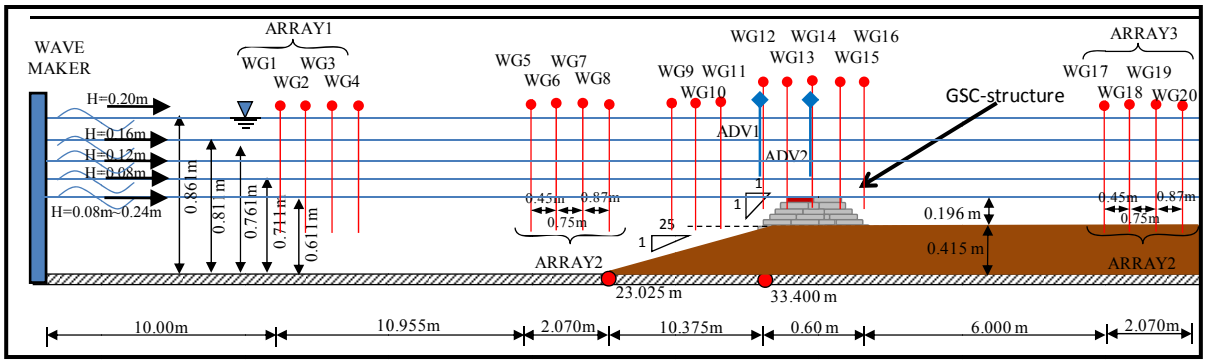

Figure 3-25: Model setup – hydraulic stability tests in the 2m wave flume of LWI

Based on several factors such as the capacity and the size of the wave flume at LWI, availability of geotextile material, experiences gained during previous model tests, existing stability formulae and few preliminary tests results, etc., the most appropriate scale of the model GSC was determined.

The decision regarding the foreshore slope should be taken carefully and only after considering all the relevant processes affecting the hydraulic stability of GSC-structure. There are advantages as well as disadvantages of having a foreshore slope. Therefore, some numerical simulations were performed using the COBRAS-UC model to identify the effect of the foreshore slope for the hydraulic stability of submerged GSC-structures (Dassanayake and Oumeraci 2010c). These simulations considered a submerged/low-crested GSC-structure with similar dimensions, but with and without the foreshore slope. Model parameters were; wave heights $H = 0.15 \sim 0.25$ m, wave periods, $T = 2.0$ s and 3.5 s and crest freeboard, $Rc = 0.000 \sim 0.313$ m. Dassanayake and Oumeraci (2010c) reported the results, which indicate that the foreshore slope might result larger horizontal particle velocities compared to the tests without a foreshore slope, which are ultimately responsible for the motion of crest GSCs. Specially, when the crest freeboard is zero, the difference between the maximum horizontal velocities (measured at the seaward edge of the crest) with the foreshore slope are much larger than those of without foreshore slopes. Therefore, it is clear that the foreshore slope will allow

large variations of test conditions. Based on these numerical modelling results and other practical concerns, it was decided to use a foreshore slope with 1:25.

Apart from that, the foreshore slope reduces the number of small scale GSCs required to construct the GSC-structures in the flume. Hence, it allows testing a wide spectrum of parameters within the limited time available for the experiments. However, the foreshore slope restricts the performance of hydraulic stability tests with surface piercing structure due to the wave breaking on the foreshore slope. Therefore, additional numerical simulations were performed with sufficiently large water depths at the toe of the structure (see Section 4.5). Three types of small scale GSCs were used during the hydraulic stability tests: (i) nonwoven 80% filled GSCs (see Figure 3-26a, series NW80H and Figure 3-26d, series NW80I) (ii) nonwoven 100% filled GSCs (see Figure 3-26b, series NW100H) and (iii) woven 80% filled GSCs (see Figure 3-26c, series W80H). As shown in Figure 3-26c, the hydraulic stability tests with woven GSCs were conducted only by constructing a woven GSC-structure to cover a 50% of the width of the 2 m wide wave flume. The next half was constructed with nonwoven 80% filled GSCs. Therefore, each type of GSCs represents 1 m width across the flume, which allows for a direct comparison of the hydraulic stability of 80% filled woven and nonwoven GSCs. The lengths and the heights of each GSC are shown in Figure 3-26 and the width of all the types of GSCs were kept as 0.70 m in order to use the same number of GSCs in each test series. Since the joint between two structures was not real (woven-nonwoven GSC interface), GSCs around the joint were not considered in the analysis. Moreover, in order to obtain the same crest height with different types of small scale GSCs, the foundation of the structure was constructed with larger GSCs of different heights. The seaward slope of the structure was 1:1 throughout the test series. When GSCs are placed with 1:1 seaward slope, always there will be small gaps between different GSC rows of the same level. These gaps were filled with relatively shorter GSCs and they were not considered during the damage analysis. Inclination angles of GSCs were 0 (horizontal) and 15^0 inclined from the horizontal line (Figure 3-26d). After each test, the model was fully reconstructed to obtain the same initial conditions.

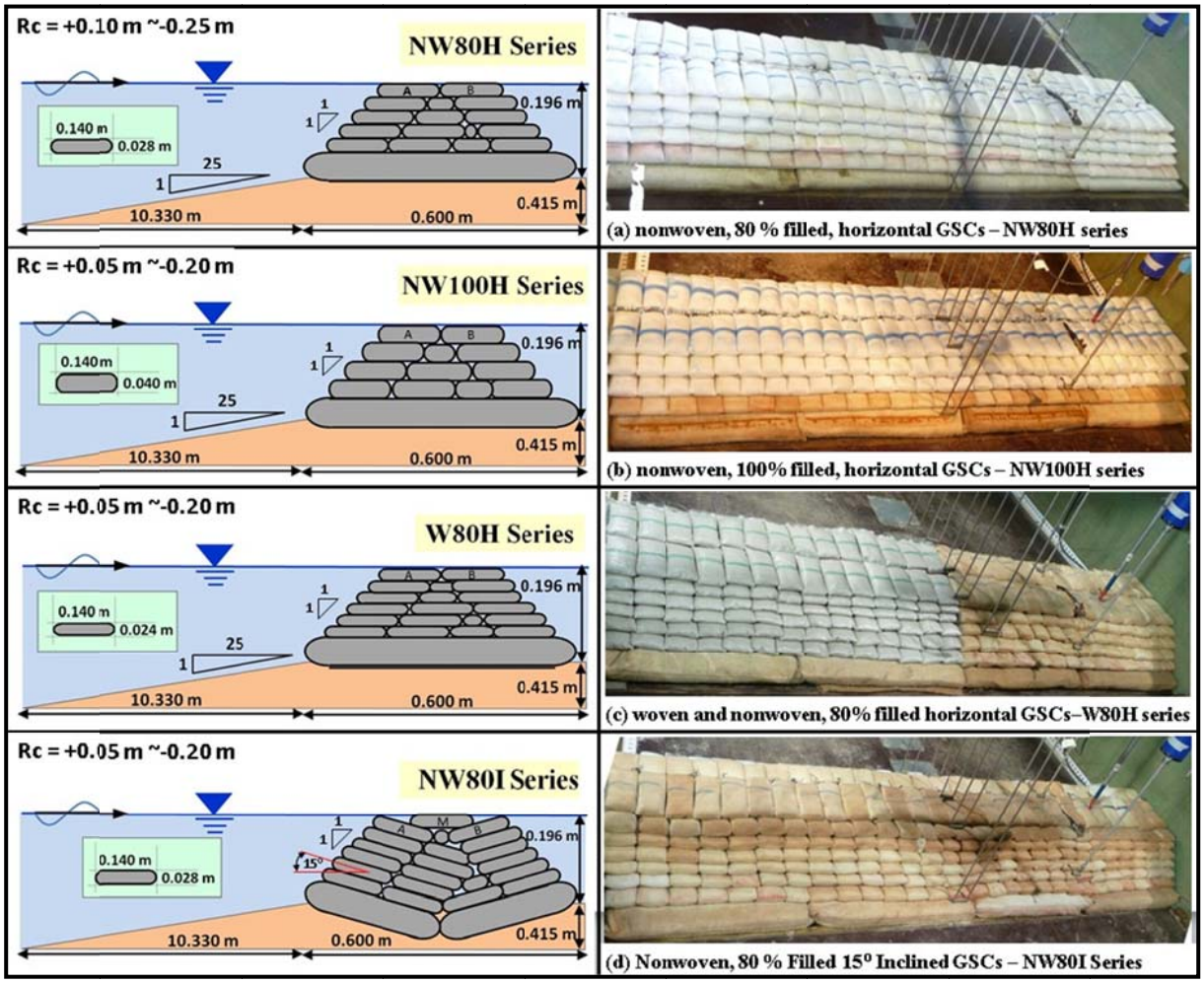

Figure 3-26: Different model configurations and test series: (a) nonwoven, 80 % filled, horizontal GSCs; (b) nonwoven, 100 % filled, horizontal GSCs, (c) woven and nonwoven, 80 % filled horizontal GSCs; and (d) nonwoven, 80 % filled 15° inclined GSCs

Table 3-5: Test programme in the 2 m wave flume of LWI

Model Configuration and Test Series	Crest Freeboard [m]	Wave Type*	Wave Height, H*** [m]	Wave Period, T [s]	Wave steepness; $S_0=H/L_0$ [-]	Relative water depth, h/L_0 [-]
(a) NW80H: nonwoven, 80% filled, horizontal GSCs	-0.25 ~ 0.096	Regular*	H_m = 0.07 ~ 0.20	T_m = 1.0 ~ 4.6	0.001~0.100	0.01~0.50
		Irregular**	H_s = 0.05 ~ 0.24	T_p = 1.0 ~ 3.4	0.005~0.060	0.01~0.22
(b) NW100H: nonwoven, 100% filled, horizontal GSCs	-0.20 ~ 0.046	Regular*	H_m = 0.09 ~ 0.20	T_m = 1 .4~ 4.0	0.005~0.056	0.03~0.20
		Irregular**	H_s = 0.04 ~ 0.11	T_p = 1.0 ~ 2.7	0.007~0.052	0.03~0.11
(c) W80H: woven and nonwoven, 80% filled horizontal GSC	-0.20 ~ 0.096	Regular*	H_m = 0.08 ~ 0.20	T_m = 1.0 ~ 4.2	0.003~0.054	0.01~0.20
		Irregular**	H_s = 0.07 ~ 0.16	T_p = 1.2 ~ 2.5	0.008~0.040	0.04~0.20
(d) NW80I: nonwoven, 80% filled, 15^0 inclined GSCs	-0.20 ~ 0.096	Regular*	H_m = 0.08 ~ 0.16	T_m = 1.2 ~ 3.2	0.004~0.070	0.01~0.20
		Irregular**	-	-	-	-

* 100 regular waves per test, ** JONSWAP spectrum with 1000 waves per test
*** Wave height measured at the beginning of the foreshore slope
Hm = mean wave period of 100 waves
Hs = Significant wave height of wave spectrum consists of 1000 waves
Tm = mean wave period of 1000 waves
Tp= peak period of the wave spectrum of 1000 waves

3.4.3 Typical Failure Modes of Low-Crested / Submerged GSC-Structures

High-speed video extracts shown in Figure 3-27 illustrate typical failure modes: sliding, "uplifting and drifting", and overturning. GSCs show different dominant failure modes for different submerged depths. For most of the low-crested structures, the crest GSCs represent the critical elements. In most of the tests a dominant failure mode was identified. This dominant failure mode apparently depends on the engineering properties of GSCs, the crest freeboard (or submergence depth) and the inclination angle of GSC. Furthermore, the importance of the engineering properties of GSCs on the hydraulic stability also varies depending on the dominant failure mechanism for a particular GSC-structure and for a particular freeboard.

The most common failure mechanism during the test series W80H (horizontally placed woven GSCs with 80% fill ratio) was sliding (Figure 3-27a). This might be due to the low friction between woven GSCs. The sliding could take place over several wave cycles in steps. Whereas, nonwoven GSCs (test series NW80H; horizontally placed woven GSCs with 80% fill ratio and test series NW100H; horizontally placed nonwoven GSCs with 100% fill ratio) were displaced mainly due to, either uplifting and drifting (Figure 3-27b) or due to overturning (Figure 3-27c). Both these failure mechanisms could occur within one wave cycle. The detailed damage analysis showed that there is a possibility that all three damage mechanisms can be seen in one model. However, in most of the test cases, there was one dominant failure mechanism.

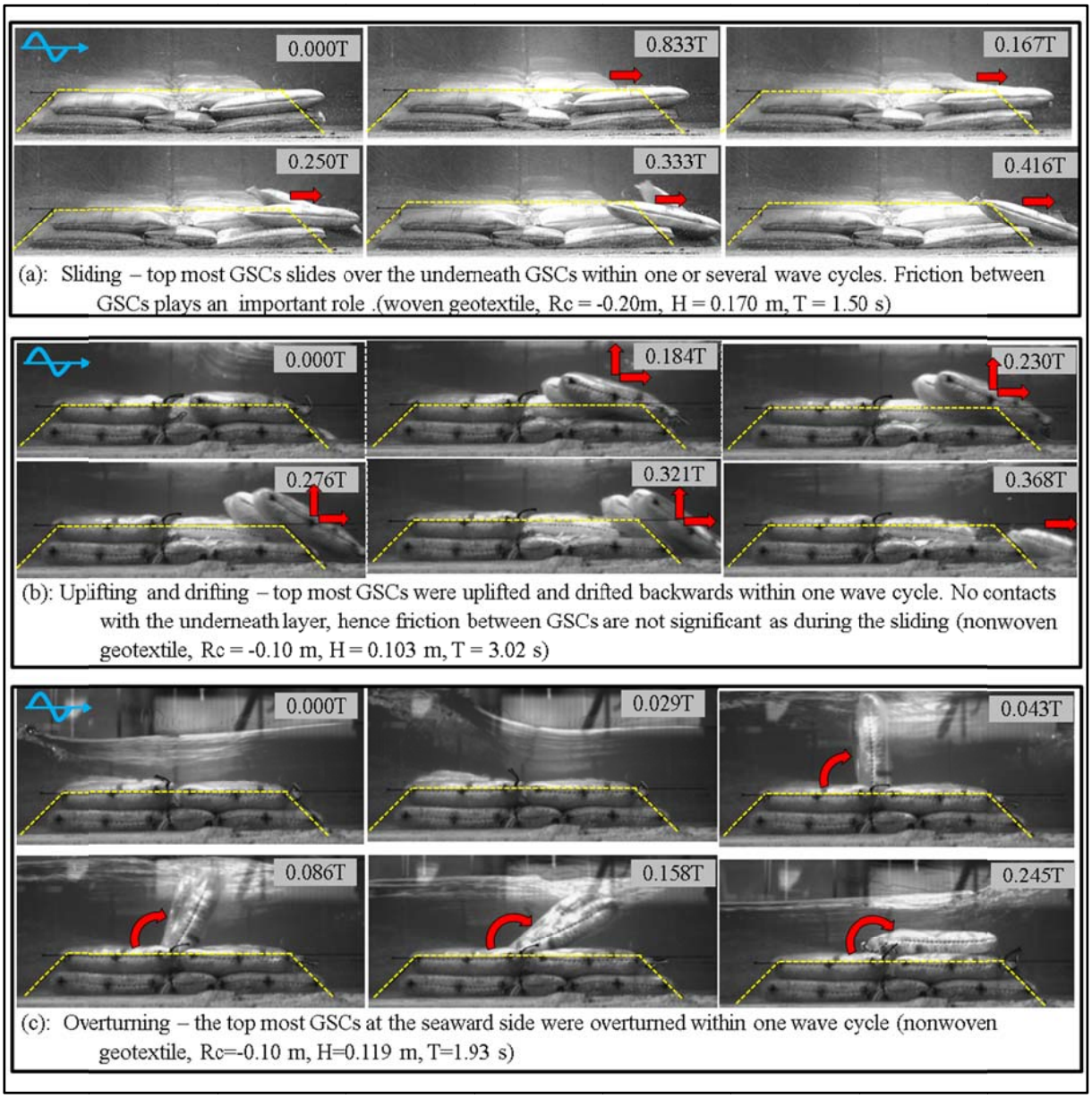

Figure 3-27: Typical failure modes observed during the wave tests: (a) sliding, (b) uplifting and drifting, (c) overturning

3.4.4 New Approach for Damage Classification for GSCs and GSC-Structures

Since the existing damage classification for conventional coastal structures (e.g. rubble mound breakwaters) is not applicable to GSC-structures, a new method of damage classification is introduced for this study (Table 3-6).

If a GSC displaces less than 10% of its length or shows an angular motion less than 10°, then it is considered as "no damage" (or "stable").

If a GSC shows a greater displacement than 10% of its length or greater angular motions than 10° it is considered either as an "incipient motion" or a "displacement" depending on the

magnitude as shown in Table 3-6. By then considering the critical GSC-layers of a GSC-structure the level of damage was classified into five categories from "no damage" (DC 0) to "total failure" (DC 4).

Table 3-6: New damage classification for individual GSCs and for entire GSC-structure (modified from Dassanayake et al. 2011c)

Damage Classification I (single GSC): considering only a single GSC in the most vulnerable position (critical GSCs)	
"Stable"	Horizontal displacement < 10% of GSC length / Upward rotation < 10^0
"Movement"	10% of GSC length, width < Horizontal displacement < 50% of GSC length 10^0 < Upward rotation < 45^0
"Detachment"	Horizontal displacement > 50% of GSC length Upward rotation > 45^0

Damage Classification II (GSC-structure): considering all critical GSC layers of a GSC-Structure ++				
No Damage [DC 0]	**Incipient Motion [DC 1]**	**Minor Damage [DC 2]**	**Moderate Damage [DC 3]**	**Total Failure [DC 4]**
< 10 % of critical GSCs moved No critical GSCs detached	10% ~ 50% of critical GSCs moved < 5 % of critical GSCs detached	> 50% of critical GSCs moved 5% ~ 20% of critical GSCs detached	20% ~ 40% of critical GSCs detached	> 40% of critical GSCs detached

++ level of damage to GSC-structures, after 100 regular waves during regular wave tests or 1000 waves with JONSWAP spectrums during irregular wave tests

3.4.5 Effect of Surf Similarity Parameter on the Hydraulic Stability of GSC-Structures

Early GSC-structures were designed using the hydraulic stability formulae for stone armour layers such as Hudson's formula (1956). Only the weight of GSCs was considered similar to other conventional coastal structures. Later, Wouters (1998) proposed a new stability formula (Eq. 2.2) for GSCs based on the Hudson's formula and the previous experimental data. This formula contains a modified stability number (Ns), which was developed explicitly for GSC structures. Then, Oumeraci et al. (2002b) and Oumeraci et al. (2003) proposed two different hydraulic stability formulae for crest GSCs and slope GSCs of a revetment using the stability number (Eq. 2.2) proposed by Wouters (1998).

According to Oumeraci et al. (2003), the hydraulic stability of crest GSCs for a structure with a relatively high crest depends primarily on the relative freeboard whereas the hydraulic stability of slope GSCs depends primarily on the surf similarity parameter. However, the results of the tests show that even the crest GSCs of submerged and low crest structures are strongly dependent on both the freeboard and the surf similarity parameter.

The result of the hydraulic stability tests are presented with modified stability number (*Ns*) similar to Wouters (1998).

$$Ns = \frac{H}{(\rho_{GSC} / \rho_W - 1) \cdot lc \sin\alpha} \quad \text{with} \quad \xi_0 = \tan\alpha / \sqrt{(H / L_0)} \tag{3.6}$$

Where;

Ns = stability number [-]
H = wave height at the beginning of the foreshore slope [m]
ρ_W = density of water [kg/m^3]
ρ_{GSC} = density of GSCs [kg/m^3]
C_w = empirical parameter derived from the stability number *Ns* [-]
l_c = length of a GSC [m]
α = slope angle of the structure [°]
$L_0 = g\,T^2/(2\pi)$ = deep water wave length calculated using the mean wave period [m]

During the data analysis, for the regular wave tests, mean wave height H_m and for the tests with JONSWAP spectrum, significant wave height, *Hs* were considered as the representative wave parameters. However, it was found that the characteristic wave height $H_{2\%}$, which is the mean of the highest 2% of the waves in the time series (mean of the highest 20 incident waves from the wave reflection analysis) is a better representative wave height to combine the data from regular and irregular wave tests. If only the significant wave height, *Hs* is known, then assuming a Rayleigh distribution, $H_{2\%} = 1.4\,H_s$.

First, hydraulic stability curves for different crest freeboards were developed based on the damage category; "Incipient motion" (DC 1) as described in Table 3-6. For the quantification of the effect of the sand fill ratio, the type of geotextile material, and the inclination angle of GSCs on the hydraulic stability, the results of different test series were compared by considering horizontally placed 80% filled nonwoven GSCs series: NW80H / *Rc* = 0; (Figure 3-28) as the basis. Figure 3-28 and Figure 3-29 present exemplarily results from NW80H test series with regular waves for two crest freeboards *Rc* = 0 m and *Rc* = -0.2 m (in model scale). For both freeboards, the "incipient motion" curves were plotted, showing a clear dependency of the stability number on the surf similarity parameter.

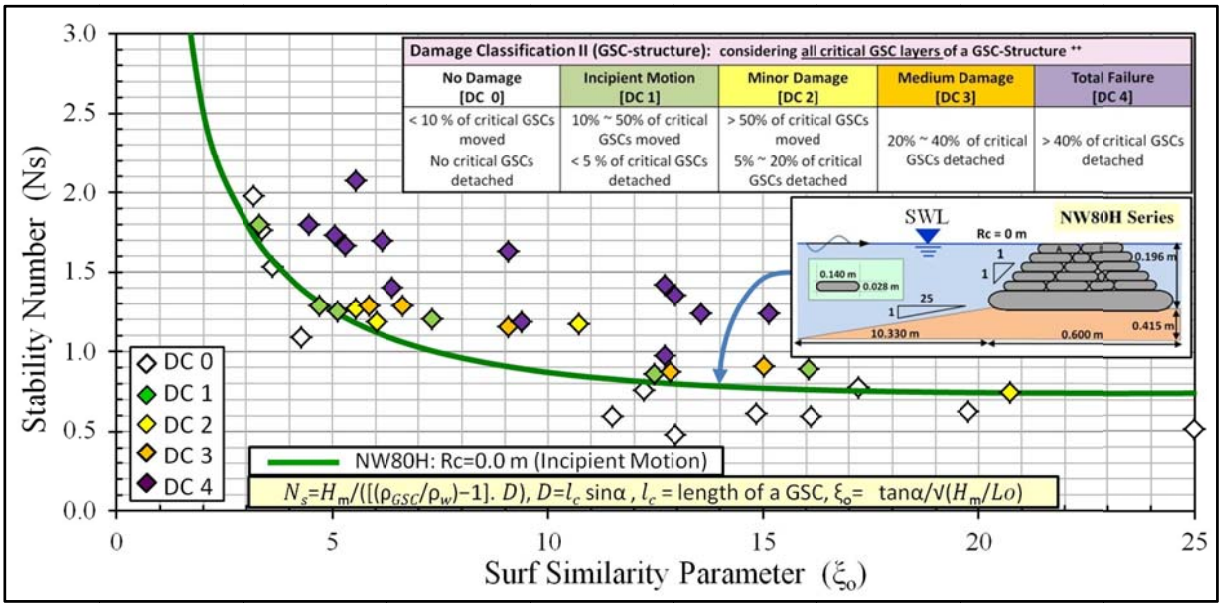

Figure 3-28: Hydraulic stability curve for low-crested GSC-structures (Rc =0 m) made of nonwoven, 80% filled GSCs (series NW80H, regular wave tests)

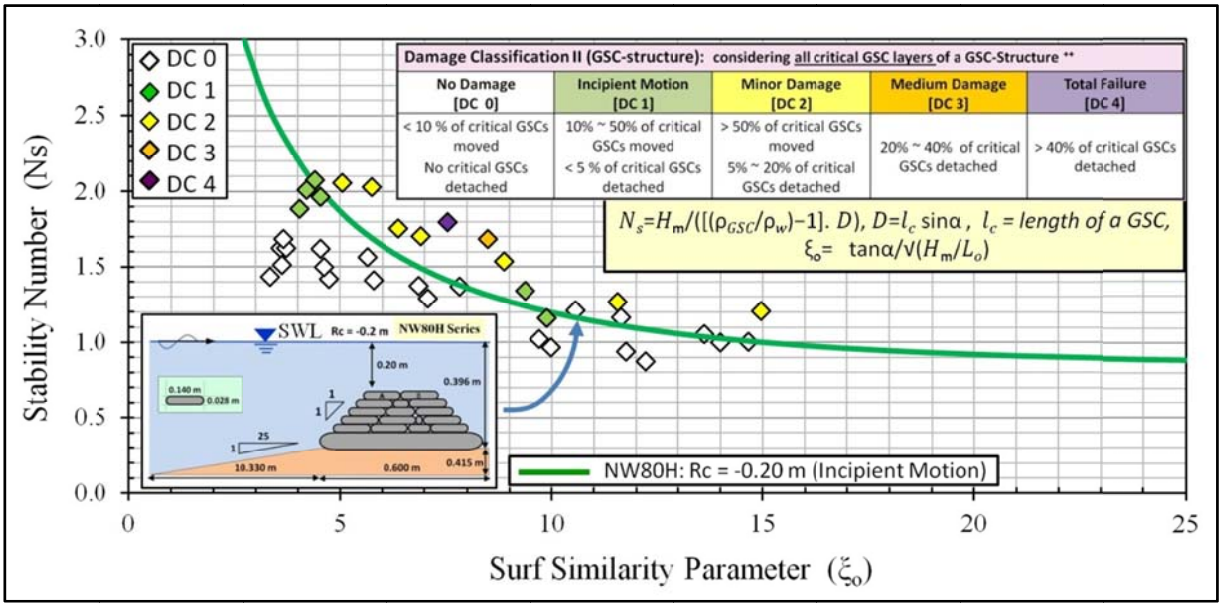

Figure 3-29: Hydraulic stability curve for submerged GSC-structures (Rc = -0.2m) made of nonwoven, 80% filled GSCs (NW80H, regular wave tests)

Moreover, the results from Oumeraci et al. (2002b) are plotted for the crest freeboards $Rc = 0.0$ m as in Figure 3-30. Despite the limited amount of data points and the tests were conducted with irregular waves, the effect of the surf similarity parameter on the damage category "little displacement" can still be observed. Therefore, the hydraulic stability of crest GSCs also depends on the surf similarity parameter.

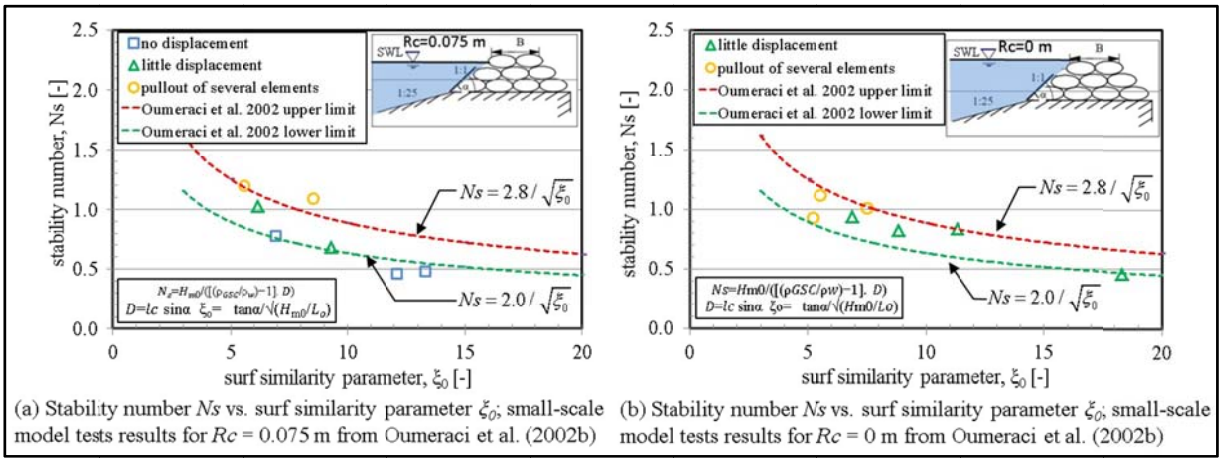

(a) Stability number *Ns* vs. surf similarity parameter ξ_0; small-scale model tests results for *Rc* = 0.075 m from Oumeraci et al. (2002b)

(b) Stability number *Ns* vs. surf similarity parameter ξ_0; small-scale model tests results for *Rc* = 0 m from Oumeraci et al. (2002b)

Figure 3-30: Small scale hydraulic stability test results from Oumeraci et al. (2002b) for crest freeboard *Rc* = 0.0 m and +0.75 m (in model scale)

3.4.6 Effect of Crest Freeboard on the Hydraulic Stability of GSC-Structures

According to Oumeraci et al. (2003), the hydraulic stability of crest GSCs depends primarily on the crest freeboard and the results from these tests confirms this finding. The hydraulic stability curves for different crest freeboards were developed based on the damage category; "Incipient motion" (DC 1) as mentioned in Table 3-6 and the curves are shown in Figure 3-31. Among the tested crest freeboards (*Rc* = -0.25 m, -0.20 m, -0.10 m, 0.00 m, +0.046 m), *Rc* = 0.0 m resulted in lowest stability. Since the data between *Rc* = -0.10 m and *Rc* = 0.0 m are missing, it is difficult to come to a conclusion.

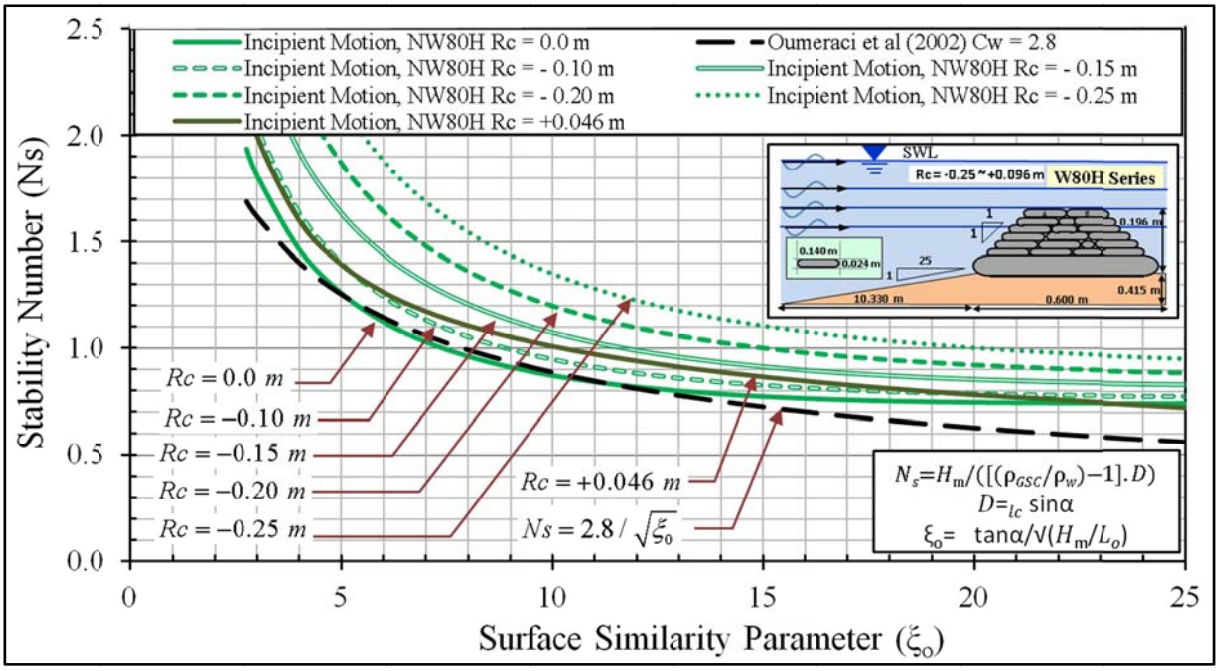

Figure 3-31: Hydraulic stability curves for regular wave tests showing the "incipient motion" cases for the tested crest freeboards *Rc* = -0.25 m ~ +0.046 m (in model scale)

3.4.7 Effect of Sand Fill Ratio on the Hydraulic Stability of GSC-Structures

In Figure 3-32 the "incipient motion" curves for 80% and 100% filled GSCs are comparatively shown (test series NW80H and NW100H). For the tested conditions (see Table 3-5), it can clearly be seen that 100% filled GSCs are more stable than 80% filled GSCs. For the 100% filled GSCs, the incipient motion occurs only when the stability number is increased by about 36% for ξ_o in the order of 5 as compared to the 80% filled GSCs. Though the overlapping length and contact area between GSCs were less for the 100% fill ratio, the 100% filled containers were more stable. This might be due to the higher weight and higher permeability of the GSC-structure associated with a 100% sand fill ratio as compared to that with an 80% sand fill ratio.

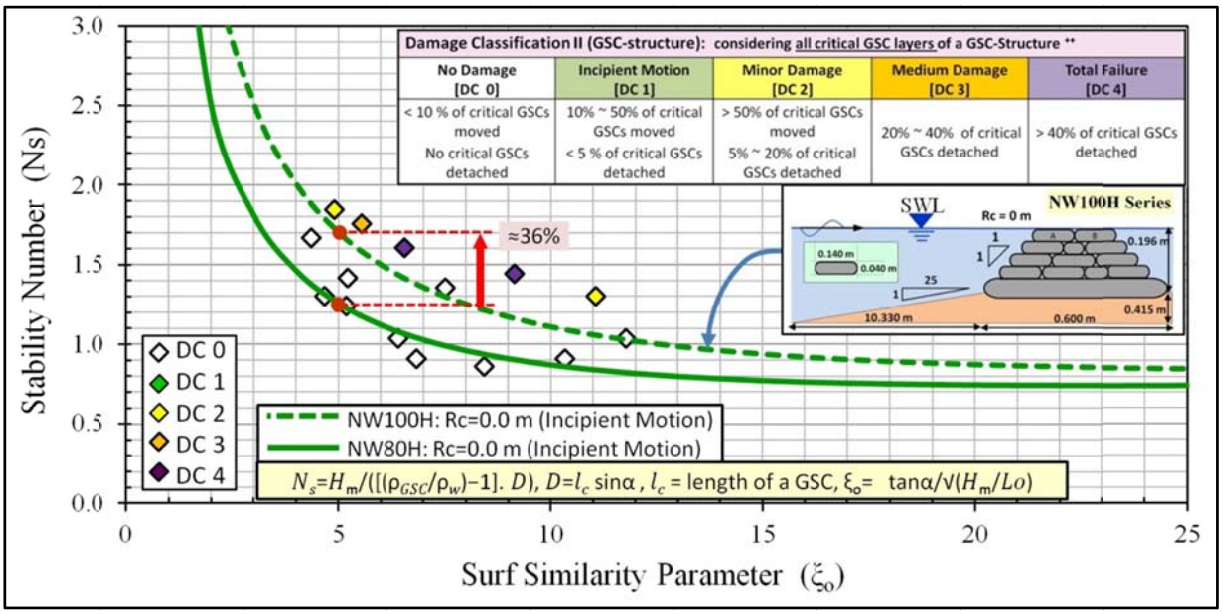

Figure 3-32: Effect of sand fill ratio on the hydraulic stability of low-crested GSC-structures: comparison of 80% and 100% filled GSCs made of nonwoven geotextile (NW80H; Rc = 0 m and NW100H; Rc = 0 m/ regular wave tests)

3.4.8 Effect of the Type of Geotextile on the Hydraulic Stability of GSC-Structures

The effects of the type of geotextile material used for the construction of GSCs on the hydraulic stability of the GSC-structure were studied by using a nonwoven (series: NW80H) and a woven (series: W80H) material (Figure 3-33). Both types of GSCs were filled 80% and had approximately the same weights under buoyancy. During the tests series, when Rc = 0 m, stability numbers of woven GSCs were ca. 40% less than those of nonwoven GSCs for "incipient motion" cases (damage category: DC 1).

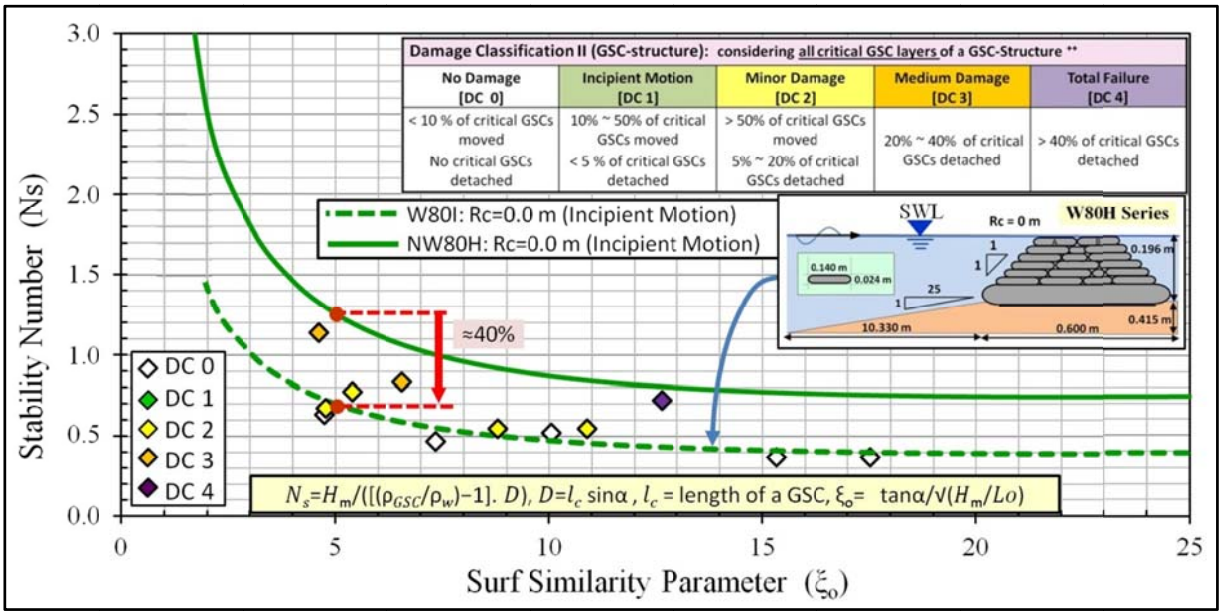

Figure 3-33: Effect of the type of geotextile on the hydraulic stability of low-crested GSC-structures: comparison of the regular wave test results of nonwoven geotextile (interface friction angle 22.64°) and woven geotextile (interface friction angle 13.33°)

As the submergence depth increases, the differences between woven and nonwoven GSCs are reduced in terms of the hydraulic stability (e.g. for *Rc* = -0.2 m, Figure 3-34), mainly because of different dominant failure mechanisms.

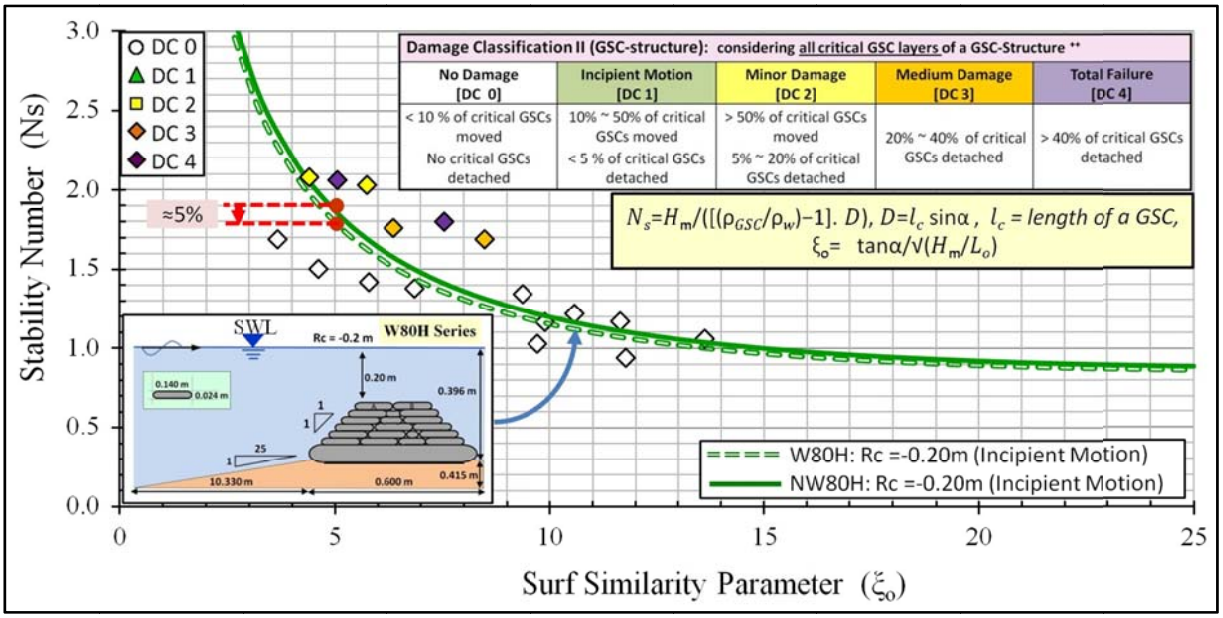

Figure 3-34: Effect of the type of geotextile on the hydraulic stability of submerged GSC-structures: comparison of the regular wave test results of nonwoven geotextile (interface friction angle; 22.64°) and woven geotextile (interface friction angle; 13.33°)

When the submergence depth is small, both woven and nonwoven GSC-structures failed due to sliding of the GSCs caused by overtopping waves, (see Figure 3-27a) whereas for relatively larger submergence depths, "uplift and drift" (see Figure 3-27b) and overturning (see Figure 3-27c) were commonly observed. For overturning and "uplift and drift" failure mechanisms, the friction between GSCs is expectedly insignificant.

Though the wave conditions that trigger the incipient motions of submerged woven and nonwoven GSCs are relatively similar, the damage progression was much more rapid in woven structures compared to nonwoven structures. For selected comparable tests, a progressive damage analysis was performed considering the number of regular waves, the type of failure mode, and the number of detached GSCs. Due to the high friction properties, nonwoven GSCs are detached mainly due to overturning (Figure 3-35a). In contrast, woven GSCs failed mainly due to sliding, which requires relatively less effort. Consequently, the damage progression of woven GSC-structure was much more rapid compared to nonwoven GSC-structures (Figure 3-35b). Therefore, not only the conditions required to start damage to a GSC-structure, but also the development of the damage is important for a comprehensive quantification of the effect of the interface friction between GSCs on the hydraulic stability.

The dominant failure mechanism of the nonwoven GSCs was overturning whereas the dominant failure mechanism for woven GSCs was sliding. Figure 3-35 provided exemplarily results on the significance of interface friction on the dominant failure mechanics.

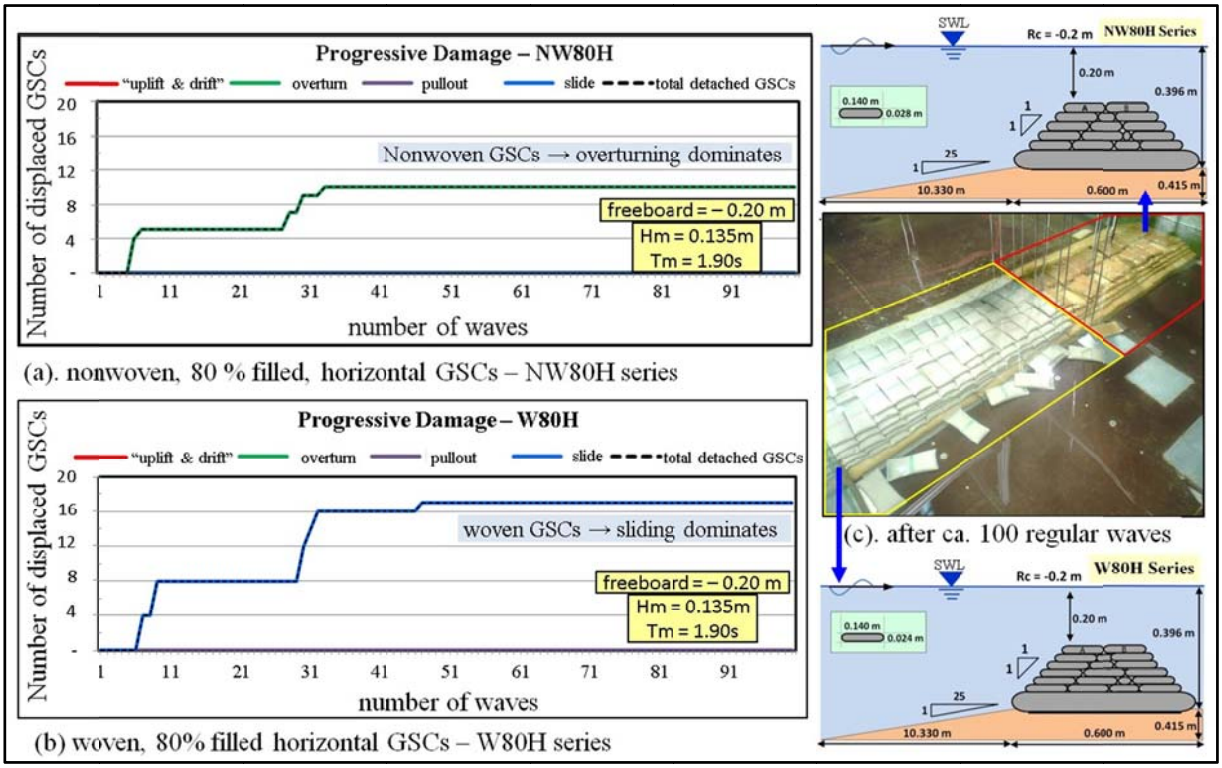

Figure 3-35: Damage progression as a function of the number of regular waves for two selected tests from NW80H and W80H test series with comparable incident wave conditions (Rc = -0.20 m)

3.4.9 Effect of Inclination Angle of GSCs on the Hydraulic Stability

The influence of the inclination angle of GSCs (between the longitudinal axis of GSCs and the horizontal plane) on the hydraulic stability was studied by comparing the stability of horizontally placed and inclined GSCs. When GSCs are placed inclined (Figure 3-36), there are several advantages. First, pulling out of GSCs from the GSC-structure is relatively more difficult compared to the horizontally placed GSCs, because, other than the friction, a component of gravitational force is also acting as a resisting force. Second, even if the incident waves caused internal movement of sand in the GSCs, the inclination angle might prevent them getting deformed (gradual enlargement of seaward end due to the internal movement of sand). Third, when construct a GSC-structure with 1:1 seaward slope using the same type of GSCs, the inclined placement resulted in larger overlapping lengths. Consequently, the friction force against the pulling out might be larger compared to those of horizontally placed GSCs.

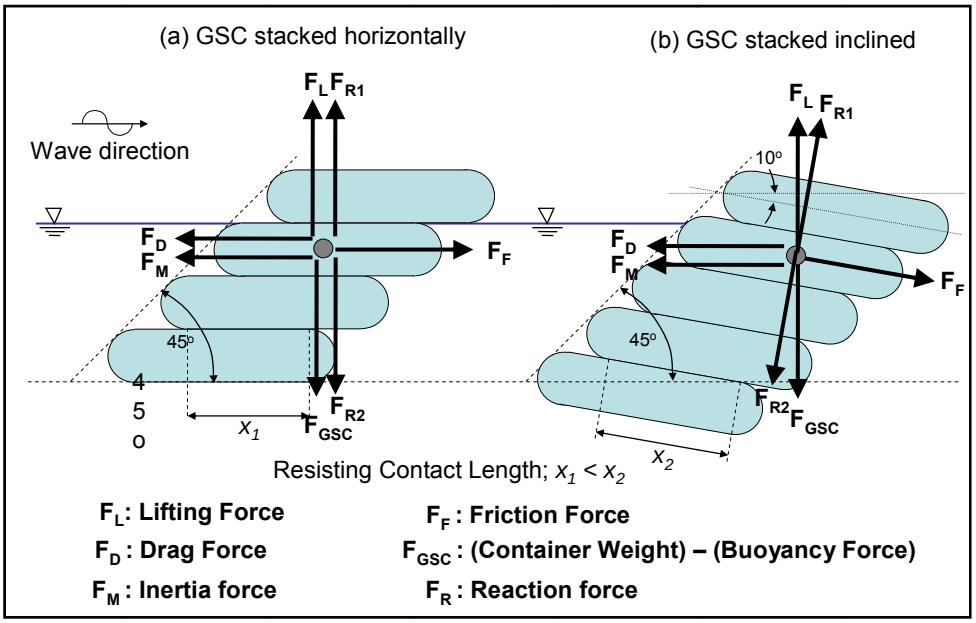

Figure 3-36: Forces acting on the GSCs under wave action

Figure 3-37 shows a comparison of the "incipient motion" (Damage category; DC1) curves for two test series NW80H (inclination angle = 0°) and NW80I (inclination angle = -15°). For *Rc* = 0 m, inclined GSC showed more stability to wave attack than horizontal GSC. For example, when the surf similarity parameter is 5, stability number is increased by 30% as compared to the horizontally placed GSCs.

Furthermore, the inclined placement of GSCs increases the hydraulic stability by restricting the internal movement of sand inside GSCs. Recio and Oumeraci (2009) described the process governing the internal movement of sand. This sand movement causes deformation of GSCs and ultimately a significant reduction in hydraulic stability against sliding. When GSCs are placed with an inclination angle instead of the conventional horizontal placement, gravitation force will prevent the movement of sand towards the seaward edge of GSCs and will thereby increase the long-term stability of GSC-structures.

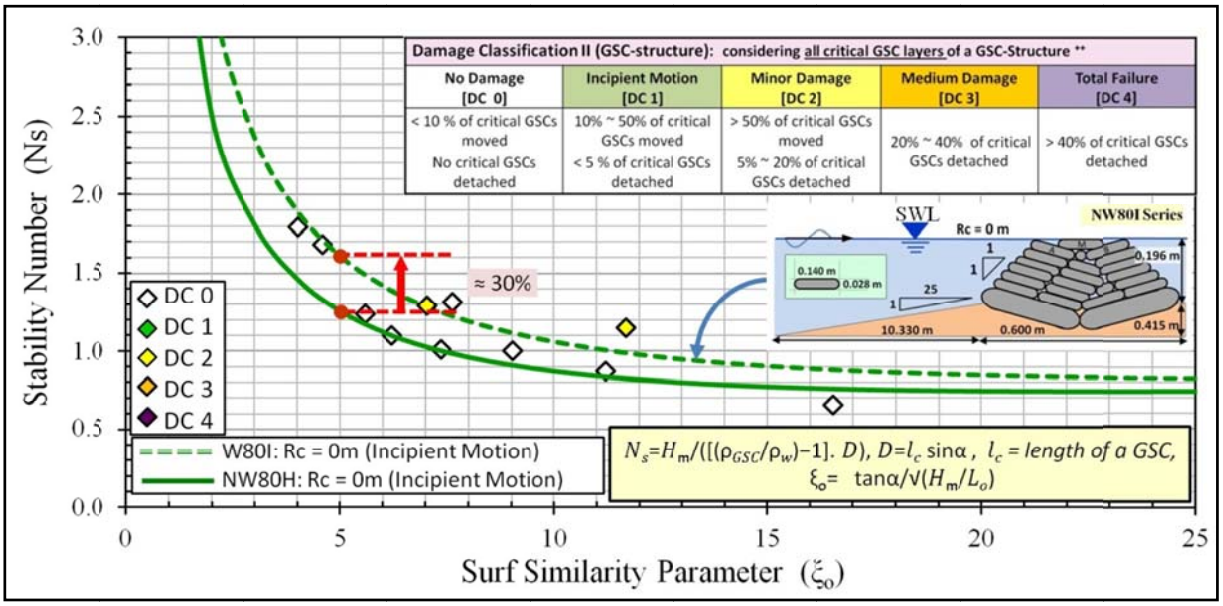

Figure 3-37: Effect of the inclination angle of GSCs on the hydraulic stability of low-crested GSC-structures: a comparison of horizontal and 15° inclined GSCs for *Rc* = 0 m (regular wave tests)

However, when the submergence depth was 0.20 m (Figure 3-38), there is no considerable difference between the wave conditions required for the initiation of damage to inclined GSC-structure in comparison to the horizontally placed GSCs. Figure 3-39 shows a progressive damage analysis of horizontally and inclined GSCs subject to regular waves and it is clear that inclined GSC have higher resistance against wave attack as the progression of damage in the NW80I test is considerably slower than in the NW80H test.

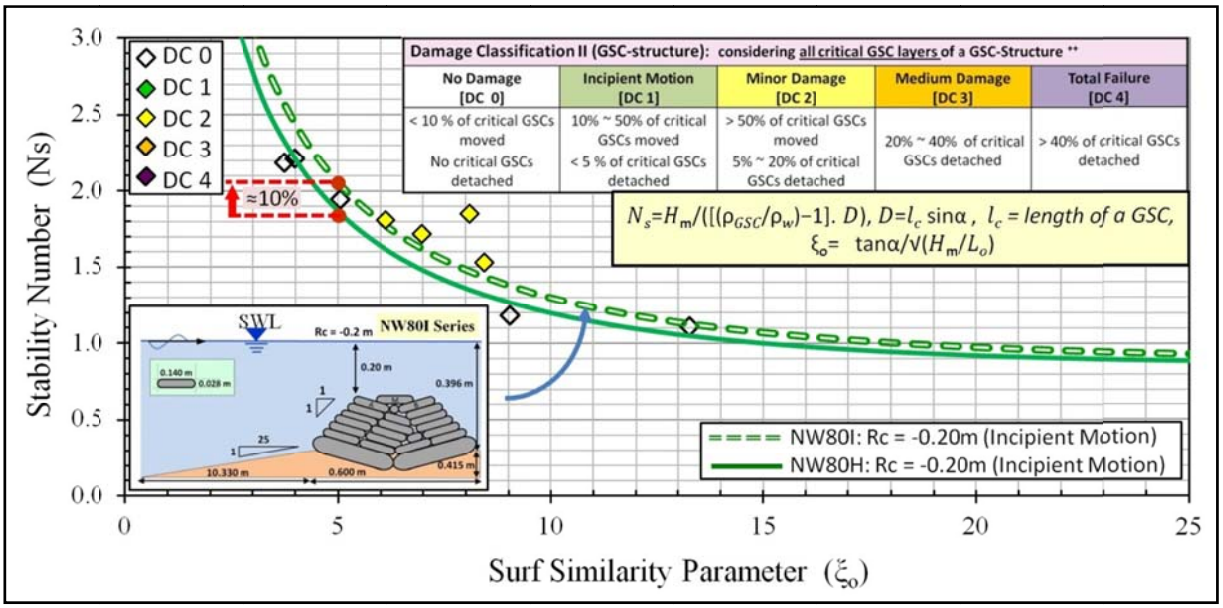

Figure 3-38: Effect of the inclination angle of GSCs on the hydraulic stability of submerged GSC-structures: a comparison of horizontal and 15° inclined GSCs for *Rc* = -0.20 m (regular wave tests)

When compare the results of two NW80H tests in Figure 3-35a and Figure 3-39a, different dominant failure mechanisms can be observed. In Figure 3-35a, ($H_m = 0.135$, $T_m = 1.90$) the dominant failure mechanism is overturning while in Figure 3-39a ($H_m = 0.144$, $T_m = 1.91$) the dominant failure mechanism is uplift and drift. During the second test (Figure 3-39a), the wave height was increased only by 7% and number of detached GSCs were more than 3 times higher. Therefore, the crest GSCs of submerged structures are extremely sensitive to the wave parameters. In addition, in Figure 3-35a, only the GSCs from the front raw at the crest were detached (mainly by overturning) and in Figure 3-39a, GSCs from both front and rear rows at the crest were detached. Once the front row is displaced, the GSCs at the rear row are exposed to the incident waves and those GSCs are mainly failed due to "uplift and drift". Further analysis on the damage developments can be found in Dassanayake and Oumeraci 2011c)

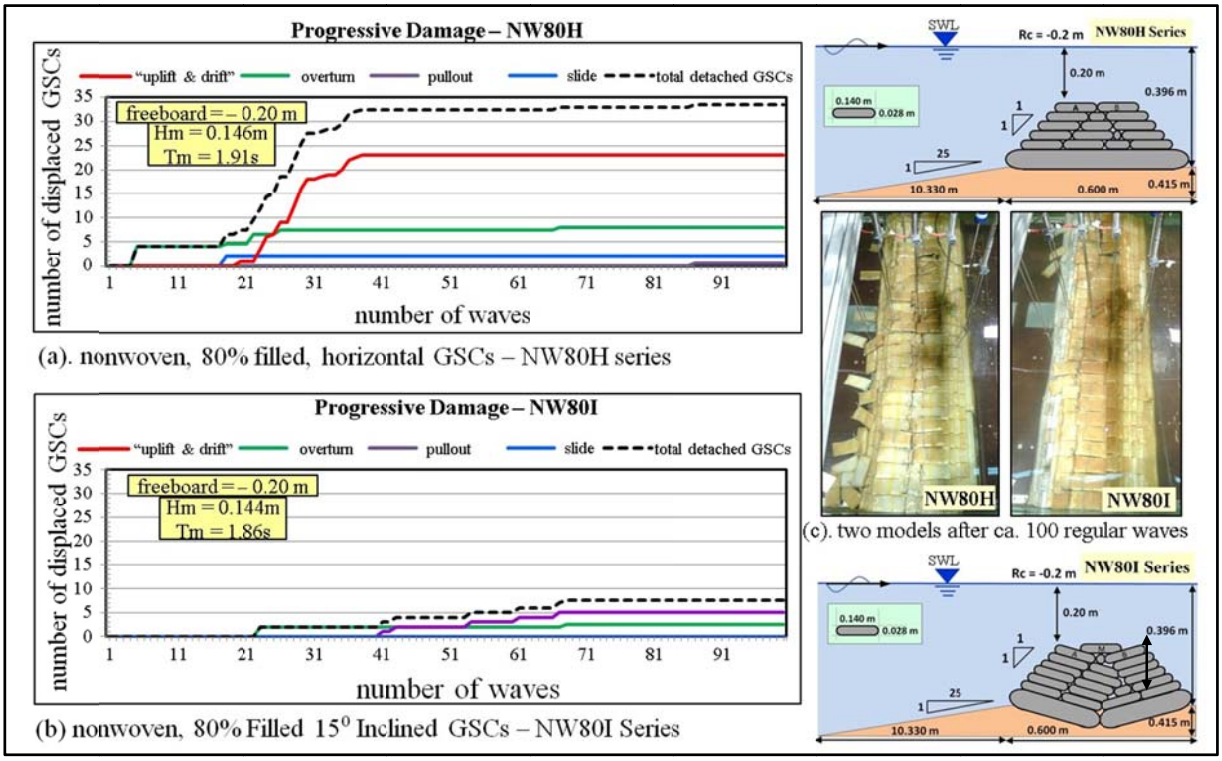

Figure 3-39: Damage progression as a function of number of waves for two selected tests from NW80H and NW80I test series with comparable incident wave conditions (Rc = -0.20 m)

3.4.10 Settlement of GSCs due to Internal Movement of Sand Under Wave Action

Another important observation made during the model testing process was the settlement of the GSC-structure. Due to continuous upward and downward movement of GSCs (e.g. incipient motion), fill material tends to accumulate at the front section of GSC. This progressive deformation process is similar to that already described by Recio (2007). Due to internal sand movement, the shape of the GSC was altered as shown in Figure 3-40a. Hence, the height of the GSC at the back section is decreased resulting in a noticeable settlement of the structure. Moreover, the GSC-structure settled as a result of the consolidation of the fill material, specially when they underwent tests with irregular waves where a single test comprises of mini-

mum number of 1000 waves. However, the maximum observed settlement was only 5%, which is lower than what Recio (2007) observed (i.e. the total reduction of height was 10%). This difference could be due to the difference in the two models used in this study and Recio's wave flume tests (see Figure 2-13 and Figure 3-26). In these model tests only five layers of GSCs were used, whereas Recio (2007) had used up to eleven GSC layers.

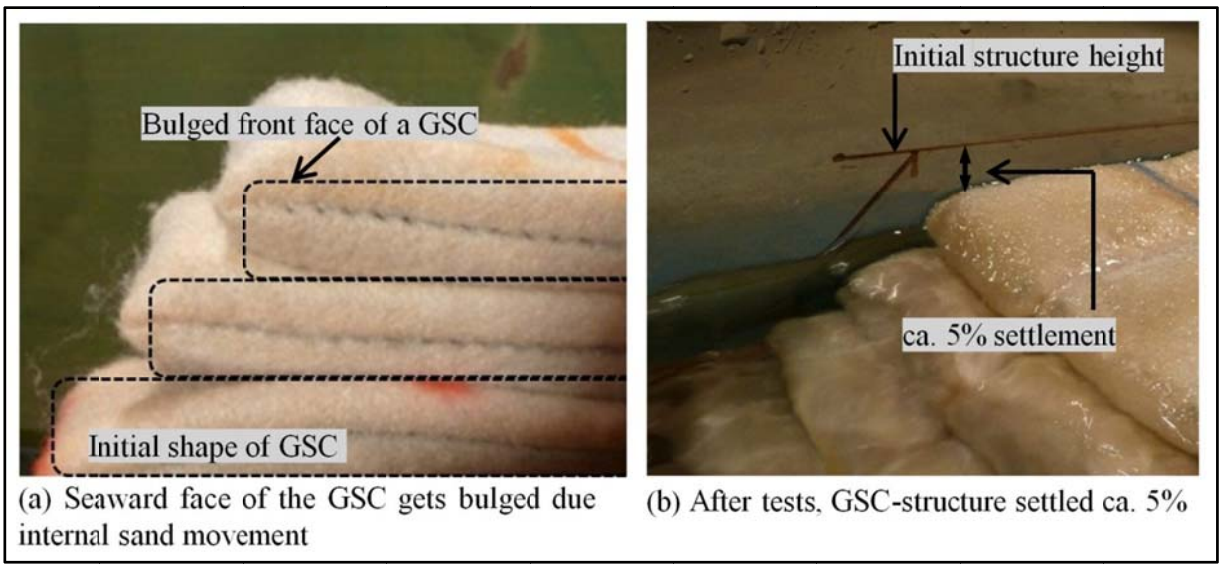

Figure 3-40: Reduction of the height of a GSC-structure due to internal movement of sand after 1000 irregular waves (Rc=-0.046, Hs=0.1 m, Tp=1.0 s)

3.4.11 Summary of Hydraulic Stability Tests and Concluding Remarks

The sand fill ratio, the type of geotextile material and the interface friction between GSCs strongly affect different processes governing the hydraulic stability of GSC-structures. These tests, therefore, represent the first attempt to systematically quantify the effects of these engineering properties and the inclined placement of GSCs on the hydraulic stability. The hydraulic stability tests were conducted on low-crested GSC-structures with both positive (submerged) and negative (emerged) crest freeboards. The most important outcomes of the experimental studies and their implications for the engineering practice can be summarised as follows:

- GSCs of a low-crested/submerged coastal structures display different failure mechanisms for different submergence depths. Furthermore, the comparative importance of the engineering properties of GSCs also varies depending on the dominant failure mechanism for a specific GSC-structure and for a particular freeboard. As expected, for most of the low-crested structures, the crest GSCs represent the critical containers in terms of the hydraulic stability. Therefore, when designing low-crested and submerged GSC structures, it is essential to carefully consider the most relevant failure mechanisms of crest GSCs, comprising the effects of the most relevant engineering properties.
- Relative crest freeboard Rc/H_m and surf similarity parameter ξ_0 are the dominant factors that govern the hydraulic stability of the crest GSCs of a low-crested/submerged GSC-structure subject to wave attack.

- GSCs made of woven geotextile (with an approximately 50% lower friction coefficient than nonwoven geotextile) resulted in 40% lower stability numbers, when the incipient motions of crest GSCs are considered for the tested conditions with a zero freeboard.
- Contrary to most of the previous studies and existing recommendations for the construction of GSC-structures (e.g. PIANC 2011) that propose a sand fill ratio of 80%, GSCs with 100% filled ratio show a 36% higher stability number for surf similarly parameters around 5. Therefore, future research and design guidance should address the definition of an optimal sand fill ratio by accounting for the elongation properties of the geotextile and by balancing the advantages and drawbacks of high and moderate sand fill ratios.
- The hydraulic stability can be increased by changing the inclination angle of GSC in a GSC-structure. When the wave conditions required for incipient motion of the GSCs are considered, GSCs inclined by -15° towards the shore resulted in nearly 30% higher stability number compared to horizontally placed GSCs.
- Key engineering parameters such as the interface friction angle, the sand fill ratio, the inclined placement of GSCs also contribute significantly to slow down the damage progress of GSC-structures over the entire storm duration. Hence, for a comprehensive quantitative assessment of the effect of the different factors considered in this study, not only the conditions essential to trigger damage to a GSC-structure, but also the development of the damage over the whole storm duration and the different damage levels that might result, are equally important .

3.5 Hydraulic Permeability of GSC-Structures - Permeability Test Results

One of the key parameters that governs the hydraulic stability of GSC-structures, which are subject to wave attack, is the hydraulic permeability (Hudson 1956, 1961, Pilarczyk 2000). In general, a more permeable structure is also more stable as it can dissipate large portion of incident wave energy. Recio (2007) extensively investigated the hydraulic permeability of different GSC-structure geometries. However, none of those tested structures were directly comparable to the model configurations, which were tested in this study (Figure 3-26). Therefore, it was indispensable to conduct new permeability tests on these model configurations. This section provides an overview of the new permeability tests and a summary of key results and the details can be found in Ozegowski (2012).

3.5.1 Results of Previous Permeability Tests

The flow through a GSC-structure is not homogeneous. The flow through the sand fill in the containers is expected to be laminar, whereas the flow through the gaps between the GSCs is turbulent. Despite the in-homogeneity of the flow and its unsteadiness, the permeability of a GSC-structure is preferably described by the Darcy's permeability coefficient k_f (Recio 2007, Recio and Oumeraci 2008a).

$$Q = v_f \times A_m = k_f \times I \times A_m = k_f \times \frac{\Delta h}{\Delta L} \times A_m \qquad (3.7)$$

where: Q: discharge [m^3/s]
v_f: velocity [m/s]
A_m: mean cross sectional area of the porous flow [m^2]
k_f: permeability coefficient [m/s]
I: hydraulic gradient [-]
Δh: difference of water height [m]
ΔL: average length of seepage path [m]

Figure 3-41 defines the relevant parameters for the quantification of permeability coefficient (k_f) of a GSC-structure.

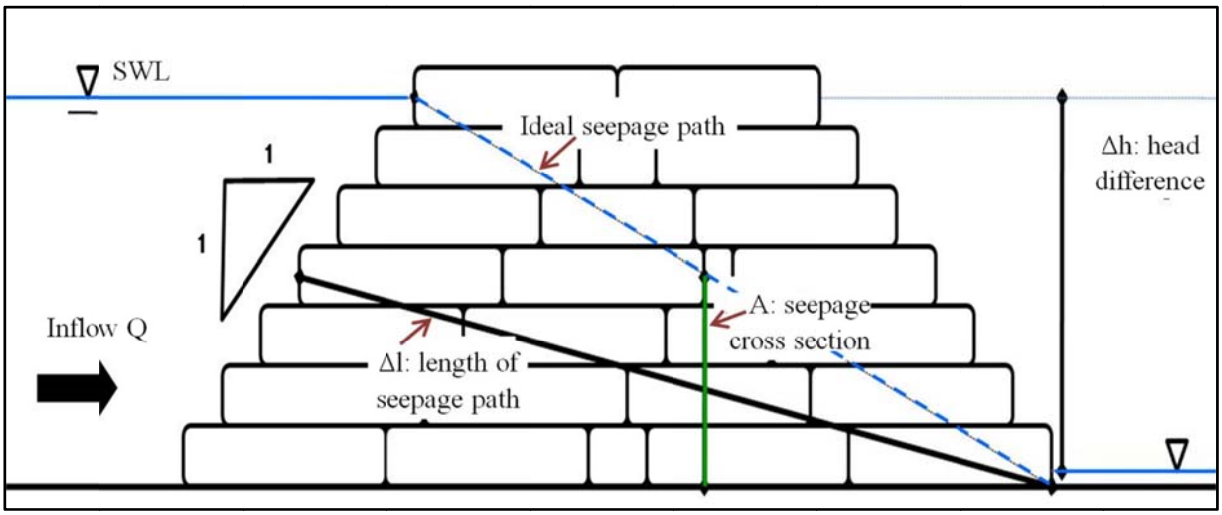

Figure 3-41: Key parameters relevant to the permeability of a GSC-structure (modified from Oumeraci 1999c)

Recio (2007) conducted two test series on the hydraulic permeability of GSC-structures. The dimensions of containers, which have been used were; 0.45 m × 0.28 m × 0.11 m, 0.35 m × 0.24 m × 0.09 m and 0.26 m × 0.13 m × 0.052 m (length × width × height). Each bag was 80% filled with sand (though the definition the sand fill ratio is vague), which has a median grain size of D_{50} = 0.2 mm, a saturated density of ρ = 1800 kg/m^3 and a permeability coefficient of approximately $k_f = 1.1 \times 10^{-4}$ m/s. Sand bag material was nonwoven geotextile with a permeability coefficient of $k_f = 1.1 \times 10^{-1}$ m/s. Figure 3-42 shows the experimental set-up of the permeability tests. During the first series, 11 different model configurations have been tested in a tank at the Leichtweiß-Institute (LWI), while varying the size of the GSCs, the size of the gaps between the GSCs and different placement modes of GSCs.

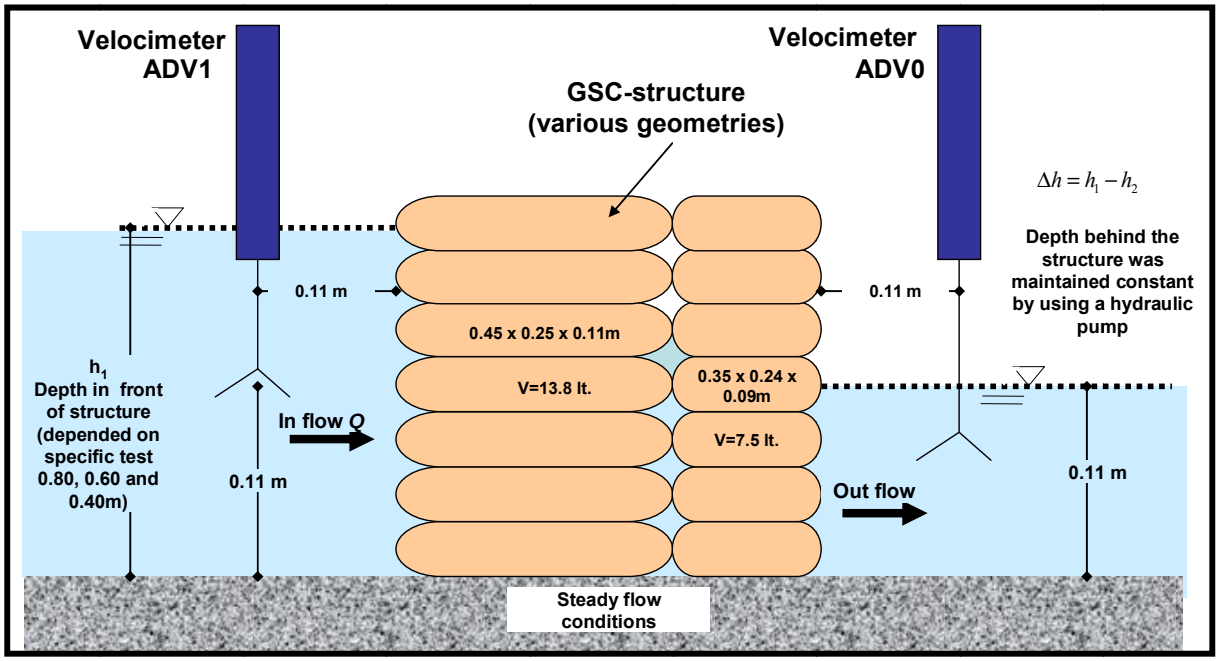

Figure 3-42: Experimental setup for basic permeability tests (Recio 2007)

The permeability coefficients have been determined using Darcy's equation. The key result of the tests performed by Recio regarding the hydraulic performance is that the size of the gaps governs the permeability of GSC-structures. The main conclusions, which were drawn from the experimental studies by Recio and Oumeraci (2008a), can be summarized as follows.

- The size of the gaps governs the overall permeability of the GSC-structure. The permeability of the fill material can be nearly neglected, because it is nearly ten times smaller than the permeability of the GSC-structure.
- The smaller the container, the smaller the permeability coefficient of the structure. If no other data is available, Recio suggested to suppose $k_f = 10^{-2}$ m/s for GSC-structures.
- longitudinal or transversal GSC arrangement will provide similar flow though the structure.
- The permeability of a GSC-structure is considerably reduced, if there is a second layer of overlapped containers that obstructs the flow coming out of the gaps of the first layer.
- The permeability coefficient of GSC-structures with elements parallel to the flow may vary from 8 x 10^{-3} m/s (medium containers) to 1.5 x 10^{-2} m/s (large containers).

Furthermore, a conceptual model was developed to assess the permeability of GSC-structures. This conceptual model can be used to approximately estimate the permeability of GSC-structures. Nevertheless, when very accurate permeability coefficients are needed, it is recommended to perform new permeability tests (Recio 2007). As shown in Table 2-5, there is a significant variation in the permeability measurements (e.g. Permeability of a single column of 13.8 *l* is lower than a complete structure with 1.7 *l* GSCs). Therefore, a different approach is necessary for the new permeability tests, in order to account for the influence of the sand fill ratio (sand fill ratio will increase the gap sizes and consequently permeability coefficients) on the hydraulic permeability (Dassanayake and Oumeraci 2009a).

3.5.2 Experimental Setup

In order to quantify the effect of engineering properties of GSCs and the inclined placement of GSCs on the overall permeability of GSC-structures, new permeability tests were performed in a 0.6 m wide hydraulic flume at LWI. These tests were performed using existing small scale GSCs that were constructed for hydraulic stability test. The main objective of the new permeability tests was to determine the Darcy permeability coefficient for each GSC-structure tested during the hydraulic stability tests (Figure 3-26).

The model setup is shown in Figure 3-43. The flow velocity was measured with an Acoustic Doppler Velocimeter (ADV). The ADV was installed 1.04 m upstream the GSC structure (Figure 3-43). In order to get the complete velocity profile, the velocities were measured at 5 different water depths. The data of the ADV was processed and the inflow discharges Q through GSC-structures were calculated. Then Darcy's Law (equation 3.7) was applied (Figure 3-43) to compute the permeability coefficients.

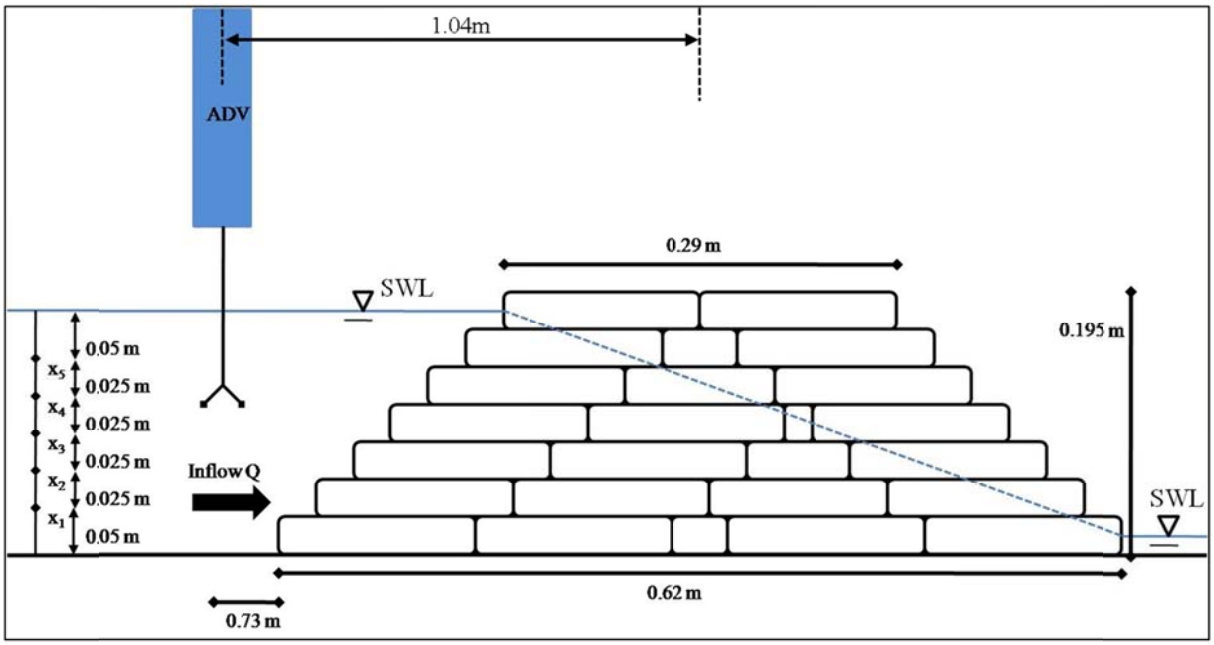

Figure 3-43: Experimental setup and measuring techniques of new permeability tests

3.5.3 Summary of Permeability Test Results and Concluding Remarks

This research study represents the first attempt to systematically quantify the effects of the sand fill ratio, the type of geotextile material and the inclined placement of GSCs on the hydraulic permeability of GSC-structures. The permeability tests were conducted on low-crested GSC-structures with a zero crest freeboards. Permeability coefficient was determined for each model configuration and results are given in Table 3-7. Since the permeability of the small scale GSC-structures were relatively low, it was difficult to perform permeability tests with high crest freeboards (with relatively lower head differences across the GSC-structure) that will result in lower discharges Q than the zero crest freeboard scenario.

Table 3-7: Results of permeability tests (modified from Ozegowski 2012)

GSC-structure	GSC-structure	GSC dimension length l_c = 0.140 m width b_c = 0.070 m height h_c : varies	Permeability coefficient k_f [m/s]
(a). NonWoven **80%** filled Horizontally placed GSCs in a Rectangular shaped structure: NW80HR		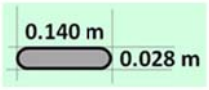	2.94×10^{-2}
(b). NonWoven **100%** filled Horizontally placed GSCs in a Rectangular shaped structure: NW100HR			11.13×10^{-2}
(c). Woven **80%** filled Horizontally placed GSCs in a Rectangular shaped structure: WW80HR			7.63×10^{-2}
(d). NonWoven **80%** filled 15° Inclined GSCs in a Rectangular shaped structure: NW80IR .		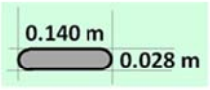	1.72×10^{-2}
(e). NonWoven **80%** filled Horizontally placed GSCs in a Trapezoidal shaped structure: NW80HT		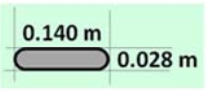	3.31×10^{-2}
(f). Woven **100%** filled Horizontally placed GSCs in a Trapezoidal shaped structure: NW100HT			8.68×10^{-2}
(g). Woven **80%** filled Horizontally placed GSCs in a Trapezoidal shaped structure: WW80HT		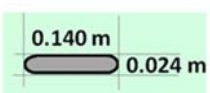	8.35×10^{-2}
(h). NonWoven **80%** filled 15° Inclined GSCs in a Trapezoidal shaped structure: NW80IT			1.81×10^{-2}

The Darcy permeability coefficient should not vary based on the shape of the structure. In order to verify the coefficient determined for the different model configurations tested in the hydraulic stability tests, it was required to have another data set. Therefore, the initial permeability tests were performed with vertical fronts and tandem orientation of GSCs (Table 3-7a, b, c, d). Then the permeability coefficient determined from the trapezoidal cross sections (Table 3-7e, f, g, h, which were tested during the hydraulic stability tests) were compared with the values obtained from the initial tests. The corresponding permeability coefficients show a good agreement and therefore, the methodology to obtain the overall permeability of the GSCs structure was also validated.

In Table 3-8, two selected permeability test results of Recio (2007) are compared with the results of this study. Though the model cross sections are fairly similar, Recio used staggered GSC arrangements, whereas the current tests were conducted with tandem arrangement. Therefore, the shapes of the gaps between GSCs are different. As a result, Recio's (2007) permeability coefficients are slightly lower than those of the current tests. However, all the results are still in the same order of magnitude.

Table 3-8: Comparison of Recio's (2007) and current permeability test results (modified from Ozegowski 2012)

GSC-structures from Recio's permeability tests (2007)	Permeability Coefficient k_f [m/s]	GSC-structures from new permeability tests (2012)	Permeability Coefficient k_f [m/s]
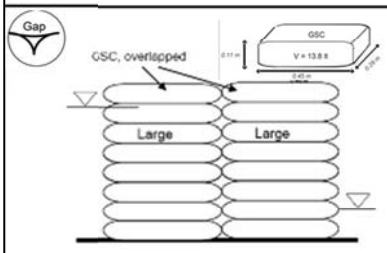 Staggered arrangement	1.40×10^{-2}	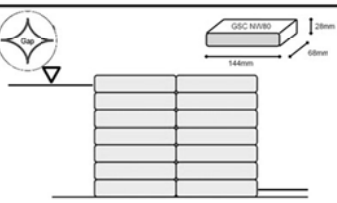 (a). NonWoven 80% filled NW80HR : tandem arrangement	2.94×10^{-2}
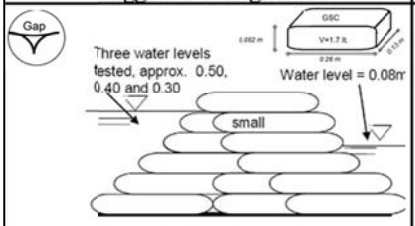 Staggered arrangement	2.274×10^{-2}	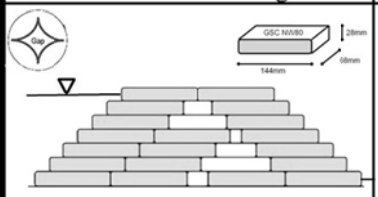 (e). NonWoven 80% filled NW80HT : tandem arrangement	3.31×10^{-2}

The main outcomes of the permeability tests are summarised below. Detailed results can be found in Ozegowski (2012).

- Both the rectangular and the trapezoidal GSC-structures resulted in nearly the same permeability coefficients. Therefore, in spite of the inhomogeneities in GSC-structures (sand fill, geotextile "skin" and gaps between GSCs), it is still possible to describe the permeability with Darcy's law due to comparatively low velocities of the porous flow.
- The obtained Darcy permeability coefficients are slightly higher than those obtained by Recio (2007) for comparable GSC-structures. This is due to the different arrangement

adopted by Recio (staggered) and in this study (tandem). These arrangements results in different gap sizes.

- The permeability test results showed that nonwoven 100% filled GSCs have a ca. 3~4 times higher permeability than nonwoven 80% filled GSCs. This might be mainly due to the larger gaps between the 100% filled GSCs compared to those of the 80% filled GSCs.
- The type of geotextile material is also a key influencing factors of the overall hydraulic permeability of a GSC-structure. Nonwoven GSCs are relatively more flexible and compact when they are in water. In contrast, woven GSCs are less flexible and leave larger gaps between GSCs. Moreover, due the different textures of the woven (smooth) and the nonwoven (rough) geotextiles, the resistance of the flow through the gaps might differ, thus resulting in lower permeability coefficients for the nonwoven GSCs. For example, 80% filled woven GSCs have ca. 2.5 times higher permeability coefficients compared to 80% filled nonwoven GSCs.
- When 80% filled nonwoven GSCs are placed with an inclination angle, the overall permeability of the structure reduces by 50% compared to horizontally placed GSCs.

Recio and Oumeraci (2007d), Werth et al. (2008) and Recio and Oumeraci (2008a) presented a conceptual model to describe the permeability of GSC-structures. In this model, gaps between GSCs are defined as several pipe flows across the structure and the conceptual model was validated with some experimental data. Later, this conceptual model was adopted in numerical simulation of GSC-structures using COBRAS model. Unfortunately, this conceptual model cannot be adopted in the numerical simulation of this study (see Section 4.4). This is mainly due to the limitations associated with the number of cells (maximum no of cells = ca. 550,000) in the COBRAS-UC model and also due to the model scale of the hydraulic stability tests. In order to model the permeability of GSCs as pipe flows, height of the pipes should be represented by at least three cells. Since, the height of a small scale GSC is 0.028 m (80% filled nonwoven GSCs), even with the maximum possible number of cells in COBRAS-UC model, the GSC height is represented by only 4 cells. Therefore, is not feasible to reproduce the hydraulic stability tests of this study with the conceptual model proposed by Recio (2007). As an alternative, GSC-structure was considered as an uniform medium and the average properties of that medium were defined to achieve a correct representation of the permeability of each tested model configuration.

3.6 Summary and Concluding Remarks

Two important engineering properties of GSCs: the sand fill ratio and the interface friction between GSCs, as well as the inclination angle of GSCs affect the different processes governing the hydraulic stability of GSC-structures. One of the first challenges of this study was to develop a physically-based definition for sand fill ratio. A new definition was developed by considering the dry bulk density of sand and the initial fully inflated volume of an empty flat bag (Section 3.1.1) and this definition was successfully implement in prototype GSCs (Oumeraci et al. 2012).

Moreover, this research study represents the first attempt to systematically quantify the effects of the sand fill ratio, the interface friction between GSCs and the inclination angle of GSCs on the hydraulic stability of GSC-structures. In order to achieve this objective, four different experimental investigations were performed, which consisted of underwater drop tests, pullout tests, hydraulic stability tests, and permeability tests. The important outcomes of the experimental studies and their implications for the engineering practice were summarised in section 3.2.7, section 3.3.8, section 3.4.11 and section 3.5.1.

First, based on the results from the drop tests and pullout tests, two sand fill ratios were selected for the hydraulic stability tests. Apart from that, pullout tests were helpful to define the scope of the hydraulic stability tests more precisely. Second, an intensive test programme was performed in the 2 m wide wave flume at LWI while varying the sand fill ratio, the type of geotextile material, the inclination angle, and other hydraulic parameters such as wave height, wav period, crest freeboard, wave type, etc. These tests generated a wide-ranging data set on the hydraulic stability of submerged and low-crested GSC-structures, which can be used for the development of new hydraulic stability formulae. Apart from that, all these test series generated required information to perform a detailed numerical study on the hydraulic stability of GSC-structures subject to wave attack.

4 Effect of Engineering Properties of GSCs on Hydraulic Stability – Numerical Studies and Results

Empirical formulae developed based on scaled model testing showed several restrictions (e.g. relatively narrow range of applicability, difficulty to reproduce some of the important factors relative to the hydraulic stability, such as friction between elements, flow in the porous structures, etc.). Given the rapid development of numerical models during the last few decades, numerical simulations of wave-structure interactions are now possible in order to extend the range of conditions tested in the laboratory. In order to simulate all the processes related to the hydraulic stability of GSC-structures, ideally a fully coupled Computation Fluid Dynamic (CFD) and Computation Structural Dynamic (CSD) model is required. Even though some research studies on combined CFD-CSD modelling have been conducted recently (Latham et al. 2008, Greben et al. 2008, Mindel 2008, Latham et al. 2009, Xiang et al. 2012) on the wave-structure interactions, most of these research studies are still limited to stiff elements such as rock or concrete armour units (e.g. Dolos, CORE-LOC, etc.). However, due to the flexible nature of GSCs, these models cannot be directly applied to GSC-structures. Recio (2007) illustrated the possibilities to numerically simulate the hydraulic stability of GSC-structures considering their flexibility. He used a weakly coupled CFD and CSD model to simulate GSC-revetments, which provided results within a reasonable accuracy for the engineering practice.

Since the experimental investigations always involve not only various expensive technical resources, but also considerable expensive consumables, the numerical modelling is also considered as a cost effective technique. Furthermore, once a calibrated numerical model is established, a range of scenarios may be investigated with relatively less effort and time than in the laboratory. As mentioned in chapter 5 of "state of the art review" report (Dassanayake and Oumeraci 2009a), COBRAS/UDEC model, which was initially proposed by Recio (2007), is still the most appropriate modelling system for GSC-structures. Therefore, the current PhD research study will focus on extending the weakly coupled COBRAS/UDEC system, where COBRAS (Liu and Lin 2002) is a RANS-VOF type flow model and UDEC (Itasca 2011) is a coupled FEM-DEM structural dynamic model.

The original COBRAS version from USA was modified in Spain and the new version was released as COBRAS-UC (Lara et al. 2008) in 2008 (see section 4.2.2). Meanwhile, a new version of UDEC (UDEC version 5) was also released in 2011 by Itasca. Therefore this chapter describes the capabilities and the limitations of using previous COBRAS/UDEC (Recio 2007) and the new COBRAS-UC/UDEC models (section 4.2.4 and section 4.2.5 respectively) for the simulation of the hydraulic stability of GSC-structures in detail. Moreover, the chapter will cover the adaptations of COBRAS-UC/UDEC models to simulate submerge GSC-structures with different sand fill ratios and different types of geotextile materials and results from the numerical simulations, etc.

The objectives of the current numerical modelling study can be summarized as follows.

(i) Examine of the capabilities and limitations of previous COBRAS/UDEC (UDEC version 4) modelling system to model the submerged GSC-structures, (ii) Extend previous COBRAS/UDEC into new COBRAS-UC/UDEC (UDEC version 5) modelling system, (iii) Further develop the "COBRAS-UC/UDEC modelling system and validate it based on the experimental results, (iv) Carry out a parameter study using the validated COBRAS-UC/UDEC modelling system in order to extend the range of the conditions tested in the laboratory.

The weakly coupled COBRAS-UC/UDEC model was adopted for the modelling of submerged/low-crested GSC-structures. The COBRAS-UC code is capable of modelling the wave structure interaction of submerged/low-crested structures and results are provided in numerous publications (Lara et al. 2008). Therefore, COBRAS-UC/UDEC modelling system could be successfully used for the modelling of submerged/low-crested GSC-structures.

This study consists of four phases (Figure 4-1), which are specified below in chronological order. Initially, COBRAS-UC model was used to study the hydrodynamics around the submerged GSC-structures and to optimise the test programme of the hydraulic stability tests (Dassanayake and Oumeraci 2010c). The next step was to introduce the necessary modifications and to validate the COBRAS-UC/UDEC modelling system to model the hydraulic stability of submerged GSC-structures. The results from the hydraulic stability tests and the pullout tests were used for the validation. Then the validated modelling system was used for a parameter study in order to extend the range of the conditions tested in the laboratory. This is indispensable to improve the understanding of the physical processes involved in the hydraulic stability of submerged GSC-structure. Based on this improved understanding, it is then possible to develop more physically-based and simpler formulae for hydraulic stability of GSC-structures, which will take into account properly the most relevant parameters affecting the stability (water depth, wave parameters, properties of GSCs, geometry of GSC-structure and inclination angle of GSCs).

The overall approach, which is adopted for this numerical study, is illustrated in Figure 4-1.

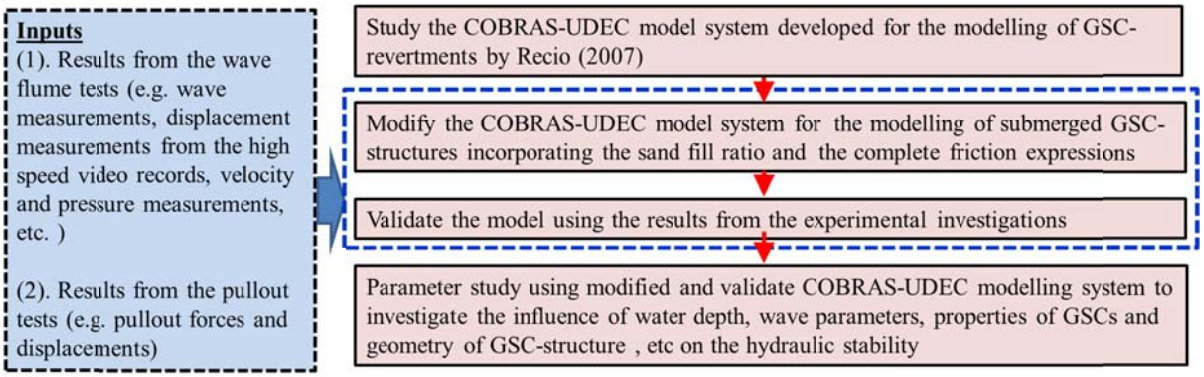

Figure 4-1: Methodology for the numerical modelling of submerged GSC-structures

4.1 Description of the Weakly Coupled CFD-CSD Modelling System

4.1.1 Description of the CFD Model COBRAS-UC Model

Among the different approaches to numerically model the wave-structure interactions, numerical models based on Navier-Stokes equations have clear advantages. By incorporating a turbulence closure model and by considering Reynolds Average Navier-Stokes (RANS) equations, they overcome the limitations associated with the use of a given wave theory and the inclusion of wave breaking. Furthermore, with the addition of Volume of Fluid (VOF) technique to track the free surface, they are able to model large and complex free surface deformations (Losada et al. 2009).

Liu et al. (1999) developed COBRAS ("Cornell Breaking Waves and Structures") to simulate the evolution of breaking waves and their interaction with coastal structures. The model is based on a previously existing model called RIPPLE, which was originally developed at "Los Alamos National Laboratory", USA. The COBRAS model describes two dimensional incompressible fluid flows with surface tension on free surfaces of general topology. Finite difference solutions to the incompressible Reynolds Averaged Navier-Stokes equations for the mean flow field and the k-ε equations for the turbulent field are obtained on a non-uniform mesh. For tracking the free surface, the VOF method is used. Different types of waves can be defined in the model: linear, Stokes II, solitary, cnoidal, Stokes V, and irregular wave. Moreover, the effect of a jet at any of the boundaries and at any position can be simulated. The turbulence model can consider linear or nonlinear eddy viscosity or Reynolds stress terms. The structures can be defined as non-porous or porous.

Hsu et al. (2002) extended the original COBRAS model by introducing the Volume-Averaged / Reynolds Averaged Navier-Stokes (VARANS). In these VARANS equations, the volume-averaged Reynolds stress is modelled by adopting the nonlinear eddy viscosity assumption. The volume averaged turbulent kinetic energy and its dissipation rate are derived by taking the volume-average of the standard k-ε equations, therefore introducing the turbulence flow in the porous media. In this study, the validation mainly focuses on the regular wave field in front of the structure. The main governing equations COBRAS/COBRAS-UC models are presented in Dassanayake and Oumeraci 2012f. The detail information of COBRAS can be found in Liu and Lin (1997) Lin and Liu (1998) and Liu and Lin (1997) and Dassanayake and Oumeraci (2012f)

4.1.2 Improvement of the Previous Version Used by Recio (2007)

Although other RANS models are available in the literature (e.g. Troch and de Rouck 1998, Kawasaki 1999, Li et al. 2004), COBRAS and COBRAS-UC are probably the most extensively validated model, especially for wave interaction with permeable low-crested structures (Garcia et al. 2004a, Garcia et al. 2004b, Losada et al. 2005, Lara et al. 2006a) and wave breaking on permeable slopes (Lara et al. 2006b). The new version of the code, COBRAS-UC

allows the possibility to consider larger and more complex computational domains and longer simulation times (Losada at al. 2008)

The mesh generation process and definition of the elements of the flume to be modelled (solid obstacles, porous media, etc.) were main limitations of previous COBRAS versions. Therefore, COBRAS-UC comprises a graphical user interface to define the initial parameters necessary for the simulation including the generation of elements with irregular shapes to describe the structures. The interface is based on a new technique to generate obstacles and avoids previously undetected sources of errors.

Moreover, validation was conducted considering the experimental data. For low-crested structures, comparisons of spatial evolution of the wave spectrums (measured and computed) were used for validation. Losada et al. (2008) showed a good comparison of experimental data (from Garcia et al. 2004a) and numerical results obtained from COBRAS-UC.

4.1.3 Description of CSD Model UDEC

Discrete (or distinct) element methods (DEM) are numerical methods for computing the motion and the interaction of large number of separate objects in a system. The Universal Distinct Element Code (UDEC) is a two-dimensional DEM code, which is based on the Finite and Discrete element methods for deformations and discontinue modelling. UDEC simulates the response of discontinuous media (e.g. jointed rock mass) subject to either static or dynamic loading. The discontinuous medium is represented as a group of discrete blocks. The discontinuities are treated as boundary conditions between blocks, where large displacements along discontinuities and rotations of blocks are allowed (DEM in UDEC). The relative motion of the discontinuities is also governed by linear or nonlinear force-displacement relations for movement in both the normal and shear directions. Individual blocks can be modelled as either rigid or deformable material. Deformable blocks are subdivided into a mesh of finite-difference elements, and each element responds according to a prescribed linear or nonlinear stress-strain law (FEM in UDEC, Itasca 2011).

UDEC has several advantages in modelling the behaviours of GSCs. One of the main problems associated with modelling of GSCs was to get the correct representation of GSC-GSC joints. The pullout test results have shown that (Dassanayake and Oumeraci 2010d) there is a significant different between static friction (peak friction) strength and dynamic friction strength. Once GSCs start to move, the required force to move GSCs were reduced considerably. However, this mechanism was difficult to model, because DEM codes generally need only a single friction angle. Fortunately, UDEC includes different representations of joint material behaviour. The basic model to represent the joints is the Coulomb slip criterion, which assigns elastic stiffness, frictional, cohesive and tensile strengths, and dilation characteristics to a joint. Furthermore, UDEC allows modifications to this basic model and also offers more complex models such as the continuously yielding joint model (Itasca 2011). Apart from that, the other challenge was to properly model the stiffness of GSCs, which is one of the unique characteristics of GSCs that differentiate GSCs from other conventional construc-

tion materials. The low stiffness of GSCs is expected to govern the hydraulic stability of GSC-structures. UDEC also has the capability of handling discrete elements with high flexibility.

4.1.4 Weakly Coupled CFD-CSD Model Used by Recio (2007)

Within the framework of his PhD, Recio (2007) proposed a methodology to simulate the hydraulic stability of GSC-revetments using a weakly coupled COBRAS and UDEC models. Both CFD and CSD models were running almost independently, only sharing input and output information among them (weak coupling). Ideally, both CFD and CSD models should run simultaneously, sharing information continuously and instantaneously (full coupling). Therefore, weak coupling might represent serious limitations (see Section 2.5.3).

The "weak coupling" of the models is performed as follows (modified from Recio 2007):

(i) The CFD model COBRAS calculates the wave-induced pressures along the surface of each element. The pressures are then integrated into forces at each nodal point of the perimeter of the finite element mesh of each GSC.

(ii) Using the results calculated in step (i) the structural dynamic model (FEM in UDEC) calculates the displacements of each node of the GSC (deformations). From the GSC-deformations, the model (FEM) derives the stresses inside the GSCs.

(iii) The structural dynamic model (DEM in UDEC) calculates the resultant forces and interactions among the GSCs in the structure from the displacements of the nodes, which are in the surface of each element that interact with the neighbouring elements and the interactions. The displacement of each element is then calculated by considering the shear properties of the joints and the derived resultant forces.

(iv) Finally, the CFD-CSD model system proceeds to the next time step with an updated geometry (if required) for the calculation of the wave-force by the CFD model as in step (i).

Since only a "partial coupling" is performed, the two main factors that control the accuracy of the simulations are the selected time step and selected threshold for updating the structure geometry in the CFD model.

Based on the knowledge obtained from various model tests and analyses of coastal structures made of sand containers, substantial efforts have been made to reduce the limitations of the models in order to improve the simulation of the hydraulic processes responsible for the instability of GSC-revetments. For instance, the flow in/on the GSC-structure is three dimensional while COBRAS (or COBRAS-UC) can simulate only two dimensional flow. Therefore, assumptions are made to simplify the 3D flow problem into a 2D problem. The size of the containers was reduced to create gaps between them (based on the conceptual model to obtain the correct permeability of the GSC-structure, see Recio 2007), while their frontal part was prescribed as vertical to maintain the wave reflection coefficient of the structure (Figure 4-2).

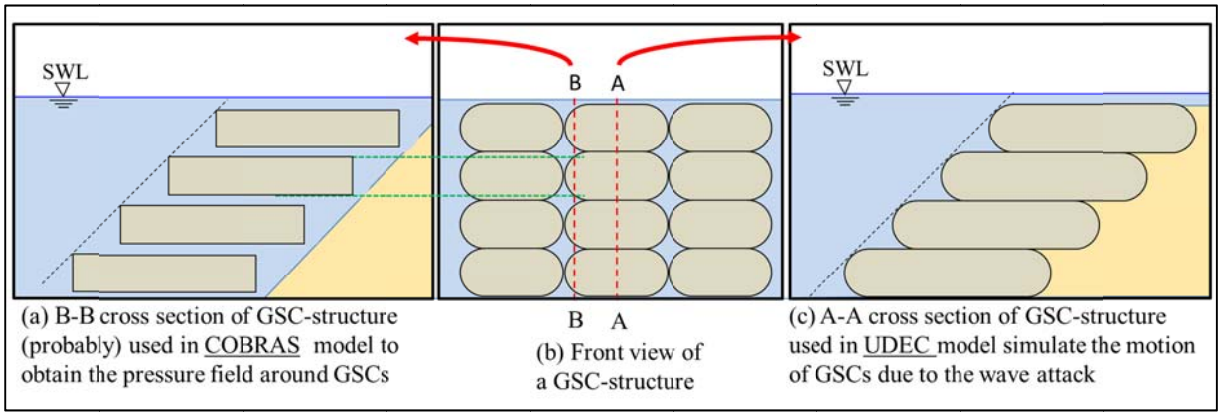

Figure 4-2: Simplifications for the conversion of 3D problem into a 2D problem with tandem arrangement

Due to the complexity of the stability problem, it is not practicable to simulate all the processes and interactions that may affect the stability of the GSCs. Moreover, a GSC is a complex composite element (3D pillow shaped element made from two materials; geotextile and sand) and Recio (2007) defined three components with different properties (i.e. (i) the surface of the GSC made of geotextile material, (ii) the interface between the geotextile and the sand and, (iii) the sand fill) to be dealt with. However, UDEC model can only handle elements made of a continuous material (no discontinuities inside elements). Therefore, some assumptions have been introduced to change the composite material of GSC to a representative homogeneous, continuous material. Thus, for the simulations, the properties of the homogeneous material in the block have "average properties" of GSCs (e.g. "average" density, "average" bulk modulus and "average" shear modulus). Table 4-1 provides an overview of the model parameters used in COBRAS/UDEC modelling systems by Recio (2007) and also during this study.

Furthermore, since the internal movement of sand inside the GSC is not simulated, it had been assumed that the sand inside GSCs are already moved and that the "folding" area is already formed. The "folding" area is created by altering the "average properties" of GSCs of the stiffness matrix that correspond to the elements that are in this area. This is usually being done by altering the bulk modulus and the shear modulus in a selected region within the GSC.

However, there are serious limitations on this existing modelling system, such as;

(i) Gaps between GSCs were simulated in COBRAS by creating smaller GSCs. However, these gaps increase the porosity of the GSC-structure and therefore, forces acting on GSCs might be overestimated.
(ii) Friction between GSCs was not accurately represented in UDEC and therefore, was not validated. Therefore, a "cohesion value" between GSCs has been introduced for the calibration of the models by considering whether the GSCs are stable or not for the tested conditions.
(iii) Even though the external dimensions of GSCs were correctly represented, neither the real contact area between GSCs nor the actual weight of the units are modelled. Instead, both of these key parameters are overestimated. Then the magnitude of the de-

stabilizing force has been increased (by introducing a calibration factor) during the model calibration (see Dassanayake and Oumeraci 2012f for the details).

(iv) Only a single vertical force and a single horizontal force component were calculated by integrating the pressure measurements around GSCs and these components were applied in UDEC. Therefore, it is not possible to simulate the rotation (or overturning) of crest GSCs.

(v) When simulating slope GSCs, force components are applied only on the limited number of free nodes of GSCs in UDEC, which limits the accuracy of simulations. (this is a limitation of UDEC model)

(vi) Only the forces due to pressure have been taken into consideration, while neglecting the forces due to shear stresses on GSCs

In order to overcome these limitations, new modifications to the existing COBRAS/UDEC modelling system were introduced during this study.

4.1.5 New Modifications to the Previous COBRAS/UDEC and Adaptation of Models to Represent Engineering Properties of GSCs

There are few challenges in modelling three dimensional GSCs in UDEC, which is a two dimensional distinct element model. These related key issue and proposed solutions are discussed below.

a) Representation of Important Geometrical Properties of GSCs

Since GSCs are stacked uniform units with finite dimensions, representation in two dimensions need additional factors. It is much simple to model GSCs as rectangular elements. However, additional care should be taken to get the weight of the elements correctly. According to small scale model tests (Dassanayake et al. 2011c), only about 0.75% of the length and width touches ($0.56 \times l_c \times b_c$) the bottom GSC. Furthermore, an 80% filled GSC will occupy only 72% of the representation box volume (i.e. $0.72 \times l_c \times b_c \times h_c$). Therefore, the GSCs in the numerical model are only $0.72 \times l_c$ long and have the same width b_c=0.07 m to ensures the same number of GSCs per unit width as it was in the hydraulic stability tests. Moreover, the density of GSCs in the numerical model is the same as the measured density (1900 kg/m^3) during the experiments. These simplified GSC models correctly represent the unit weight of GSCs and has approximately the same contact lengths in the longitudinal direction (length = $0.72 \times l_c$). However, the contact width is larger than that was in the experiments, which results in ca. 28% higher contact areas (previously 46% higher) between GSCs (Figure 4-3). Then these simplified GSCs model were used for the simulation of pullout tests and validated by comparing both numerical and experimental pullout test results (see Section 4.3.3).

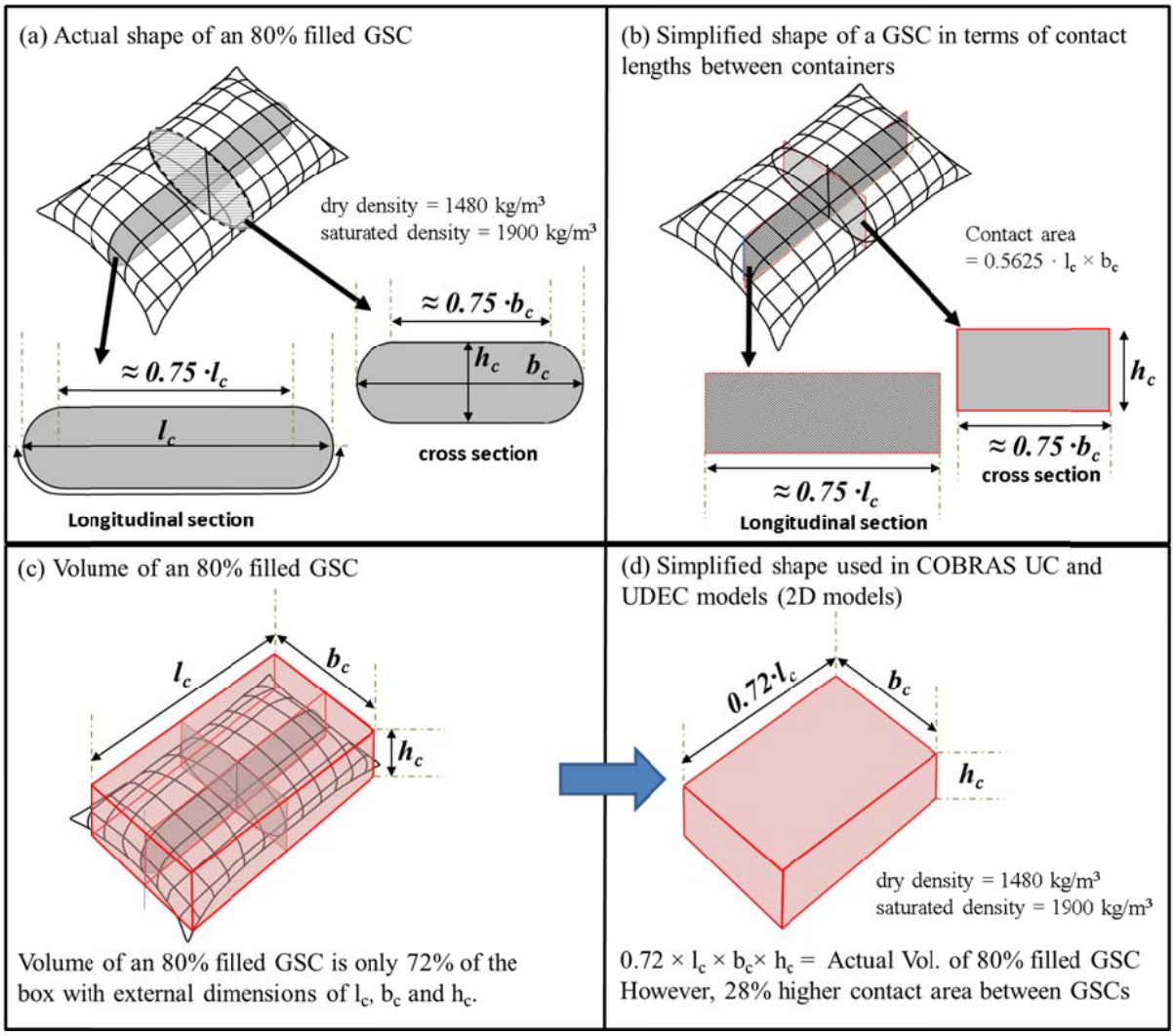

Figure 4-3: Simplified shape of 80% filled GSCs used in COBRAS-UC/UDEC model

b) Sand Fill Ratio

Three types of small scale GSCs were used during the hydraulic stability tests: (i) nonwoven 80% filled GSCs (Figure 4-4a, series NW80H) (ii) nonwoven 100% filled GSCs (Figure 4-4b, series NW100H) and (iii) woven 80% filled GSCs (Figure 4-4c, series W80H). The initial dimensions of the empty flat bags, which were used for the construction of these small scale GSCs, were similar in all three cases (length $a = 0.082$ m and width $b = 0.148$ m). Then, different sand fill ratios resulted in different GSC geometries (Figure 4-4) and these different geometries should be properly taken into account as they might influence the overall hydraulic stability of GSC-structures. The GSC lengths *lc* of all three GSCs were also similar, but the overlapping lengths and the height were varied as shown in below (seaward slope: 1:1). For example, the GSC-GSC contact lengths for 80% filled nonwoven GSCs were ca. 0.75% of the length (*0.75·lc*) when they placed horizontally and at a seaward slope of 1:1. Similarly, the overlapping length for 100% filled nonwoven GSCs was 70% of the GSC length (*0.7·lc*) and that for woven 80% filled GSCs was ca. 72% (*0.72·lc*). Apart from that different sand fill

ratios and different types of geotextiles might result in different flexural properties and they might result in different "average properties" (see Section 4.2.4) of GSCs. However, once these small scale GSCs are submerged and compacted by the waves, it is difficult to distinguish between the different flexural properties related to different sand fill ratios. Therefore, the flexural properties of all the GSCs were treated equally.

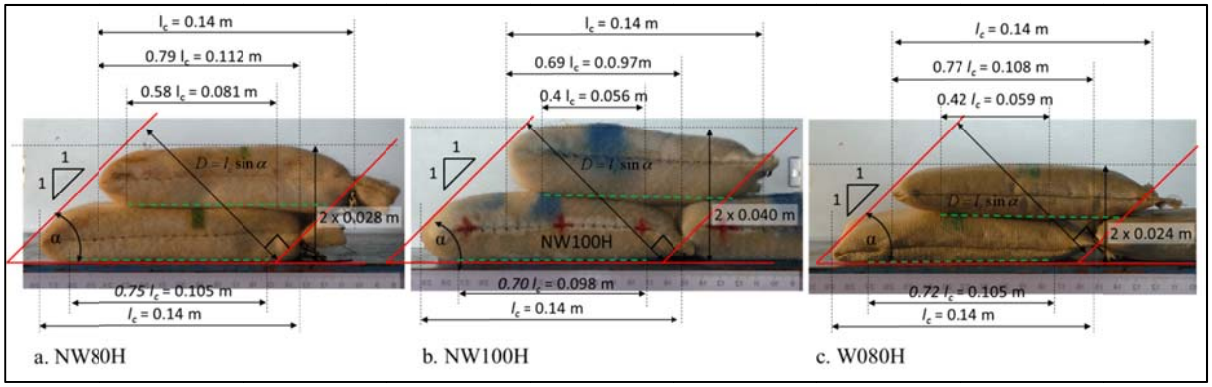

Figure 4-4: Overlapping length of GSCs for different sand fill ratios (80% & 100%) and type of geotextile (Nonwoven and woven)

c) Type of Geotextile Material and Interface Friction Between GSCs

In order to determine the interface friction properties of GSCs, first direct shear tests were performed using the small shear box apparatus. The shear box tests were conducted with the same types of geotextile materials used for the hydraulic stability tests and both static and kinetic friction angles for geotextile-geotextile contact surfaces were found. The shear box test results showed considerably different static and kinetic friction angles for nonwoven geotextile (static friction angle = 22.62°/ μ = 0.41 and kinetic friction angle = 14.88°/ μ = 0.27), whereas for woven geotextile only a small difference was observed (static friction angle = 13.33°/ μ = 0.24 and kinetic friction angle = 12.23 / μ = 0.22). In both cases, woven and non-woven geotextile, the friction angles calculated based on the pullout tests are much higher than those of the shear box tests (see Section 3.3.5). Based on the pullout tests, dry nonwoven 80% filled GSCs resulted in a friction angle of 38°/ μ = 0.8 and dry woven 80% filled GSCs resulted in a friction angle of 19.2 °/ μ = 0.35.

Therefore, the friction angles used during the numerical simulations were ca. 25% higher than those resulted in the shear box tests. Later, the result from numerical pullout tests (Section 4.3.3) were compared with the experimental results and the agreement was good for both nonwoven and woven GSCs.

Recio and Oumeraci (2007c) have introduced a cohesion value for GSCs (Cohesion of GSCs = 1.4×10^4). However, the direct shear test results do not show any cohesion between two geotextile surfaces. Therefore, zero cohesion was assumed for the joints between GSCs.

Nonwoven and woven geotextiles show different friction behaviours. Nonwoven geotextile shows about 7° difference between static and kinetic friction angles, whereas woven geotex-

tile shows less than 1° difference between static and kinetic friction angles. Therefore, two different joint models were used for the representation of interface friction properties of nonwoven and woven GSCs. In UDEC, the joints (discontinuities) between nonwoven GSCs were modelled with Coulomb slip model with residual strength, which simulates displacement-weakening of the joint by loss of frictional (Itasca 2011) and the joints between woven GSCs were modelled with the standard Mohr-Coulomb slip model.

d) Forces Acting on a Single GSC:

Figure 4-5 describes the representation of the forces acting on GSCs in UDEC model. As the force apply on each element considered as force per unit length in UDEC model, force on a single GSC need to be multiply by number of GSCs per unit length.

Recio (2007) has performed small scale pressure measurements on an instrumented container to obtain wave-induced loads on GSCs (Figure 4-9). This instrumented container was placed at different elevations in the structure to investigate the influence of the location of the GSC with respect of the still water level, on the wave-induced pressures (see Section 4.4.1). Then, by integrating the pressures around the containers, the total wave-induced forces have been derived for each time steps. A similar method was followed in the current simulations. Figure 4-5 describes the representation of the forces acting on GSCs in UDEC model.

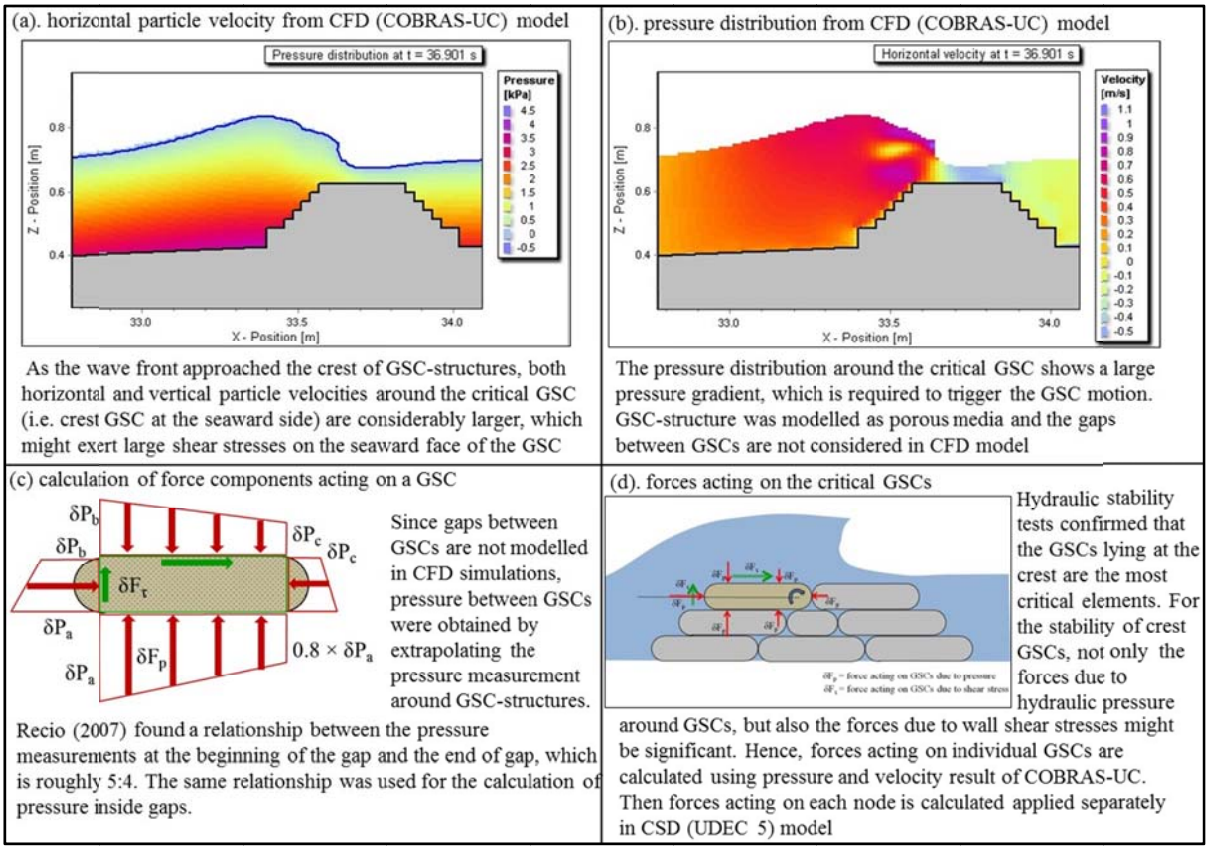

Figure 4-5: Simulation of forces acting on a single GSC in the CFD-CSD model system

Since UDEC is also a 2D model, the forces acting on each element should be provided as forces per unit length. Therefore, the force components on a single GSC (which are calculated based on COBRAS-UC results) need to be multiplied by number of GSCs per unit length to obtain the force per unit length and then applied on each element in UDEC model.

4.2 Simulation of GSC Pullout Tests Using UDEC

Many authors (Lohani et al. 2006, Krahn et al. 2007, Matsushima et al. 2008) have already reported that the properties of GSCs do not always depend directly on the properties of the geotextile material. This was confirmed by the results of the pullout tests with GSCs showing that 30% ~ 50% higher pullout resistance forces were obtained than those estimated only on the basis of the interface friction properties of geotextile materials without the sand fill. Therefore, it is necessary to define proper interface properties for GSCs, in order to simulate hydraulic stability of GSCs more accurately. Therefore, an attempt was made to simulate the pullout tests using UDEC model (numerical pullout tests) and to validate the selected joint models in UDEC.

4.2.1 Computational Domain and Discretization

During the numerical pullout tests, the measured pullout forces were applied as an input and the motion of the GSC, which was pulled out, was later compared with the displacement measurements from the experiments for the model validation. Figure 4-6d is a typical plot where the numerical pullout results are compared with the measured displacement.

Figure 4-6e shows a typical geometry of a tested GSC-structure of three GSCs (GSCs were placed in tandem placement). An addition fixed blocks was introduced at the bottom of the structure to make the computational domain more stable. The GSC-structure was then divided into finite triangular meshes and the material and the joint properties were defined (see Table 4-1). Then the pullout force is applied on an external node at the right boundary of the middle GSC during the simulation of slope GSCs. Figure 4-6a, Figure 4-6b, and Figure 4-6c show different computational steps, where displacement vectors are shown with red arrows. As shown in these figures, the numerical model correctly reproduces the beginning of the motion. However, the numerical model predicts a rapid displacement than what was measured during the pullout tests. Although there is a different between the magnitude of the measured and the calculated displacements for a given time, UDEC model can still be successfully used for the determination of whether the GSC-structure is stable or not for a given load. Moreover, UDEC model often overestimates the motion. Therefore, the results from the numerical modelling will be slightly conservative.

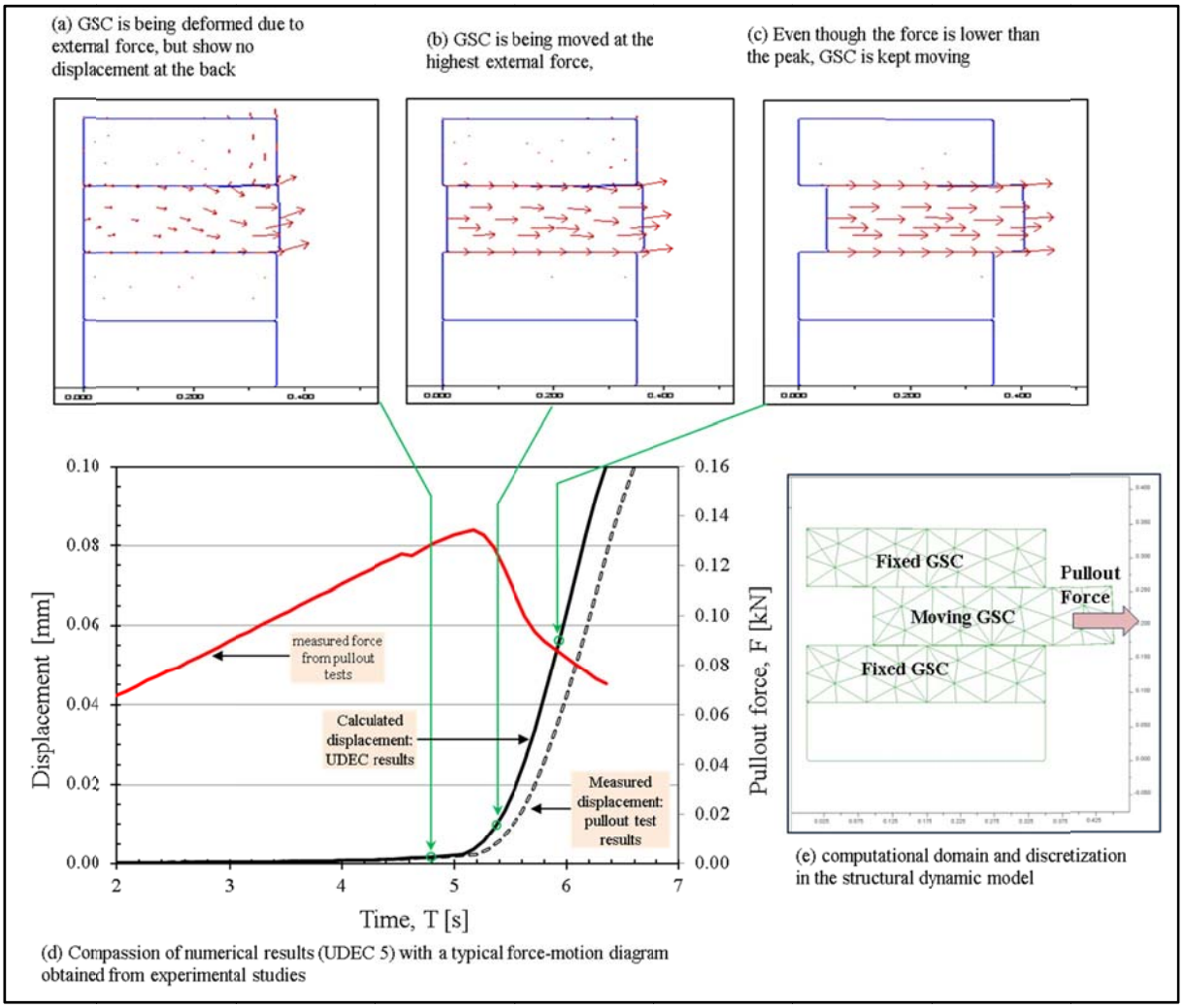

Figure 4-6: Numerical model setup and results for pullout tests of slope GSCs

4.2.2 Input Parameters for the Numerical Pullout Tests

In addition to the new modifications in COBRAS-UC/UDEC modelling system (compared to the previous version by Recio 2007), which are mentioned in Section 4.2.5, new values were introduced to some of the important parameters; the density of GSCs ρ_{GSC} = 1900 kg/m^3 and the friction angle between GSCs (Nonwoven: 28° and woven: 16°). Other than those, most of the parameters that describe the deformability of GSCs and the behaviour of GSC-GSC joints were adopted from the previous modelling system. A comparison of the model parameters used by Recio (2007) and model parameters used during current pullout simulations (UDEC) are summarised in Table 4-1

Table 4-1: Comparison between model parameters used in the CSD (UDEC) model

Descriptions of UDEC model parameters	UDEC 4.0 Input values by Recio (2007)	UDEC 5.0 input values for the current study	References / Remarks
Time step	0.02 s	0.02 s	Time step of input files containing forces acting on GSCs
Density of all non-submerged GSCs (fully saturated)	1800 kg/m^3	1900 kg/m^3 *	* Recent laboratory and prototype measurements suggest slightly higher value than Recio (2007)
Density of all submerged GSCs (fully saturated)	800 kg/m^3	900 kg/m^3 **	** Recent laboratory and prototype measurements suggest higher value
Bulk modulus of GSCs	2.5 × 10^6 Pa or N/m2	2.5 × 10^6 Pa or N/m2	Adopted from Recio (2007)/ Assuming loose sand
Shear modulus of GSCs	1.1 × 10^6 Pa or N/m^2	1.1 × 10^6 Pa or N/m^2	Adopted from Recio (2007)/ Assuming loose sand
Bulk modulus of "folding" area inside GSCs	9 × 10^4 Pa or N/m^2	9 × 10^4 Pa or N/m^2	Adopted from Recio (2007)
Shear modulus of "folding" area inside GSCs	4 × 10^4 Pa or N/m^2	4 × 10^4 Pa or N/m^2	Adopted from Recio (2007)
Cohesion between GSCs	1.4 × 10^4 Pa or N/m^2	0	Shear box tests showed no cohesion between geotextile-geotextile interface. However, apparent cohesion due to "interlocking" between GSCs might occur
Friction between GSCs	Nonwoven: 28º	Woven: 16º Nonwoven: 28º	Statistic friction angles will be 19º +9º =28º
Dilatancy angles between GSCs †	-	Woven: 0 Nonwoven: 9	Dynamic friction angle or residual friction angle
Constitutive model for friction between GSCs	Coulomb slip model	Coulomb slip model with residual strength	New model simulates the both static and dynamic friction
Constitutive model for the deformation of GSCs	Mohr-Coulomb	Mohr-Coulomb	
† Krahn et al. (2007) reported that the shear stiffness of sand bag-sand bag is about 33% higher than that of the sand bag material. This was explained as the dilatants behaviour that occurs with the large shear deformations of sand bags.			

4.2.3 Numerical Pullout Tests Results and Validation

The results from different model scenarios used during the pullout tests are comparatively shown in Figure 4-7. During each simulation, respective measured pullout forces were applied either on crest GSCs or on slope GSCs. The displacements were then compared with the measured displacements. Both woven and nonwoven crest GSC models show a good agreement with the measured data.

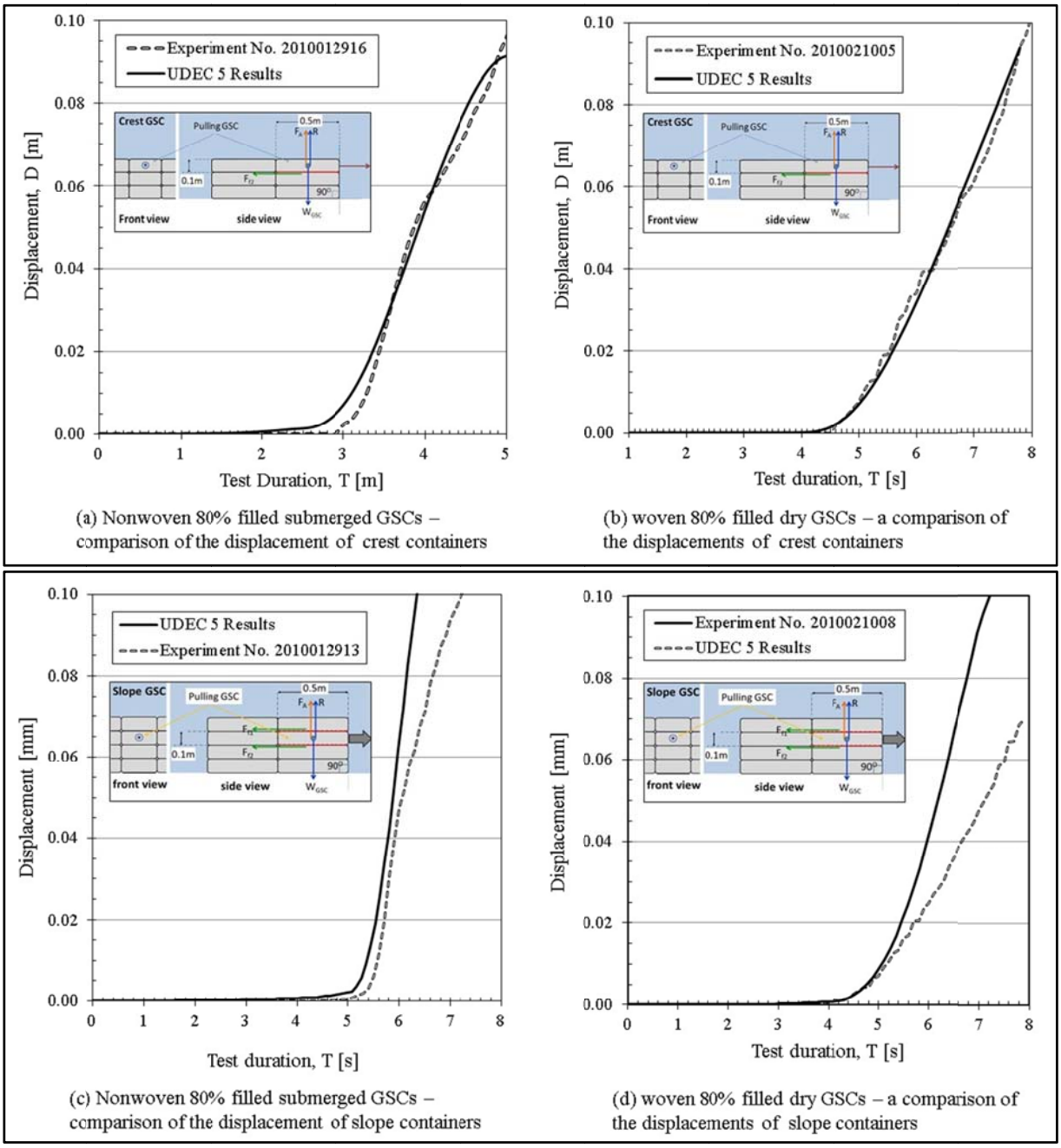

Figure 4-7: Comparison of measured (pullout tests) and computed (UDEC 5) displacements, when GSCs are subject to pullout forces

Figure 4-7a and Figure 4-7b show the result from both experimental and numerical pullout tests for nonwoven and woven crest GSCs, which are the critical elements for hydraulic stability of submerged and low-crested Structures. Both figures show very good agreement with the measurements.

However, slope GSCs shows an increasing deviation from the measured values, as the displacement gets larger. Hence, the numerical model slightly underestimates the stability of GSCs against the pullout forces. Therefore, numerical modelling results from COBRAS-

UC/UDEC modelling system might also be slightly conservative. Overall, the initiation of motion, which is the most critical point relevant with respect to the hydraulic stability, is within the acceptable limit for all scenarios. All the numerical model scenarios correctly predict the initiation of motion as the pullout force approached its maximum or less than 0.2 s before it reaches the peaks. During the pullout tests, force was applied at a uniform rate of ca. 24 N/s. Therefore, the accuracy is within 5 N that is less than 4% of the peak force (required force to trigger the motion of GSCs) for slope GSCs. The differences between the numerical and the experimental results for crest GSCs were also in the same range (less than 4% difference, when compare the peak forces). Additional numerical pullout results and the detailed on the different constitutive models for the representation of GSC-GSC contacts are described in Dassanayake and Oumeraci 2012f.

4.2.4 Summary and Concluding Remarks

According to Recio (2007), the hydraulic stability of GSC-structures is highly sensitive to the friction properties of GSCs. However, there were no detailed investigations on the effect of friction properties of GSCs. Moreover, the correct representation of friction between elements is a key factor for a reliable numerical model. Therefore, several inbuilt models available in UDEC 5 for the representation of interfaces between distinct bodies were tested with experimental data and the most appropriate constitutive models for the adequate representation of both woven and nonwoven GSCs were found. Based on the experimental and the numerical pullout test, interface friction between nonwoven GSCs can be better represented using the Coulomb slip model with residual strength, while the standard Mohr-Coulomb slip model is sufficient for the representation of the interface between woven GSCs.

According to the numerical modelling results, the required forces to pull numerical GSCs out are slightly less than those obtained from the experimental results. Whereas, the slope GSCs show an increasing deviation from the measured values, as the displacement gets larger. This might be mainly due to the 2D simplification of the 3D problem as the side effects from neighbouring GSCs are not properly represented in the 2D numerical model. Furthermore, the GSCs were modelled as rectangular blocks with horizontal contacts between them, which ignore the effect of the irregular GSC surfaces (curvatures) on the pullout forces. Therefore, 2D numerical modelling might result in a slightly less hydraulic stability compared to the experimental results.

4.3 CFD-CSD Simulation of GSC Hydraulic stability tests

This section outlines the procedure to simulate the hydraulic stability tests using weakly coupled CFD-CSD models (COBRAS-UC/UDEC) and some key results. Further results and more detailed analysis can be found in and Dassanayake and Oumeraci (2012e).

4.3.1 Forces acting on GSCs

COBRAS-UC version is limited to approximately 550,000 cells. Since the height of a small scale GSC tested in the wave flume is only 28 mm, cell size close to GSC-structure was kept as 28 mm × 7 mm, which is the smallest possible mesh size to represent the flow around GSC with a reasonable accuracy. Even with this grid size, only ca. 40 m of the flume can be modelled, because of the limitation with the maximum number of cells (see Section 3.5.3). Therefore, it is not possible to model the flow through the gaps of GSCs. According to Recio (2007), at least 3 cells are required to represent the gaps and 10 cells to represent the height of GSCs. Since Recio had been modelled the experiments with relatively larger GSCs (height = 0.10 m), it was possible to simulate with 10 mm × 10 mm cells and by reducing the length of the flume to 44 m. Due to this limitation, during the current study, CFD simulation were performed excluding the flow between GSCs. Then, the pressure inside the GSC structure was obtained by extrapolating the pressure measurements around the GSCs structure using the relationships proposed by Recio (2007) based on experimental results.

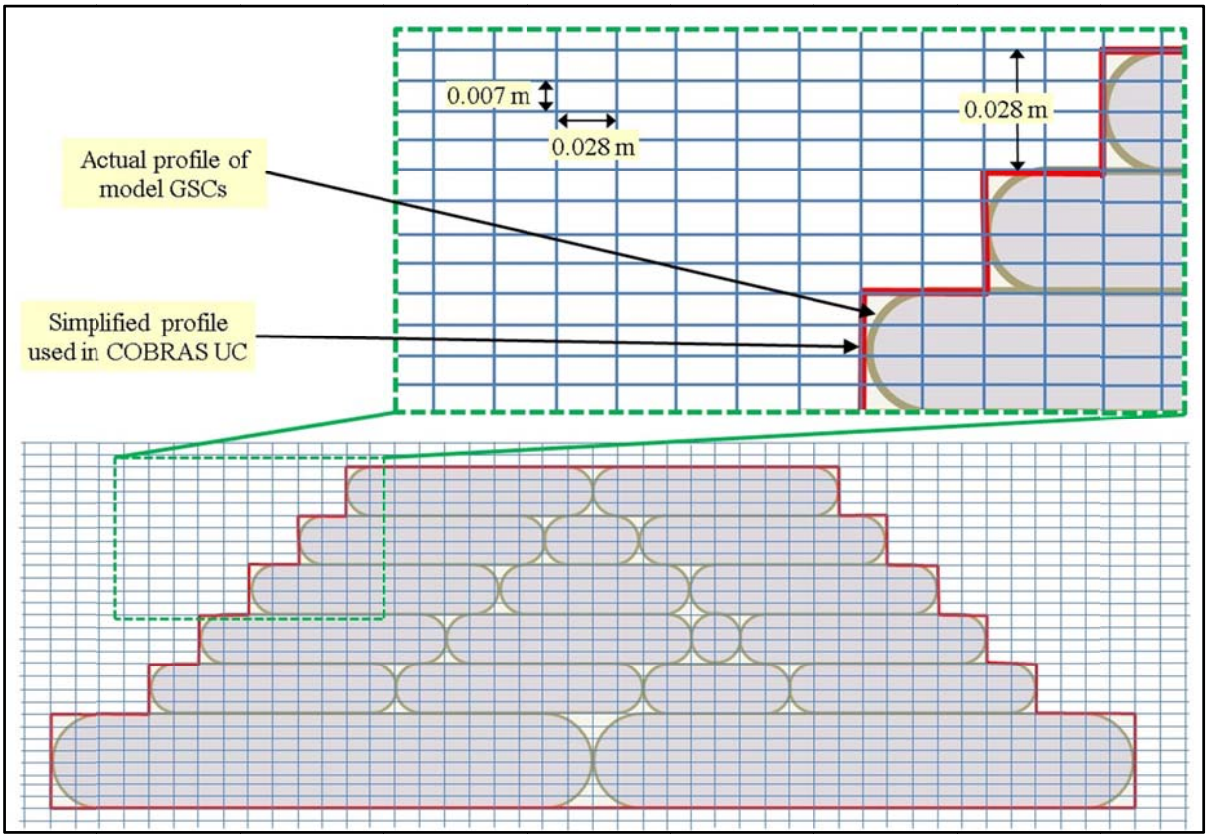

Figure 4-8: Mesh size used in COBRAS-UC model

Recio (2007) has performed pressure measurements on an instrumented container to record wave-induced pressures. This instrumented container was placed at different elevations in the structure to investigate the influence of the location of the GSC (with respect to the still water level) on the wave-induced pressures. Then, by integrating the pressures around the containers, the total wave-induced forces have been derived (Figure 4-9). Later, these pressure meas-

urements were used for the validation of the numerical simulations. However, the current experiments were performed with relatively smaller GSCs, so that it was not possible to install pressure transducers within the GSCs. For the numerical simulations of the hydraulic stability of GSC-structures, one of the important inputs is the pressure between GSCs. For this purpose,, Recio (2007) succeeded to derive some relationship between the external pressure and the pressure at various locations inside the GSC-structure. These empirical relationships which have also been verified by numerical simulations (Recio and Oumeraci 2006a, 2007b, 2007c, 2007d, 2007e) are applied in this study in order to obtain the pressure inside the GSC-structures.

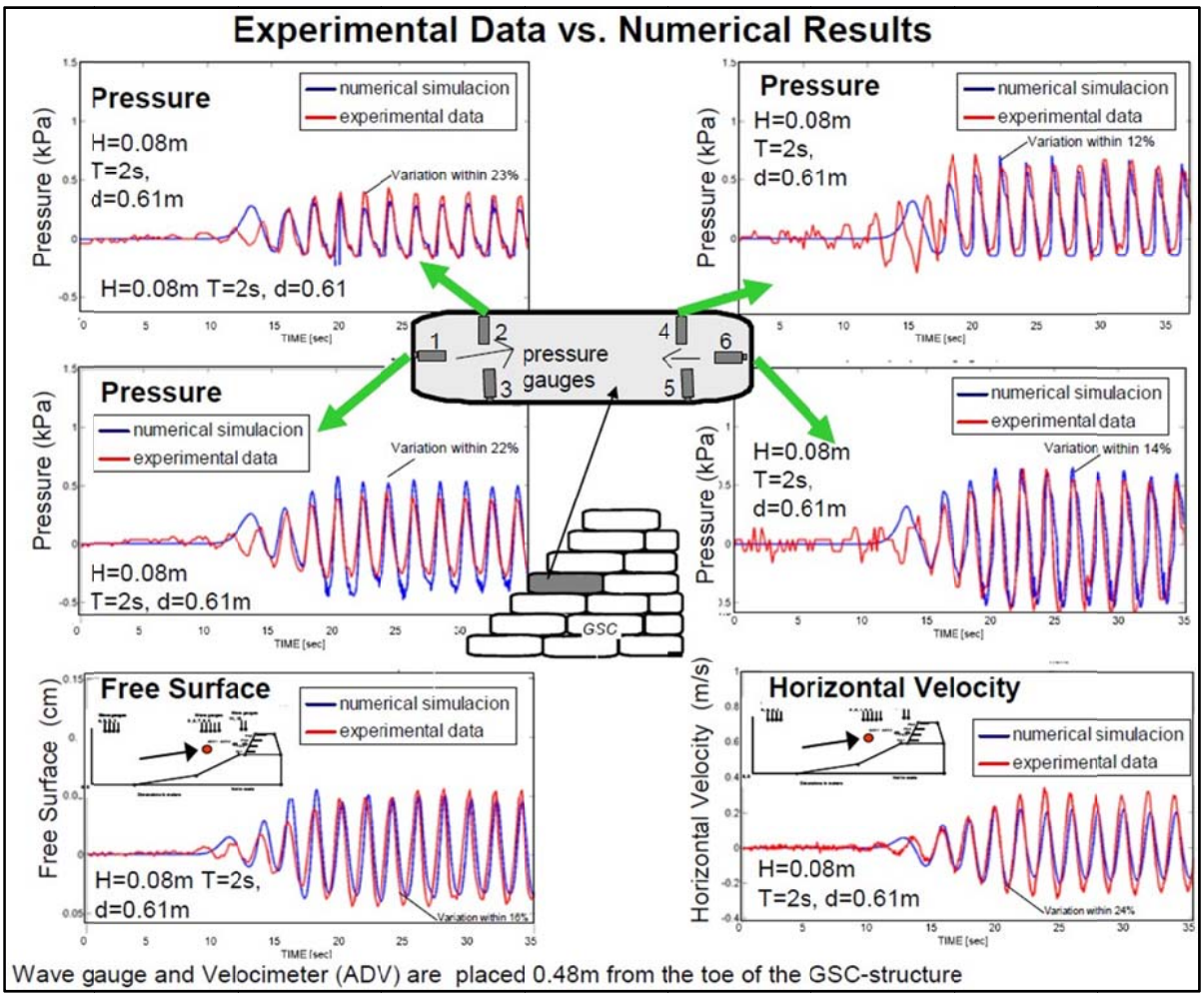

Figure 4-9: Measured and computed (using COBRAS model results) wave-induced pressures, velocities and free surface elevation (Recio, 2007)

Then, by integrating the pressures around GSCs, forces at each nodal point of the perimeter of the finite element mesh (FEM of UDEC) in each GSC were derived and the total wave-induced forces on each GSCs were calculated. Figure 4-10 shows a typical time series used by Recio (2007) during his COBRAS – UDEC simulations. The GSCs at different locations show a clear difference in termers of both total vertical and horizontal forces. the total vertical and the horizontal forces acting on them. These forces were applied on the external nodes of

the GSC structures in the UDEC model. Figure 4-11 describes the process of obtaining the pressure values from COBRAS model and the application of the calculated total forces on the external nodes in the UDEC model (Figure 4-11).

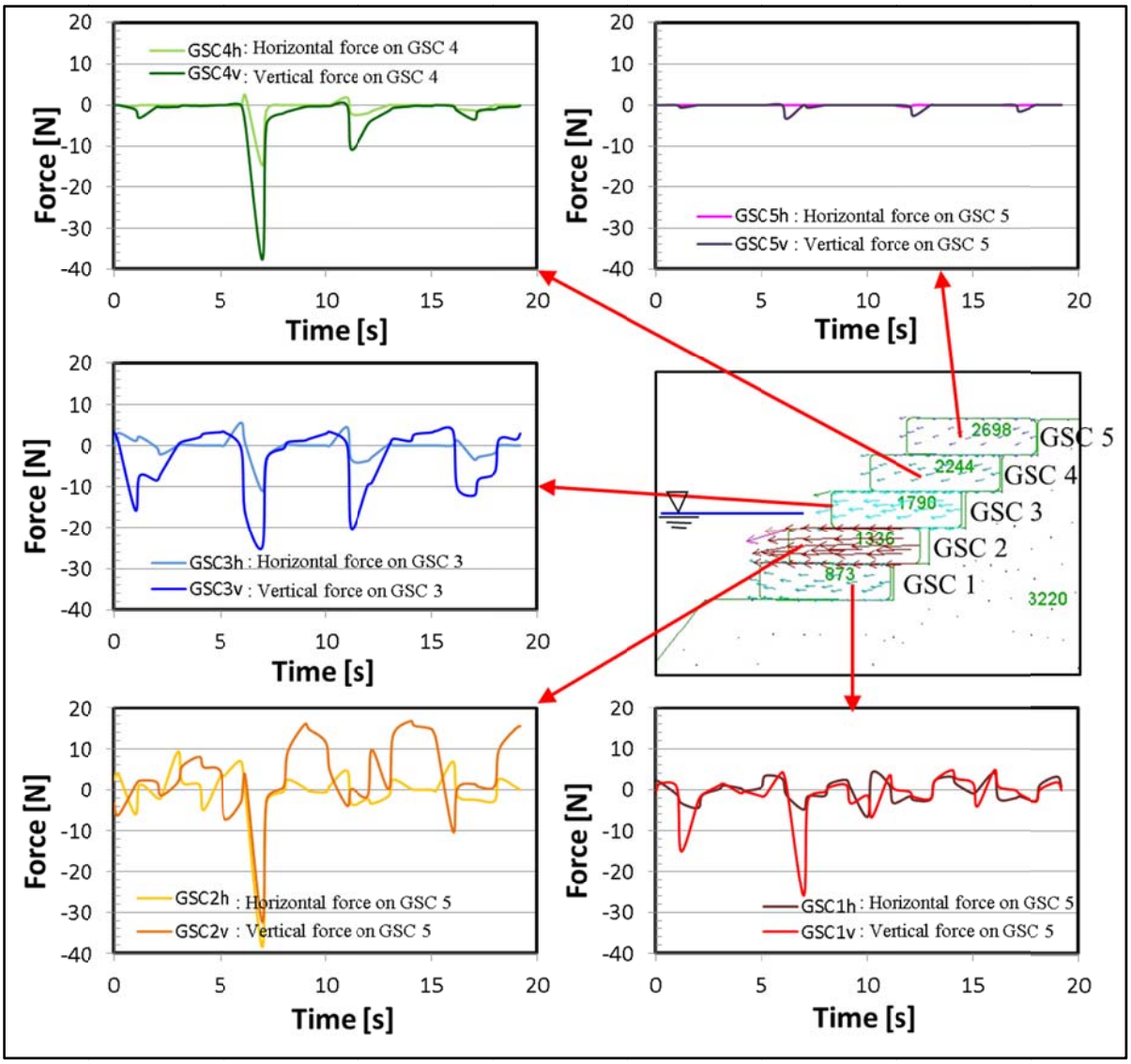

Figure 4-10: Resultant forces acting on GSCs. horizontal and vertical components are applied separately on each GSC in the model (modified from Recio 2007)

Figure 4-11 elaborates the functionality of the weakly coupled CFD-CSD by Recio (2007). The CFD model COBRAS calculate the pressure around GSCs and the pressure results are extracted using numerical wave/pressure gauges. Then the wave-induced pressures along the surface of each GSC are calculated and provide to CSD model UDEC (pressures are integrated into forces, see Recio and Oumeraci 2007c). These forces are then applied on each nodal point of the perimeter of the finite element mesh (FEM in UDEC) in each GSC. Detailed information on this weakly couple models can be found in Dassanayake and Oumeraci (2009a), Dassanayake and Oumeraci (2012f) and Recio and Oumeraci (2007c). Even though this method has some limitations in modelling the hydraulic stability of slope GSCs it can better

be used for the simulation of the hydraulic stability of crest GSCs from the current hydraulic stability tests (Dassanayake and Oumeraci 2012f). This is mainly due to most of the nodes at the perimeter of the crest GSCs are exposed and different force components can be assign to each of them.

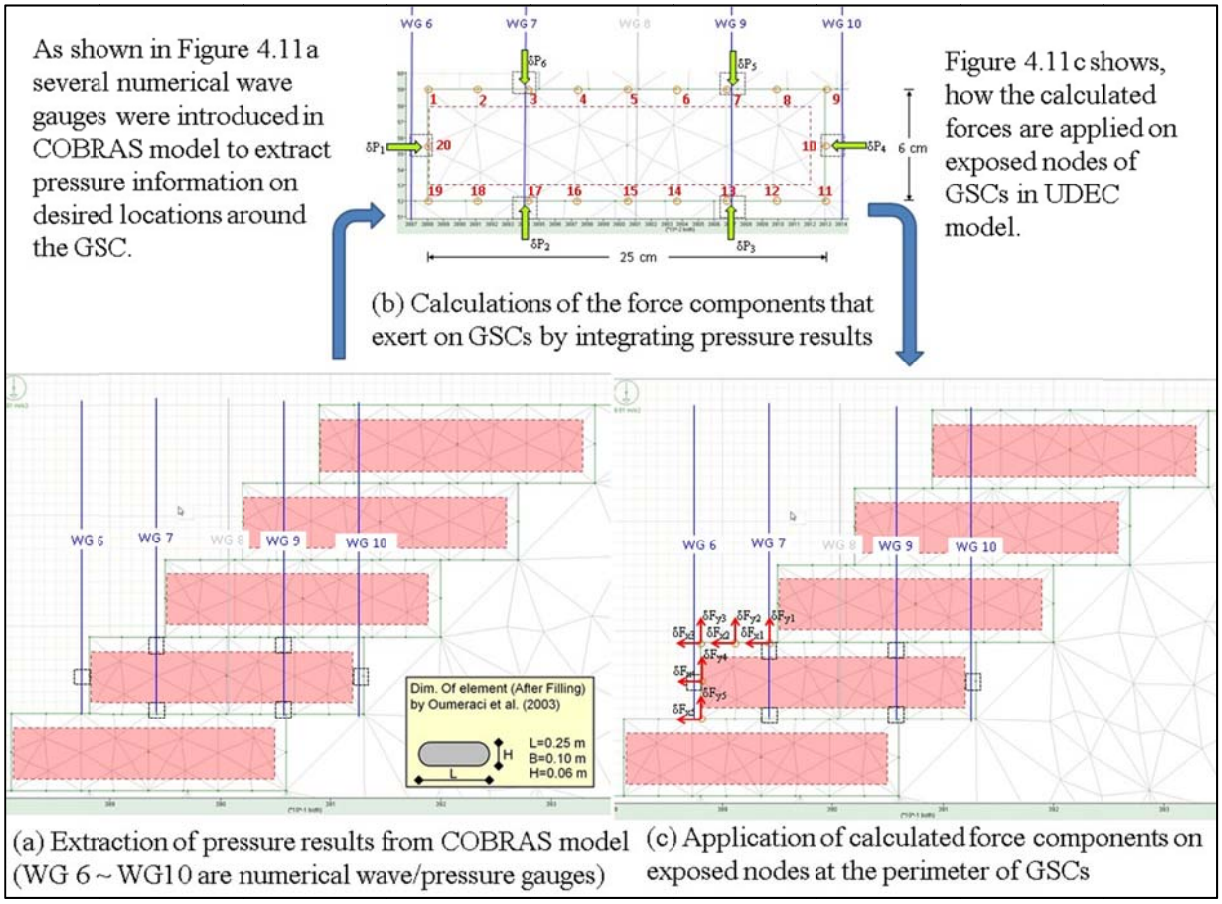

Figure 4-11: Calculation of forces components around GSCs using pressure measurements from COBRAS and application of those computed pressure results on a slope GSC in the UDEC model

The results of the current hydraulic stability tests (see Section 3.4 and Dassanayake et al. 2011c) show that for submerged/low-crested ($Rc/H_m \leq +0.5$) GSC-structures, the initiation of damage always at the crest of the structure. Even if the total number of displaced GSCs during the entire series of experiments were considered, more than 70% of GSCs are displaced from the crest (Figure 4-12). Therefore, it was decided to apply the COBRAS-UC/UDEC modelling system to study the incipient motion of crest GSCs, which are much more critical and thus more relevant than slope GSCs.

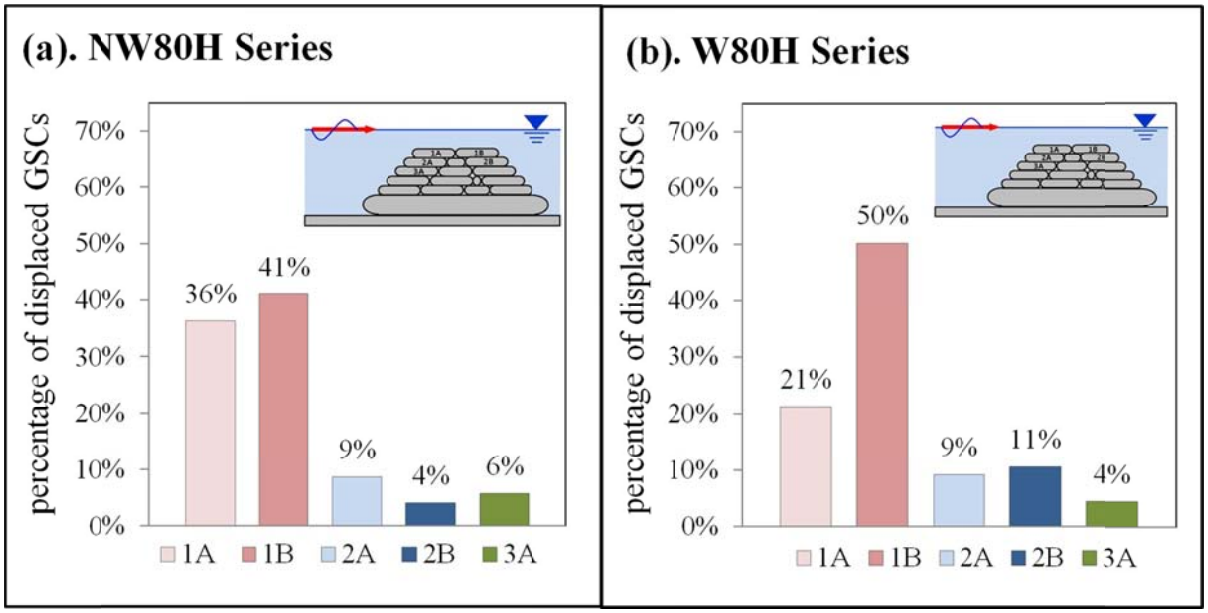

Figure 4-12: Percentages of displaced GSCs during 366 model tests in four test series (Dassanayake et al. 2011c)

Every motion of GSCs in this weakly couple COBRAS-UC/UDEC modelling system will disturb the wave-induced flow in the CFD model (COBRAS-UC) and thus, the wave-induced forces on them in the next time step. This can only be solved with a fully coupled model, which is outside the scope of this PhD.

Even within the COBRAS-UC/UDEC, is possible to update the geometry of the GSC-structure in CFD model, but updating the geometry at every time step will not be practicable. Therefore, a more feasible option is to update the geometry of the structure only after a predefined tolerance has been exceeded. Therefore, it is assumed that as soon as a GSC starts to show a significant movement (movement >10% of the length of the GSC or an upward rotation of $>10^0$), the hydraulic boundary conditions as well as the forces acting on the GSC will be significantly altered. Hence, the simulation of this weakly coupled modelling system deviated from real situation and the geometry should be updated in order to continue the simulation. Moreover, the detailed analysis of the hydraulic stability test results (see Dassanayake et al. 2011c) showed that this is the threshold limit to distinguish whether a GSC is stable or not (Table 3-6). Therefore, the COBRAS-UC/UDEC modelling system can be successfully used for the determination of the hydraulic stability of a crest GSC on a submerged/low-crested structure.

4.3.2 Computational Domain and Discretization in the CSD Model (UDEC)

The computational domain of UDEC is shown in Figure 4-13. The numerical model setup and geometry of the GSC-structure follow the conditions tested in the wave flume. The foreshore slope and the podest (Figure 3-25) acts as the bottom boundary (fixed boundary), which make the computational domain more stable. The GSC-structure was discretized in finite triangular meshes (triangular elements in the mesh are approx. 7 mm x 7 mm).

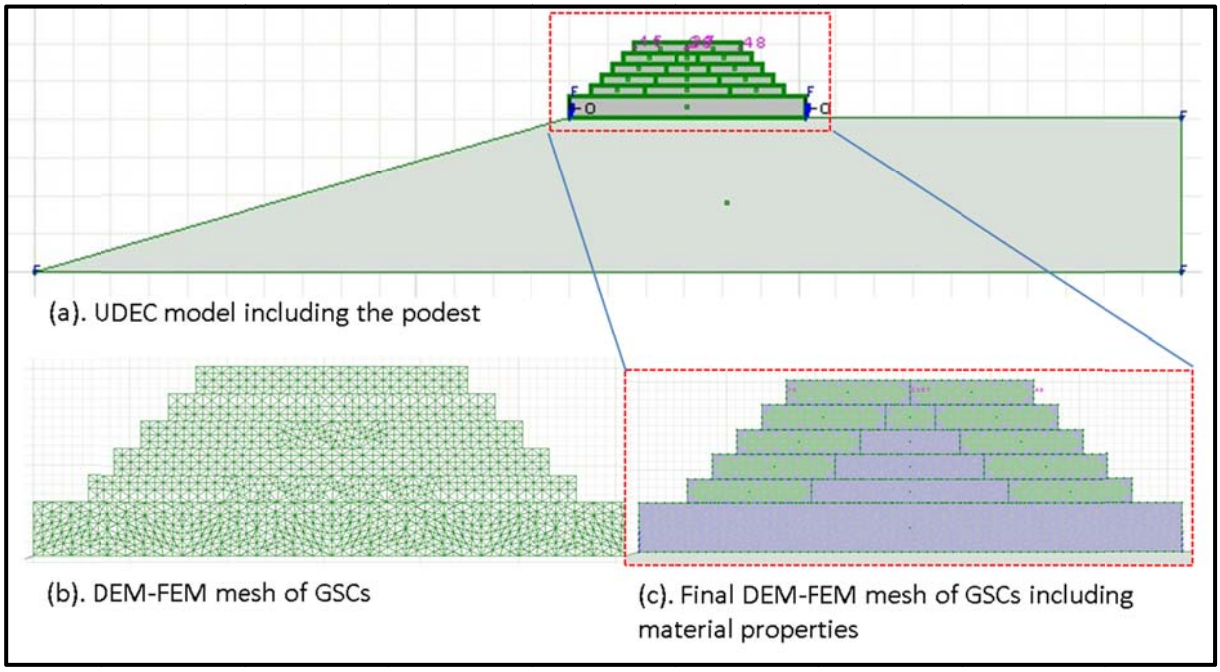

Figure 4-13: Numerical set up in the UDEC model for simulation of 80% filled nonwoven GSCs

4.3.3 Input Parameters for the Weakly Coupled CFD-CSD Numerical Simulations

The main input values used for the COBRAS by Recio (2007) and the COBRAS-UC models are summarized in Table 4-2. The main inputs values for the UDEC model are comparatively shown in Table 4-1. The values for the COBRAS-UC/UDEC modelling system were selected, following the results of Recio (2007) and newly conducted experiments and numerical studies (e.g. numerical pullout tests, preliminary CFD simulations, Dassanayake and Oumeraci 2010c.)

Table 4-2: Comparison of the main input parameter and assumptions used in the numerical simulations

"COBRAS" parameters by Recio (2007)		**COBRAS-UC parameters used during this study**	
Description	**Input values**	**Description**	**Input values**
Time step	0.02 s	Time step	0.02 s (or dynamic time steps)
Density of water	1000 kg/m^3	Density of water	1000 kg/m^3
Type of wave	Stokes V, internal wave maker	Type of wave	Airy waves, wave dynamics as boundary conditions at the left boundary of the simulation area
Kinematic viscosity of water	1×10^{-6} m^2/s	Kinematic viscosity of water	1×10^{-6} m^2/s
Turbulence model	$k-\varepsilon$ (nonlinear eddy viscosity)	Turbulence model	$k-\varepsilon$ (nonlinear eddy viscosity)
Turbulence seed parameter	0.5	Turbulence seed parameter	0.5
Eddy viscosity behaviour parameter	5	Eddy viscosity behaviour parameter	5
Max Courant number	0.3	Max Courant number	0.3
Wave heights	0.08 ~ 0.20 m	Wave heights	0.06–0.20 m
Wave period	1.5 ~ 3 s	Wave period	1.5 ~ 4.5 s
Water depth	0.61 m	Water depth	0.5 ~ 0.8 m
Mesh in domain	1600 × 100	Mesh in domain	3190 × 172

4.3.4 Validation of the CFD Model (COBRAS-UC)

Results from COBRAS-UC simulations were compared with the experimental data obtained from the hydraulic stability tests. Both the incident wave conditions as well as the particle velocity around the GSC-structure and the pressure results are compared. Figure 4-14 shows some typical results from two model tests with Rc = -0.1. More results are reported in Dassanayake and Oumeraci (2012f). There is very good agreement between the measured and the computed results for free surface elevations. The particle velocities and pressure measurements show some discrepancies only for the peak values. (scatter up to about 20% which may be considered as acceptable).

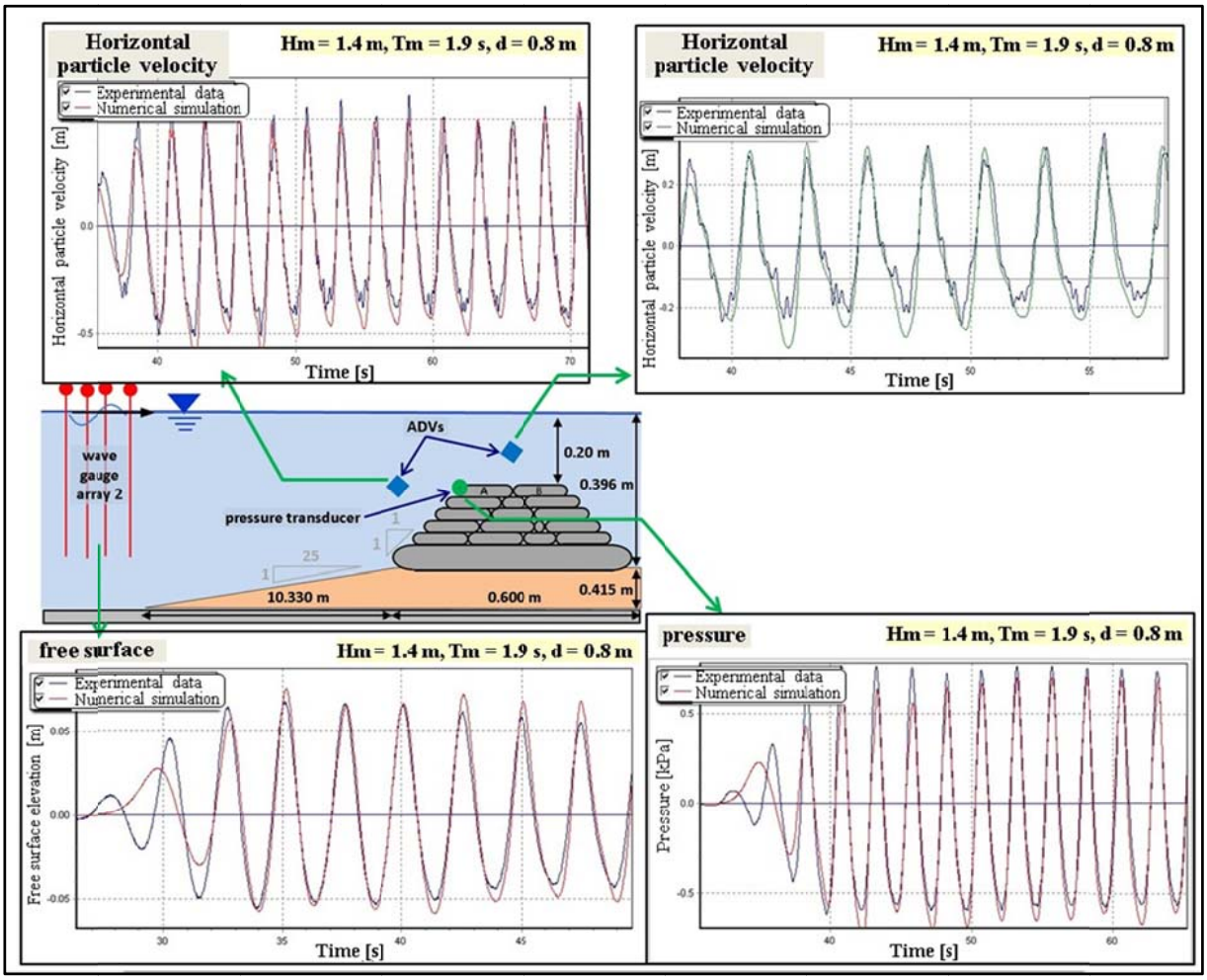

Figure 4-14: Measured (hydraulic stability tests) and computed (COBRAS-UC simulations) wave induced pressured, velocities and fee surface elevation

The data from numerical wave gauges were then analysed to obtain incident and reflected wave parameters. Figure 4-15 compares target and generated values wave heights and wave periods from COBRAS-UC simulations, showing a very good agreement (Scatter in wave heights < 5% and scatter in wave periods < 3%). Wave reflection and wave transmission characteristics of different test series from the hydraulic stability tests were studies and reported in Ozegowski (2012). Same parameter form the numerical model also computed and no significant difference (scatter < 5%) were found (Dassanayake and Oumeraci 2012f).

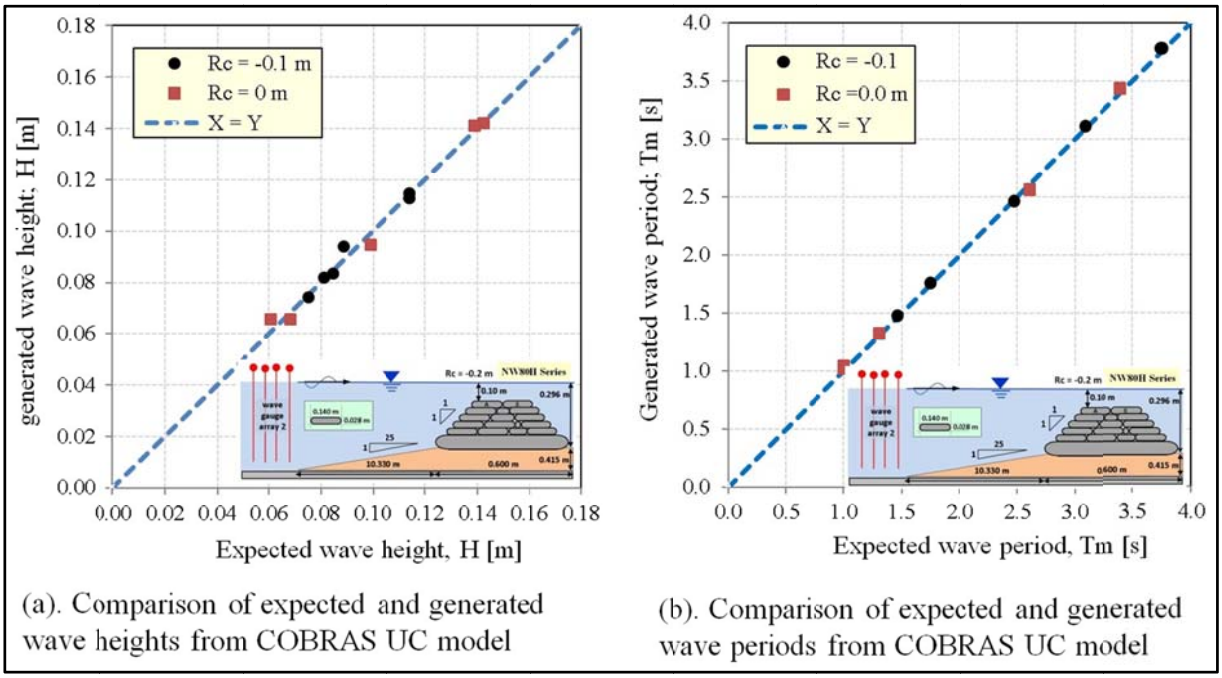

Figure 4-15: Comparison of input and output wave parameter from COBRAS-UC model.(exemplary results from *Rc* = -0.10 m)

4.3.5 Validation of CFD-CSD Modelling System (COBRAS-UC–UDEC)

Results from the numerical simulations and the video records obtained during the flume tests were carefully analysed to identify the conditions required for the initiation of motion of the critical GSCs. There are two main types of forces acting on GSCs due the presence of water; forces due to hydrostatic/dynamic pressure and forces due to shear stresses on the GSC surface. Recio (2007) simplified this problem probably by assuming forces acting on a GSC due to hydraulic pressure are dominant compared to the shear stress on the surface of the GSC. However, the forces due to shear stresses might influence the cyclic deformation of GSCs and the sliding of crest GSCs towards the landward side. From the video records, it is apparent that up rushing water results in the upward movement of the front section of GSCs. At this moment, pressure values around the face of GSC might also be large, but shear forces due to high velocities cannot be ignored.

Instead of only two force components (horizontal total force and vertical total force), current simulations were performed with 14 deferent force components acting on each exposed node of a single GSC (Figure 4-16). These force components consist of both vertical and horizontal force components which are induced by both pressure and shear stress on different nodes of GSCs. Figure 4-16 shows time series of total vertical and horizontal forces acting on crest GSCs (critical GSCs) calculated by integrating all of these components.

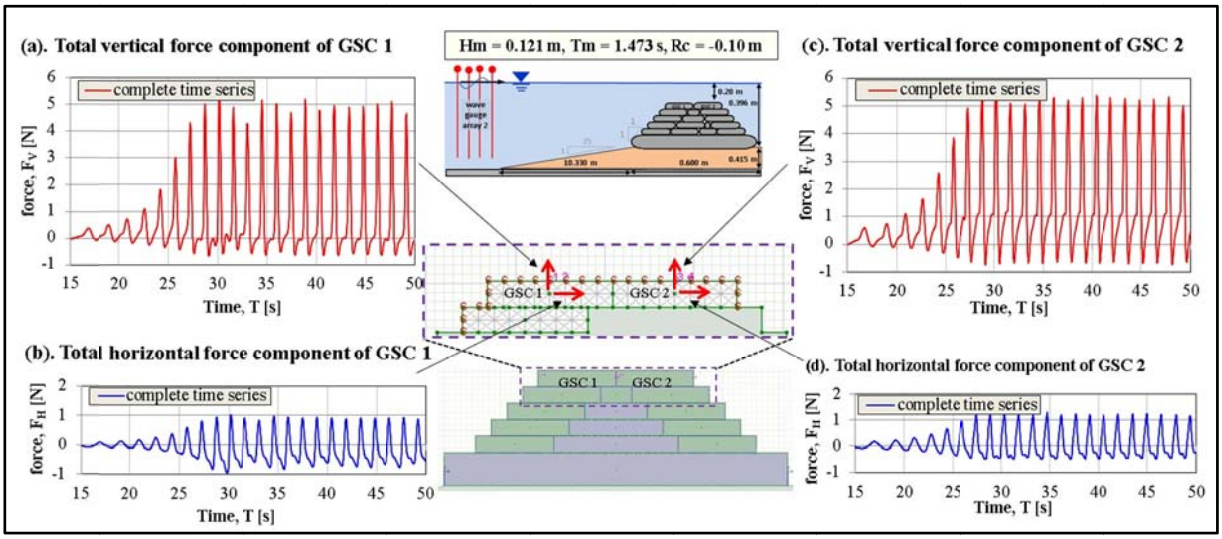

Figure 4-16: Total vertical and horizontal forces on crest GSCs

The displacements of a crest GSC during a wave cycle are comparatively shown in Table 4-3 using extracted images from high speed video records and the COBRAS-UC/UDEC results. The results show a reasonably good agreement with the magnitude of the upward rotation, and motion towards the seaward side.

As the wave approaches the GSC-structures, displacement vectors from the UDEC model indicate an upward rotation of the crest GSC at the seaward side (note: displacement vectors from the UDEC model are drawn with a dynamic scale). At time $t = 2T/9$, the UDEC model shows an upward rotation and the same could be observed from the high-speed video records. Then the GSC from the hydraulic stability tests shows a maximum of ca. 15° upward rotation whereas the UDEC model predicts an upward rotation of 12° (at time $t = 5T/9$). Even though the UDEC model predicts a slightly smaller rotation, this is already larger that the predefined threshold limit for "no damage" (stable) condition (Table 3-6). Therefore, the crest GSC shows an "incipient motion" (DC =1, Table 3-6) and hence, agrees with the results from hydraulic stability test. Moreover, the difference between two maximum rotation angels might be due to the limitation of this weakly coupled modelling system. Right after time $t = 7T/9$, both experimental and numerical GSCs return to their original horizontal position, but show a sliding motion towards the seaward side. At the end of the wave cycle, experimental GSC shows a sliding distance of ca. 7.5% of the GSC length and the UDEC model predicts the sliding distance of 6% of the GSC length. If the models continue, after few wave cycles, both GSCs will be detached from the structures.

Based on the experimental results from "no damage" and "incipient" motion tests (DC =0 and DC =1, Table 3-6), model parameters were fitted so that it can reproduced those test cases with a reasonable accuracy (Dassanayake and Oumeraci, 2012f). Table 4-3 represent an exemplary result of calibrated COBRAS-UC/UDEC modelling system. Then the calibrated model was used for the simulation of new hydraulic stability tests.

Table 4-3: Upward and downward rotation of GSCs within a wave cycle, $H = 0.134$ m, $T = 1.76$ s, $Rc = 0.1$ m-nonwoven, 80% filled GSCs (NW80H series)

video frames from high-speed video camera (speed = 50 fps)	pressure distribution around GSC-structures (COBRAS-UC results)	displacement of crest GSCs (UDEC results)
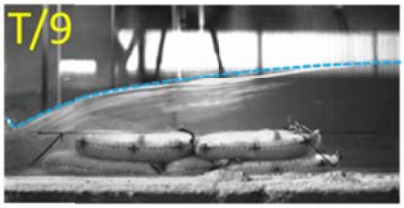	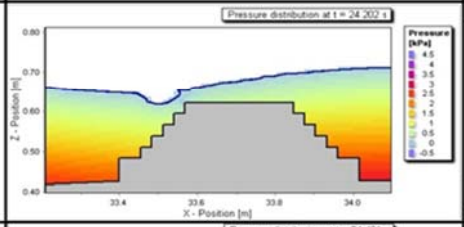	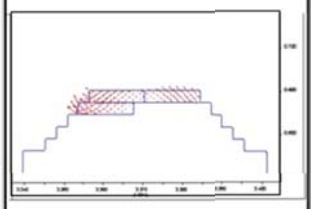
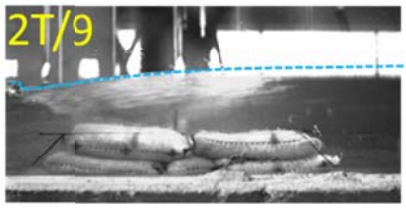	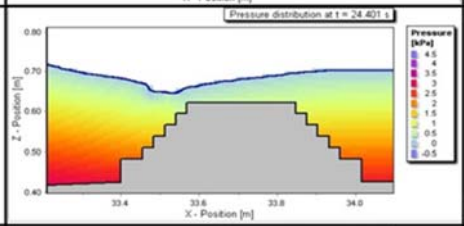	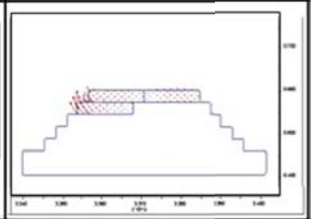
	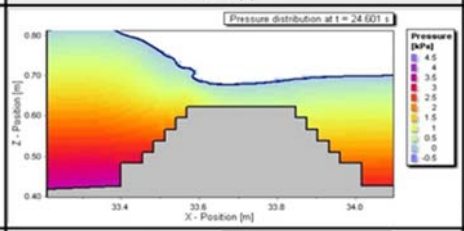	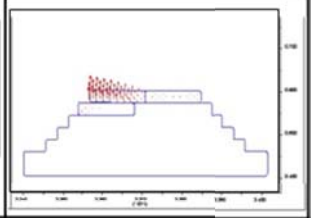
	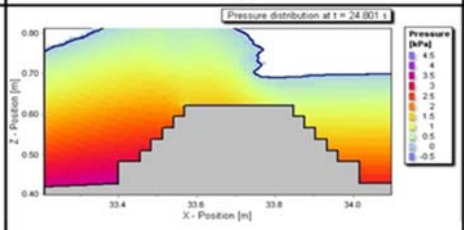	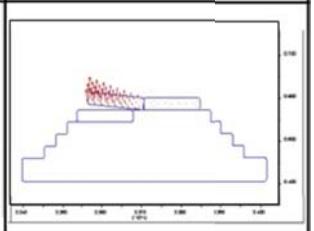
	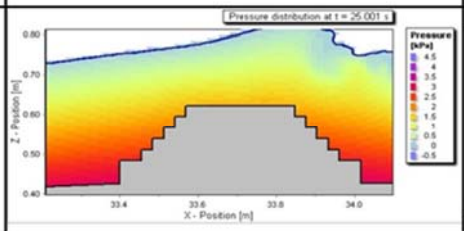	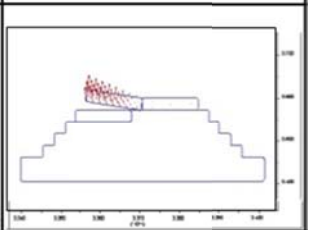
	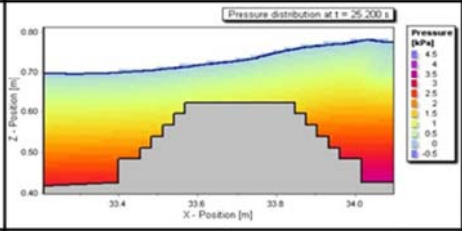	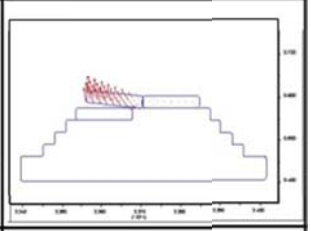
	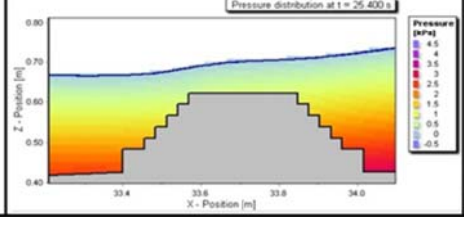	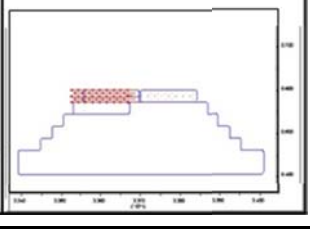

4.4 Detailed Numerical Simulations and Analysis of Hydraulic Stability

Initially, a set of selected hydraulic stability tests (stable and incipient motions cases, Dassanayake et al. 2011c) were reproduced with COBRAS-UC/UDEC modelling system and the results were compared to calibrate the modelling system and then to verify it (see Dassanayake and Oumeraci, 2012f for further details). Once the COBRAS-UC/UDEC modelling system was verified, further simulations were conducted to obtain additional data to fill the gaps in the date set and also to extend it. These new numerical simulations were conducted mainly with varying crest freeboard from three test series (NW80H, NW100H and W80H, see Figure 3 26).

Table 4-4: Test programme for the numerical simulations with COBRAS-UC/UDEC modelling system

Model configuration and test series for COBRAS UC – UDEC modelling system	Crest freeboard [m]	Height of the GSC-structure [m]	Relative depth at the toe, H_m/d [-]	Wave steepness, S_0 [=]
(a) NW80H: nonwoven, 80% filled, horizontal GSCs	-0.05 ~ 0.096	0.196	-0.1 ~ 0.8	0.01 ~ 0.06
		0.392	-0.1 ~ 0.4	0.01 ~ 0.06
(b) NW100H: nonwoven, 100% filled, horizontal GSCs	-0.05 ~ 0.096	0.196	-0.1 ~ 0.8	0.01 ~ 0.06
		0.392	-0.1 ~ 0.4	0.01 ~ 0.06
(c) W80H: woven and nonwoven, 80% filled horizontal GSC	-0.05 ~ 0.096	0.196	-0.1 ~ 0.8	0.01 ~ 0.06
		0.392	-0.1 ~ 0.4	0.01 ~ 0.06
H_m = mean wave period of 50 waves measured at the beginning of the foreshore slope				

4.4.1 Pressure Acting on Critical GSCs

The hydraulic stability tests did not cover the crest freeboard between -0.01 m and 0.0 m (model scale). Therefore, it was necessary to identify the most critical crest freeboard in terms of the hydraulic stability of crest GSCs. Hence, in order to identify the most critical crest freeboard in terms of the hydraulic stability of the crest GSCs, the wave induced pressures at the bottom of the seaward edge of the crest GSCs were compared using COBRAS-UC simulations (Regular waves with Hm = 0.14 m and Tm = 1.5s). According to Figure 4-17 the maximum dynamic pressure values were recorded when the crest freeboard is Rc = -0.05 m. Therefore, it was decided to study the hydraulic stability for Rc = -0.05 m case in detail.

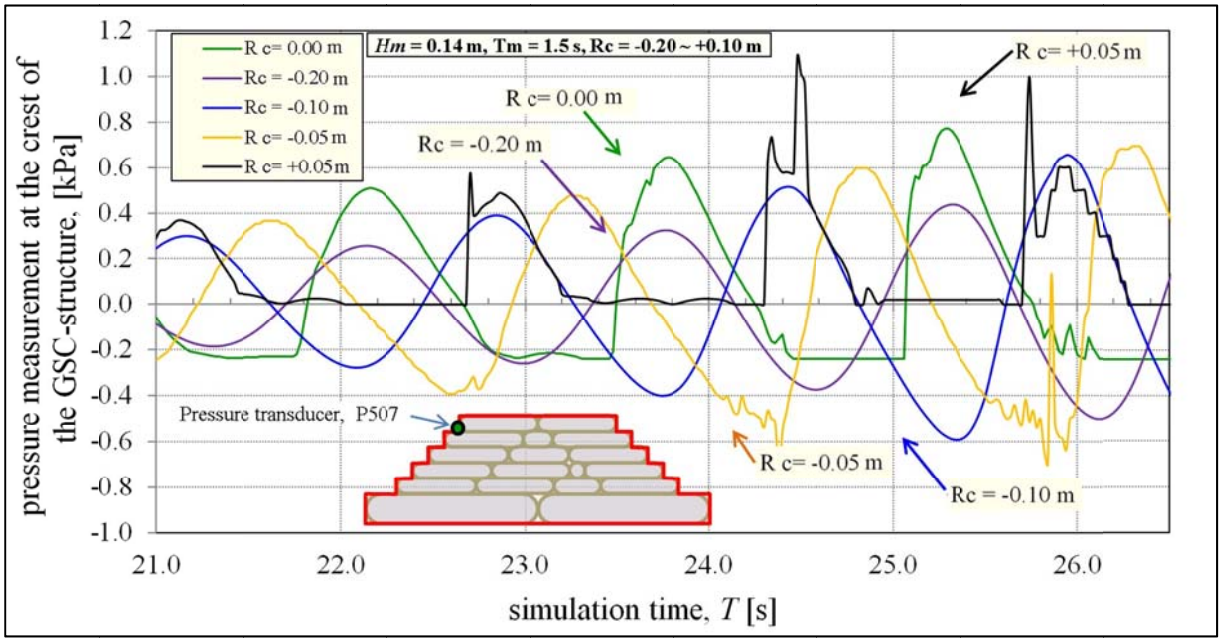

Figure 4-17: pressure acting on the seaward edge of crest GSCs

4.4.2 Extended Hydraulic Stability Tests with COBRAS-UC/UDEC Modelling

Figure 4-18 shows a comparison of COBRAS-UC/UDEC results of 80% filled GSCs made of nonwoven geotextile and Rc = -0.05 m with hydraulic stability curve derived from the hydraulic stability test for Rc = 0 (NW80H, see Figure 3 26). The numerical model results for Rc = -0.05 m show a slightly lower stability than that for Rc = 0 m.

Since the COBRAS-UC/UDEC simulations were performed for a limited duration (simulation duration: 3 ~ 5 wav periods compared minimum 100 regular waves were used during the hydraulic stability tests), it is not possible to accurately distinguish whether the degree of damage to the GSC-structure, but it can only distinguish whether the structure is stable or not.

Then the COBRAS-UC/UDEC results for $_{Rc}$ = -0.05 m were plotted in Figure 4-19, which contains the data from all the experiments form NW80H test series for varying crest freeboards from Rc = -0.25 m to Rc = +0.096 m. As expected from Figure 4-17 and Figure 4-18, numerical model results from Rc = -0.-0.05 m shows the lowest hydraulic stability among tested crest freeboards.

Not only in the test series NW80H, but also in other test series; NW100H and W80H, there were gaps in the data set. First, new simulations were performed to bridge these gaps in the data set in order to have a continuous stability curve with higher degree of certainty. In addition, data set was increases with additional simulation with larger relative crest freeboards up to Rc/H_m = + 2.0 and the results are shown in Figure 4-19, Figure 4-20 and Figure 4-21.

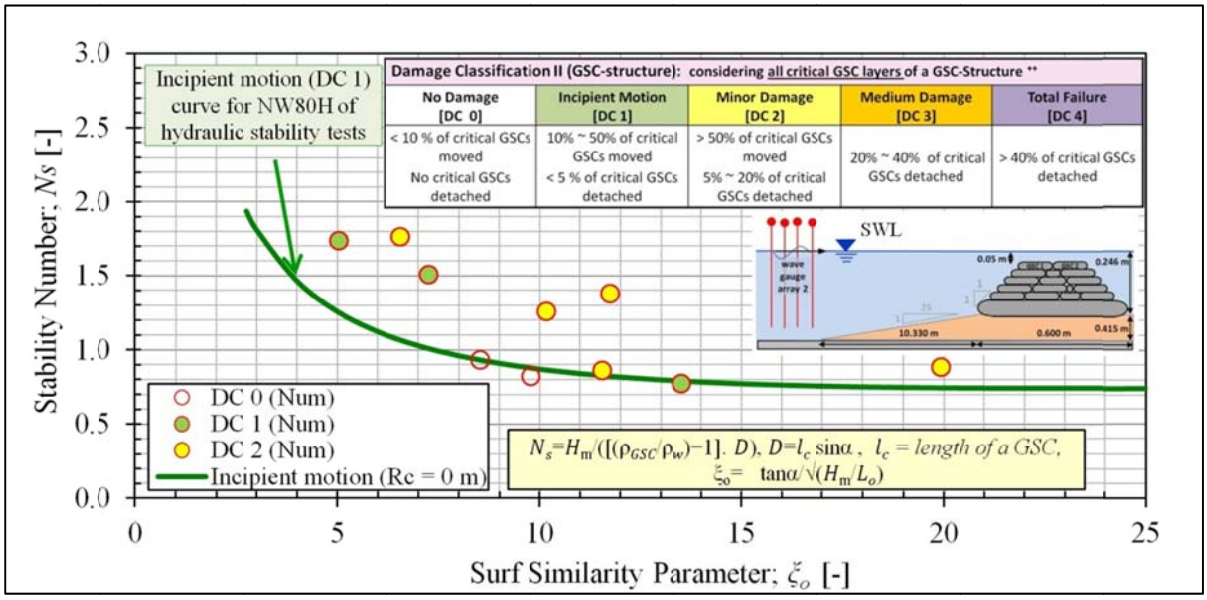

Figure 4-18: COBRAS-UC/UDEC results of the hydraulic stability of low-crested GSC-structures: comparison of 80% filled GSCs made of nonwoven geotextile (*Rc* = -0.05 m) with the hydraulic stability curves for (NW80H; *Rc* = 0 m

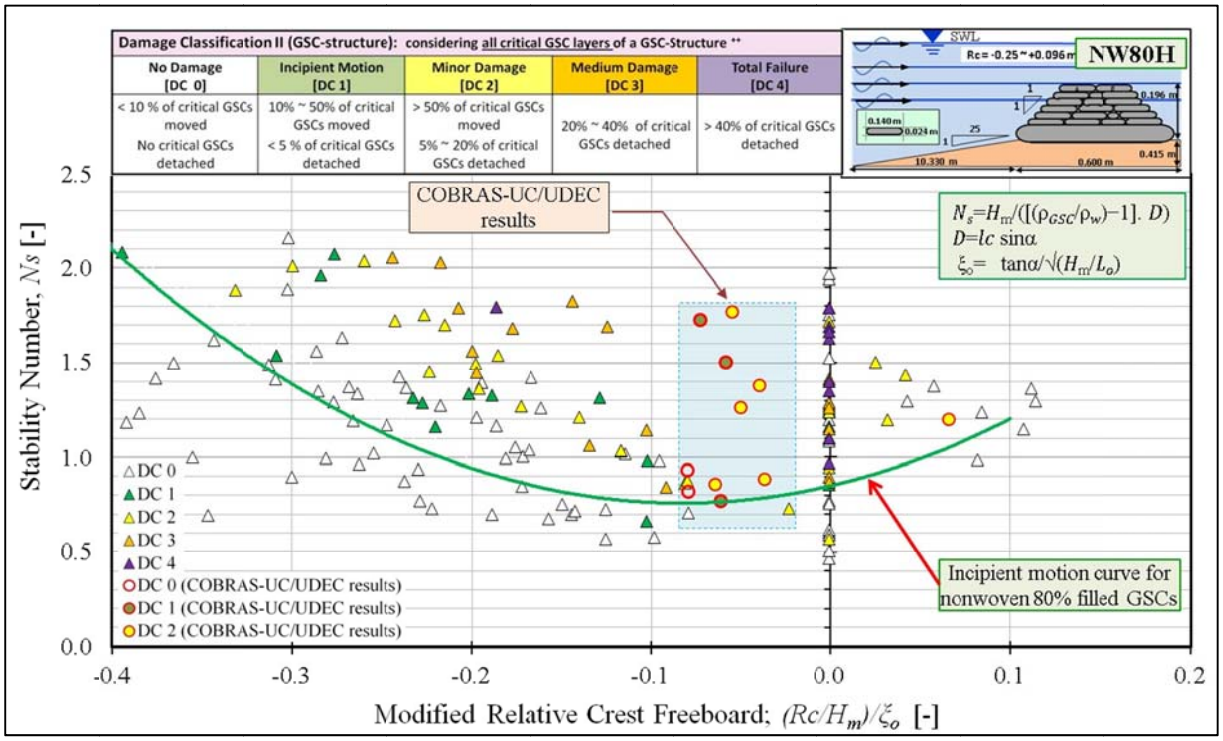

Figure 4-19: Hydraulic stability curve for low-crested and submerged GSC-structures made of nonwoven, 80% filled GSCs (series NW80H/*Rc* = -0.25 m ~ +0.096 / regular wave tests with H_m) including COBRAS-UC/UDEC results

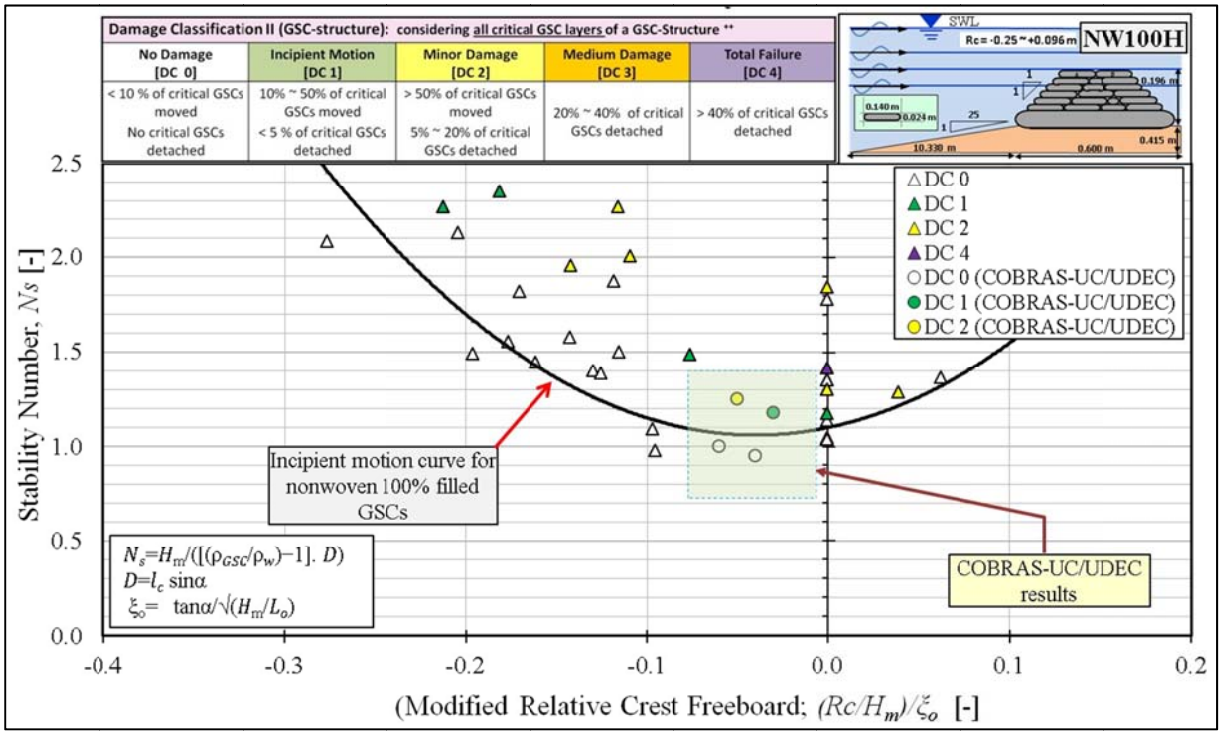

Figure 4-20: Hydraulic stability curve for low-crested and submerged GSC-structures made of nonwoven, 100% filled GSCs (series NW100H/*Rc* = -0.25 m ~ +0.096 / regular wave tests with H_m) including COBRAS-UC/UDEC results

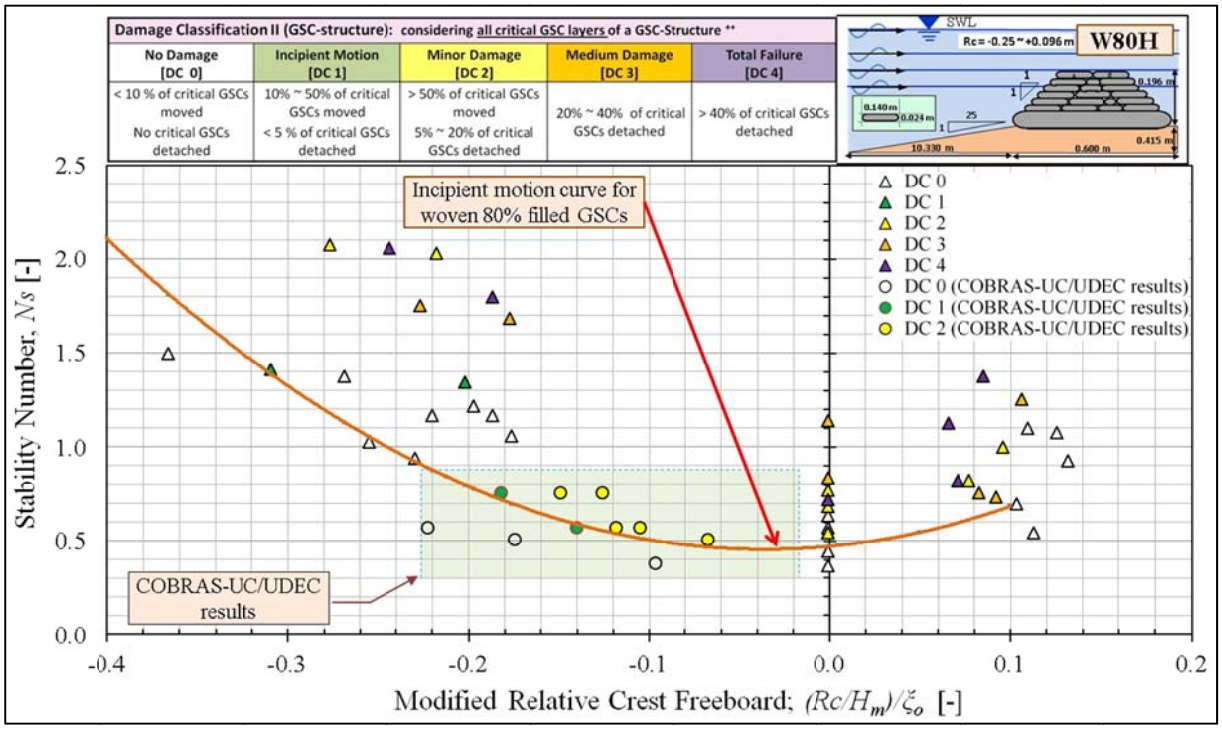

Figure 4-21: Hydraulic stability curve for low-crested and submerged GSC-structures made of woven, 80% filled GSCs (series W80H / *Rc* = -0.25 m ~ +0.096 m / regular wave tests with H_m) including COBRAS-UC/UDEC results

4.5 Summary and Concluding Remarks

Recio (2007) demonstrated the possibilities to numerically simulate the hydraulic stability of GSC-structures considering their flexibility. He used a weakly coupled CFD and CSD model (COBRAS/UDEC), which resulted in reasonably accurate results. According to the available literature, this was the first numerical study on the hydraulic stability of GSC-structure subject to wave attack with weakly coupled CFD and CSD models. There are several limitations in the COBRAS/UDEC as discussed in this chapter. In spite of these limitations, COBRAS/UDEC is the most reasonable modelling system for GSC-structures up to date.

In current study, COBRAS and UDEC 4 versions were replaced with recently released COBRAS-UC and UDEC 5 models. Apart from that, new modifications were introduced to simulate the simplified GSC model in COBRAS-UC/UDEC modelling system such as simplified GSCs with the correct masses and accurate overlapping lengths. UDEC has several options to defined properties of GSC-GSC joints. From those, the best matching model were selected to represent the GSC-GSC contacts and verified using the pullout test results. Moreover, forces acting on each node at the perimeter of the GSCs were calculated and applied separately, which allows more accurate simulations (both sliding and rotation motions of GSCs can be properly simulated).

Then several hydraulic stability tests were simulated with the COBRAS-UC/UDEC model and a good comparison of experimental data and numerical results were found. This step verifies capability of the COBRAS-UC/UDEC modelling system to simulate the hydraulic stability of submerged/low-crested GSC-structures.

Finally, a parameter study was carried out using the validated model system to extend the range of the conditions tested in the laboratory. The main objective of these simulations was to obtain additional data for three test series, NW80H, NW100H and W80H that were later used for the development of hydraulic stability curves

In conclusion, COBRAS-UC/UDEC results show a relatively good agreement with the experimental data. Hence, this CFD-CSD model system has an encouraging potential for practical applications. However, this system has serious limitations because of the 2D simplification of a truly 3D-problem. Therefore, one of the future research tasks is to extend the COBRAS-UC/UDEC to a coupled 3D-model system. Meanwhile, the 2D-modelling system should be applied cautiously.

5 Hydraulic Stability Formulae and Stability Nomograms

One of the main objectives of the current research study is to develop new simplified formulae and/or nomograms for the hydraulic stability of GSCs subject to wave loads based on recent and past experimental/numerical investigations. The existing formulae and nomograms from published literature were critically reviewed/analysed in Section 2.7 and already summarised in Table 2-8. In this chapter, the possibilities to simplify the process-based stability formulae of Recio (2007) are first examined (Section 5.1), before starting with the development of new hydraulic stability nomograms and simplified formulae (Sections 5.2-5.4). In Section 5.5 the possibility of using the same stability curves for both regular and irregular waves were studied and Section 5.6 summarises the outcomes of Chapter 5.

5.1 Simplifications of Recio's Formulae

The complicated process-based stability formulae of Recio (2007) are compared to the less complicated formulae of Wouters (1998) and Oumeraci et al. (2002b) by considering the sliding stability of crest containers for the zero-freeboard case, i.e. when the water surface and the crest of the structure are at the same level (Figure 5-1).

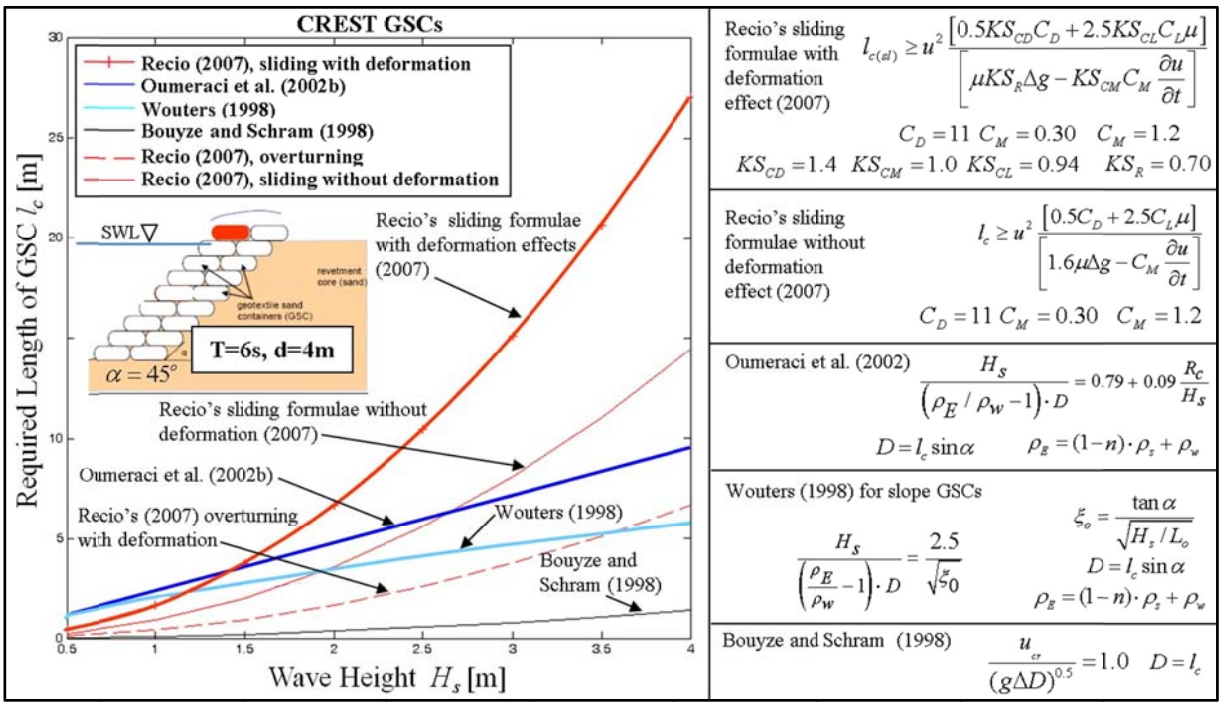

Figure 5-1: Comparison between Recio's stability formulae with and without deformation effects including further available formulae (Recio 2007)

In Recio's (2007) formulae (Figure 5-2), the required container length l_c is a function of u^2 ($l_c \propto u^2 \propto H^2$ with u being the horizontal flow velocity and H the wave height), whereas in the Hudson-like formulae l_c is approximately proportional to $H^{3/4}$ ($l_c \propto H^{3/4}$). Moreover, in the stability formula for crest GSCs by Oumeraci et al. (2002b), when $Rc = 0$, l_c is proportional to

H ($l_c \propto H$). Therefore, Recio's formulae are much more sensitive to the wave height. As shown in Figure 5-1, for smaller wave heights (H<1.5 m) the formulae of Wouters (1998) and Oumeraci et al. (2002b) provide slightly larger GSCs than Recio´s formula. For larger wave height larger (H>1.5 m) this is rather the opposite. The comparison in Figure 5-1 is mainly focused only on Recio's (2007) formula with and without the deformation effect, and the other simple Hudson-like formulae which implicitly include the effect of GSC-deformation.

Furthermore, in shallow water, the calculated GSC length l_c from Recio's (2007) formulae is less sensitive to the wave period ($l_c \propto u^2$ with u independent of T in shallow water but $u \propto 1/T$ in deeper water), whereas l_c is dependent of T in Oumeraci et al. (2002b) and Wouters (1998) for slope containers (see Table 2-8). However, in the formula by Oumeraci et al. (2002b) for the crest containers, l_c is independent from the wave period T (see Figure 5-1).

In order to analyse the performance of Recio's formulae, a new MATLAB routine was developed for the formulae to calculate the required size (characteristic length, l_c) of GSCs (Dassanayake and Oumeraci 2013c). In this routine, the required length l_c for the crest GSCs of a submerged GSC-structure is calculated as shown in Figure 5-2. Figure 5-3 shows the approach used in the new routine, which can be easily modified for other structures.

Stability formulae for crest GSCs of a submerged reef including the effect of deformation (Recio 2007)

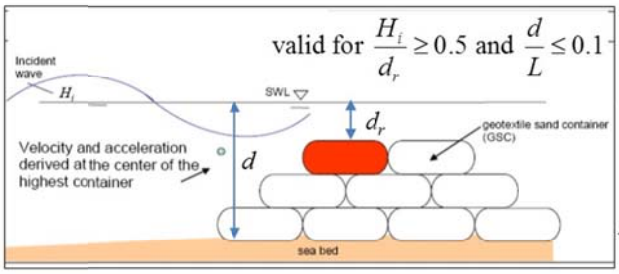

deformation factor for force coefficient during overturning

$KO_{CD} = 1.54,\ KO_{CL} = 0.80,\ KO_{CM} = 1.1,\ KO_R = 0.92$

deformation factor for force coefficient during overturning

$KS_{CD} = 1.40,\ KS_{CL} = 0.94,\ KS_{CM} = 1.00,\ KS_R = 0.70$

Overturning formula

$$l_{c(sl)} \geq u^2 \frac{\left[0.5KS_{CD}C_D + 2.5KS_{CL}C_L\mu\right]}{\left[\mu KS_R\Delta g - KS_{CM}C_M\frac{\partial u}{\partial t}\right]} \quad \text{.....(5.1)}$$

Sliding formula

$$l_{c(ov)} \geq u^2 \frac{\left[0.05KO_{CD}C_D + 1.25KO_{CL}C_L\right]}{\left[0.5\Delta KO_R g - 0.1KO_{CM}C_M\frac{\partial u}{\partial t}\right]} \quad \text{.....(5.2)}$$

$C_D = -9\times10^{-5}\,\mathrm{Re} + 23.04$ with $4 \leq C_D \leq 15$ .....(5.3)

$C_M = 0.30$ .....(5.4)

$C_L = 1\times10^{-5}\,\mathrm{Re} - 0.587$ with $0.3 \leq C_L \leq 1.2$ .....(5.5)

$\mathrm{Re} = \frac{u \cdot D}{\nu} = \frac{u \cdot l_c \sin\alpha}{\nu}$ .....(5.6)

Where;

C_D : drag coefficient [-]
C_L : lift coefficient [-]
C_M : inertia coefficient [-]
Cu : coefficient of uniformity [-]
d : water depth [m]
d_r : water depth at crest [m]
H_i : incident wave height [m]
l_c : length of container [m]
L_0 : deep water wave length [m]
Re : Reynolds number [-]
L_0 : deep water wave length [m]
u : wave induced horizontal particle velocity [m/s]
ν : kinematic viscosity of water [m²/s]
μ : friction coefficient [-]
$\frac{\partial v}{\partial t}$: wave induced horizontal particle acceleration [m/s²]

Figure 5-2: Process based hydraulic stability formulae for crest GSCs of a submerged reef (Recio 2007)

The main calculation steps of the MATLAB routine as illustrated in Figure 5-3 are:

(i) Define the design parameters relevant for the selected GSC-structure. Then calculate the horizontal particle velocity and acceleration at the elevation of the critical GSC using an appropriate wave theory.

(ii) Select the appropriate deformation factors K_{CD}, K_{CM}, K_{CL} and K_R (see Recio and Oumeraci 2009)

(iii) Calculate the minimum characteristic GSC length l_c by assigning the values corresponding to the lower limits of the force coefficients; C_D, C_M and C_L for the selected GSC-structure (see Recio and Oumeraci 2009)

(iv) Calculate the Reynolds number using the calculated GSC length l_c with equation 5.6 and calculate the new force coefficient with equations 5.3 and 5.5.

(v) Using new force coefficient from step (iv), recalculate the new required l_c and determine the difference between the previous value.

(vi) If, the length difference calculate in step (v) is larger than a threshold limit (e.g. 5%), then increase the calculated GSC length by 5% and follow steps (iv) to (vi) until the difference is lower than the threshold limit.

(vii) Steps (ii) to (vi) should be performed for both sliding and overturning to determine which formulae gives the largest required length l_c.

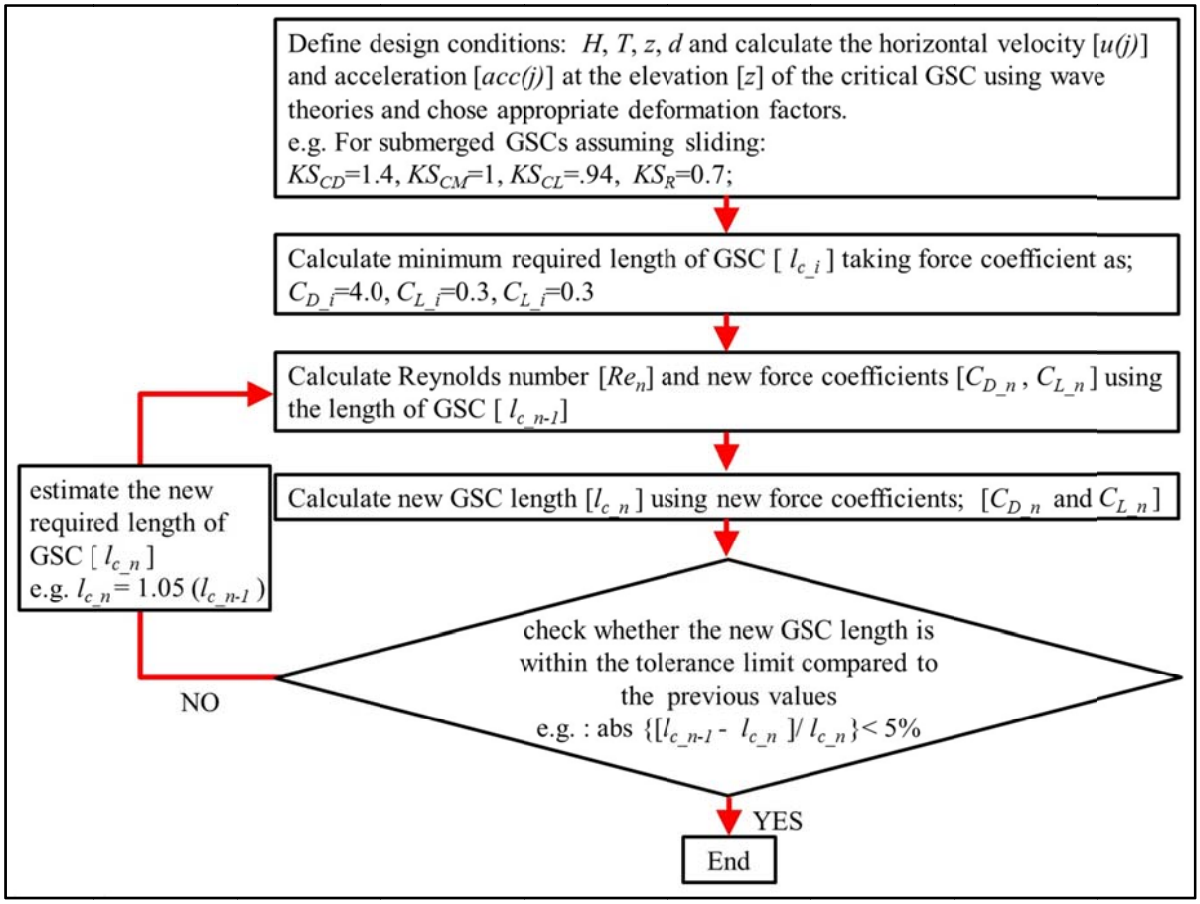

Figure 5-3: Flow chart for the application of the Recio (2007) stability formulae (developed for the new MATLAB routine)

By using the new MATLAB routine, the applicability and limitations of different forms of Recio's formulae were analysed and reported in Dassanayake and Oumeraci (2013c). In addition, a simplified version for this process - based stability formulae were proposed. This section provides an overview of this simplifying process, while considering exemplarily the most relevant formulae for the current study.

Based on the experimental data, Recio (2007) suggested a separate set of formulae for the calculation of force coefficients (Eqs. 5.3, 5.4 and 5.5). In most of the cases, once the wave height reached ca. 0.2 m ~ 0.6 m, the lower limit of the drag coefficient and the upper limit of the lift coefficient are considered in the formulae. Therefore, for prototype applications, only the lower limits of the drag coefficient and the upper limit of lift coefficient might be sufficient (Figure 5-4). The formulae were developed considering relatively smaller Reynolds number; ($Re = uD/\nu$ and $Re = 10^4 \sim 10^6$). Therefore, the formulae should be applied cautiously as most of the prototype cases might results in Reynolds number well beyond this limit. If the trend shown in Figure 5-4 continues, the drag coefficients might still be reduced for larger Re numbers ($Re > 10^6$) and consequently might result in smaller GSC lengths than the calculated values with constant (e.g. lower limit of C_D) force coefficients.

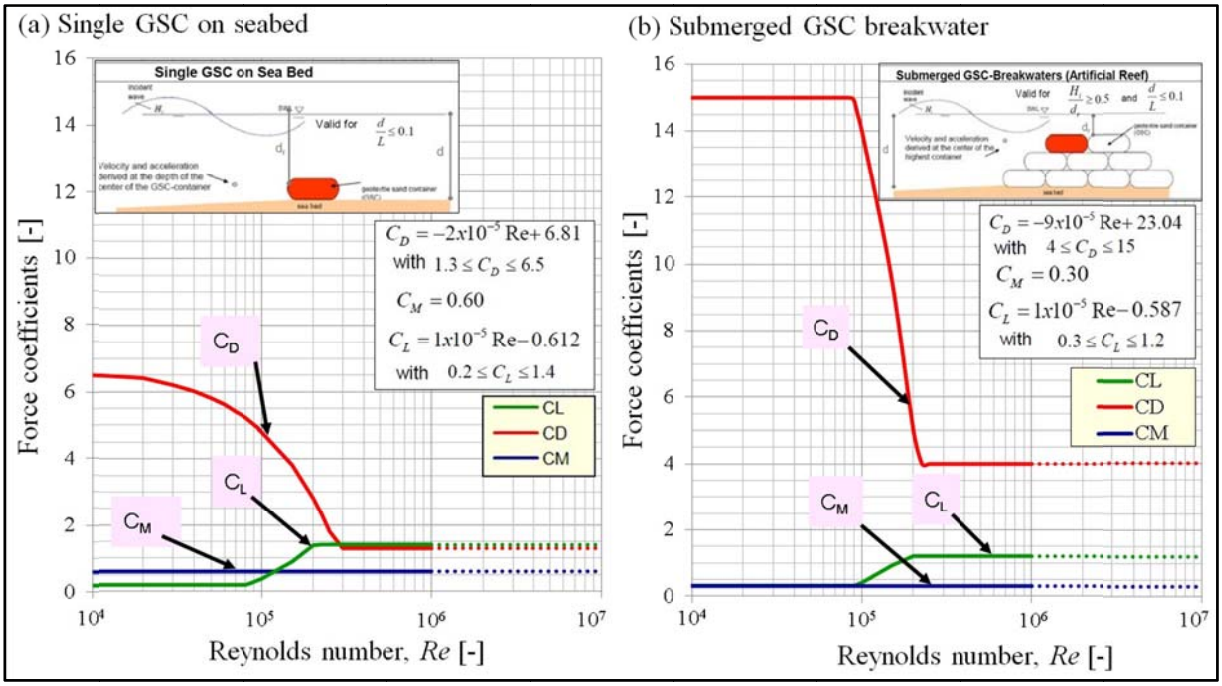

Figure 5-4: Example calculations of force coefficients using Recio's (2007) formulae for two GSC applications

The results of example calculations with model scale dimensions are shown in Figure 5-5 for design wave periods, $T = 1.0$ s and $T = 2.0$ s and a negative crest freeboard $Rc = -0.15$ m. According to the formulae, which calculate the force coefficients, as the Reynolds number increases drag coefficient C_D drops from 15 to 4. In contrast, the lift coefficient C_L increases from 0.3 to 1.2 (Figure 5-5e and Figure 5-5f). Since the formula is more sensitive to the drag coefficient, a drop of the required GSC length l_c occurs for wave heights between

$H = 0.175$ m and $H = 0.225$ m. For larger wave heights, GSC length l_c increases again exponentially with increasing wave height.

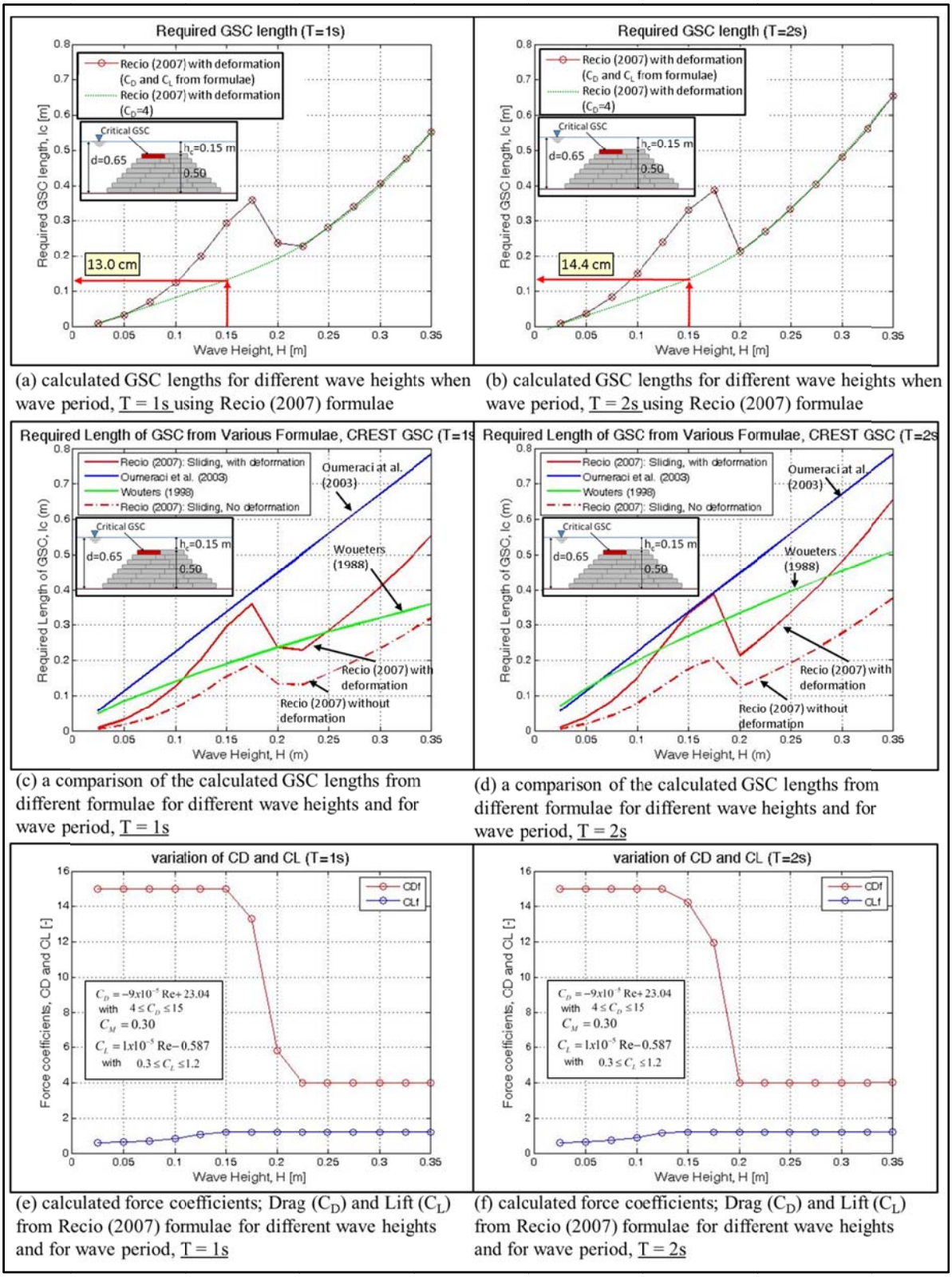

(a) calculated GSC lengths for different wave heights when wave period, T = 1s using Recio (2007) formulae

(b) calculated GSC lengths for different wave heights when wave period, T = 2s using Recio (2007) formulae

(c) a comparison of the calculated GSC lengths from different formulae for different wave heights and for wave period, T = 1s

(d) a comparison of the calculated GSC lengths from different formulae for different wave heights and for wave period, T = 2s

(e) calculated force coefficients; Drag (C_D) and Lift (C_L) from Recio (2007) formulae for different wave heights and for wave period, T = 1s

(f) calculated force coefficients; Drag (C_D) and Lift (C_L) from Recio (2007) formulae for different wave heights and for wave period, T = 2s

Figure 5-5: Calculated length of GSCs for different wave parameters using Recio's sliding formulae (calculations were performed with model scale dimensions)

Figure 5-6 further illustrates the application of Recio's formulae exemplarily for the hydraulic stability of crest GSCs of a submerged GSC-structure at prototype scale (calculations were performed with prototype dimensions). In order to apply the formulae, first, the structure should satisfy two conditions; $H_i/d_r \geq 0.5$ and $d/L \leq 0.1$. Hence, if the submergence depth is 1.5 m, then the minimum wave height, which satisfies this condition ($H_i/d_r \geq 0.5$), is $H_i = 3.0$ m. For example, a wave period of 7 s and a water depth of 10 m would satisfy the other criterion ($d/L \leq 0.1$). Second, the force coefficients that satisfy equations 5.3 and 5.5 reach their upper limits in terms of Reynolds number, consequently, the lower limit of the drag coefficient ($C_D = 4$) and the upper limit of the lift coefficient ($C_L = 1.2$) as illustrated in Figure 5-6a. Third, as shown in Figure 5-6b, the contribution from the horizontal particle velocity is significant (u^2). Therefore, the inertia force acting on the GSC can be neglected as they have a phase difference of ca. $\pi/2$. Based on these results, the formulae were simplified (Figure 5-7) and the simplified Recio formula is used for the calculation of GSC length l_c for different incident wave heights (Figure 5-6d and Figure 5-19).

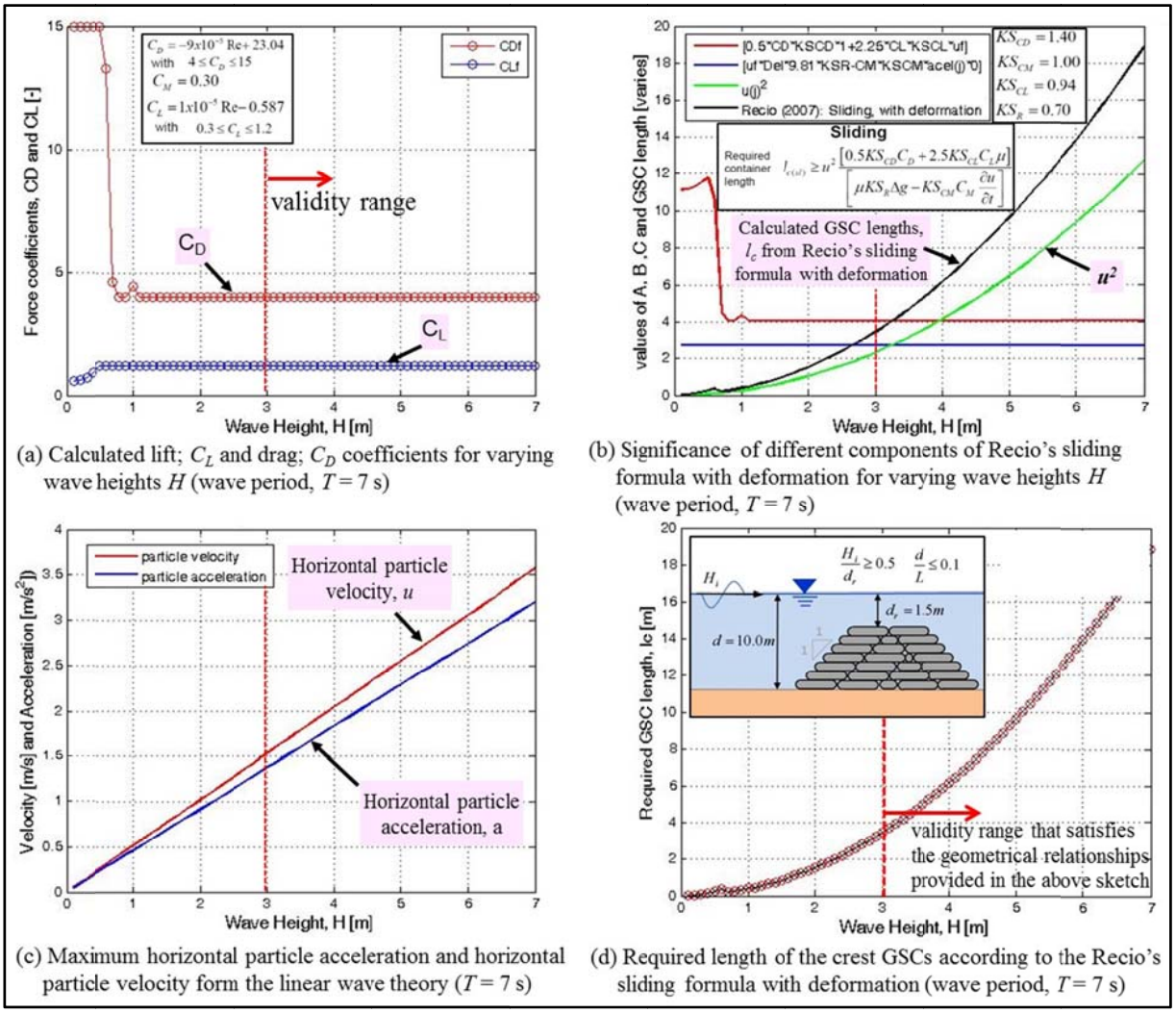

(a) Calculated lift; C_L and drag; C_D coefficients for varying wave heights H (wave period, $T = 7$ s)

(b) Significance of different components of Recio's sliding formula with deformation for varying wave heights H (wave period, $T = 7$ s)

(c) Maximum horizontal particle acceleration and horizontal particle velocity form the linear wave theory ($T = 7$ s)

(d) Required length of the crest GSCs according to the Recio's sliding formula with deformation (wave period, $T = 7$ s)

Figure 5-6: Application of Recio's formulae for submerged GSC-structures (prototype scale dimensions)

The process based hydraulic stability formulae of Recio (2007) were critically evaluated (Dassanayake and Oumeraci 2013c) and the results from the most relevant applications for this study namely for the hydraulic stability of crest GSCs of a submerged reef, are presented here. Two major simplifications were suggested for the formulae considering the prototype applications.

(i). Omissions of the iteration process to calculate the force coefficient based on the GSC length l_c and the Reynolds number, when the formulae are applied for the prototype scale. Instead of using the supplementary equations (eqs. 5.3 and 5.5) given in the formulae, it is sufficient to use the lower limit of the drag coefficient and the upper limit of the lift coefficient as the values of C_D and C_L in the formulae (eqs. 5.1 and 5.2).

(ii). Recio's formulae are more sensitive to the horizontal particle velocity than to the horizontal particle acceleration (Dassanayake and Oumeraci 2013c). Even though the maximum wave induced forces on a submerged body does not reach its maximum for the maximum horizontal particle velocity, it is accurate enough for the engineering practice to consider only the maximum velocity (where acceleration is zero) for the calculation of the required GSC length l_c.

Figure 5-7 presents the simplified Recio's formulae for the hydraulic stability of crest GSCs of a submerged GSC-structure. Since, these are simplified formulae, some of the influencing factors (e.g. Inertia force) are ignored. Therefore, these formulae should be used cautiously as in some flow regimes, which are outside the tested range (i.e. $Re > 2\times10^5$), combinations of inertia and drag forces might be crucial for the hydraulic stability. More details on the Recio's formulae and the simplification process can be found in Dassanayake and Oumeraci (2013c).

Simplified Recio formulae for the hydraulic stability of crest GSCs of a submerged GSC-structure including the effect of deformation

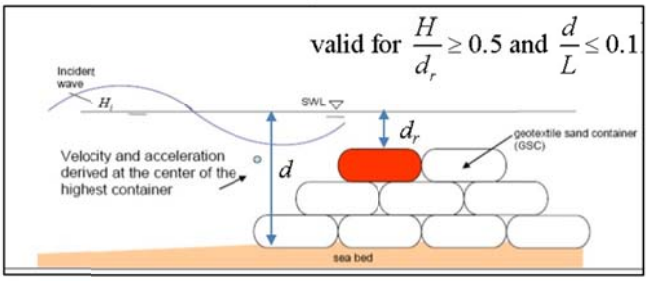

deformation factor for force coefficient during overturning: $KO_{CD} = 1.54$ $KO_{CL} = 0.80$ $KO_{CM} = 1.1$ $KO_R = 0.92$

deformation factor for force coefficient during overturning: $KS_{CD} = 1.40$ $KS_{CL} = 0.94$ $KS_{CM} = 1.00$ $KS_R = 0.70$

force coefficients: $C_D = 4$ $C_M = 0.3$ $C_L = 1.2$

Overturning formula

$$l_{c(ot)} \geq u^2 \frac{\left[0.5KS_{CD}C_D + 2.5KS_{CL}C_L\mu\right]}{\left[\mu KS_R \Delta g\right]} \quad (5.6)$$

Sliding formula

$$l_{c(sl)} \geq u^2 \frac{\left[0.05KO_{CD}C_D + 1.25KO_{CL}C_L\right]}{\left[0.5\Delta KO_R g\right]} \quad (5.7)$$

Where;

C_D : drag coefficient [-]
C_L : lift coefficient [-]
C_M: inertia coefficient [-]
Cu : coefficient of uniformity [-]
d : water depth [m]
d_r : water depth at crest [m]
H_i : incident wave height [m]
l_c : length of container [m]
L_0 : deep water wave length [m]
Re : Reynolds number
L_0 : deep water wave length [m]
u : wave induced horizontal particle velocity [m/s]
ν : kinematic viscosity of water [m²/s]
μ : friction coefficient [-]
$\frac{\partial v}{\partial t}$: wave induced horizontal particle acceleration [m/s²]

Figure 5-7: Simplified Recio's formulae for the hydraulic stability of crest GSCs of a submerged GSC-structure

5.2 Effect of the Engineering Properties of GSCs on Hydraulic Stability

The influence of the sand fill ratio (test series NW80H and NW100H), the interface friction between GSCs (test series NW80H and W80H) and the inclined placement of GSCs (NW80H and NW80I)] on the hydraulic stability were comparatively analysed through four test series (Figure 3-26). The effects of these parameters on the hydraulic stability of submerged and low-crested GSC-structures were quantified by considering the test series *NW80H (nonwoven 80% filled and horizontally placed GSCs*) as the reference case as it represents one of the most commonly used GSC types. The differences between stability numbers N_s, which correspond to "incipient motion" (DC 1) of crest GSCs of the test series NW80H and the other test series were calculated using equation 5.8 and presented in Figure 5-8 as percentage differences.

$$\left(\begin{array}{l}\textit{Percentage change}\\ \textit{in stability number}\left(N_{s\_k}\right)\end{array}\right)\% = \left(\frac{\textit{stability number}\left(N_{s\_k}\right) - \textit{stability number}\left(N_{s\_NW80H}\right)}{\textit{stability number}\left(N_{s\_NW80H}\right)}\right)\% \qquad (5.8)$$

k = Test Series (i.e. $NW80H$, $NW100H$, $W80H$, and $NW80I$), see Figure 3-26 for descriptions

The experimental results show different failure mechanisms for different submergence depths and the importance of the engineering properties of GSCs also varies depending on the dominant failure mechanism for a particular GSC-structure and for a particular freeboard (Dassanayake et al. 2011c, Dassanayake and Oumeraci 2012b, 2012c and 2012d). The relative importance of the engineering properties (woven and non-woven geotextile, 80% and 100% sand fill, horizontal and inclined GSC placement) is shown in Figure 5-8 as a function of the surf similarly parameter and for two crest freeboard (Rc = -0.2 m in Figure 5-8a and Rc =0.0 m in Figure 5-8b).

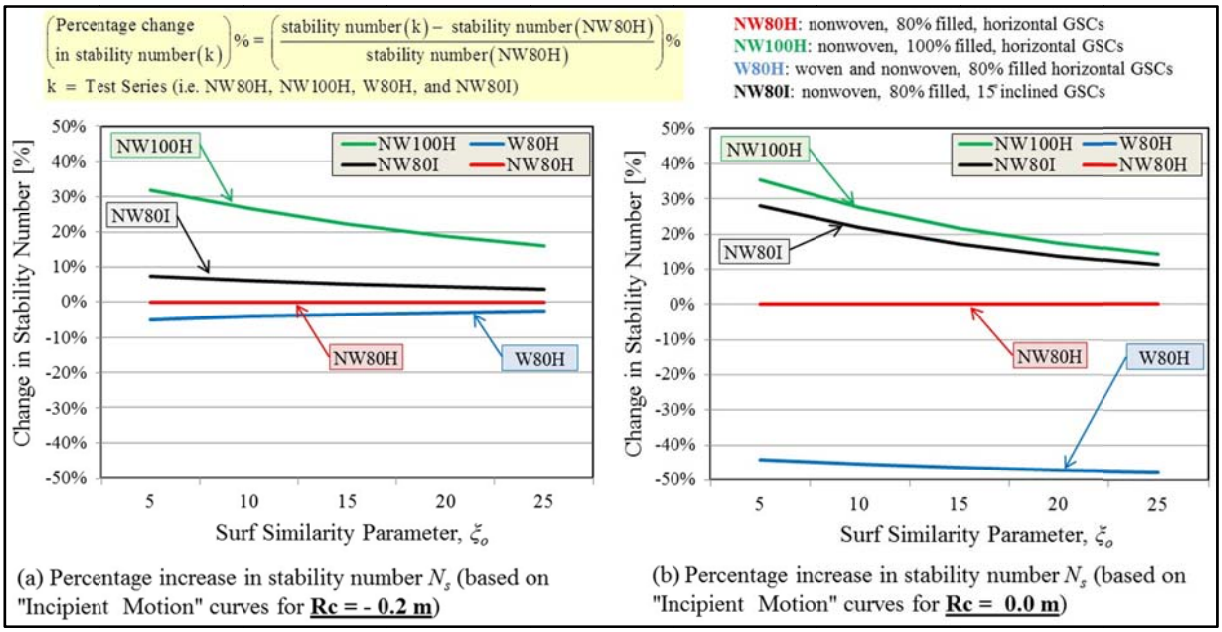

Figure 5-8: Effect of the sand fill ratio, the geotextile material, and the inclined placement of GSC on hydraulic stability of GSC-structures for crest freeboards Rc = 0.2 m (a) and Rc = 0.0 m (b).

For the tested conditions with a zero crest freeboard, GSCs made of woven (interface friction angle = 13.33°) geotextile (with an approximately 50% lower friction coefficient than nonwoven geotextile with interface friction angle = 22.64°) resulted in ca. 44% lower stability numbers, when considering the "incipient motion" of crest GSCs (Figure 5-8b). Though most of the existing studies (e.g. PIANC 2011) on GSC-structures recommend a sand fill ratio of 80%, a 100% filled GSC shows a 36 % higher stability number for a surf similarly parameter of 5, compared to 80% filled GSC (Figure 5-8b).

Apart from changing the engineering properties of GSCs, the hydraulic stability can be increased by changing the inclination angle of GSCs during placement. An inclination angle of only 15^0 resulted in approximately 28% higher stability number compared to horizontally placed GSCs, when the wave conditions required for incipient motion of the GSCs are considered. In addition to the improvements of the hydraulic stability which is achieved by a higher friction angle between GSCs, higher sand fill ratios and inclined placement of GSCs, these parameters significantly retard the damage development of GSC-structures over the entire storm duration (Dassanayake et al. 2011c, Dassanayake and Oumeraci 2012c). Therefore, not only the conditions required for incipient damage to a GSC-structure, but also the temporal development of the damage and the different damage levels that might result, are important for a proper the comprehensive quantification of the effect of the different factors considered in this study.

With this background, it was required to develop separate hydraulic stability curves for the three aforementioned test series (NW80H, NW100H and W80H). In order to develop a single stability curve/formula accounting for the effect of friction between GSCs and the sand fill ratio, a more detailed study on several sand fill ratios and several types of geotextiles with varying friction properties would be required. Such a detailed study was not feasible within the frame of this study.

5.3 New Hydraulic Stability Nomograms for Submerged and Low-Crested GSC-Structures

By combining previous and current hydraulic stability tests and numerical modelling results, new hydraulic stability nomograms and simplified formulae for the hydraulic stability of low-crested/submerged GSC-structures are developed. This section outlines the new stability curves and the stability formulae for horizontally placed; nonwoven 80% filled GSCs (NW80H), nonwoven 100% filled GSCs (NW100H) and woven 80% filled GSCs (W80H). Ideally, a single hydraulic stability curve should be found, which can describe the behaviour of both submerged (Rc<0) and surface piercing low-crested GSC-structures (Rc>0). For example, Vidal et al. (1992) showed a relationship with the relative freeboard ($Rc^* = Rc/D_{50}$) and the stability number ($N_s=H_s/\Delta D_{50}$) of low-crested rubble mound breakwaters by considering four different damage categories. The possibility of developing a similar relationship for the submerged/low-crested GSC structures is also examined in this PhD study. Based on the new damage classification developed in this study (Table 3-6), the relationship between the stability number N_s and the relative crest freeboards Rc^* is first analysed (Figure 5-9).

Figure 5-9 provides an impression of the tested relative crest freeboards ($Rc^*=Rc/H$) that indicate the applicability range of each of the new prospective formulae (only the hydraulic stability results from the regular wave tests are shown). Moreover, Figure 5-9a~ Figure 5-9d suggest the specific freeboards that need to be covered by the planned numerical simulations in order to fill the gaps in the data set. Test series NW80H, which is the reference case for the comparison, covered a large spectrum (- 3.0 $<Rc^*<$ + 0.5) of relative crest freeboards (Figure 5-9a). The experiences gained during this test series were important to optimise the test programmes for the other 3 test series (NW80I: Figure 5-9b, W80H: Figure 5-9c, NW100H: Figure 5-9d).

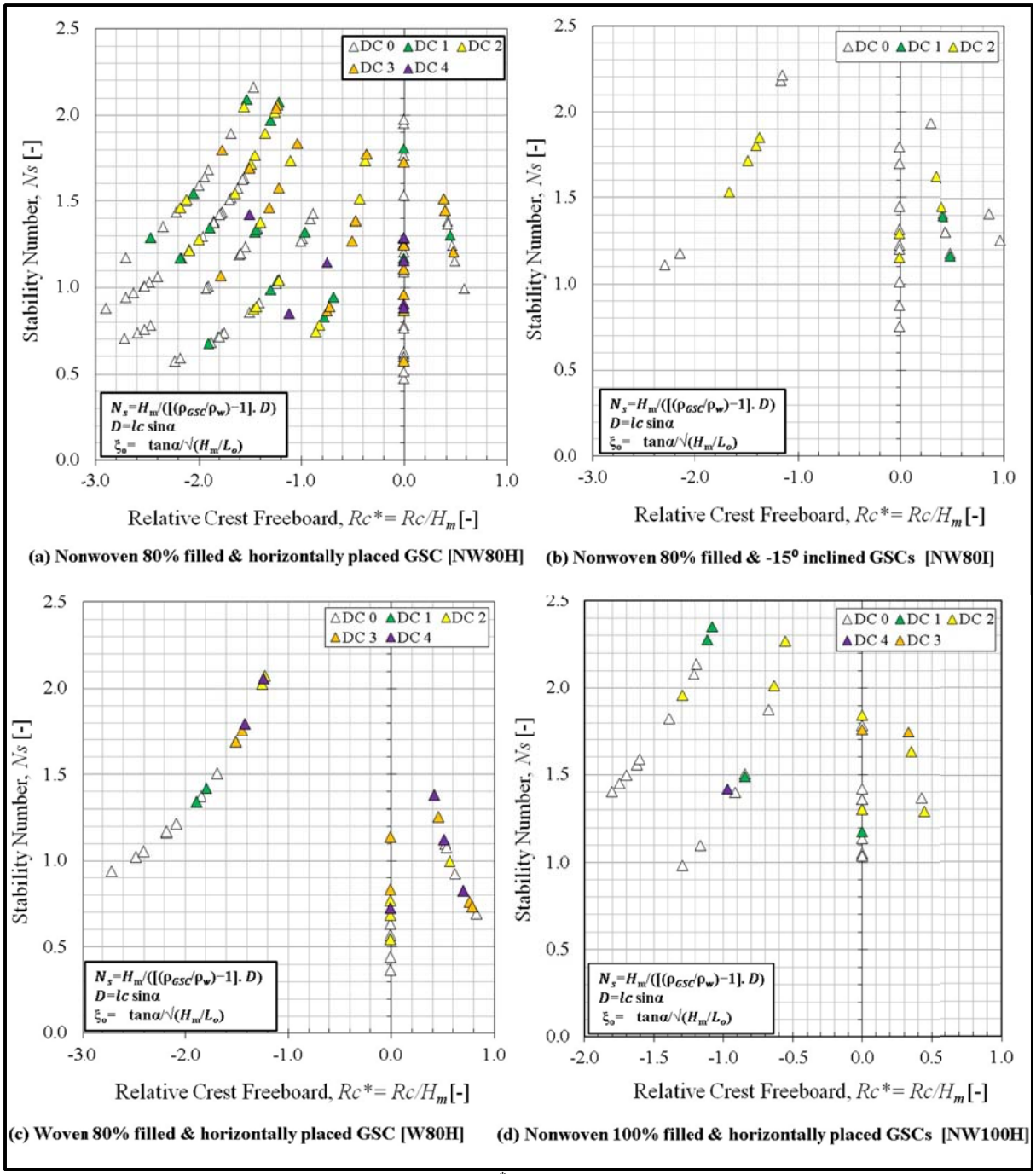

Figure 5-9: Influence of the relative crest freeboard Rc^* on the hydraulic stability of GSC-structures.

Most of the tests for test series NW80I (Figure 5-9b), W80H (Figure 5-9c) and NW100H (Figure 5-9d) were performed with the parameters required for the "incipient motion" (DC 1) of crest GSCs. Therefore, the amount of data showing the "no damage" damage level (DC 0) is relatively small. During the test series NW80I (Figure 5-9b), the wave maker reached its limit in terms of maximum wave parameters. Therefore, most of the tests were showing damage levels from "no damage" (DC 0) to "minor damage" (DC 2). Therefore, no stability curve/formula is developed for that case. Woven GSCs were tested in three crest freeboards (Rc = -0.2 m, 0.0 m, +0.496 m, in model scale) and therefore numerical simulation were performed to obtain additional data between Rc = -0.2 m and Rc = 0.0 m. Figure 3-31 well-illustrated that the hydraulic stability of crest GSCs of a submerged/low-crested GSC-structure depends on both the relative crest freeboard and the surf similarity parameter which is confirmed by Figure 5-9 . Since there are no clear boundaries between the two important damage categories, "no damage" (DC 0) and "incipient motion" (DC 1), data were plotted with the stability number Ns and a modified relative freeboard $Rc^*mod = Rc^*/\xi_0$ where $Rc^* = Rc/H_m$ represents the relative crest freeboard and ξ_0 the surf similarity parameter, and new hydraulic stability curves were then developed. Based on the hydraulic stability results from regular wave tests, a curve which distinguishes the "no damage" (DC 0) and the "incipient motion" (DC 1) damage levels was first drawn (Figure 5-10). Here, stability numbers were plotted against modified relative crest freeboard (i.e. $Rc^*_{mod} = Rc^*/\xi_0$, with $Rc^* = Rc/H_m$). Each regular wave test consists of 100 waves and the mean wave height H_m and mean wave period T_m from the time domain analysis were considered when calculating the stability number N_s and the wave steepens S_0 .

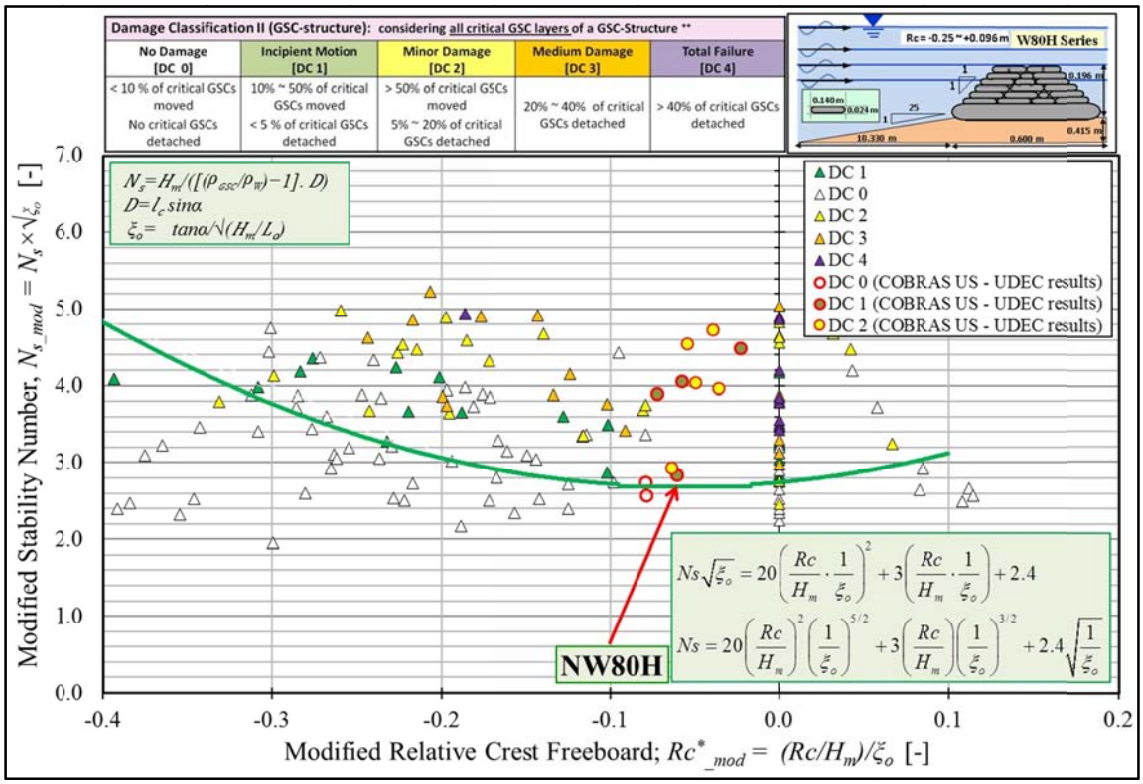

Figure 5-10: Hydraulic stability curve for low-crested and submerged GSC-structures made of nonwoven, 80% filled GSCs (series NW80H with Rc = -0.25 m ~ +0.096 m / regular wave tests with H_m)

The "incipient motion" curve shows the lowest hydraulic stability around Rc^*_{mod} = -0.08, which corresponds to a crest freeboard of ca. Rc = -0.05 m (in model scale). Therefore, numerical modelling was mainly focusing on this range of crest freeboards. For all non-zero relative crest freeboards there is a tendency of increasing damaged levels as the test parameters move upwards from the curve. However, one of the main limitations of the modified relative crest freeboards $Rc^*_{mod} = (Rc/H_m)/\xi_o$ is, when $Rc = 0$, it does not show the influence of the surf similarity parameter (see Figure 3-28). Therefore, there are no clear differences in the damage categories when moved upwards from the "incipient motion" curve.

Similarly, new stability curves are developed for other two test series, nonwoven 100% filled GSCs (NW100H - Figure 5-11) and woven 80% filled GSCs (W80H - Figure 5-12). In both figures, the data points showing "no damage" (DC 0) are less than those in Figure 5-10, because the test parameters were carefully selected to obtain the threshold limit between "no damage" and "incipient motion" (DC 1) damage levels. Whenever it was evident that the wave parameters were not sufficient to damage the structures, those tests were omitted from the original test programme.

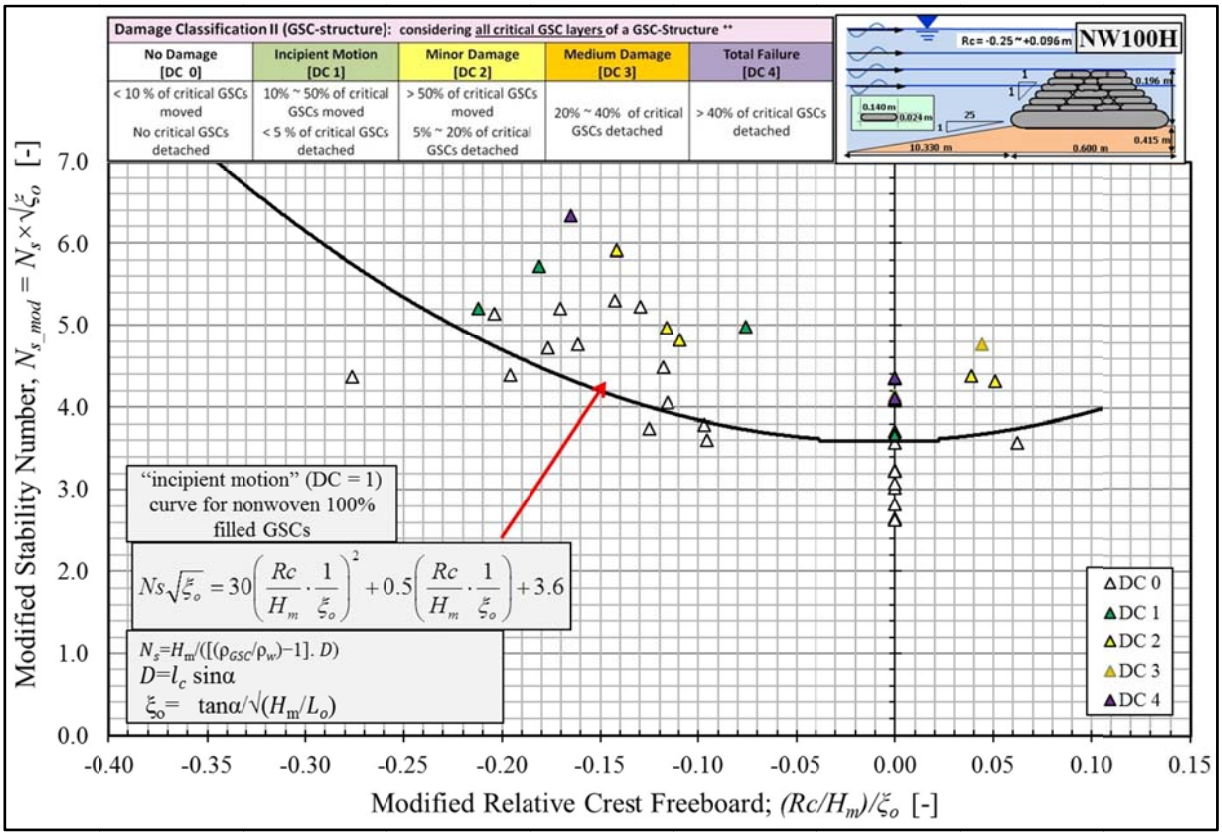

Figure 5-11: Hydraulic stability curve for low-crested and submerged GSC-structures made of nonwoven, 100% filled GSCs (series NW100H with Rc = -0.25 m ~ +0.096 / regular wave tests with H_m)

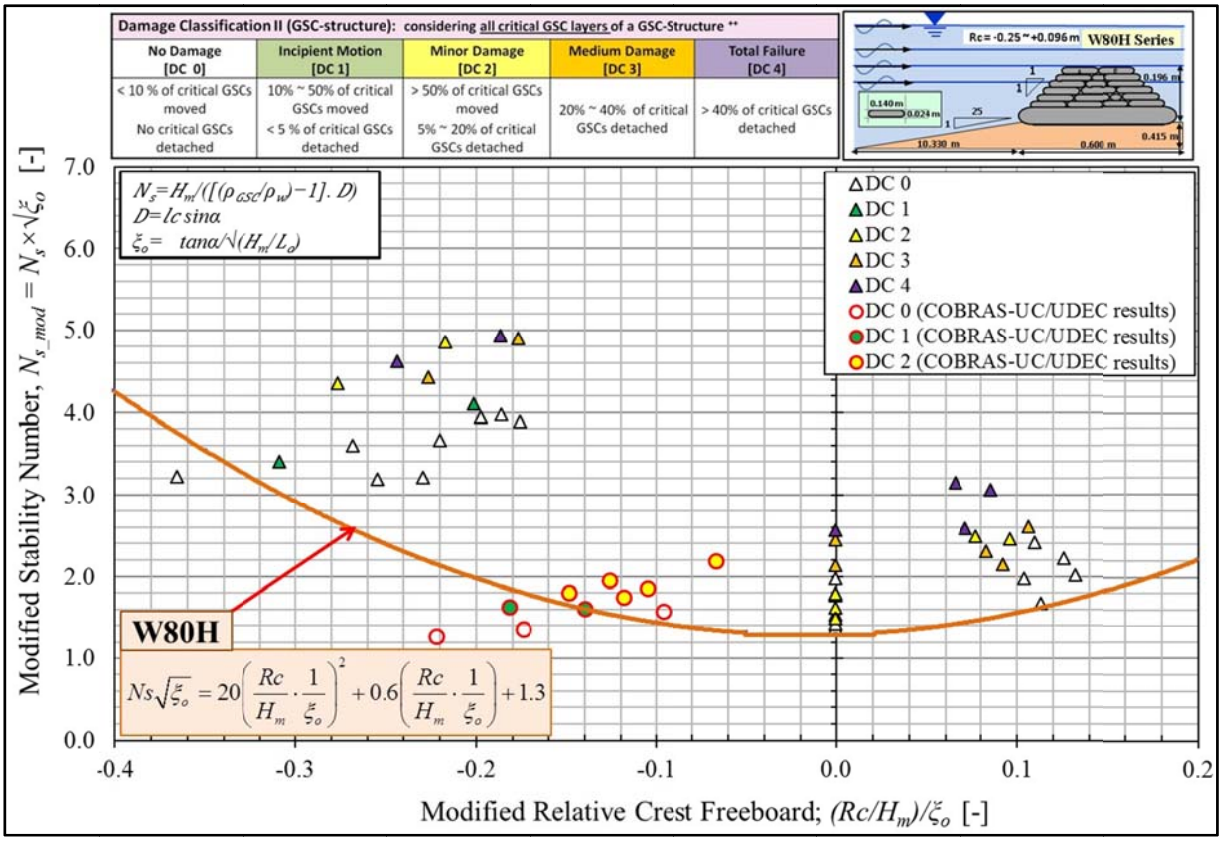

Figure 5-12: Hydraulic stability curve for low-crested and submerged GSC-structures made of woven, 80% filled GSCs (series W80H / Rc = -0.25 m ~ +0.096 / regular wave tests with H_m)

Since nonwoven GSCs were tested only with three crest freeboards, there is a large gap of data. This gap was filled with the numerical simulation results (COBRAS-UC/UDEC).

Furthermore, if some damage level is accepted in the engineering practice, then there is a possibility to select parameters above the hydraulic stability curves presented in Figure 5-10, Figure 5-11 and Figure 5-12, even though in GSC-structures, generally no damage is allowed (Hornsey et al. 2011).

5.4 Simple Stability Formulae

The hydraulic stability of rock armours at the crest of a low-crested and submerged breakwater has been extensively investigated by several researchers over the last three decades and several hydraulic stability formulae were developed based on those results. Among them, Van deer Meer (1988), Van der Meer and Pilarczyk (1990), Vidal et al. (1992), Vidal et al. (1995), Burger (1995), Burcharth et al. (2005), Cappietti (2011), etc. are noteworthy. Apart from that, Kramer et al. (2005), Van der Linde (2010) and van den Bosch et al. (2012), etc. studied the hydraulic stability of interlocking armour units at the crest (e.g. Dolos, X-block, etc.). However, the investigations on the hydraulic stability of crest GSCs of low-crested and/or submerged GSC-structures (See Dassanayake and Oumeraci 2013c for further details) are limited to a few series of experimental studies (Figure 5-13) namely; Oumeraci et al. (2002a), Oume-

raci et al.(2002b) and Mori (2009). Given the range of Rc/H_s values tested in previous studies (Figure 5-13), the formulae developed under the current study (eq. 5.9) covers relative crest freeboards of $-2.0 \leq Rc/Hs \leq +0.5$ in order to bridge the knowledge gaps on the hydraulic stability of low-crested and submerged GSC-structures. The possibilities to extend the range of validity of the formulae by incorporating previous hydraulic stability tests were examined and results are presented in Section 5.5.

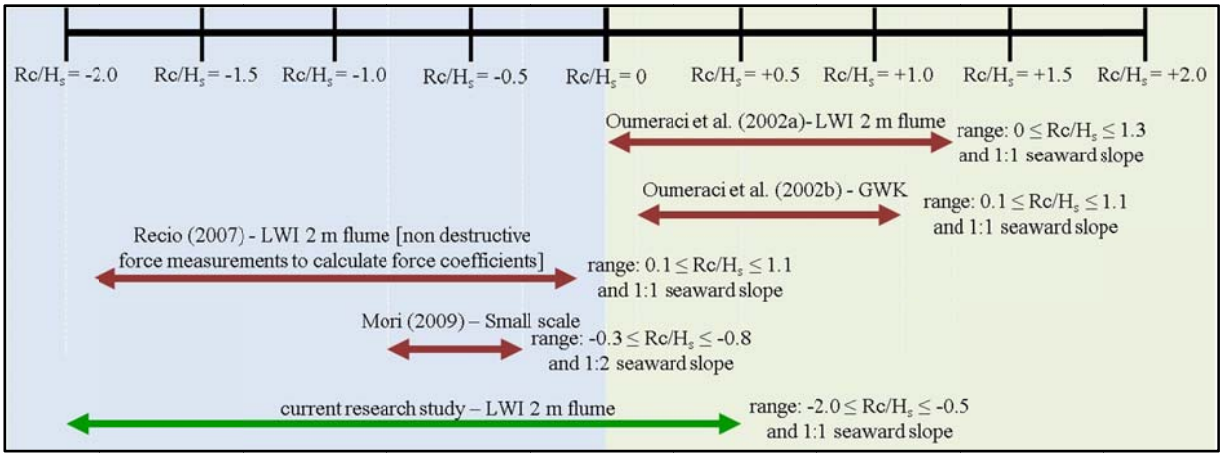

Figure 5-13: Applicability of previous and current formulae in terms of relative crest freeboard

A new hydraulic stability formula for "incipient motion" of crest GSCs in a low-crested/submerged GSC-structure was developed using the stability curves drawn in Figure 5-10, Figure 5-11 and Figure 5-12. This formula can be written as;

$$Ns\sqrt{\xi_o} = A\left(\frac{Rc}{H}\cdot\frac{1}{\xi_o}\right)^2 + B\left(\frac{Rc}{H}\cdot\frac{1}{\xi_o}\right) + C \qquad (5.9)$$

where; $Ns = H / \left[\{(\rho_{GSC}/\rho_w) - 1\}\cdot l_c \sin\alpha\right]$ and $\xi_o = \tan\alpha / \sqrt{H / L_0}$

and where;

A, B, and C = empirical parameters depending on the type of geotextile material and the sand fill ratio, which are derived from the hydraulic stability tests [-]

$H = H_m$ for regular wave tests or $H_{2\%}$ for irregular wave tests [m]

H_m = incident mean wave height from regular wave tests measured at intermediate water depth (at the beginning of the foreshore slope) [m]

$H_{2\%}$ = mean of the highest 2% of the incident waves in a time series (mean of the highest 20 incident waves from the wave reflection analysis of 1000 waves and for a Rayleigh distribution the values $H_{2\%} = 1.4\ H_s$)[m]

Rc = crest free board [m]

L_0 = wave length at deep water

Ns = stability number [-]

ρ_w = density of water [kg/m^3]

ρ_{GSC} = density of GSCs [kg/m^3]

l_c = length of a GSC [m],

α = slope angle of the structure [°],

$L_0 = g\,T^2/(2\pi)$ = deep water wave length calculated using the mean wave period [m]

When eq. 5.9 is used for the stability calculations with the data from irregular wave tests, the mean wave height H_m can be replaced by $H_{2\%}$. Here $H_{2\%}$ is the representative wave height for tests with wave spectrums instead of the commonly applied H_s. In some coastal engineering applications such as the designing of low-crested rubble mount breakwaters on depth limited foreshores, $H_{2\%}$ was found as a better representative value for design than the significant wave height H_s (Van der Meer 1988, Van der Meer 1998, Rock Manual 2007). Therefore, both H_s and $H_{2\%}$ were considered in the analysis and found, $H_{2\%}$ is a better representative value for the hydraulic stability of crest GSCs of a low-crested or submerged GSC-structure (see Section 3.4.5 and section 5.5).

The applicability range is given in Table 5-1 and the values for A, B and C constant for the tested test series are provided in Table 5-2. The curves are plotted in Figure 5-14 for comparison.

Table 5-1: Validity range of the new hydraulic stability formulae

parameter	valid range of the formulae
relative crest freeboard; $Rc^* = Rc / H_m$	-2.0 ~ +1.2
wave steepness; $S_0 = H_m / L_0$	0.001 ~ 0.01
sand fill ratio; FR	80% and 100%
friction angle of geotextile; ϕ (from underwater direct shear tests)	woven: 13.33^0 (tan Φ=0.237) nonwoven: 22.62^0 (tan Φ=0.417)
seaward slope	1:1
crest width	$2 \times l_c$, where l_c is the GSC length
foreshore slope	1:25
relative depth at the toe; d / L_0 and H_m / d	$0.01 \le d / L_0 \le 0.04$ and $0.125 \le H_m / d \le 0.8$

Table 5-2: Empirical parameters for the new hydraulic stability formula

Empirical parameters	A	B	C
nonwoven 80% filled and horizontally placed GSCs	20	3.0	2.4
nonwoven 100% filled and horizontally placed GSCs	30	0.5	3.6
woven 80% filled and horizontally placed GSCs	20	0.6	1.3

As shown in Figure 5-14, the hydraulic stability curves for two different geotextile materials (woven and nonwoven) tend to converge as the submergence depth increases. The differences between woven and nonwoven GSCs are reduced in terms of the hydraulic stability (e.g. for Rc = -0.2 m, Figure 3-34), mainly because of different dominant failure mechanisms (see Section 3.4.8 and Figure 5-8).

Furthermore, 100% filled GSCs show smaller overlapping lengths compared to 80% filled GSCs. The overlapping length is important for the overall stability of low-crested structures as the possibility of pulling out or overturning of slope elements could be higher. However, as the submergence depth increases, only the crest elements govern the stability of the entire

structure. Therefore, nonwoven 80% and 100% filled curves tend to diverge as the submergence depth increases (see Section 3.4.7 and Figure 5-14).

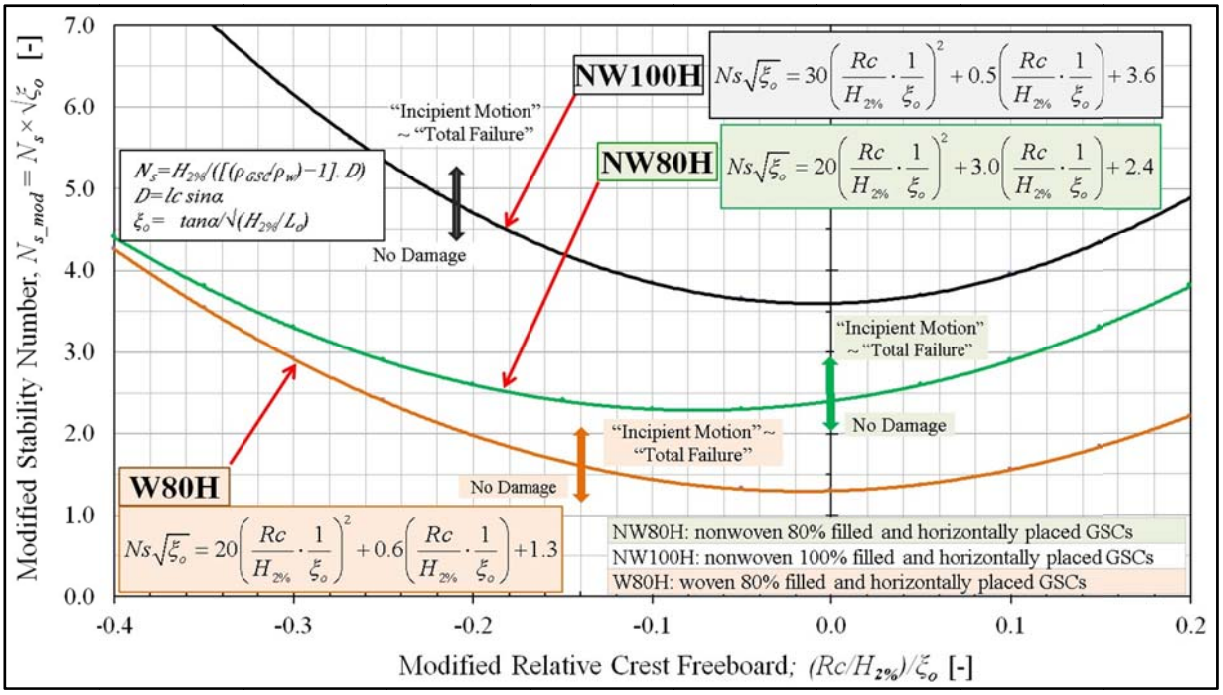

Figure 5-14: Incipient motion curves derived from regular wave tests

Even though equation 5.9 was developed based on an extensive series of experimental studies, the results from previous experimental studies and numerical simulations were used for the validation (see Section 5.5).

Nonwoven 80% filled and 100% filled GSCs were tested for several crest freeboards, whereas the woven 80% filled GSCs were tested only for three different crest freeboards. Therefore, the stability curve for woven geotextile is relatively less reliable unless more data from the numerical simulations are added to the plots. Therefore, the validated COBRAS-UC/UDEC model was used for the simulation of additional crest freeboards, in order to extend the range validity of the formulae (Dassanayake and Oumeraci 2012f)

Moreover, Coghlan et al (2009) and Hornsey et al. (2011) have conducted experimental studies on the hydraulic stability of GSC-revetments with three non-overtopping seaward slopes; 1:1, 1:1.5 and 1:2 and found 1:1 slope provided the highest stability against wave attack. Therefore, only 1:1 slope is considered in this PhD study.

5.5 Validity of Proposed Stability Nomograms and Formulae

Finally, instead of defining two separate stability curves for the tests with regular waves and irregular waves, the possibility of using the same stability curves (Figure 5-14) for both type of waves were studied. Here, the irregular wave test data (test series NW80H) are plotted in Figure 5-18 by using the characteristic wave height $H_{2\%}$, which is the mean of the highest 2% of the waves in the time series (mean of the highest 20 incident waves from the wave reflection analysis and for a Rayleigh distribution of the values $H_{2\%} = 1.4\ H_s$). The results show a better agreement with the initial curve developed for regular wave test (see Figure 5-10).

Moreover, the hydraulic stability curve for 80% nonwoven GSCs is validated by comparing the data from two previous model tests conducted by Oumeraci et al. (2002a and 2002b) in a small scale model (2 m wide wave flume of LWI, Braunschweig) and in a large scale model (large wave flume GWK, Hannover) to study the hydraulic stability and the hydraulic performances of low-crested GSC-structures. One of the main objectives of these experiments was to identify the most relevant parameters for the hydraulic stability of high overtopping GSC-structures. In addition, the hydraulic performance of these GSC-structures was also investigated. Two different types of structures were tested: low-crested reef structures and revetments (Figure 5-15). The applicability of new formula (eq. 5.8) for nonwoven 80% filled GSCs was verified using the hydraulic stability results from these two scale model studies.

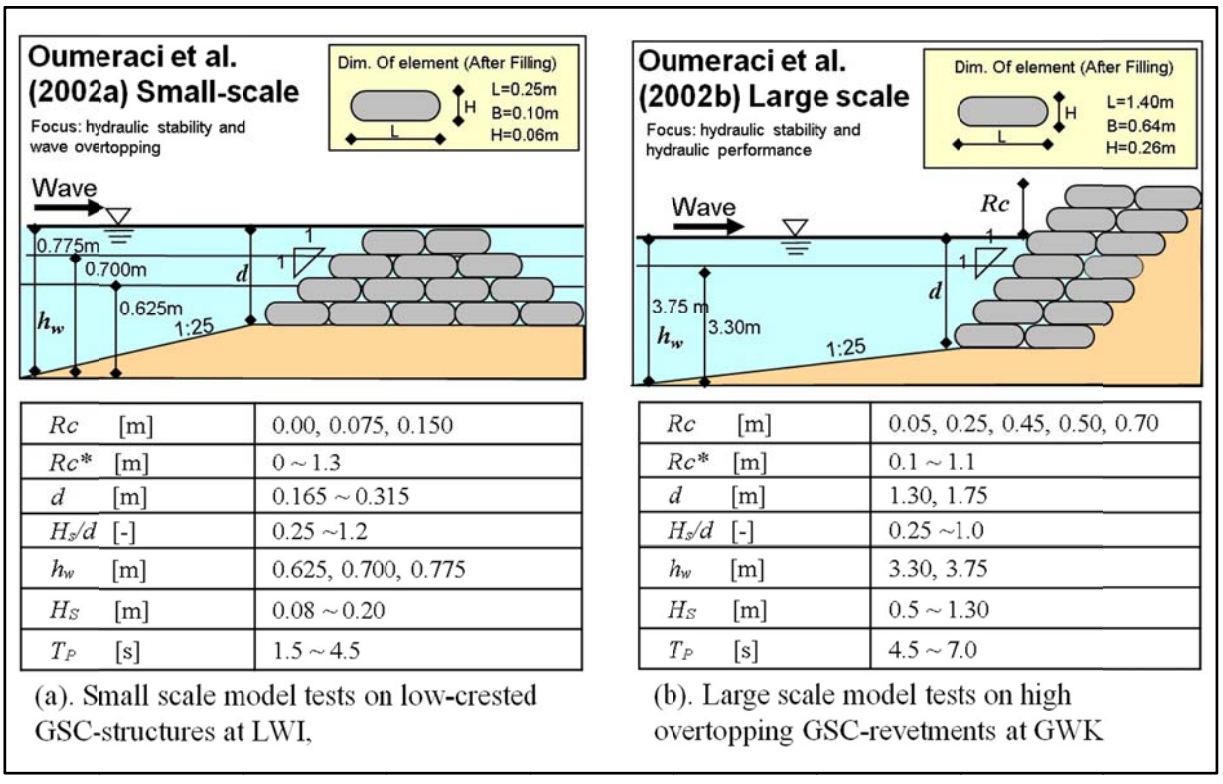

Rc [m]	0.00, 0.075, 0.150
Rc^* [m]	0 ~ 1.3
d [m]	0.165 ~ 0.315
H_s/d [-]	0.25 ~1.2
h_w [m]	0.625, 0.700, 0.775
H_S [m]	0.08 ~ 0.20
T_P [s]	1.5 ~ 4.5

(a). Small scale model tests on low-crested GSC-structures at LWI,

Rc [m]	0.05, 0.25, 0.45, 0.50, 0.70
Rc^* [m]	0.1 ~ 1.1
d [m]	1.30, 1.75
H_s/d [-]	0.25 ~1.0
h_w [m]	3.30, 3.75
H_S [m]	0.5 ~ 1.30
T_P [s]	4.5 ~ 7.0

(b). Large scale model tests on high overtopping GSC-revetments at GWK

Figure 5-15: Small (LWI) and large (GWK) scale model tests on the hydraulic stability of crest GSCs by Oumeraci et al. (2002a and 2002b)

The main reasons for the selection of these two specific model studies are;

(i) the current PhD study is focused on submerged/low-crested GSC-structures and the data sets from these two studies are most relevant as in both cases the tests were performed with 80% filled nonwoven GSC and with 1:1 seaward slope.

(ii) Since most of the model tests were performed either with zero crest freeboard or with negative crest freeboards, with the help of these data sets, it is possible to extend the range of validity of the new formula.

Figure 5-16 provides an impression of the tested relative crest freeboards ($Rc^*=Rc/H$) with irregular tests performed in the current PhD study and from the previous hydraulic stability tests by Oumeraci et al. (2002a and 2002b). The crest freeboards of irregular wave tests from the current study cover a wide range from $-3.0<(Rc/H_s)<+1.0$. However, most of the tests were performed with negative crest freeboards. Therefore, the results from Oumeraci et al. (2002a and 2002b) are useful to extend the validity of the formula for low-crested structure.

Even though the damage classification system used by Oumeraci et al. (2002a and 2002b) is different from what was proposed in Table 3-6, damage definitions; "stable" and "little displacement" in the two former studies are considered as equivalent to the damage level "no damage" (DC 0) and "incipient motion" (DC =1) in the current study.

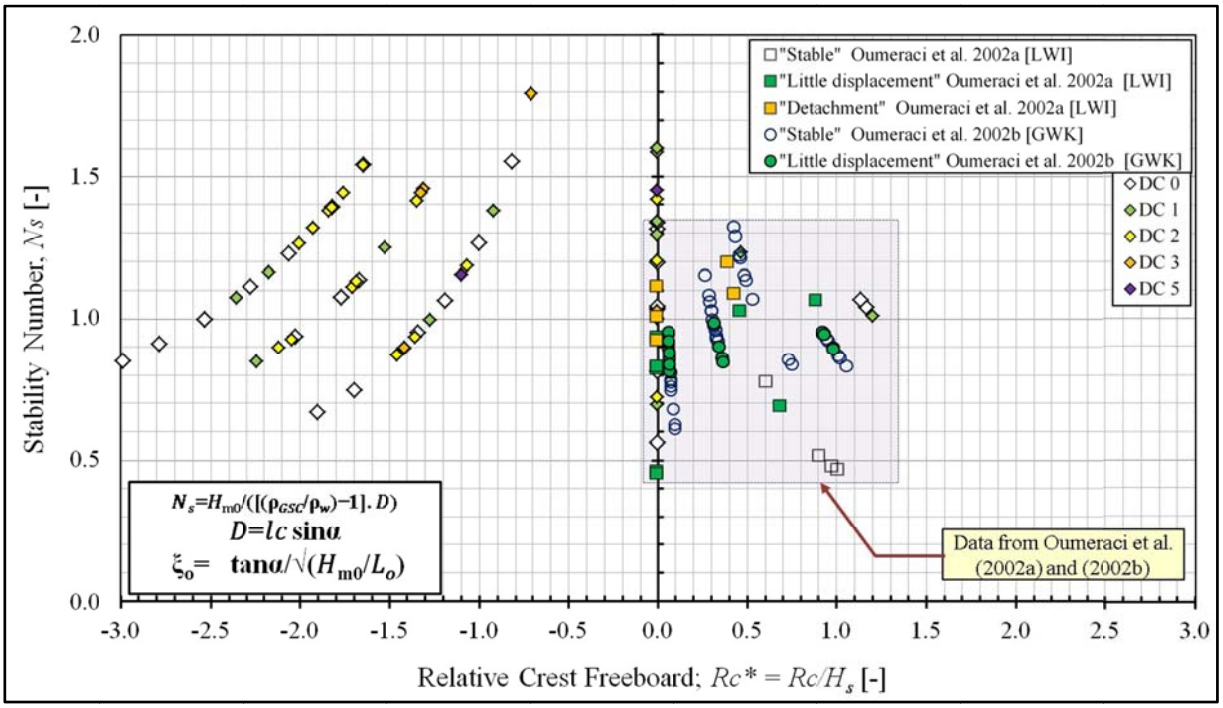

Figure 5-16: Hydraulic stability test data for low-crested/submerged GSC-structures made of nonwoven, 80% filled GSCs (series NW80H with Rc = -0.25 m ~ +0.096 / Irregular wave tests with H_s)

The stability curve derived from regular wave tests (Figure 5-10) was then compared with the hydraulic stability results from irregular wave tests. Each irregular wave test consists of 1000 irregular waves (JONSWAP spectrum). Here, the characteristic wave height H_{m0} and the peak

wave period T_p from the frequency domain analysis were considered when calculating stability number Ns and wave steepness S_o. As shown in Figure 5-17, when the stability number is plotted against the modified crest freeboard, the stability number appears to be lower for irregular waves with height H_{m0} than for regular waves with height H_m. Therefore, in order to develop an "incipient motion" curve for the irregular wave tests, the test data should either be plotted with different parameters (e.g. $H_{2\%}$ or H_{max}) or new empirical parameters for the new formulae should be found.

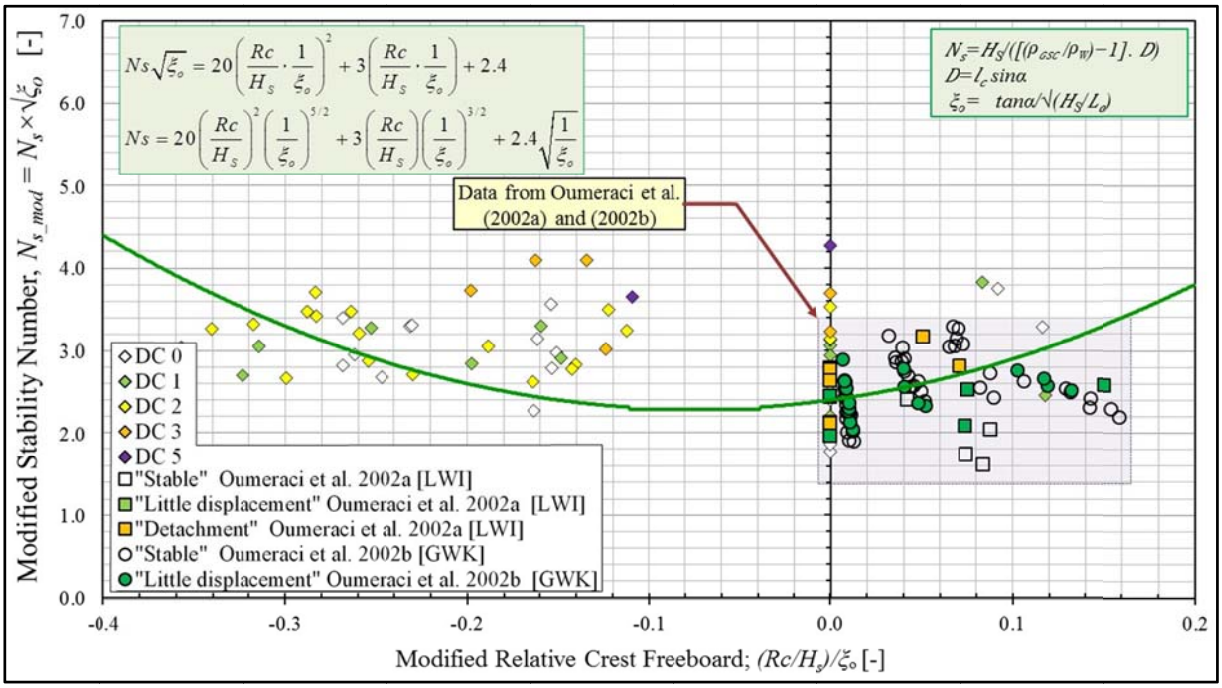

Figure 5-17: Hydraulic stability curve for low-crested and submerged GSC-structures made of nonwoven, 80% filled GSCs (series NW80H with Rc = -0.25 m ~ +0.096 / Irregular wave tests with significant wave height, H_s)

Finally, instead of defining a separate stability curves (or finding new empirical parameters for the new formula) for the tests with regular waves and irregular waves, the irregular wave test data are plotted in Figure 5-18 by using the characteristic wave height $H_{2\%}$. When plotting the data from Oumeraci et al. (2002a and 2002b), assuming a Rayleigh distribution in the measured wave heights, characteristic wave height $H_{2\%}$ is obtained as $H_{2\%} = 1.4\ H_s$. The results show a better agreement with the initial curve developed for regular wave test using the mean wave height H_m. Therefore, when using the formula (eq. 5.9), it is possible to use $H_{2\%}$ as the representative wave height for irregular waves.

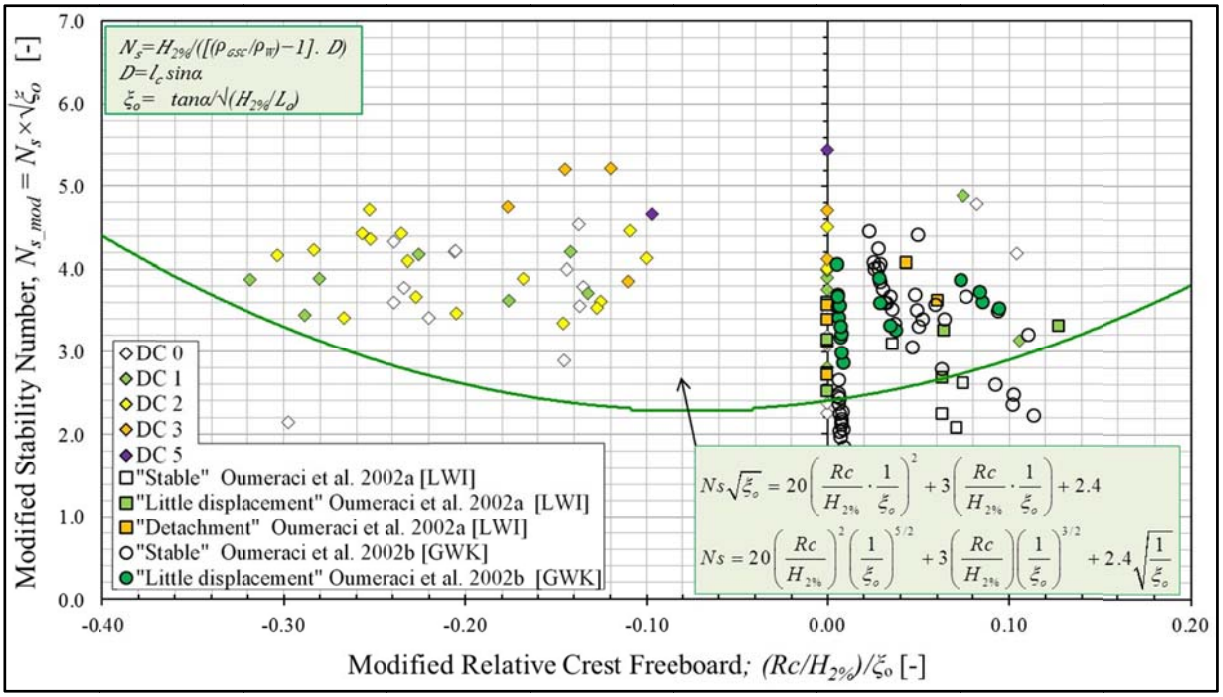

Figure 5-18: Hydraulic stability curve for low-crested and submerged GSC-structures made of nonwoven, 80% filled GSCs (series NW80H/*Rc* = -0.25 m ~ +0.096 / Irregular wave tests with $H_{2\%}$)

The new hydraulic stability formula is then plotted in Figure 5-19 together with other available formulae (Table 2-8) for the *Rc = 0* m case. The new formula resulted in slightly larger GSC lengths l_c than those from the simple stability formula for crest containers by Oumeraci et al. (2002b). Since the crest formula by Oumeraci et al. (2002b) was developed after several small scale (at LWI) and large scale (at GWK) laboratory tests (sand fill ratio = 80%) with relative crest freeboards of $Rc/H_s = 0 \sim 1.3$, the reliability of the formula for low-crested GSCs-structure with those crest freeboards is high. Therefore, the new formula was compared with the formula from Oumeraci et al. (2002b).

The new formula for nonwoven 80% filled GSCs provides slightly larger (ca. 10%) GSC lengths l_c than the formula of Oumeraci et al. (2002b). Therefore, the new formula might result in slightly conservative results for relative crest freeboards; $Rc/H_s = 0 \sim 1.3$.

Moreover, as expected the curve for NW100H resulted in slightly smaller (ca. 8%) GSC lengths l_c than those calculated with the formulae of Oumeraci et al. (2002b) for 80% filled GSCs. Therefore the new formula predicts the hydraulic stability of 80% and 100% filled GSCs with a reasonable accuracy for the low-crested structure subject to irregular wave attack. However, no experimental data are yet available to perform a final validation of the new formula for fully submerged GSC-structures (Rc<0).

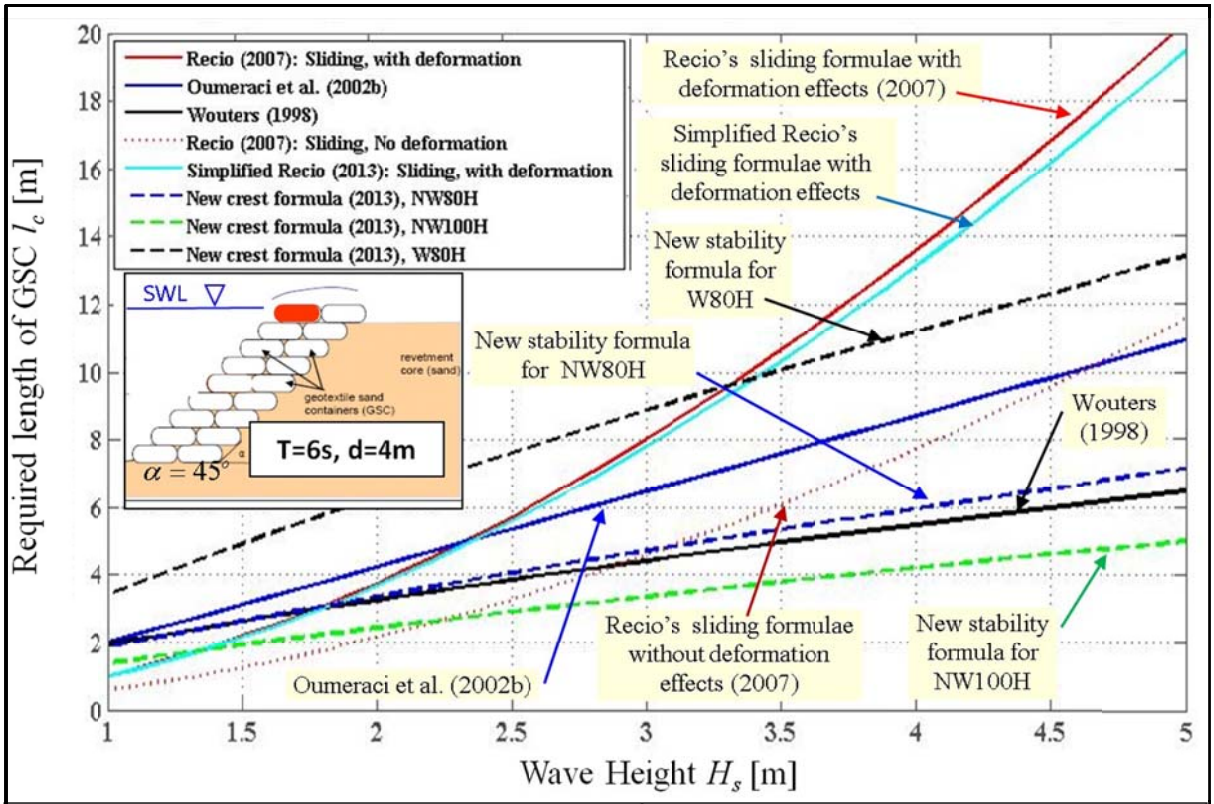

Recio's sliding formulae with deformation effect (2007)

$$l_{c(sl)} \geq u^2 \frac{\left[0.5KS_{CD}C_D + 2.5KS_{CL}C_L\mu\right]}{\left[\mu KS_R\Delta g - KS_{CM}C_M\frac{\partial u}{\partial t}\right]}$$

$C_D = -9\times10^{-5}\,\mathrm{Re} + 23.04$ with $4 \leq C_D \leq 15$

$C_L = 1\times10^{-5}\,\mathrm{Re} - 0.587$ with $0.3 \leq C_L \leq 1.2$

$C_M = 0.30$

$$\mathrm{Re} = \frac{u\cdot D}{\nu} = \frac{u\cdot l_c \sin\alpha}{\nu}$$

$KS_{CD} = 1.4 \quad KS_{CM} = 1.0 \quad KS_{CL} = 0.94 \quad KS_R = 0.70$

Recio's sliding formulae without deformation effect (2007)

$$l_c \geq u^2 \frac{\left[0.5C_D + 2.5C_L\mu\right]}{\left[1.6\mu\Delta g - C_M\frac{\partial u}{\partial t}\right]}$$

$C_D = -9\times10^{-5}\,\mathrm{Re} + 23.04$ with $4 \leq C_D \leq 15$

$C_L = 1\times10^{-5}\,\mathrm{Re} - 0.587$ with $0.3 \leq C_L \leq 1.2$

$C_M = 0.30$

$$\mathrm{Re} = \frac{u\cdot D}{\nu} = \frac{u\cdot l_c \sin\alpha}{\nu}$$

Oumeraci et al. (2002)

$$\frac{H_S}{\left(\rho_E/\rho_W - 1\right)\cdot D} = 0.79 + 0.09\frac{R_c}{H_S}$$

$$D = l_c \sin\alpha$$

New crest formula

$$Ns\sqrt{\xi_o} = A\left(\frac{Rc}{H_{2\%}}\cdot\frac{1}{\xi_o}\right)^2 + B\left(\frac{Rc}{H_{2\%}}\cdot\frac{1}{\xi_o}\right) + C$$

where; $Ns = \dfrac{H}{\left((\rho_{GSC}-\rho_w)-1\right)\cdot l_c \sin\alpha}$

and $\xi_o = \dfrac{\tan\alpha}{\sqrt{H_{2\%}/L_0}}$ for a Rayleigh distribution the values $H_{2\%} = 1.4\,H_s$ [m]

Simplified Recio's sliding formulae with deformation effect (2007)

$$l_{c(sl)} \geq u^2 \frac{\left[0.5KS_{CD}C_D + 2.5KS_{CL}C_L\mu\right]}{\left[\mu KS_R\Delta g\right]}$$

$C_D = 4 \quad C_M = 0.30 \quad C_M = 1.2$

$KS_{CD} = 1.4 \quad KS_{CM} = 1.0 \quad KS_{CL} = 0.94 \quad KS_R = 0.70$

Wouters (1998)

$$\frac{H_S}{\left(\frac{\rho_E}{\rho_W} - 1\right)\cdot D} = \frac{2.5}{\sqrt{\xi_0}} \qquad \xi_o = \frac{\tan\alpha}{\sqrt{H_s/L_o}}$$

$$D = l_c \sin\alpha$$

Empirical parameters	A	B	C
nonwoven 80% filled and horizontally placed GSCs NW80H	20	3.0	2.4
nonwoven 100% filled and horizontally placed GSCs NW100H	30	0.5	3.6
woven 80% filled and horizontally placed GSCs W80H	20	0.6	1.3

Figure 5-19: Comparison between new hydraulic stability formula and other available formulae for the design of crest GSCs of a low-crested GSC structure with *Rc* = 0 m

5.6 Summary and Concluding Remarks

A main objective of this study is to find out how recent and past experimental investigations and numerical simulations are incorporated for the development of new simplified hydraulic stability formulae based on . Chapter 2 critically reviews existing stability formulae and nomograms with a summary of the results are provided in Table 2 8. Compared to sufficiently high surface-piercing structures (i.e. without excessive wave overtopping), submerged and low-crested GSC-structures have critical knowledge gaps related to the hydraulic stability. Therefore, systematic investigations were carried out, primarily to recognize the parameters important for the hydraulic stability. The main results of Chapter 5 can be recapitulates as:

- As a part of chapter 5, a thorough and a systematic analysis of the process-based stability formulae of Recio (2007) was performed. Based on the outcomes of this analyses, a simplified versions of the formulae were proposed (Figure 5 7).
- Using the new experimental and numerical results from regular wave tests, new hydraulic stability nomograms were developed for horizontally placed, nonwoven 80% filled GSCs, nonwoven 100% filled GSCs and woven 80% filled GSCs. The stability curve for 80% filled nonwoven GSCs was later extended to irregular waves combining the results of the current and past experimental studies with wave spectra. It was then shown that the stability curves developed using regular wave test data can also be applied for irregular waves by substituting the mean wave height H_m of regular waves by characteristic wave height $H_{2\%}$. This stability curve was validated for low-crested structure using the experimental data from small and large scale tests from Oumeraci et al. (2002a, 2002b)
- Finally a new hydraulic stability formula was proposed for submerged/low-crest GSC-structures. Not only in submerged structures, but also in most of the low-crested structures, the critical element are the GSCs at the crest. Therefore, this formula applies only for the incipient motion of crest GSCs (Figure 6 1 and Figure 6 2).
- For sufficiently high structures such as none overtopping revetments, where stability of slope GSCs close to the free water surface is critical, Hudson like stability formula from Oumeraci et al. (2002b) can be applied as the formula is developed and validated with both small and large scale experimental data.

It is important to stress that the stability curves are developed solely based on small scale experiments (average length of a model GSC ≈ 0.14 m) and two types of geotextiles (woven geotextiles with interface friction angle = 13.33° and nonwoven geotextile with interface friction angle = 22.64°). Due to the lack of large scale data or field data, it is still not possible to fully validate (for submerged GSC-structures) the curves for different scales though the stability curves are presented in a non-dimensional form. Some of the previous experimental investigations (e.g. Oumeraci et al. 2002a, 2002b) have shown scale effects when compare small scale test results with large scale results. Therefore, these curves should be used cautiously.

6 Summary, Conclusions, Recommendations and Outlook

More versatile materials and innovative solutions are required for the design of new, cost effective shore protection structures. Geotextile Sand Containers (GSC) is a low cost, soft and reversible solution for the above problem with a history of more than 50 years in hydraulic and marine applications. In the earlier applications, coastal GSC-structures were considered as temporary or short term solutions. The main concerns were the durability issues such UV-resistance, biological effects, abrasion and damage resistance, etc. However the extensive research works conducted during the recent past and their findings remarkably reduced the weaknesses of coastal structures made of GSCs.

Nevertheless, GSC is still an emerging technology and no proper guidelines are available for the design of GSC-structures on a sound scientific base. Due to the flexibility and the lower specific gravity of GSCs as compared to rock or concrete armour units, GSCs behave differently and therefore, the established design formulae for rock or concrete units are not applicable. A few formulae were developed for the prediction of the hydraulic stability of GSC-structures and among those, the formulae developed by Recio (2007) are the only process-based hydraulic stability formulae for GSCs. However, these formulae still need to be simplified and refined in order to make them more user friendly for practicing engineers.

This PhD study attempts to evaluate the effect of the most important engineering properties on the hydraulic stability of GSC-structures and to develop new formulae for the hydraulic stability of crest GSCs for submerged/low-crested GSC-structures. The most important engineering properties of GSCs are the mechanical properties of the geotextile material, the sand fill ratio, the type of the fill material and the interface friction. However, the knowledge about the influence of the sand fill ratio and the interface friction of GSCs on the hydraulic stability of GSC-structure is still very poor. None of the exiting formulae for the hydraulic stability of GSC-structures accounts for the sand fill ratio. Moreover, a clear definition for a sand fill ratio is still lacking. Therefore, a proper definition for the sand fill ratio based on a systematic investigation on the relationships between the sand fill ratio and the hydraulic stability of GSC-structures is crucial, to achieve a better understanding of the hydraulic functioning GSC-structures under the wave attack. Furthermore, Recio (2007) identified the interface friction between GSCs as an important parameter that considerably affects the hydraulic stability of GSC-Structures. Moreover, a friction factor between containers (μ) is already included in the formulae of Recio. Despite of the interface friction already incorporated in the formulae of Recio (2007), the effect of interface friction properties is still not fully explained or experimentally verified.

Therefore, the main contributions of this thesis are: (i) improvement of the understanding of the influence of key engineering properties of GSCs; the sand fill ratio and the interface friction between GSCs on the hydraulic stability of coastal GSC-structures and (ii) development of stability formula that account for these two engineering properties.

To achieve an improved understanding on the important engineering properties of GSCs that affect the hydraulic stability of GSC-structures, experimental and numerical studies were performed focusing on the following issues:

(i) factors influencing the sand fill ratio of GSCs, (ii) Development of a physically-based and practically feasible definition of the sand fill ratio of GSC (iii) effect of the sand fill ratio on the hydraulic stability of structures made of GSCs (iv) factors influencing the friction between GSCs (v) influence of the properties of geotextile materials and the sand fill ratio on the friction between GSCs and ultimately on the hydraulic stability of GSCs (vi) methodology to properly represent friction between GSCs in the numerical modelling of GSC-structures (vii) Refining the Recio's (2007) formulae, mainly considering the stability of submerged GSC-structures (viii) Development of empirical relationships for the hydraulic stability of GSCs based on further experimental and numerical investigations

First, the present knowledge related to the engineering properties of GSCs and their effects on the stability of GSC-structures, and existing hydraulic stability formulae for GSC-structures were critically reviewed. Second, four series of especially designed laboratory experiments, which allowed to have an insight into the influence of the above mentioned properties on the stability of GSC-structures and also to obtain the required parameters for the numerical modelling of their stability, were performed. Experimental investigations consisted of two types of laboratory experiments (drop tests and pullout tests), small scale wave flume tests (hydraulic stability tests) and hydraulic flume tests (permeability tests). Third, numerical modelling of GSC-structures was conducted using a weakly coupled RANS-VOF model and FEM-DEM models (COBRAS-UC/UDEC). This was the best feasible option to numerically model the hydraulic stability of GSC-structures in the framework of this PhD. Finally, combining both the experimental and numerical results, new stability curves and a simple formula was developed for the hydraulic stability of crest GSCs and validated with the previous experimental data from small and large scale hydraulic stability tests. The newly developed stability curves and simple stability formulae are expected to foster the applications of GSC structures for coastal protection.

This chapter summarises the main results and conclusions drawn from this study and provides recommendations with respect to the practical application of the proposed hydraulic stability formula, including their limitations. Finally, the import tasks for future research are proposed.

6.1 Summary of Main Results and Conclusions

6.1.1 Sand Fill Ratio: New Definition

Based on the results of an extensive analysis of the current knowledge, several model GSCs were constructed with varying geometries, geotextile materials and sand fill ratios. The main objective was to determine practical sand fill ratios and to develop a method to predict final external dimensions of a GSC, once the sand fill ratio and the dimensions of empty flat bag is known. The main outcomes of this exercise can be summarised as follows:

(i) After considering various parameters and processes that affect the sand fill ratio, a new definition for the sand fill ratio of GSCs was proposed. The new definition can be described as the initial sand fill ratio, which can be used as the representative parameter to describe GSCs. The initial sand fill ratio of a GSC is defined using the fully inflated volume of the empty bags described by (eq. 3.1) of Robin (2004) and the dry bulk density of the sand fill.
(ii) Two types of nomograms (for nonwoven and woven geotextile) were developed to predict the final external dimensions of GSC, once the sand fill ratio and the dimensions of empty flat bag is known (see Figure 3 3). .
(iii) The sand fill ratio is expected to change due to both short and long term processes. Most relevant processes that contribute to alter the sand fill ratio were identified and the evolution of the sand fill ratio is presented as a flow chart (Figure 3 4).
(iv) A procedure was developed to determine the final sand fill ratio of GSC under field conditions (see Figure 3 15)

6.1.2 Drop Tests: New Insights in the Sinking and Deformation Behaviour of GSCs

A new Underwater Drop Testing Facility (UDTF) was developed and constructed to systematically investigate the sinking behaviour of GSCs. Some of the main design concerns such as sink velocities, spreading of GSCs when released from the water surface, deformations resulted from filling, handling and due to instantaneous loads when hitting the bottom of the model were studied and the most important results can be summarised as follows:

(i) In still water, the sink trajectories and the deviations from the initial dropping axis mainly depend on the initial orientation of the GSC. When a GSC dropped with its largest cross section parallel to the water surface, it deviates only 0.2 ~ 1.2 GSC lengths after it sinks 10 times its length, while other initial orientations results in much larger deviations, which could even reach 5 GSC lengths.
(ii) The results from the drop tests with fully dry GSCs (0% saturation) showed about 25% less sink velocities than those with fully saturated GSC (100% saturation).
(iii) A significant decrease (20~50%) in sink velocity was observed near the bottom (when the distance between the GSC and the bottom is less than ca. 0.5 GSC length) and just before hitting the seabed
(iv) Drag coefficients for GSCs, when they released with their largest cross section parallel to the water surface, are comparable to those of smooth cylinders (C_D = 1.0 ~ 1.2) for the tested Reynolds numbers $Re = 2.0\times10^4 \sim 1.5\times10^5$ with Re defined using the sink velocity, u and the length scale of GSC in the sinking direction, D. However, when a GSC released with its smallest cross section parallel to the water surface, it shows drag coefficients between 0.6 and 1.2, which are higher than that of a smooth cylinder for tested Reynolds numbers $Re = 4.0\times10^5 \sim 1.5\times10^6$.
(v) The results on the deformation of 80%~110% filled GSCs show that 90% filled containers are less sensitive to deformation due to filling process and due to the impact on the bottom, when dropped in deeper water. According to the small scale drop test results, GSCs can expand during the filling process (due to the elongation of the geotex-

tile material) by 3% ~ 12%. Furthermore, dropping in deeper water could further elongate the geotextile skin of GSCs (after 15 drop tests, the small scale GSCs showed further 3% ~ 18% expansions).

6.1.3 Pullout Tests: New Insights on the Effects of Sand Fill Ratio and Friction

The pullout tests were conducted to quantify the effect of the sand fill ratio, the type of geotextile material, seaward slope of GSC-structures (overlapping length), stacking pattern, test conditions (dry or submerged), etc. on the underwater pullout forces. The influence of these parameters on pullout forces of crest and slope GSCs were then analysed in detail. Some concluding remarks drawn from the results study may be summarized as follows:

(i) From the five different tested sand fill ratios (80%, 90%, 100%, 110%, and 120%), the results of the pullout tests have shown that the pullout forces increase with increasing sand fill ratios (or increment of the weight of GSC). In this comparison only the amount of sand filled into the GSCs was varied and the size of the empty bag was unchanged (same amount of geotextile). Hence, the weight of each GSC increases as the sand fill ratio increases.

(ii) In order to determine the optimum sand fill ratio, a non-dimensional parameter was introduced as a relative pullout force (Ratio between pullout force and the weight of the GSCs). Optimal sand fill ratios in terms of the resistance against pullout of the GSCs were found to be between 90% ~ 100%. The slope containers have in average at least 130% higher resistance than the crest containers.

(iii) All the GSCs showed 30% ~ 50% higher pullout resistances than what was estimated based on the interface friction properties of geotextile materials. The pullout resistance is roughly proportional to the friction coefficients for geotextile materials obtained from direct shear tests.

(iv) GSCs showed ca. 10~15% higher pullout forces, when GSCs are submerged. There is no apparent reduction in interface friction properties. Therefore, this slight difference might be due to the settlement of GSCs, once they are wet. Consequently, it is not required to alter the joint properties in numerical modelling, because, GSCs in a low-crested/submerged structure are wet at least once during each test and all the GSCs (emerged and submerged) will show nearly a similar behaviour.

6.1.4 Hydraulic Stability Tests: New Insights on the Effect of Sand Fill Ratio, Friction and GSC Placement

The sand fill ratio, the type of geotextile material and the interface friction between GSCs strongly affect different processes governing the hydraulic stability of GSC-structures. These tests therefore represent the first attempt systematically quantify the effects of these engineering properties and the inclined placement of GSCs on the hydraulic stability. The hydraulic stability tests were conducted on low-crested GSC-structures with both positive (emerged) and negative (submerged) crest freeboards. The most important outcomes of the experimental studies and their implications for the engineering practice can be summarised as follows:

(i) GSCs show different failure mechanisms for different submergence depths. Moreover, depending on the dominant failure mechanism for a particular GSC-structure and for a particular crest freeboard, the relative significance of the engineering properties of GSCs also varies.

(ii) As expected, for most of the low-crested structures, the crest GSCs represent the critical elements in terms of the hydraulic stability. Therefore, when designing low-crested and submerged GSC structures, it is important to consider more carefully the most relevant failure mechanisms of crest GSCs, including the effect of the most relevant engineering properties.

(iii) The hydraulic stability of the crest GSCs depends on both relative crest freeboard Rc/H_m and surf similarity parameter ξ_0.

(iv) For the tested conditions with a zero freeboard, GSCs made of woven geotextile (with an approximately 50% lower friction coefficient than nonwoven geotextile) resulted in 40% lower stability numbers, when the incipient motions of crest GSCs are considered.

(v) Though most of the existing studies and recommendations for the construction of GSC-structures (e.g. PIANC, 2011) suggest a sand fill ratio of 80%, GSC with 100% filled GSC show a 36 % higher stability number for surf similarly parameters around 5.

(vi) Apart from changing the engineering properties of GSC, the hydraulic stability can be increased by changing the inclination angle of GSCs in a GSC-structure. GSCs inclined by -15° towards the shore resulted in approximately 30% higher stability number compared to horizontally placed GSCs, when the wave conditions required for incipient motion of the GSCs are considered.

(vii) In addition to the improvements of the hydraulic stability (in terms of incipient damage) which are achieved by a higher friction angle between GSCs, higher sand fill ratios and inclined placement of GSCs, these parameters also contribute significantly to retard the damage development of GSC-structures over the entire storm duration. Therefore, not only the conditions required to trigger damage to a GSC-structure, but also the development of the damage over the entire storm duration and the different damage levels that might result, are equally important for a comprehensive quantitative assessment of the effect of the different factors considered in this study.

6.1.5 Permeability Tests: New Insights on the Effect of Sand Fill Ratio, Type of Geotextile and GSC Placement

These tests represent the first attempt to systematically quantify the effects of the sand fill ratio, the type of geotextile material and the inclined placement of GSCs on the hydraulic permeability of GSC-structures. The permeability tests were conducted on low-crested GSC-structures with a zero crest freeboard. The permeably coefficient was determined for each model configurations and results are given in Table 3 7. Main outcomes may be summarised as follows:

(i) In spite of the inhomogeneities in GSC-structures (and fill, geotextile and gaps between GSCs), it is still possible to describe the permeability with Darcy's law due the relatively low velocities of the porous flow

(ii) Nonwoven 100% filled GSCs have a ca. 3~4 times higher permeability than nonwoven 80% filled GSCs. This might be mainly due to the larger gaps between the 100% filled GSCs compared to those of the 80% filled GSCs.

(iii) 80% filled woven GSCs have ca. 2.5 times higher permeability coefficients compared to 80% filled nonwoven GSCs. Nonwoven GSCs are relatively more flexible and compact when they are in water. In contrast, woven GSCs are less flexible and leave larger gaps between GSCs. Moreover, due the different textures of the woven (smooth) and the nonwoven (rough) geotextiles, the resistance of the flow through the gaps might differ, thus resulting in low permeability coefficients for 80% filled nonwoven GSCs.

(iv) Inclined placement of nonwoven 80% GSCs reduces the permeability of the structure by 50%.

6.1.6 Numerical Simulation of Pullout Tests: Identification of Proper Constitutive Models for Friction Between GSCs

The hydraulic stability of GSC-structures is highly sensitive to the friction properties of GSCs. However, there were no detailed investigations on the effect of friction properties of GSCs. Moreover, the correct representation of friction between elements is a key factor for a reliable numerical modelling. Therefore, pullout tests were simulated with the computational dynamic 2D model UDEC 5 and the main outcomes are:

(i) A parameterised simple rectangular shape was proposed for the simulation of GSCs in the UDEC model by taking into account the external dimension, sand fill ratio, type geotextile material, overlapping lengths, GSC mass, etc.

(ii) Different joint models available in UDEC 5 were tested by performing several numerical pullout tests. Then the numerical results were compared with experimental data and the most appropriate constitutive models for adequate representation of both woven and nonwoven GSCs were determined. Based on the experimental and the numerical pullout tests, interface friction between nonwoven GSCs can be better represented using the Coulomb slip model with residual strength, whereas the standard Mohr-Coulomb slip model is sufficient for the representation of the interface between woven GSCs.

6.1.7 Numerical Simulations of Hydraulic Stability of GSC-Structures: Improvement and Validation of a Partially Coupled CFD-CSD Model

(i) Numerical simulations were performed mainly to obtain additional data to fill the gaps in the laboratory data obtained from the hydraulic stability tests. During the process, some important improvements were proposed to the exiting weakly coupled CFD-CSD model system “COBRAS-UC/UDEC”, including a systematic validation of the system component and the overall weakly coupled model system based on the experimental results.

(ii) COBRAS and UDEC 4 versions by Recio (2007) were replaced with recently released COBRAS-UC and UDEC 5 models. Apart from that, new modifications were intro-

duced to simulate the simplified GSC model in COBRAS-UC/UDEC modelling system such as parameterised GSCs with more accurately defined physical properties.

(iii) Forces acting on each node at the perimeter of the GSCs were calculated and applied separately, which allows more realistic simulations (both sliding and rotation can be simulated).

(iv) Several hydraulic stability tests were successfully reproduced with the COBRAS-UC/UDEC model (validation).

(v) Using the validated model system a parameter study was then carried out in order to extend the range of the conditions tested in the laboratory. The main objective of these simulations to obtain further data for the development of hydraulic stability curves for three test series, NW80H, NW100H and W80H (See Figure 6-1 and Figure 6-2) .

6.1.8 New stability formulae: Applicability and Limitations

One of the main objectives of this study is to develop new simplified hydraulic stability formulae based on recent and past experimental investigations and numerical simulations. In Chapter 2, existing stability formulae and nomograms were critically reviewed/analysed with a summary of the results in Table 2-8. Most of the knowledge gaps were found to be rather related to the hydraulic stability of submerged and low-crest GSC-structures as compared to sufficiently high surface-piercing structures (i.e. without excessive wave overtopping). Therefore, systematic investigations were conducted, mainly to identify the parameters relevant for the hydraulic stability. The main results can be summarizes as:

(i) A more detailed analysis of the process based stability formulae of Recio (2007) and a simplified versions of the formulae were developed (Figure 5-7).

(ii) Then new hydraulic stability nomograms were developed for horizontally placed, nonwoven 80% filled GSCs, nonwoven 100% filled GSCs and woven 80% filled GSCs by combining experimental results from regular wave tests and from numerical simulations.

(iii) The stability curve for 80% filled nonwoven GSCs was extended to irregular waves using the results of the current and past experimental studies with wave spectra. It was then shown that the stability curves developed using regular wave test data can also be applied for irregular waves by substituting the mean wave height H_m of regular waves by characteristic wave height $H_{2\%}$. This new stability curve was validated for low-crested structure using the experimental data from small and large scale tests from Oumeraci et al. (2002a, 2002b)

(iv) Finally a new formula was proposed for the hydraulic stability of submerged/low-crest GSC-structures. In most of those structure, the critical element are the GSCs at the crest. Therefore, this formula applies only for the incipient motion of crest GSCs (Figure 6-1 and Figure 6-2).

(v) For sufficiently high structures, Hudson like stability formula from Oumeraci et al. (2002b) can be applied as the formula is developed and validated with both small and large scale experimental data.

$$Ns\sqrt{\xi_o} = A\left(\frac{Rc}{H}\cdot\frac{1}{\xi_o}\right)^2 + B\left(\frac{Rc}{H}\cdot\frac{1}{\xi_o}\right) + C$$

where; $Ns = \dfrac{H}{((\rho_{GSC}/\rho_w)-1)\cdot l_c \sin\alpha}$ and $\xi_o = \dfrac{\tan\alpha}{\sqrt{H/L_0}}$

Empirical parameters	A	B	C
nonwoven 80% filled and horizontally placed GSCs	20	3.0	2.4
nonwoven 100% filled and horizontally placed GSCs	30	0.5	3.6
woven 80% filled and horizontally placed GSCs	20	0.6	1.3

Where;
A, B, and C = empirical parameters depending on the type of geotextile material and the sand fill ratios [-]
$H = H_m$ for regular wave tests or $H_{2\%}$ for irregular wave tests [m]
H_m = incident mean wave height from regular wave tests measured at intermediate water depth (at the beginning of the foreshore slope) [m]
$H_{2\%}$ = mean of the highest 2% of the incident waves in a time series (mean of the highest 20 incident waves from the wave reflection analysis of 1000 waves and for a Rayleigh distribution the values $H_{2\%} = 1.4\ H_s$)[m]

Rc = crest free board [m]
L_0 = wave length at deep water
Ns = stability number [-]
ρ_w = density of water [kg/m³]
ρ_{GSC} = density of GSCs [kg/m³]
l_c = length of a GSC [m],
α = slope angle of the structure [°],
$L_0 = g\,T^2/(2\pi)$ = deep water wave length calculated using the mean wave period [m]

Figure 6-1: New hydraulic stability formula for crest GSCs of low-crested/submerged GSC-structures

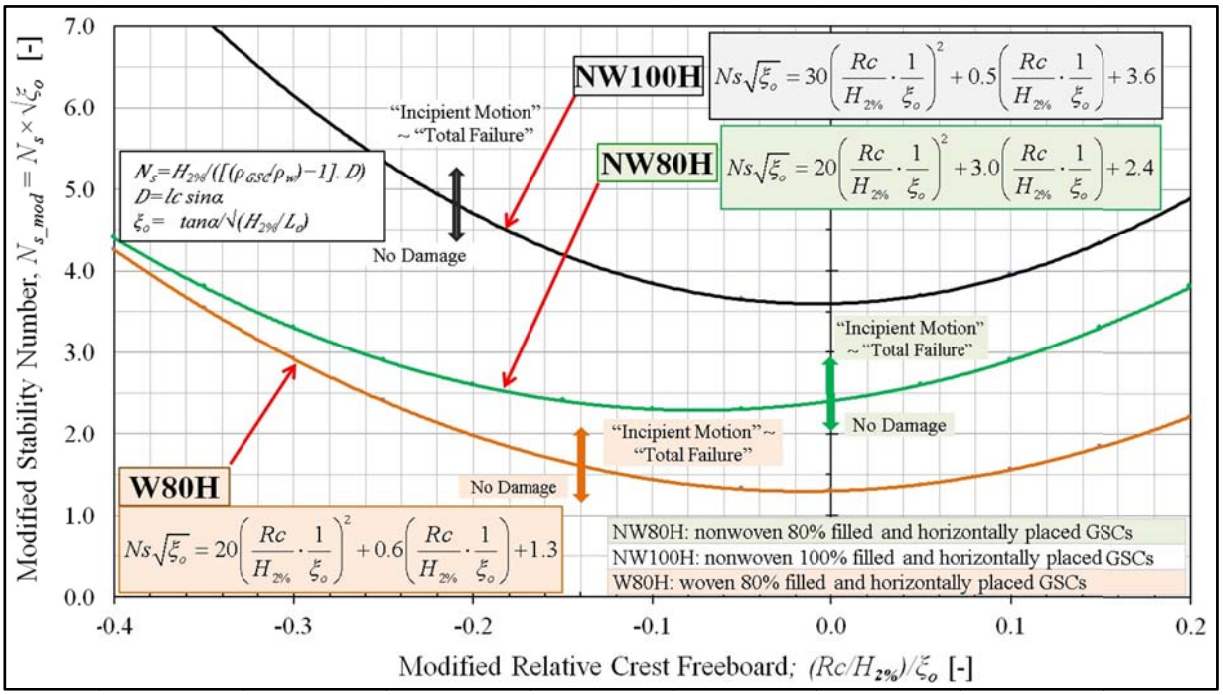

Figure 6-2: Incipient motion curves derived from regular wave tests

6.1.9 Applicability and Limitations of the Proposed Stability Formula

It is important to stress that the new stability formula and the related curves in Figure 6-1and Figure 6-2 were developed solely based on small scale experiments (average length of a mod-

el GSC ≈ 0.14 m) and two types of geotextiles (woven geotextiles with interface friction angle = 13.33^0 and nonwoven geotextile with interface friction angle = 22.64^0). Due to the lack of large scale data or field data for submerged GSC-structures, it is still not possible to fully validate the stability curves for different scales though the stability curves are presented in a non-dimensional form.

Also, if the geometrical proportions of GSCs substantially differ from those considered in this study, (i.e. length : width : height = 10 : 5 : 1), the stability curves might not be directly applicable. Therefore, it is advisable to use similar geometrical proportions as this research study because, they represent most commonly used (see Recio 2007, Oumeraci et al. 2002a, Oumeraci et al. 2002b, Oumeraci et al. 2007, Oumeraci et al. 2012, Wilms et al. 2012) length/width ratio of empty bag (length : width = 1.8 : 1.0).

6.2 Recommendations for the Engineering Practice and Future Research

Based on the knowledge gained during this research study, some recommendations were drawn for the engineering practice and for future research as follows:

(i) The COBRAS-UC/UDEC results show a relatively good agreement with the experimental data. Hence, this CFD-CSD model system has an encouraging potential for practical applications. However, this system has serious limitations because of the 2D simplification of a truly 3D-problem. Therefore, one of the future research tasks is to extend the COBRAS-UC/UDEC to a coupled 3D-model system. Meanwhile, the 2D-modelling system should be applied thoughtfully.

(ii) Before starting any detailed investigations on hydraulic stability of GSCs, it is necessarily required to determine the actual dimensions of the prototype GSC to be used. Two nomograms (for nonwoven and woven geotextile, Figure 3-3) developed during this study can be used for the prediction of the final external dimensions of GSC, once the sand fill ratio and the dimensions of empty flat bag is known (Figure 3-3). However, the exact final dimensions of GSCs can only be found by constructing prototype containers and by performing measurements. For this purpose, a comprehensive methodology to determine the final sand fill ratio of a GSC is developed by considering all relevant processes associated with the construction of GSC structures, which can be applied in practice (Figure 3 15). This procedure will guide through field investigation is to quantify the deformations of GSC during different phases of construction.

(iii) For conventional rubble mound structures, studies are available for the prediction of the damage for a series of storms throughout the lifetime of the structure. This allows engineers to balance initial costs with expected maintenance costs in order to reduce the overall costs of the structure and also to possibly reduce unexpected maintenance costs (Melby, 2005). Since GSC structures are highly sensitive to the changes in wave parameters, it is essential to know the damage development in order to achieve optimal GSC-structures by selecting the proper material for GSCs and the most appropriate inclination angle of GSCs. This series of experiments has highlighted the effects of engineering properties and inclined placement of GSCs on both temporal and spatial

damage development. In addition, the awareness of dominant failure modes will help to create site specific GSC solutions by altering the most relevant engineering properties of GSCs.

(iv) For prototype GSC-structure a comprehensive monitoring programme is essential to ensure an optimum performance over the entire design life time and to obtain data for the validation of the hydraulic stability formulae. A separate budget is required for the collection of "baseline data set" and for the monitoring programme to ensure that the monitoring will be performed regularly and properly by competent personnel. Results of such a monitoring programme can also so used for the validation of the hydraulic stability formulae, which are based on small scale experimental results.

This research study has significantly enhanced the understanding of the engineering properties of GSCs and their influence on the hydraulic stability of submerged/low-crested GSC-structures. However, substantial research and development still needs to be performed.

(i) As the sand fill ratio, the interface friction between GSCs, and the inclination angle of GSCs considerably affect the hydraulic stability and the long term performance of GSC-structures, the future research and development should address the definition of an optimal sand fill ratio by accounting for the elongation properties of the geotextile and by balancing the advantages and drawbacks of high and moderate sand fill ratios. Ultimately, future standards and guidelines should explicitly consider the engineering parameters of GSCs.

(ii) The ratio between the weight of GSCs and the maximum tensile strengths of the bag material (geotextile) could be a relevant parameter to determine the degree of deformation during the construction and the installation process of GSCs. However, this can only be confirmed by prototype tests, because the tensile strength of the geotextile material cannot be properly scale down.

(iii) COBRAS-UC/UDEC modelling system has serious limitations because of the 2D simplification of a truly 3D-problem. Therefore, one of the future research tasks is to extend the COBRAS-UC/UDEC to a coupled 3D-model system. A fully coupled model can then be used for the performance of more detailed and more systematic parameter studies to analyse the effect of further friction angles between GSCs, seaward slope angle of the structure, further sand fill ratio of GSCs on the hydraulic stability. A similar study will generate knowledge to develop a single hydraulic stability formula containing the aforementioned key engineering properties of GSCs. Moreover, properly calibrated 3D-mode systems can be used for the simulation of large scale models with prototype dimensions. Thereby, the scaling problems can be answered. Furthermore, additional numerical simulations can also be performed to verify the formulae developed for small scale.

References

Abelev, A.V., Valent, P.J, Plant, N.G., and Holland, K.T. (2003), "Evaluation and Quantification of Randomness in Free-fall Trajectories of Instrumented Cylinders." Proceedings, Oceans 2003 marine technology and ocean science conference, San Diego, CA, September 22-26 (DVD-ROM).

Ante Munjiza, A. (2004), The Combined Finite-Discrete Element Method, John Wiley & Sons Ltd, England, ISBN 0-470-84199-0

ASR (2005a), Artificial Surfing Reef Construction -Technical Document 3 ASR Construction Document 3 – Reef Construction Summary

ASR (2005b), Artificial surfing reef construction – Technical Document 4, ASR Construction Documents-Geotextile Materials

BAW (1993), Merkblatt Anwendung von Geotextilen Filtern an WasserstraXen. Bundesanstalt für Wasserbau, Karlsruhe, Germany.

Bear, J. (2000), Modelling Groundwater Flow and Contaminant Transport, Course demo website (http://www.cmdlet.com/demos/mgfc-course/mgfcclas.html), Faculty of Civil Engineering, Technion-Israel Institute of Technology, Haifa, Israel

Bergado, D.T., Manivannan, R. and Balasubramaniam, A.S. (1996), Filtration Criteria For Prefabricated Vertical Drain Geotextile Filter Jackets In Soft Bangkok Clay, eosynthetics International S 1996, Vol. 3, No. 1

Bezuijen A, Schrijver R.R., Klein Breteler M., Berendsen E., Pilarczyk K.W. (2002b) Field tests on GSCs. Proceeding of 7th Int. Conference on Geosynthetics, Nice, France

Bezuijen A., Adel H. den, Groot M.B. de and Pilarczyk K.W. (2000), Research on GSCs and its application in practice, Proceedings of 27th International Conference on Coastal Engineering (ICCE) Conference, Sydney, Ausralia

Bezuijen A., de Groot M. and Klein Breteler M. (2001), Geotextile tubes - analyse resultaten Brutusbakproeven, Delftcluster , The Netherlands (in Dutch)

Bezuijen A., de Groot M.B., Klein Breteler M., Berendsen E. (2004), Placing accuracy and stability of GSCs, Proc. EuroGeo 3, Munich, Germany

Bezuijen A., Oung O., Klein Breteler M., Berendsen E., Pilarczyk K.W. (2002a). Model tests on GSCs, placing accuracy and geotechnical aspects. Proc. 7th Int. Conf. on Geosynthetics, Nice, France

Bezuijen, A. and Vastenburg, E. (2008), Geosystems, Possibilities And Limitations For Applications, Proceeding of EuroGeo4; Fourth European Geosynthetics Conference, Edinburgh, Scotland, United Kingdom

Blacka, M. J., Carley, J.T., Cox, R.J., Hornsey, W.P. and Restall, S.J. (2007), Field Measurements of Full Sized Geocontainers, Proceedings of Australasian Coasts and Ports Conference 2007, Melbourne, Australia

Blacka, M.J., Carley, J.T. and Cox, R.J. (2008), Field Measurement of ELCOMAX® ELCOROCK® Geocontainers at Clifton Springs Boat Harbour, Victoria

Bleck M. and Werth K. (2012), Geotextile sand-filled containers as structures against erosion of sandy coasts - a comparison to rock material relating design, functionality, eco-effectiveness and costs, 12th Baltic Sea Geotechnical Conference, Rostock, Germany

Bourzaev, A. (2003), Hydraulische Prozesse an und in einem Deckwerk aus Geotextilen Sandcontainern, Diplom-Arbeit (Master Student Project Report) LWI, TU Braunschweig, Germany (in German).

Bouyze, J.G. and Schram, A.R. (1990), Stabiliteit van Grondkribben en Onderwatergolbrekers Opgebouwd uit Zandworsten, TU-Delft, Studentarbeit (Master Student Project Report) (in Dutch).

Breteler, M.K. and Pilarczyk, K.W. (1998), Alternative revetments, Pilarczyk, K. (editor), Dikes and Revetments, A.A. Balkema (publisher)

Bukreev, V. I. and Gusev, A. V. (1996), Motion of a sphere in a fluid due to gravity, Journal of Applied Mechanics and Technical Physics, Vol. 37, No. 4, pp 494–501

Burger, G. (1995), Stability of low-crested breakwaters. Final Proceedings, EU research project Rubble mound breakwater failure modes, MAST 2 contract MAS2-CT92-0042. Also published in Delft Hydraulics report H1878/H2415.

Cappietti, L. (2011), Converting Emergent Breakwaters Into Submerged Breakwaters, Journal of Coastal Research, pp 479 – 483

Cazzuffi, D., Mazzucato, A., Moraci, N. and Tondello, M. (1999), A New Test Apparatus for fhe Study of Geotextiles Behaviour As Filters in Unsteady Flow Conditions. Geotextiles and Geomembranes Journal, Vol. 17, Elsevier, pp 313-329.

CFGG (1986), AFNOR G38017, Association Franc¸aise de Normalisation (French Committee on Geotextiles), La Plaine Saint-Denis, France (in French).

Chen, R.H., Ho, C.C. and Hsu, C.Y. (2008), The Effect of Fine Soil Content on The Filtration Characteristics of Geotextile Under Cyclic Flows. Geosynthetics International, 15, No. 2, pp 95–106. [doi: 10.1680/gein.2008.15.2.95]

Chew, S.H., Tian, H., Tan, S.A. and Karunaratne, G.P. (2003), Erosion stability of punctured geotextile filters subjected to cyclic wave loadings—a laboratory study, Geotextiles and Geomembranes Journal, Vol. 21, pp 221–252.

Christopher, B.R. & Holtz, R.D. (1985), Geotextile Engineering Manual, US Federal Highway Administration, Report FHWA-TS-86/203, National Highway Institute, Washington, DC, USA.

Chu, P.C., Gilles, A.F. and Fan, C.W. (2004), Experiment of falling cylinder through the water column, Experimental Thermal and Fluid Scinece 29, pp 555-568 Crowe C.T., Roberson J.A. and Elger D.F.(2001), Engineering Fluid Mechanics, seventh ed., John Wiley & Sons Inc, New York, p. 714.

Chu, P.C., Gilles, A.F., Fan, C.W., Lan, J. and Fleischer, P. (2002), Hydrodynamics of falling cylinder in water column, Advances in Fluid Mechanics, 4, 163-181.

Coghlan, I.R., Carley, J.T., Cox R.J., Blacka,chu M.J., Mariani, A., Restall, S.J., Hornsey, W.P., and Sheldrick, S.M. (2009), Two-Dimensional Physical Modelling of Sand Filled Geocontainers for Coastal Protection, Proceedings of Australasian Coasts and Ports Conference 2009, Wellington New Zealand

Corbella, S. and Stretch, D.D. (2012), Geotextile sand filled containers as coastal defence: South African experience, Geotextiles and Geomembranes Journal, Vol. 17, Elsevier, pp120-130

Cundall, P.A. and Hart, R.D. (1989) Numerical of discontinua, In Golden, Colo

CUR (2006), CUR 217: Ontwerpen met Geotextiele Zandelementen, Stichting CUR, Gouda

Dael N. (2009) SPAN 1.3 (SPatial ANnotation) MATLAB code and Instructions for SPAN 1.3, downloaded from File Exchange, MATLAB central, Website accessed on Jan 2010, [http://www.mathworks.com/matlabcentral/fileexchange/authors/67813]

das Neves, L., Lopes, M.L., Veloso-Gomes, F. Taveira-Pinto, F., Iglesias, G. and Garcia, S. (2008), Sand Filled Containers In Dune Erosion Control: Experimental Stability Analysis, Proceeding of EuroGeo4; Fourth European Geosynthetics Conference, Edinburgh, Scotland, United Kingdom

Dassanayake, D.T. and Oumeraci, H. (2009a), Experimental and numerical modelling of the hydraulic stability of geotextile sand containers for coastal protection - State of the art report, Internal report (Nr. 1), Leichtweiß-Institute for Hydraulic Engineering and Water Resources, Braunschweig, Germany.

Dassanayake, D.T. and Oumeraci, H. (2009b), Planned Research on the Hydraulic Stability of Geotextile Sand Containers. Proceedings of 7. FZK-Kolloquium "Potentiale für die Maritime Wirtschaft", Hannover, Germany, pp. 45-49.

Dassanayake, D.T. and Oumeraci, H. (2010a), Sinking Behaviour and Deformation of Geotextile-Sand Containers- State of the Art Review, Internal Report (Nr. 6), Leichtweiß Institute for Hydraulic Engineering and Water Resources, Braunschweig, Germany

Dassanayake, D.T. and Oumeraci, H. (2010b), Design and construction aspects of fully submerged geotextile sand container (GSC) structures: sinking behaviour and deformation of GSCs, International Workshop on Geosynthetics and Modern Materials in Coastal Protection and Related Applications, IIT Madras, India, pp. 242-244.

Dassanayake, D.T. and Oumeraci, H. (2010c), Hydraulic Stability of Submerged GSC-Structures-Planned Flume Test- Internal Report (Nr. 08), Leichtweiß Institute for Hydraulic Engineering and Water Resources, Braunschweig, Germany

Dassanayake, D.T. and Oumeraci, H. (2010d), Experimental Study on the Effect of Sand Fill Ratio on Pullout Forces of Geotextile Sand Containers Structures-Model test results- Internal Report (Nr. 09), Leichtweiß Institute for Hydraulic Engineering and Water Resources, Braunschweig, Germany

Dassanayake, D.T. and Oumeraci, H. (2010e), Preliminary drop tests on GSCs: Preliminary laboratory investigations results, Internal Report (Nr. 07), Leichtweiß Institute for Hydraulic Engineering and Water Resources, Braunschweig, Germany

Dassanayake, D. T. and Oumeraci, H. (2010f): Field measurement of prototype geotextile sand containers - draft field investigation report - Internal report (Nr. 10), Leichtweiß-Institut für Wasserbau, Technische Universität Braunschweig

Dassanayake, D.T. and Oumeraci, H. (2011d), Effect of the Engineering Properties of Geotextile Sand Containers on their Hydraulic Stability under Wave Loads, CoastDoc 2011 Graduate Seminar, Braunschweig, Germany.

Dassanayake, D.T. and Oumeraci, H. (2012a), Important engineering properties of geotextile sand containers and their effect on the hydraulic stability of GSC-structures, 8th International Conference on Coastal and Port Engineering in Developing Countries (COPEDEC VIII), Chennai, India, pp 1940-1951.

Dassanayake, D.T. and Oumeraci, H. (2012b), Important Engineering Properties of Geotextile Sand Containers and Their Effect on The Hydraulic Stability of GSC-Structures, Terra et Aqua Journal, Issue 127, International Association of Dredging Companies, The Netherlands, pp 3-11.

Dassanayake, D.T. and Oumeraci, H. (2012c), Engineering properties of geotextile sand containers and their effect on hydraulic stability and damage development of low-crested / submerged structures, The International Journal of Ocean and Climate Systems, Vol. 3, Issue 3, Multi Science Publishing, Essex, UK, pp 135-150.

Dassanayake, D.T. and Oumeraci, H. (2012d), Hydraulic stability of coastal structures made of geotextile sand containers: Effect of engineering properties of GSCs, 33rd International Conference on Coastal Engineering (ICCE) 2012, Santander, Spain, p14

Dassanayake, D.T. and Oumeraci, H. (2012e), Effect of fill ratio and type of geotextile on the hydraulic stability of Geotextile Sand Containers in coastal engineering. Eurogeo 5, 5th European Geosynthetics Congress, Valencia, Spain

Dassanayake, D.T. and Oumeraci, H. (2012f), Numerical modelling of the hydraulic stability of GSCs with COBRAS-UC and UDEC 5, Internal report (Nr. 13), Leichtweiß-Institute for Hydraulic Engineering and Water Resources, Braunschweig, Germany.

Dassanayake, D.T. and Oumeraci, H. (2013a), Experimental and numerical modelling of the hydraulic stability of geotextile sand containers under wave loads, Proceedings of 9. FZK-Kolloquium "Modellierung im Seebau und Küsteningenieurwesen", Hannover, Germany

Dassanayake, D.T. and Oumeraci, H. (2013b), Geotextile sand container structures for shore protection – hydraulic stability formulae and nomograms, 2nd International Workshop on Geosynthetics and Modern Materials in Coastal Protection and Related Applications, IIT Madras, Cheanni, India, pp 68-81.

Dassanayake, D.T. and Oumeraci, H. (2013c), New Hydraulic Stability Formulae for GSC-Structures, Internal report, Leichtweiß-Institute for Hydraulic Engineering and Water Resources, Braunschweig, Germany.

Dassanayake, D.T. and Oumeraci, H., Werth, K. and Heerten, G. (2013), Setting up monitoring plans to assess the performance and the durability of exposed geotextile encapsulated sand elements in coastal engineering applications, 2nd International Workshop on Geosynthetics and Modern Materials in Coastal Protection and Related Applications, IIT Madras, Cheannai, India, pp 115-128.

Dassanayake, D.T., Oumeraci, H. and Streicher, M. (2011a), Sinking behaviour and deformation of geotextile sand containers during installation of scour protection for marine and offshore structures, Proceedings of 8. FZK-Kolloquium "Maritimer Wasserbau und Küsteningenieurwesen", Hannover, Germany, pp. 33-38

Dassanayake, D.T., Oumeraci, H. and Streicher, M. (2011b), Sinking behaviour and deformation of geotextile sand containers – Experimental Investigations and Results, Internal Report (Nr. 11), Leichtweiß Institute for Hydraulic Engineering and Water Resources, Braunschweig, Germany

Dassanayake, D.T., Soysa, A., Munith-Hadi, F. and Oumeraci, H. (2011c), Hydraulic stability of low-crested GSC-structures, Internal report (Nr. 12), Leichtweiß-Institute for Hydraulic Engineering and Water Resources, Braunschweig, Germany.

Davidson, M. A., Bird, P.A.D., Bullock, G.N. and Huntley, D.A. (1996), A new non-dimensional number for the analysis of wave reflection from rubble mound breakwaters, Coastal Eng., 28, 93- 120.

De Groot . M.B., Klein Breteler M. and Bezuijen A. (2003), Results of geotextile tube research (Resultaten geotextile tube onderzoek), Final project report (DC1-321-11), Delftcluster , The Netherlands (in Dutch)

De Groot, M.B., Klein Breteler M. and Berendsen E. (2004), Feasibility of Geocontainers At The Sea, Proceedings Of 29th International Conference on Coastal Engineering (ICCE 2004) Conference, Lisbon, Portugal

Delft Hydraulics (1975), Artificial Island in the Baufort-sea: M 1271 part III, Comparison of stabilty of shore protection with gabions and sand sausages (2-dim); M 1271 part V, stabilty of shore protection with san dsauges on circular insland (3-dim), Delft, The Netherlands

Delft Hydraulics (1994), Stability of Geotubes® and Geocontainers®, Report Prepared for Nicolon b.v., Delft, The Netherlands

Deltrares (2008), Large Scale Physical Model Test on the Stability of Geocontainers, by Van Steeg, P and Klein Breteler, M., Deltares report prepared for Delft cluster

Deltrares (2010), Large Scale Physical Model Test on the Stability of Geotextile Tubes, by Van Steeg and Vastenburg, E.W., Deltares report prepared for Delft cluster

EurOtop (2007), European Overtopping Manual. Eds Pullen, T., Allsop, N.W.H., Bruce, T., Kortenhaus, A., Schüttrumpf, H.., Van der Meer, J.W., www.overtopping-manual.com.

Fakhimi, A. (2008), A hybrid discrete-finite element model for numerical simulation of geomaterials, Elsevier, Computers and Geotechnics, Vol 36 (2008), pp 386-395.

Fowler, J. and Trainer, E. (1998), Overview of geocontainer projects in the United States. Proceedings of the Western Dredging Conference, Houston, TX, USA.

Fowler, J., Toups, D. and Duarte, F. and Gilbert, P. (1995), Geotextile Contained Dredged Material, Red Eye Crossing, Baton Rouge, LA." Proceedings, Western Dredging Association 16th Technical Conference, 28th Annual Texas AandM Dredging Seminar, University of Wisconsin Sea Grant Dredging Workshop, May 23-24, 1995, Minneapolis, MN

Garcia, N., Lara, J.L., Lomonaco, P., Losada, I.J. (2004b), Flow at low-crested breakwaters under breaking conditions. Proceedings of the 29th International Conference on Coastal Engineering, World Scientific, pp 4240–4252.

Garcia, N., Lara, J.L., Losada, I.J. (2004a), 2-D numerical analysis of near-field flow at low-crested breakwaters. Coastal Engineering 51 (10), pp 991–1020.

Giroud, J-P. (1982),Filter criterial for geotextile, Proceedings of 2nd internaitonal conference on geotextile, Las Vegas, pp 103-108

Greben, J.M., Cooper, A.K., Gledhill, I.M.A. and de Villiers, R. (2008), Numerical modelling of structures of dolosse and their interaction with waves , 2nd CSIR Biennial Conference, CSIR International Convention Centre Pretoria, ISBN 9780798855730.

Grett, H. (1984), Das reibungsverhalten von Geotextilien in bindigem und nichtbindigem Boden, Mitteilungen des Franzius-Instituts für Wasserbau und Küsteningenieurwese der Universität Hannover (in German).

Grobler, J.H., de Villiers, R, and Cooper, A.K. (2010), Modelling of fluid-solid interaction using two stand-alone codes, 7th South African Conference on Computational and Applied Mechanics (SACAM10), Pretoria, 10-13 January 2010, pp 10

Grüne, J., Sparboom, U., Schmidt-Koppenhagen, R., Wang, Z. and Oumeraci, H. (2006), Large-Scale Investigations Of Geotextile Sand containers Used For Scour Protection Of Offshore Monopiles Supporting Wind Energy Turbines, Proceedings of OMAE2006 : 25th International Conference on Offshore Mechanics and Arctic Engineering, Hamburg, Germany

Hald, T. and Burcharth, H. F. (2000), An alternative stability equation for rock armoured rubble mound breakwaters. In Proceedings of the 27th international conference on coastal engineering (ICCE 2000) Sydney, Australia, pp. 1921–1934

Heerten, G. (1982), Dimensioning the filtration properties of geotextiles considering long-term conditions. Proceedings of the 2nd International Conference on Geotextiles, Las Vegas, USA, Vol. 1, pp. 115–120.

Heerten, G., Jackson, A., Restall, S. and Saathoff, F. (2000), New Developments with Mega Sand Containers of Nonwoven Needle-Puncture Geotextile for the Construction of Coastal Structures, Proceedings of International Conference on Coastal Engineering 2000, Australia

Heerten, G., Klompmaker, J. and Partridge, A. (2008), Design and Construction of Waterfront Structures With Special Designed Nonwoven Geotextiles, 7th International Conference on Coastal and Port Engineering in Developing Countries (COPEDEC VII), Dubai, UAE.

Heieh, C., Wang, J.B. and Chiu, Y.F. (2006), Weathering properties of Geotextiles in Ocean environment, Geosynthetics International, pp 210-217.

Hendar, P. A. (1960), Stability of Rock-fill breakwaters, PhD Thesis, Chalmers Univ. of Technology. Dept. of Hydr. Göteborg, Sweden.

Holland, K.T., Green, A.W. Abelev, A. and Valent, P. J. (2004), Parameterization of the in-water motions of falling cylinders using high-speed video, Experiments in Fluids 37, pp 690–700

Hornsey, W.P. Carley, J.T., Coghlan, I.R. and Cox, R.J. (2011), Geotextile sand container shoreline protection systems: Design and application, J. Geotextiles and Geomembranes Journal, Vol. 29, pp 425-439

Hsu, T.-J., Sakakiyama, T., Liu, P.L.-F. (2002), A numerical model for wave motions and turbulence flows in front of a composite breakwater, Coastal Engineering Journal, Elsevier, Volume 46, pp 25–50

Hudson, R. (1956), Laboratory Investigation of Rubble-Mound Breakwaters. Journal of the Waterways and Harbour Division, pages 93-118.

Hudson, R. (1961), Laboratory Investigation of Rubble Mound Breakwater, Trans. ASCE 126, pages 492-541.

Hughes, S.A. (1993), Physical Models and Laboratory Techniques in Coastal Engineering, Volume 7. Coastal Engineering Research Center, USA.

Hughes, S.A. (2003), Physical Modelling Considerations for Coastal Structures, Advances in Coastal Structure Design, editors Mahan, R.K., Magoon, O. and Pirrello M, Ametica Society of Civil Engineering, pp 97-116

Itasca Consultants (2011), UDEC Manual, Volume 4, Theory and Background and Volume 1 Users Guide, USA

Jackson, L.A. and Corbett, B.A. (2007), Review of Existing Multi-Functional Artificial Reefs, Australasian Conference On Coasts And Ports 2007.

Jackson, L.A. and Hornsey, W.P. (2002), Engineering and Artificial Reef, Geotechnical Fabric Report, Australia

Jackson, L.A., Corbett, B.A., Restall, S.J. (2006), Failure modes and stability modelling for design of sand filled geosynthetic units in coastal structures, International Conference on Coastal Engineering 2006, World Scientific, San Diego, USA, Book of Abstracts.

Jackson, L.A., Russell, E.R., Restall, S.J, Corbett, B.A., Tomilinson, R. and McGrath J. (2004), Marine Ecosystems Enhancement of a Geotextile Coastal Protection Reef-Narrowneck Reef Case Study, Proceedings of International Conference on Coastal Engineering 2004, Lisbon, Portugal.

Jackson, A.; Recio, J.; Mocke, Z.; Jackson, L. (2012), Case Studies and Lessons Learnt from Applications of Sand Filled Geotextile Containers in the Arabian Gulf. 8th International Conference On Coastal And Port Engineering In Developing Countries PIANC-COPEDEC 2012, Chennai, INDIA., pp 1068-1073.

Jacobs, B.K. and Kobayashi, N. (1983), Sandbag stability and wave runup on bench slopes. University of Delaware , Research Report No. CE-83-36.

Jacobs, B.K. and Kobayashi, N. (1985), Experimental Study on sandbag stability and runup.Proceedings Coastal Zone.

Kawasaki, K. (1999), Numerical simulation of breaking and post-breaking wave deformation process around a submerged breakwater, Coastal Engineering Journal, Elsevier, Volume 41, pp 201–223

Klein Breteler, M., Uittenboogaard, R.E. and Eysink, W.D. (2001), Dumping accuracy of geotextile tubes in flow and waves (Storten van geotextile tube in stroming en golven), Project leader: De Groot M.B., DC1-321-5, Nov 2001, Delftcluster , The Netherlands (in Dutch)

Koerner, G.R. and Koerner, R.M. (2006), Geotextile tube assessment using a hanging bag test, Geotextiles and Geomembranes Journal, Vol. 24, Elsevier, pp 129–137

Kortenhaus, A., Van der Meer, J., Burcharth, H.F., Geeraerts, J., Pullen, T., Ingram, D. and Troch, P. (2005), Quantification of Measurement Errors, Model and Scale Effects Related to Wave Overtopping, Work package 7, CLASH programme

Krahn, T., Blatz, J., Alfaro, M. and Bathurst, R. J. (2007), Large-scale interface shear testing of sand bag dyke materials. Geosynthetics International, 14, No. 2, 119–126.

Kramer, M., Zanuttigh, B., Van der Meer, J.W., Vidal, C., Gironella, F.X. (2005), Laboratory experiments on low-crested breakwaters. Coastal Engineering 52 (10–11), 867–885

Kübler, S. (2002), Hydraulische Stabilität von geotextilen Sandcontainern unter Seegangseinwirkung. Diplomarbeit (Master Research Project Report) am Leichtweiß-Institut für Wasserbau.

Kutay, M. E. and Aydilek, A. H. (2004), Retention performance of geotextile containers confining geomaterials, Geosynthetics International, 11, No. 2, pp 100-113.

Lara, J. L., Losada I. J., del Jesus, M., Barajas, G. and Guanche R. (2010a), Numerical Modelling of Wave-Structure Interaction With a Three Dimensional Navier-Stokes Model, V European Conference on Computational Fluid Dynamics, Lisbon, Portugal

Lara, J. L., Losada, I. J., del Jesus, M., Barajas, G., Guanche, R. (2010b), IH-3VOF: A Three-Dimensional Navier-Stokes Model for Wave and Structure Interaction, In Proceedings of the 32nd International Conference On Coastal Engineering (ICCE 2010) Shanghai, China.

Lara, J.L., Garcia, N. and Losada, I.J. (2006), RANS modelling applied to random wave interaction with submerged permeable structures, Coastal Engineering 53 (10), Elsivier, pp 395–417.

Lara, J.L., I.J. Losada and R. Guanche. (2008), Wave interaction with low mound breakwaters using a RANS model, Ocean Engineering, ELSEVIER, 35, pp 1388-1400.

Lara, J.L., Losada, I.J. and Liu, P.L.-F. (2006), Breaking waves over a mild gravel slope: experimental and numerical analysis, Journal of Geophysical Research, AGU, 111, p. C11019 (2006)

Latham J.P., Mindel J., Xiang J., Guisesa R., Garciaa X., Paina C., Gormana G., Piggotta M. and Munjizab A. (2009), Coupled FEMDEM/Fluids for coastal engineers with special reference to armour stability and breakage., Geomechanics and Geoengineering, 2009, Vol:4, pp 797-805

Latham, J.P., Munjiza, A., Mindel, J., Xiang, J., Guises, R., Garcia, X., Pain, C., Gorman, G. and Piggott, M. (2008), Modelling of massive particulates for breakwater engineering using coupled FEMDEM and CFD,), Chinese Society of Particuology and Institute of Process Engineering, Chinese Academy of Sciences, Elsevier B.V., Particuology 6 (2008) pp 572–583

Lawson, C.R. (2008), Geotextile Containment for Hydraulic and Environmental Engineering, Geosynthetics International 2008

Lenze, B., Heerten, G., Saathoff, F. and Stelljes, K. (2002), Geotextile Sand Containers - Successful Solutions Against Beach Erosion at Sandy Coasts and Scour Problems under Hydrodynamic Loads, Littoral 2002, The Changing Coast. EUROCOAST / EUCC, Porto – Portugal, Ed. EUROCOAST – Portugal, ISBN 972-8558-09-0

Li, T., Troch, P. and De Rouck, J. (2004a), Wave overtopping over a sea dike, Journal of Computational Physics 198, pp 686–726

Lin P.and Liu, P.L.-F. (1998), A numerical study of breaking waves in the surf zone. Journal of Fluid Mechanics 359, 239-264.

Liu P. 2004, A finite volume/volume of fluid method for solving the Navier-Stokes-equation with application to water-wave problems, Lecture Notes of the 3 Days Compact Course, LWI, Germany.

Liu, P.L.-F. and Lin P. (1997), A numerical model for breaking wave: the Volume of Fluid method. Research Report. No. CACR-97-02, Centre for Applied Coastal Research, Ocean Engineering Laboratory, University of Delaware, U.S.

Liu, P.L.-F. and Lin P. (2002), Cobras Manual, Cornell Breaking Wave and Structures, Cobras Manual, a VOF- based RANS-model. Cornell University U.S.

Liu, P.L.-F., Lin P., Chang K.A. and Sakakiyama T. (1999), Numerical modelling of wave interaction with porous structures. J. Waterway, Port, Coastal and Ocean Engineering, ASCE 125 (6), pp 322-330.

Lohani, T. N., Matsushima, K., Aqil, U., Mohri, Y. and Tatsuoka, F. (2006), Evaluating the strength and deformation characteristics of a soil bag pile from full-scale laboratory tests. Geosynthetics International, 13, No. 6, pp246–264.

Losada, I.J., Lara, J.L., Christensen, E.D., Garcia, N. (2005), Modelling of velocity and turbulence fields around and within low-crested rubble-mound breakwaters.Coastal Engineering 52, pp 887-913.

Losada, I.J., Lara, J.L., Guanche, R., Gonzalez-Ondina, J.M. (2008), Numerical analysis of wave overtopping of rubble mound breakwaters. Coastal Engineering 55, pp 47-62.Munjiza, A. (2004), The Combined Finite-Discrete Element Method, ISBN 0-470-84199-0, John Wiley and Sons, 348.

Matsuoka, H., Sihong, L. and Yamaguchi, K. (2001), Mechanical Properties of Soilbags and their Application to Earth Reinforcement, Proceedings of the International Symposium on Earth Reinforcement, Fukuoka, Japan, pp 587-592.

Matsushima, K., Aqil, U., Mohri, Y. and Tatsuoka, F. (2008), Shear strength and deformation characteristics of geosynthetic soil bags stacked horizontal and inclined, Geosynthetics International, 2008, 15, No. 2, pp119-135

McGranahan, G., Balk, D. and Anderson, B. (2007), The rising tide: assessing the risks of climate change and human settlements in low elevation coastal zones, Environment and Urbanization, Vol. 19, No. 1, 17-37 (2007)

Mindel, J. E. (2008), Interface Tracking and Solid-Fluid Couupling Techniques with Coastal Engineering Applications, PhD Thesis, Imperial College of Science, Technology, and Medicine, London, UK

Mirafi (2004), Physical Properties of Geosynthetics, Technical Brochure.

Moraci, N. and Mandaglio, M.C. (2008), The Design of Geotextile Filters for Granular Soils, The First Pan American Geosynthetics Conference and Exhibition, Cancun, Mexico

Mori, E. (2009), Coastal Structures Made of Geotextile Elements Filled With Sand: Field and Experimental Research, PhD Thesis, Università degli Studi di Firenze, Florence, Italy

Mori, E., D'eliso, C. and Aminti, P.L. (2008), Physical Modelling on Geotextile Sand Container Used for Submerged Breakwater, Proceeding so the second international conference on the application of physical modelling to port and coastal protection, Coastlab08, Bari, Italy

Muttray, M. (2001), Wellenbewegung an und in Einem Geschuetteten Wellenbrecher - Laboruntersuchungen Im Grossmassstab Und Theoretische Untersuchungen-. PhD-Thesis, Mitteilungen Leichtweiss-Institut fuer Wasserbau der TU Braunschweig, Germany, pp. 1-304. (in German)

Muttray, M. and Oumeraci, H. (2002), Wave Transformation at Sloping Perforated Walls, Proceedings of the International Conference on Coastal Engineering 2002, p 2031-2043

Muttray, M. and Oumeraci, H. (2005), Theoretical and experimental study on wave damping inside a rubble mound breakwater. Amsterdam, The Netherlands: Elsevier, Coastal Engineering, vol. 52, no. 8, pp. 709-725.

NAUE (2009), Submerged Direct Shear Stress Results, Internal Communication.

NAUE and Soil Filters Australia (2003), Designing with Geotextile Sand Containers, Technical Brochure.

NAUE Fasetechnik (2004a), Direct Shear Stress Results, Internal Communication

NAUE Fasetechnik (2004b), Secutex GRX, Technical Brochure (in German).

Oberhagemann K., Stevens M.A., Haque S.M.S. and Faisal M.A. (2006), Geobags for Riverbank Protection, 3rd International Conference on Scour and Erosion, Amsterdam

Oberhagemann, K. and Hossain, M.M. (2011), Geotextile bag revetments for large rivers in Bangladesh, Geotextiles and Geomembranes Journal, Vol. 29, pp 402-414

Ogink, M.J.M., (1975), Investigations on the hydraulic characteristics of synthetic fabrics, Delf Hydraulics Laboratory, Publication No. 146, Delft, The Netherlands,

Oumeraci, H , Kortenhaus, A. and Werth, K. (2008), Core Made of Geotextile Sand Containers for Rubble Mound Breakwaters and Seawalls: Effect on Hydraulic Stability and Performance, 7th International Conference on Coastal and Port Engineering in Developing Countries (COPEDEC VII), Dubai, UAE

Oumeraci, H. (1999a), Physical modelling, field measurements and numerical modelling in coastal engineering: synergy or competition? 2nd German-Chinese Joint Seminar on Recent Developments in Coastal Engineering - Sustainable Development in the Coastal Zone, Tainan, Taiwan, pp. 513-537.

Oumeraci, H. (1999b), Strengths and limitations of physical modelling in coastal engineering - synergy effects with numerical modelling and field measurements. In: Evers, K.-U.et al. (eds.): Keynote Address, Proceedings Hydralab Workshop on Experimental Research and Synergy Effects with Mathematical Models, Keynote lecture, Hannover, Germany, pp. 7-38.

Oumeraci, H. (1999c), Hydromechanik. Vorlesungsumdruck für das Grundfach "Hydromechanik", Leichtweiß-Institute for Hydraulic Engineering and Water Resources Braunschweig, Germany

Oumeraci, H. (2000), The Sustainability Challenge in Coastal Engineering (Keynote Lecture). Proceedings 4th International Conference of Hydrodynamics

Oumeraci, H. (2004), Sustainable coastal flood defences: scientific and modelling challenges towards an integrated risk-based design concept. Keynote Lecture. Proc. First IMA International Conference on Flood Risk Assessment. Bath, UK, IMA - Institute of Mathematics and its Applications: pp. 9-24.

Oumeraci, H. (2009), Wasserbauliches Versuchswesen und Dimensionsanalyse, Hydromechanics and Coastal Engineering Lecture Notes – SS 2009, Leichtweiss Institute for Hydraulic Engineering and Water Resource, Technical University Braunschweig, Germany (In German)

Oumeraci, H. and Recio, J. (2010), Geotextile sand containers for shore protection, Invited Chapter in Handbook of Coastal and Ocean Engineering, Editor: Kim Y.C., World Scientific Publishing, Singapore, pp 553-600

Oumeraci, H., Bleck, M. and Hinz, M. (2002a), Untersuchungen zur Funktionalität geotextiler Sandcontainer. Berichte Leichtweiß-Institut für Wasserbau, Technische Universität Braunschweig, Nr. 874, Braunschweig, Germany, (in German).

Oumeraci, H., Bleck, M., Hinz, M. and Kübler, S. (2002b), Großmaßstäbliche Untersuchungen zur hydraulischen Stabilität geotextiler Sandcontainer unter Wellenbelastung. Berichte Leichtweiß-Institut für Wasserbau, Technische Universität Braunschweig, Nr. 878, Braunschweig, Germany, (in German).

Oumeraci, H., Bleck, M., Hinz, M. and Möller, J. (2002c), Theoretische Untersuchungen zur Anwendung geotextiler Sandcontainer im Küstenschutz. Berichte Leichtweiß-Institut für Wasserbau, Technische Universität Braunschweig, Nr. 866, Braunschweig, Germany, (in German).

Oumeraci, H., Grüne, J., Sparboom, U., Schmidt-Koppenhagen, R., and Wang, Z. (2007a), Stability Tests of Geotextile Sand containers for Monopile Scour Protection (Untersuchungen zur Kolkbildung und zum Kolkschutz bei Monopile-Gründungen von Offshore-Windenergieanlagen), Final Research Report, Coastal Research Centre (FZK), (in German)

Oumeraci, H., Hinz, M., Bleck, M. and Kortenhaus, A. (2003), Sand-filled geotextile containers for shore protection, 6th International Conference on Coastal and Port Engineering in Developing Countries (COPEDEC VI), Colombo, Sri Lanka.

Oumeraci, H., Kortenhaus, A. and Dassanayake, D.T. (2012), Prototype Drop Tests on Optimisation on the Construction of Scour Protection Systems Using GSCs (GeoDumping-Phase I), Final research report, Leichtweiß-Institut für Wasserbau, Technische Universität Braunschweig, Nr. 1029, Braunschweig, Germany

Oumeraci, H., Kortenhaus, A. and Werth, K. (2007b), Hydraulic performance and armour stability of rubble mound breakwaters with core made of geotextile sand containers - Comparison with conventional breakwaters. Intern. Conf. on Coastal Structures, ASCE, Venice, Italy.

Ozegowski, J. (2012), Hydraulic Performances of Low-Crested and Submerged Coastal Structures Made of Geotextile Sand Containers, Bachelor Thesis supervised by Dassanayake, D.T. and Oumeraci, H., Leichtweiß-Institut für Wasserbau, Technische Universität Braunschweig, Braunschweig, Germany

Pain, C. C., Umpleby, A. P., de Oliveria, C. R. E., and Goddard, A. J. H. (2001), Tetrahedral mesh optimisation and adaptively for steady-state and transient finite element calculations. Computer Methods in Applied Mechanics and Engineering, 190, 3771–3796.

Patterson Britton & Partners (2008), Manly Ocean Beach Emergency Action Plan for Coastal Erosion, Issue No. 6, March, for Manly Council,

PIANC (2011), The Application of geosynthetics in waterfront areas-PIANC Report No. 113 by MarCom Working Group 113.

Pilarczyk, K. (1998), Dikes and Revetments, design, maintenance and safety assessment, A.A. Balkema, Rotterdam, the Netherlands.

Pilarczyk, K. (2005), Coastal Stabilization and Alternative Solutions in International Perspective, Keynote lecture, Arabian Coast, Dubai, UAE

Pilarczyk, K. W. (2000), Geosynthetics and Geosystems in Hydraulic and Coastal Engineering. A.A. Balkema, Rotterdam, the Netherlands.

Porraz M.J.L., Masa A. J. A. and Medina, R.R. (1979), Mortar-filled Containers, Lab and ocean experiences. Proceedings Coastal Structures, pp 270-289

Ray, R. (1977), A Laboratory Study of The Stability of Sand-Field Nylon Bag Breakwater Structures, US Army Coastal Engineering Research Centre, Vickburg, USA

Recio, J. (2007), Hydraulic stability of geotextile sand containers for coastal structures- effect of deformations and stability formulae. Leichweiss-Institute for Hydraulic Engineering and Water Resources. Braunschweig, Germany, Technical University Braunschweig, PhD, http://deposit.ddb.de/cgi-bin/dokserv?idn=987929720

Recio, J. and Oumeraci, H. (2006a), A numerical study on the hydraulic processes associated with the instability of GSC-structures using a VOF-RANS model, LWI Report No. 941, Leichtweiss-Institute for Hydraulic Engineering and Water Resources, Technische Universität Braunschweig, Germany.

Recio, J. and Oumeraci, H. (2006b), Processes affecting the stability of revetments made with geotextile sand containers, 31st International Conference on Coastal Engineering (ICCE 2006) Conference, World Scientific, San Diego, USA, Vol. 5, 5080-5092.

Recio, J. and Oumeraci, H. (2006c), Geotextile sand containers for coastal structures, hydraulic stability formulae and tests for drag, inertia and lift coefficients, LWI Report No. 936, Leichtweiss-Institute for Hydraulic Engineering and Water Resources, Technische Universität Braunschweig, Germany.

Recio, J. and Oumeraci, H. (2007a), Effect of Deformations on the Hydraulic Stability of Coastal Structures made of Geotextile Sand Containers. Geotextile and Geomembrane Journal, vol. 25. Elsevier, pp. 278–292.

Recio, J. and Oumeraci, H. (2007b), Hydraulic processes associated with the instability of GSC-structures — A numerical study using the "COBRAS-Model". Leichtweiß Institute for Hydraulic Engineering and Water Resources, LWI-Report Nr 941.

Recio, J. and Oumeraci, H. (2007c), Numerical simulations on the stability of coastal structures made of geotextile sand containers (GSC). Leichtweiß Institute for Hydraulic Engineering and Water Resources, LWI-Report Nr. 942.

Recio, J. and Oumeraci, H. (2007d), Permeability of GSC-structures, model tests and analyses, LWI Report No. 943, Leichtweiss-Institute for Hydraulic Engineering and Water Resources, Technische Universität Braunschweig, Germany.

Recio, J. and Oumeraci, H. (2007e), Processes affecting the hydraulic stability of geotextile sand containers — experimental studies. Leichtweiß Institute for Hydraulic Engineering and Water Resources, LWI-Report Nr. 944.

Recio, J. and Oumeraci, H. (2008a), Hydraulic permeability of structures made of geotextile sand containers: Laboratory tests and conceptual model. Geotextiles and Geomembranes Journal, Vol. 26, Elsevier, pp. 473-487.

Recio, J. and Oumeraci, H. (2008b), Processes affecting the hydraulic stability of coastal revetments made of Geotextile sand containers. Coastal Engineering (2009a), pp 260-284

Recio, J. and Oumeraci, H. (2009), Process based stability formulae for coastal structures made of geotextile sand container, Coastal Engineering, Vol. 56, Elsevier, pp 632-658

Recio, J., Hocine Oumeraci, H., Mocke, G. (2010), Stability Formula and Numerical Model for Structures made with Geotextile Sand Containers used for Coastal Stabilization, 2nd International Conference on Coastal Zone Engineering and Management (Arabian Coast 2010), Muscat, Oman

Restall, S. and Saathoff, J. (2002), Australian and German Experiences with Geotextile Containers for Coastal Protections, EuroGeo 2002.

Restall, S., Hornsey, W., Oumeraci, H., Hinz, M., Saathoff, F., and Werth, K. (2004), Australian and German Experiences with geotextile Containers for Coastal Protection, proceedings Eurogeo 2004

Robin, A.C. (2004), Paper bag problem, Mathematics today, Bulletin of the Institute of Mathematics and its Applications 40 (June 2004), pp 104-107.

Rock Manual (2007), The Rock Manual. The use of rock in hydraulic engineering, CIRIA, CUR, CETMEF, 2nd edition, C683, CIRIA, London.

Saathoff, J., Oumeraci, H. and Restall, S. (2007), Australian and German experiences on the use of geotextile containers, Geotextiles and Geomembranes Journal, Vol. 25, Elsevier, pp 251–263

Seelig, W.N. (1983), Wave Reflection from Coastal Structures. Proceedings Conference on Coastal Structures 1983, American Society of Civil Engineers (ASCE), pp. 961-973.

Shin, E.C. and Oh, Y.I. (2004), Consolidation Process of Geotextile Tube Filled with Fine-Grained Materials, International Journal of Offshore and Polar Engineering, Vol. 14, No. 2, June 2004 (ISSN 1053-5381)

Sierra, J.P., González-Marco,D. Mestres, M., Gironella,X., Oliveira, T.C.A., Cáceres I. and Mösso, C. (2010), Numerical model for wave overtopping and transmission through permeable coastal structures, Environmental Modelling & Software 25 (2010), Elsevier, pp 1897-1904

Slinn, D.N. (2011), Numerical Simulations Techniques applied to Coastal and Oceanographic Engineering - Computational Fluid Dynamics (CFD), Lecture Notes, Department of Civil and Coastal Engineering University of Florida, USA, (Accessed on 02-08-2011, http://users.coastal.ufl.edu/~slinn/),

Smid,R. (2001), Untersuchungen zur Ermittlung der mittleren Wellenüberlaufrate an einer senkrechten Wand und einer 1:1.5 geneigten Böschung für Versuche mit und ohne Freibord. Studienarbeit LWI., (Master Research Project Report) (in German)

Sorensen, R.M. (2006), Basic Coastal Engineering, ISBN-10: 0-387-23333-4, Springer Science + Business Media, Inc., 233 Spring Street, New York, NY 10013, USA.

Tan, C.Y. and Chew, S.H. (2008), Modelling Geotextile Container In Marine Construction Using Geotechnical Centrifuge, Proceedings of the 4th Asian Regional Conference on Geosynthetics, Shanghai, China, pp 615-620

Tekmarine Inc. (1982), Large-scale model studies of artic island slope protection. Sierra California.

TenCate (2007), Determination of the Long Term Properties for Mirafi® PET-Series Reinforcement Geotextiles by GRI-GT7 and NCMA Guidelines, Technical Note by TenCate Geosynthetics North America

Ting C.L., Lin M.C., Cheng C.Y. (2004), Porosity Effects on Non-breaking Surface Waves over Permeable Submerged Breakwaters. Coastal Engineering Journal, Elsevier, Vol. 50 Issue 4, pages 213-224.

Troch P. and De Rouck J. (1998), Development of 2D numerical Wave flume for simulation of Wave interaction with rubble mound breakwaters. In: Proceedings 26th International Conference on Coastal Engineering (ICCE 1998) Conference, Copenhagen, Denmark.

Troch P. and De Rouck J. (1999), An Active Wave Generatíng-Absorbing Boundary Condition for VOF type numerical model. Coastal Engineering, Vol. 38(4), pp. 223- 247, Elsevier, The Netherlands.

U.S.-CEM (2004), Coastal Engineering Manual, U.S. Army Corps Of Engineers, Engineering Use of Geotextiles

van den Bosch, I., ten Oever, E., Bakker, P., and Muttray, M. (2012), Stability of interlocking armour units on a breakwater crest, Proceedings of the 33rd International Conference On Coastal Engineering (ICCE 2012) Santander, Spain.

Van der Linde, J.P. (2010), Stability of single layer armour units on low-crested structures, Delft University of Technology, The Netherlands

Van der Meer, J.W. (1987), Stability of breakwater armour layers - Design formulae. Journal of Coastal Engineering, 11, pp. 219-239

Van der Meer, J.W. (1988), Rock slopes and gravel beaches under wave attack, PhD thesis, Delft Hydraulics Laboratory, The Netherlands

Van Der Meer, J.W. (1998), Application and stability criteria for rock and artificial units, Chapter 11 in: "Seawalls, dikes and revetments". Edited by K.W. Pilarczyk. Balkema, Rotterdam, The Netherlands

Van der Meer, J.W., Pilarczyk, K.W. (1990), Stability of low-crested and reef breakwaters. Proc. 22nd International Conference on Coastal Engineering, Delft, The Netherlands, pp. 1375–1388.

Venis, W.A., (1968), Closure of estuarine channels in tidal regions, Behaviour of dumping material when exposed to currents and wave action, De ingenieur, 50, 1968

Verhagen, H.J. (2004), Classical, Innovative and Unconventional Coastal Protection Methods, keynote address, Nato Advanced Workshop on Environment friendly coastal protection structures, Varna, Bulgaria

Vidal, C., Losada, M.A., Mansard, E.P.D. (1995), Stability of low-crested rubble mound breakwater heads. Journal of Waterway, Port, Coastal, and Ocean Engineering vol. 121, No. 2. ASCE, pp. 114–122

Vidal, C., Losada, M.A., Medina, R., Mansard, E.P.D., Gomes-Pina, G. (1992), An universal analysis for the stability of both low-crested and submerged breakwaters. Proc. 23rd International Conference on Coastal Engineering, Italy, pp. 1679–1697.

Wang, Y.W. and Lin, Y.W. (2008), Combination of CFD and CSD packages for fluid-structure interaction, Journal of Hydrodynamics, Volume 20 (6), pp 756-761

Warnock, J. E. (1950), Hydraulic Similitude, In: H. Rowe, Editor, Engineering Hydraulics, Wiley, New York, N.Y (1950), pp. 136–17

Weerakoon, S.; Mocke, G.P.; Smit, F.; Al Zahed, K. (2003), Cost Effective Coastal Protection Works Using Sand Filled Geotextile Containers. 6th International Conference on Coastal and Port Engineering in Developing Countries (COPEDEC VI), Colombo, Sri Lanka.

Werth, K., Recio, J., Oumeraci, H. and Heerten, G. (2008), Hydraulic permeability of GSC-structures: Laboratory tests and results. Proc. 31st International Conference Coastal Engineering (ICCE 2008), Hamburg, Germany

Wilms, M., Wahrmund, H., Stahlmann, A., Heitz, C. and Schlurmann, S. (2011), Kolkbildung und dimensionierung des Kolkschutzsystems eines OWEA Schwerkraftfundaments, Hydraulische dodellversuche zum STRABAG Schwerkraftfundament, HTG Kongress 2011, Germany, 395-404.

Won, M.S. and You-Seong Kim, Y.S. (2007), Internal Deformation Behavior of Geosynthetic-Reinforced Soil Walls, Geotextiles and Geomembranes J, Vol. 25, Elsevier, pp 10-22

Wouters, J. (1998), Open Taludbekledingen; stabiliteit van geosystems (Stability of Geosystems) Deftt Hydraulics Report H1930, Annex 7 (in Dutch).

Wu, C. S., Hong, Y.S. and Wang, R.H. (2008), The influence of uniaxial tensile strain on the pore size and filtration characteristics of geotextiles, Geotextiles and Geomembranes Journal, vol. 26 (2008), Elsevier, pp 250–262

Xiang J., Latham J.P., Vire A., Anastasaki E. and Pain, C.C. (2012), Coupled FLUIDITY/Y3D technology and simulation tools for numerical breakwater modelling, Proc. 33rd International Conference Coastal Engineering (ICCE 2012), Santander, Spain

Zanuttigh, B. and Van der Meer, J.W. (2006), Wave reflection from coastal structures. ASCE, Proceedings of the International Conference on Coastal Engineering 2006, San Diego, pp 4337-4349

Zanuttigh, B., and Van der Meer, J.W. (2008), Wave Reflection From Coastal Structures in Design Conditions, Coastal Engineering Journal, Elsevier, Volume 55, Issue 10, October 2008, pp 771-779

Zellweger, H., (2007), Geotextile bags for river erosion control in Bangladesh, underwater behaviour and environmental aspects. Diploma thesis, ETH Zürich.

Zhao, Z.K., Chew, S.H., Karunaratne, G.P., Tan, S.A., Delmas, Ph. and Loke, K.H. (2000), Geotextile Filter In Revetment Subjected To Cyclic Wave Loading, GeoEng 2000, Melbourne, Australia